Modelling the crosstalk between residual normal haematopoietic stem/progenitor cells, acute myeloid leukaemia and their microenvironment

Alexander Waclawiczek

Imperial College London
Department of Life Sciences
PhD Supervisor: Dr. Dominique Bonnet

A thesis submitted for degree of
Doctor of Philosophy
Imperial College London
March 2019

Declaration of Originality

I Alexander Waclawiczek confirm that the work presented in this thesis is my own. Where information has been derived from other sources, I confirm that this has been indicated in the thesis.

Copyright Declaration

The copyright of this thesis rests with the author. Unless otherwise indicated, its contents are licensed under a Creative Commons Attribution-Non Commercial 4.0 International Licence (CC BY-NC). Under this licence, you may copy and redistribute the material in any medium or format. You may also create and distribute modified versions of the work. This is on the condition that: you credit the author and do not use it, or any derivative works, for a commercial purpose. When reusing or sharing this work, ensure you make the licence terms clear to others by naming the licence and linking to the licence text. Where a work has been adapted, you should indicate that the work has been changed and describe those changes. Please seek permission from the copyright holder for uses of this work that are not included in this licence or permitted under UK Copyright Law.

Acknowledgement

Firstly, I would like to thank my supervisor Dr Dominique Bonnet for her support during my Ph.D. I could always rely on her valuable input and patience even in those plentiful times when results were discouraging. She gave me the freedom and space to develop as an independent and critically thinking scientist but also provided the necessary framework to exchange ideas and tackle technical problems. Importantly, she showed trust when negative results encouraged me to rethink my project and to develop somewhat unorthodox methods to study haematopoiesis. Furthermore, she selected three excellent Ph.D. committee members which also deserve my greatest gratitude for the advice during numerous thesis committee meeting.

Furthermore, this work would not have been possible without all present and particularly former Bonnet lab members. Scientific and, more often, non-scientific topics could always be discussed and the diverse scientific background of each member guaranteed a great spectrum of advice. Each one was very engaged to develop a cheerful work atmosphere, organize retreats, dinners or simply a drink after work. Certainly, the friendships that developed will be long-lasting. Furthermore, I very much appreciated their comradery during tea breaks and lunches, their audience, and feedback to complain and discuss results and their patience and understanding with my inappropriate jokes, pranks and a 3-hour lab meeting (it only happened once though).

Certainly, outside the lab, I could always count on friends and family to provide support for the difficult work schedules during hectic phases of the PhD. Especially my girlfriend, helped me through many struggles and I could always rely on her for support no matter the outcome of experiments. Her, often painful but valid, criticism and advice made me a better scientist and allowed me to progress my project.

Lastly, the FCI core facilities especially the flow cytometry and biological research facility were always supportive and provide invaluable expertise and great company during long FACS-sorting sessions.

Abstract

In acute myeloid leukaemia (AML) the suppression of haematopoietic stem and progenitor cell (HSPC) differentiation and proliferation is a major factor contributing to treatment complications and mortality rates. Previous studies associated an altered microenvironment with dysregulated haematopoiesis but the precise molecular mechanisms are still not fully understood.

To mimic AML infiltrated human bone marrow (BM), we utilised our published humanised 3D BM model. Healthy donor MSCs were cultured on a 3D collagen scaffold, co-injected with normal $CD34^+$ HSPCs with AML and transplanted into NSG-SGM3 mice. In analogue, we co-cultured healthy BM MSCs with HSPCs and AML.

Both ex vivo and in vivo models replicated a suppression of normal haematopoiesis. Similar to AML patients, cell death was affected minimally but the majority of HSPCs were quiescent and showed an enrichment of serial colony-forming cells and LTC-ICs.
Ex vivo, HSPC suppression was largely dependent on the presence of MSCs but not in a direct contact manner. Stroma secretome analysis identified the previously uncharacterized stanniocalcin-1 (STC1). STC1 is exclusively expressed in MSCs and upregulated 2 to 30-fold after AML contact. Supplemented recombinant STC1 significantly enriches for quiescent HSPCs and helps to preserve their functionality, while the proliferation of AML was unchanged. Neutralisation of STC1 in AML scaffolds improved HSPC cell number through increased proliferation.
Further transcriptomic interrogation of the MSCs after AML exposure also identified an upregulation of Hypoxia-inducible factor -1 alpha (HIF-1α) target genes and increased stabilisation of HIF-1α. Knockdown of HIF-1α in MSCs not only abrogates secreted STC1 but also improves HSPC proliferation in the presence of AML.

In conclusion, the newly developed humanised ex vivo and in vivo models mimic the suppression of HSPCs by AML but are dependent on an altered MSC niche and the HIF-1α-STC1 axis. Inhibition of niche remodelling may be an interesting new approach to improve recovery after AML treatment.

Table of Contents

Declaration of Originality ***2***

Copyright Declaration ***3***

Acknowledgement ***4***

Abstract ***5***

Table of Figures ***10***

List of Tables ***11***

Abbreviations ***12***

Chapter 1. Introduction ***19***

1.1 Normal Haematopoiesis **19**

1.1.1 The origins of haematopoiesis 19

1.1.2 Adult haematopoiesis 21

1.1.2.1 Haematopoietic stem cells 21

1.1.2.2 MPPs and downstream progenitors 23

1.1.2.3 Immunophenotypic HSCs 25

1.2 **Assays to analyse HSPCs** **25**

1.2.1 Mouse models 25

1.2.2 *Ex vivo* models 26

1.2.3 Humanised niche models 27

1.3 Acute myeloid leukaemia **28**

1.3.1 Classification and outcome stratification 30

1.3.2 Clonal haematopoiesis 31

1.3.3 Therapeutic options and disease progression 32

1.3.4 AML heterogeneity 33

1.4 The healthy bone marrow microenvironment **35**

1.4.1 The anatomy of bone marrow 35

1.4.1.1 The endosteal niche 38

1.4.1.2 The perivascular niche 38

1.4.1.3 Mesenchymal stroma cells (MSCs) 39

1.4.1.4 Other non-haematopoietic SCN members 41

1.4.1.5 Haematopoietic SCN members 41

1.5 The malignant bone marrow niche **42**

1.5.1 AML interactions with the niche 42

1.5.2 The location of AML in the niche 43

1.5.3 AML remodels the niche 44

1.5.4 The niche remodels AML 46

1.6 Normal haematopoiesis in AML **48**

1.6.1 Clinical perspective 48

1.6.2 HSPCs in acute leukaemias 49

1.6.3 Mechanistic perspective 50

1.6.3.1 Displacement of HSPCs from the niche 50

1.6.3.2 Cell cycle 51

1.6.3.3 Microenvironment 52

1.7 Hypoxia in BM during normal and malignant haematopoiesis **55**

1.7.1 Oxygen distribution in the BM 55

1.7.2 The HIF family of transcription factors 55

1.7.3 Role of hypoxia for normal haematopoiesis 56
1.7.4 Role of hypoxia for malignant haematopoiesis 57
1.7.5 HIF in the BM microenvironment 57

1.8 The Stanniocalcin family of secreted proteins 59
1.8.1 STC in fish and mammals 59
1.8.2 The roles of STC 60
1.8.3 STC1 in cancer 61

1.9 Objective of study 63

2 Chapter 2 Materials and Methods 64

2.1 Cell culture 64

2.2 Primary Samples 65
2.2.1 Mesenchymal Stroma Cells 65
2.2.2 Umbilical Cord Blood Cells 65
2.2.2.1 Separation of mononuclear cells by Ficoll density centrifugation 65
2.2.2.2 CD34 Positive Purification of HSPCs 66
2.2.3 Acute Myeloid Leukaemia Samples 66

2.3 Lentivirus production 67
2.3.1 Determination of virus titre 67
2.3.2 Lentivirus transduction 68
2.3.2.1 MSC 68
2.3.2.2 HSPCs 68

2.4 In vitro assays 68
2.4.1 Culture of MSCs with primary CB $CD34^+$HSPCs/AML patient samples and AML cell lines 68
2.4.2 Culture of MSCs with primary HSPCs and primary AML cells. 69
2.4.3 Culture comparing feeder-free $CD34^+$ with AML and MSC co-cultured $CD34^+$ with AML 69

2.5 Cell division tracking 69

2.6 Preconditioning of MSCs 70
2.6.1 Generation of AML expressing inducible caspase 9 fragment 70
2.6.2 Preconditioning with AML 70
2.6.3 Preconditioning with hypoxia 70

2.7 Analysis of reactive oxygen species and mitochondrial membrane potential 70

2.8 Colony-forming assay 71
2.8.1 Primary CFU-assay 71
2.8.2 Secondary CFU-assay 71

2.9 Long term colony initiation cell – Assay (LTC-IC) 71
2.9.1 Limiting dilution LTC-IC 71
2.9.2 Bulk Culture LTC-IC 72

2.10 *In vivo* assays 72
2.10.1 Mice 72
2.10.2 Human Xenografts 73
2.10.2.1 Analysis of human engraftment (12 weeks) 73
2.10.2.2 Bone marrow aspiration (8 weeks) 73

2.11 Scaffold 73
2.11.1 Scaffold preparation 73
2.11.2 Surgery and pre- and post-surgery care 74

2.12 Flow Cytometry 75
2.12.1 Extracellular Staining and Analysis Parameters 75
2.12.2 AnnexinV Staining 75

2.12.3 Intracellular Staining 75
2.12.4 Ki67 and EdU staining 76
2.12.5 Cell Sorting 76

2.13 Molecular Biology 76
2.13.1 RNA Extraction 76
2.13.2 Reverse Transcription 77
2.13.3 Quantitative real-time PCR 77
2.13.4 Western blotting 77

2.14 Statistical Analysis 77

3 Chapter 3. Ex vivo modelling the AML crosstalk with microenvironment and normal haematopoietic HSPCs 81

3.1 Introduction 81

3.2 Results 83
3.2.1 Quantitative analysis of normal CB HSPCs co-cultured of with BM MSCs and AML 83
3.2.1.1 Time course analysis with AML cell line 84
3.2.1.2 Screen with AML cell lines and AML patient samples 85
3.2.1.3 HSPC Viability 89
3.2.1.4 Cell cycle and proliferation assay 89
3.2.2 Qualitative analysis of normal CB HSPCs co-cultured of with BM MSCs and AML 91
3.2.2.1 Serial CFU-assay 94
3.2.2.2 LTC-IC Assay 95
3.2.2.3 Serial transplantation Assay 95
3.2.3 Impact of an AML-remodelled microenvironment on AML proliferation 98

3.3 Discussion 100

4 Chapter 4. Development of an in vivo fully humanised scaffold model 104

4.1 Results 104
4.1.1 Time course analysis 105
4.1.2 Screen of AML cell lines and AML patient samples 106
4.1.3 Viability of non-leukaemic haematopoietic cells in scaffolds 109
4.1.4 Proliferation of non-leukaemic haematopoietic cells 110

4.2 Discussion 114

5 Chapter 5. An AML remodelled mesenchymal niche suppresses normal HSPCs 118

5.1 Introduction 118

5.2 Results 120
5.2.1 The impact of AML on the MSC transcriptome 120
5.2.2 Impact of mesenchymal microenvironment on HSPC repression 121
5.2.3 AML pre-conditioned MSCs suppress HSPC expansion 122
5.2.4 Hypoxia and hypoxia-regulated genes from MSCs promote HSPC quiescence 124

5.3 Discussion 127

6 Chapter 6. The MSC secreted factor STC1 suppresses normal HSPCs 129

6.1 Introduction 129

6.2 Results 131
6.2.1 AML suppresses is partially dependent on direct contact 131
6.2.2 Investigation of stromal secretome after AML culture 132
6.2.3 AML triggers STC1 secretion from MSCs 134
6.2.4 STC1 as biomarker to measure HSPC suppression 136
6.2.5 STC1 suppresses normal HSPCs expansion and differentiation 137

6.2.5.1 Phenotypic and functional characterisation of STC1-treated HSPCs *ex vivo* 137
6.2.5.2 Phenotypic and functional characterisation of STC1-treated HSPCs *in vivo* 140
6.2.6 Antibody neutralisation of STC1 ameliorates HSPC differentiation blockage *ex vivo* 141
6.2.7 Antibody neutralisation of STC1 ameliorates HSPC differentiation blockage *in vivo* 142
6.2.8 Mechanistic analysis of STC1 on normal HSPCs and MSCs 143

6.3 Discussion: 145

7 Chapter 7. HIF-1α regulates STC1 expression in AML MSCs and suppresses HSPCs .. 150

7.1 Introduction 150

7.2 Results 152

7.2.1 Expression of STC1 and other hypoxia-response genes in hypoxia is mediated by HIF-1α stabilisation 152
7.2.2 AML stabilises HIF-1α triggering expression of STC1 and other hypoxia-response genes 153
7.2.3 Investigation of other STC1 regulators 154
7.2.4 HIF-1α overexpression in MSCs suppresses expansion of normal HSPCs in co-culture 156
7.2.5 HIF-1α knockdown ameliorates HSPC suppression *ex vivo* 157
7.2.6 HIF-1α knockdown ameliorates HSPC suppression *in vivo* 158

7.3 Discussion 160

8 Summary and discussion 166

References 171

Table of Figures

Figure 1. The human haematopoietic hierarchy. Adapted from (Doulatov et al., 2012) and (Laurenti and Gottgens, 2018) 22
Figure 2. Molecular classes of AML with frequency (>1 %); adapted from (Dohner et al., 2017) 29
Figure 3. Anatomy of long and flat bones adapted from (Clarke, 2008) 36
Figure 4 The bone marrow niche for HSCs adapted from (Boulais and Frenette, 2015) 37
Figure 5. Schematic of in vitro culture protocol and cell separation 83
Figure 6. 4-day time course analysis of HSPC cultured with and without AML cell line U937 84
Figure 7. Lineage Distribution of normal CB MNCs 86
Figure 8. Relative cell counts and phenotypic distributions of non-leukaemic haematopoietic cells after 4 days 87
Figure 9. Relationship between numbers of AML cells and total non-leukaemic haematopoietic cells 88
Figure 10. Cell counts of HSPCs and sub-populations after co-culture with purified normal CB MNCs fractions. 88
Figure 11. Viability of HSPCs alone or co-cultured with AML 89
Figure 12. Cell cycle analysis of HSPCs and sub-populations alone or co-cultured with AML 90
Figure 13. 4-day time course analysis of cell divisions of $CD34^+$ 91
Figure 14. Tracking of HSPC divisions cultured alone or co-cultured with AML 91
Figure 15. Schematic depicting the functional analysis of $CD34^+$ cells isolated from HSPCs cultured alone or with AML for 4 days 92
Figure 16. Comparison of transwell versus direct contact exposure of AML to CB HSPCs and MSCs 93
Figure 17. Results from serial CFU-assay and LTC-IC assay of sorted $CD34^+$ cells from HSPC-AML co-cultures 94
Figure 18. Lymphoid and myeloid lineage distribution of human CD45 from primary recipients 96
Figure 19. Engraftment and phenotypic HSC frequencies of primary recipients 97
Figure 20. AML patient samples and HSPCs co-cultured with AML cell lines 99
Figure 21. Schematic presentation of experimental design and fundamental scaffold properties 105
Figure 22. Kinetics of AML and normal haematopoietic cells over a 3-week time course 106
Figure 23. Engraftment of AML patient samples + normal CB $CD34^+$ in scaffolds 107
Figure 24. Engraftment of normal HSPCs alone or + AML patient samples/cell lines 108
Figure 25. Engraftment of non-leukaemic and leukaemic human CD45 in spleen and BM of mice 109
Figure 26. Viability of non-leukaemic human haematopoietic cells 110
Figure 27. Analysis of cycling non-leukaemic human haematopoietic cells via EdU incorporation 111
Figure 28. Tracking of proliferation using pulse-chase cell tracer experiments 112
Figure 29. Proportions of $CD34^+$ among total non-leukaemic human haematopoietic cells 113
Figure 30. Schematic overview of different MSC scaffold models (adapted from (Abarrategi et al., 2017)) 115
Figure 31. Expression of hypoxia-regulated genes in MSCs co-cultured with AML in normoxia 120
Figure 32. Comparison of HSPC suppression by AML on feeder-free and MSC supported conditions 121
Figure 33. Experimental setup for pre-conditioning MSCs with AML (iCASP) 123
Figure 34. Results of HSPC co-culture with AML-preconditioned MSCs 124
Figure 35. Regulation of HSPC proliferation by hypoxia and hypoxia-regulated genes from MSCs 125
Figure 36. Comparison of HSPCs proliferation in direct contact or in transwell inserts 132
Figure 37. Schematic of transcriptome analysis of MS5 exposed to AML 132
Figure 38. Expression of STC1 in MSCs 135
Figure 39. Correlation between normal haematopoietic cells and STC1 concentration in supernatant of HSPC-AML co-cultures 136
Figure 40. Correlation between normal haematopoietic cells and STC1 concentration in supernatant of HSPC-AML co-cultures 137
Figure 41. Comparative analysis of viability and proliferation of HSPCs treated with vehicle or STC1 138
Figure 42. Functional analysis of FACS-sorted $CD34^+$ HSPCs treated with vehicle or STC1 139
Figure 43. Investigation of HSPCs treated with vehicle or STC1 in scaffold model 140
Figure 44. STC1 neutralisation in AML-HSPC co-cultures *ex vivo* 141
Figure 45. STC1 expression and neutralisation of STC1 in AML-HSPC scaffold model 143
Figure 46. Role of STC1 for ROS and mitochondrial membrane potential in MSCs 144
Figure 47. Expression of STC1 and other hypoxia-response genes is mediated by HIF-1α stabilisation. 152
Figure 48. Hypoxia-response gene expression in MSCs is caused by HIF-1α stabilisation 154
Figure 49. HIF-1α knockdown abrogates STC1 accumulation in supernatant 155
Figure 50. HIF-1α stabilisation in MSCs suppresses HSPC expansion in co-culture 156
Figure 51. HIF-1α stabilisation in MSCs suppresses HSPC expansion in co-culture 157
Figure 52. HIF-1α knockdown in MSCs ameliorates the HSPC suppression *ex vivo* 158
Figure 53. HIF-1α knockdown in MSCs ameliorates the HSPC suppression *in vivo* 159

List of Tables

Table 1. **Overview of mutations in commonly used immunodeficient mouse models** 26
Table 2. **Detailed genomic classification of AML proposed by (Papaemmanuil et al., 2016)** 29
Table 3. **Risk classifications from 2017 European LeukaemiaNet (ELN) based on genetic and molecular abnormalities adapted from (Dohner et al., 2017)** 31
Table 4. **Cell line/Primary cells and culture conditions** 64
Table 5. **Genetic abnormalities in AML patient cohort** 66
Table 6. **Antibodies** 78
Table 7. **shRNA sequences** 78
Table 8. **RT-PCR primer sequences** 78
Table 9. **AML cell lines and patient samples and their respective symbols in graphs** 85
Table 10. **Commonly up-and down-regulated putative secreted genes in MS5 exposed to AML** 133
Table 11. **Gene name, associated protein product and function obtained from Uniprot database** 133

Abbreviations

α-SMA	α-actin-2
ADP	Adenosine diphosphate
AGM	Aorta-gonad-mesonephros
AhR	Aryl hydrocarbon receptor
AKT1	AKT serine/threonine kinase 1
α-MEM	Minimum essential medium eagle - α modification
AML	Acute myeloid leukaemia
AMPK	AMP-activated protein kinase
Ara-C	Cytarabine
ASCT	Allogenic stem cell transplant
ASXL1	Additional sex combs-like 1
ATP	Adenosine triphosphate
B-ALL	B-cell acute lymphoblastic leukaemia
B/NK	B-cell/natural killer cell progenitor
BCR-ABL	Fusion gene of Abelson murine leukaemia viral oncogene homolog 1 and breakpoint cluster region
BM	Bone marrow
BMP2	Bone morphogenetic protein 2
BrdU	Bromodeoxyuridine
CAD	C-terminal activating domain
CAF	Cancer-associated fibroblast
cAMP	Cyclic adenosine monophosphate
CaR	Calcium-sensing receptor
CB	Umbilical cord blood
CBP	CREB-binding protein
CCL3	Chemokine (C-C motif) ligand 3
CD	Cluster of differentiation
cDNA	Copy Deoxyribonucleic acid
CEBPA	CCAAT enhancer-binding protein α
CFSE	Carboxyfluorescein succinimidyl ester
CFU	Colony-forming unit

CFU-F	Colony-forming unit - fibroblast
CFU-S	Colony-forming unit – spleen
CH	Clonal haematopoiesis
CLL	Chronic lymphoid leukaemia
CML	Chromic myeloid leukaemia
CMP	Common myeloid progenitor
CMV	Granulocyte-macrophage colony-stimulating factor
CO_2	Carbon dioxide
CODDD	C-terminal oxygen-dependent degradation domains
CR	Complete remission
CRi	Complete remission with incomplete blood count
CTV	Cell trace violet
CXCL4	Chemokine (C-X-C motif) ligand 4
CXCR4	CXC-motif-chemokine receptor 4
DAPI	4′,6-Diamidin-2-phenylindol
DCL	Donor cell leukaemia
dHLH	Domain helix loop helix
DMEM	Dulbecco's modified eagle's medium
DMNT3a	DNA methyltransferase 3a
DNA	Deoxyribonucleic acid
Dnase	Deoxyribonuclease
dT	Deoxythymidine
EC	Endothelial cells
EdU	5-Ethynyl-2′-deoxyuridine
EFS	Event-free survival
Egr 1-3	Early growth response 1-3
EMP	Erythromyelo-progenitors
EPAS1	Endothelial PAS domain protein 1
EPAS1	HIF prolyl hydroxylase
EPO	Erythropoietin
ER	Endoplasmic reticulum
ERK1/2	Extracellular signal–regulated kinases
ETP	Immature lymphoid progenitors

FA	Fatty acids
FABP4	Fatty acid binding protein 4
FACS	Fluorescence assisted cell sorting
FAP	Fibroblast activation protein α
FBS	Foetal bovine Serum
FCCP	Carbonyl cyanide 4-(trifluoromethoxy) phenylhydrazone
Fgd5	FYVE, RhoGEF And PH Domain Containing 5
FIH	Factor-inhibiting HIF1a
FKBP1A	Peptidyl-prolyl cis-trans isomerase
FL	Foetal liver
FLT3	Fms like tyrosine kinase 3
FLT3-ITD	FMS-like tyrosine kinase 3 internal tandem duplication
FLT3L	FMS-like tyrosine kinase 3 ligand
G-CSF	Granulocyte-colony stimulating factor
GDF15	Growth/differentiation factor 15
GLUT1	Glucose transporter 1
GM-CSF	Granulocyte-macrophage colony-stimulating factor
GMP	Granulocyte-monocyte progenitors
HBSS	Hanks' balanced salt solution
HDAC	Histone deacetylase
HEPES	(4-(2-hydroxyethyl)-1-piperazineethanesulfonic acid)
HES1	Hes Family BHLH transcription factor 1
HEY1	Hairy/enhancer-of-split related with YRPW motif protein 1
HIF	Hypoxia-inducible factors
HLH	Helix-loop-helix
HMOX1	Heme oxygenase (decycling) 1
HRE	Hypoxia response elements
HSC	Haematopoietic stem cell
HSPC	Haematopoietic stem and progenitor cells
IDH1/2	Isocitrate dehydrogenase 1
IGF	Insulin-like growth factor
IGF-BP	Insulin-like growth factor - binding protein
IκBα	Nuclear factor of κ light polypeptide gene enhancer in B-cells inhibitor, α

IL-15	Interleukine-15
IL-2	Interleukine-2
IL-21	Interleukine-21
IL-3	Interleukine-3
IL-4	Interleukine-4
IL-7	Inteleukine-7
IL-9	Interleukine-9
IL-1α/β	Interleukine-1 α/β
IL-2Rγ	Interleukine-2 Receptor common γ chain
IL-3	Interleukine-3
IL-7R	Interleukine-7 receptor
IP	Intraperitoneal
IS	Intra-scaffold
IV	Intravenously
JAK2	Janus Kinase 2
Ki67	Antigen identified by monoclonal antibody Ki-67
KO	Knockout
KRAS	Kirsten rat sarcoma 2 viral oncogene homolog
LDHA	Lactate dehydrogenase A
LepR	Leptin receptor
LIC	Leukaemia initiating cells
Lin	Lineage marker
LT-HSC	Long-term haematopoietic stem cell
LTC-IC	Long-term cell - initiation cell
MAPK	Mitogen-activated protein kinase
MDS	Myelodysplastic syndrome
MEF	Mouse embryonic fibroblast
MEIS1	Homeobox protein Meis1
MEP	Megakaryocyte-erythrocyte progenitors
MIB1	E3 ubiquitin-protein ligase
MLL-AF9	Acute lymphoblastic leukaemia 1
MLP	Immature lymphoid progenitors
mmHg	Millimetre of mercury or Torr

MOI	Multiplicity of infection
MPN	Myeloproliferative neoplasm
MPP	Multipotent progenitor cells
MRS	Minimal residual disease
MSCs	Mesenchymal stroma cells
mTOR	Mechanistic target of rapamycin
MYC	MYC proto-oncogene
N-MSCs	Healthy donor MSCs
NAD	Nicotinamide adenine dinucleotide (oxidized)
NADH	Nicotinamide adenine dinucleotide (reduced)
NF-κB	Nuclear factor 'κ-light-chain-enhancer' of activated B-cells
NK-Cell	Natural killer cell
NO	Nitric oxide
NOD	Non-obese diabetic
NODDD	N-terminal oxygen-dependent degradation domains
NPM1	Nucleophosmin 1
NRAS	Neuroblastoma RAS viral oncogene homolog
NSG	NOD-scid IL-2R γ null
O_2	Oxygen
OCR	Oxygen consumption rate
ON	Overnight
OS	Overall survival
OXPHOS	Oxidative phosphorylation
P/S	Penicillin/Streptomycin
PAPP-A	Pregnancy-associated plasma protein A
PAS	Per-Arnt-Sim
PBS	Phosphate-buffered saline
PDGF	Platelet-derived growth factor
PDK1	Phosphoinositide-dependent kinase-1
PDZK1IP1	PDZK1-interacting protein 1
PFA	Paraformaldehyde
PI	Propidium Iodide
PI3K	Phosphoinositide 3-kinase

PKA	Protein kinase A
PTPN11	Protein tyrosine phosphatase, non-receptor type 11
PPAR-γ	Peroxisome proliferator-activated receptor γ
PPM1D	Protein phosphatase, $Mg2^{+}$/$Mn2^{+}$ dependent 1D
PRKDC	Protein kinase, DNA-activated, catalytic subunit
ProB	Pro B-Cell
RANKL	Receptor activator of NF-κB ligand
RARγ	Retinoic acid receptors γ
RAS	Rat sarcoma gene
RBPJk	Recombining binding protein suppressor of hairless
ROS	Reactive oxygen species
RPL18A	Ribosomal protein L18a
RPMI 1640	Roswell Park memorial institute
RT	Room temperature
RUNX1	Runt-related transcription factor 1
S6K1	Ribosomal protein S6 kinase beta-1
SCA-1	Stem cell antigen-1
SCF	Stem cell factor
SCID	Severe combined immune deficiency
SCN	Stem cell niche
SDF1	Stroma derived factor 1
SEM	Standard error of the mean
SF3B1	Splicing factor 3B subunit 1
SIRPα	Signal regulatory protein α
SIRT1	Sirtuin1
SMAD	Mothers against decapentaplegic homolog 2
SMC3	Structural maintenance of chromosomes protein 3
SOD2	Superoxide dismutase 2
SRSF2	Serine and arginine rich splicing factor 2
ST-HSC	Short term haematopoietic stem cell
STAG2	Stromal antigen 2
STAT	Signal transducers and activators of transcription
STC	Stanniocalcin

STIM1	Stromal interaction molecule 1
STR	Short tandem repeat
T-ALL	T-Cell acute lymphoblastic leukaemia
TET2	Tet methylcytosine dioxygenase 2
TGF-β1	Transforming growth factor β 1
TH	Tyrosine hydroxylase
TIE2	Angiopoietin-1 receptor
TMRE	Tetramethylrhodamine, ethyl ester
TNF-α	Tumour necrosis factor α
TP53	Tumour protein 53
TPO	Thrombopoietin
TRAP	Tartrate-resistant acid phosphatase
U2AF1	U2 small nuclear RNA auxiliary factor 1
UCP2	Uncoupling protein 2
VEGF-A	Vascular endothelial growth factor - A
VHL	Von Hippel-Lindau protein complex
VLA-4	Very late antigen-4
WHO	World health organisation
WNT	Wingless-type MMTV integration site Family, member 1
WT1	Wilms tumour 1

Chapter 1. Introduction

1.1 Normal Haematopoiesis

Since ancient times blood signifies the bearer of life. In Germanic and Greek mythology, humans were created from the blood of gods and religions like Judaism, and Christianity treat blood as the symbol of a person's soul. Nowadays, charming and handsome vampires are perpetuating the fascination for blood into the 21st century and probably beyond.

Today's scientific perception of blood has come a long way, but our understanding is far from complete. Blood is a genuinely multitasking tissue. To name a few of its many functions, it transports nutrients and signalling molecules throughout the body, coagulation factors and platelets to prevent haemorrhage, erythrocytes carrying oxygen (O_2) and carbon dioxide (CO_2) allowing respiration and cells of the innate and adaptive immune system, which circle the body scouting for pathogens. The average human adult has around 5 litres of blood, of which each ml consists of 4.1-5.9x10^9 erythrocytes, 0.8-3.2x10^6 leukocytes and 150-400x10^6 platelets (Dean, 2005; Sharma and Sharma, 2018). More than 99,9999 % of these cells are fully differentiated and except specific immune cells unable to re-initiated proliferation. Additionally, studies of leukocyte kinetics and half-life determined that most haematopoietic cells have a limited lifespan ranging from several months to a few hours (Athens et al., 1961; Franco, 2012; Fulcher and Basten, 1997). This means that an estimated 1012 cells need to be replenished every day through a pyramid-shaped hierarchy of haematopoietic stem and progenitor cells (HSPCs) (Doulatov et al., 2012). The top of the pyramid is colonized by a small number of haematopoietic stem cells (HSCs) capable of generating differentiated cells of all lineages and giving rise to other HSCs throughout a lifetime (Bhatia et al., 1998; Eaves, 2015; Notta et al., 2011). However, the lion's share of regeneration is performed downstream of HSCs by a complex layer of rapidly dividing progenitors whose multi-lineage potential and self-renewal capacity decrease as they differentiate.

1.1.1 The origins of haematopoiesis

The first haematopoietic cells are formed at multiple locations during several haematopoietic waves during mammalian development. Once the growing embryo becomes too large to rely on oxygen diffusion, the first emergence called "primitive" wave of non-self-renewing primitive erythrocytes, macrophages and megakaryocytes takes place in the blood islands of

the extra-embryonic yolk sac (Palis et al., 1999; Tober et al., 2007). Subsequently, a second pro-definitive wave of erythromyelo-progenitors (EMP) ensures further erythromyelopoiesis and are the origin for an HSC-independent population of tissue-resident macrophages in the adult (Dzierzak and Bigas, 2018; Gomez Perdiguero et al., 2015). The emergence of HSCs termed the “definitive” wave, marks the onset of a haematopoietic system driven by self-renewing HSCs (Pei et al., 2017). Specialised hemogenic endothelial cells give rise to the first HSCs when they transition from an endothelial to a haematopoietic state in the dorsal aorta of the aorta-gonad-mesonephros (AGM) region of the embryo (Medvinsky and Dzierzak, 1996; Muller et al., 1994; Swiers et al., 2013). More HSCs are found in the placenta and the umbilical arteries and from a wave of definitive haematopoiesis in the yolk sac (Hirschi, 2012). Afterwards, these HSCs are combined as they lead a nomadic existence migrating from their site of origin to the foetal liver (FL) before they ultimately settle in the neonatal bone marrow (Orkin and Zon, 2008).

HSCs from different stages of ontogeny show distinct self-renewal, proliferation and lineage bias which is governed by distinct transcriptional programs. From the FL stage to shortly after birth, the HSC pool expands drastically and generates a complete HSPC hierarchy (Bowie et al., 2007; Morrison et al., 1995). On the contrary, adult bone marrow (BM) HSCs retain the ability to expand, but the majority lays dormant and cycles on average once every 175-350 day (Catlin et al., 2011; Wilson et al., 2008). Additionally, the proportion of HSCs with predominantly myeloid lineage output (termed myeloid biased) is higher and further increases with ageing (Gekas and Graf, 2013).

An intermediary HSC, which rose to primary clinical importance in recent year for bone marrow transplantation, is found in the umbilical cord blood (CB). Furthermore, CB HSCs are essential to study human HSCs since the minimally invasive collection of CB during childbirth provides large numbers of HSCs. CB HSCs are similar to their BM counterparts regarding quiescence and multipotency but enter cell cycle more readily in response to cytokines ex vivo and reconstitute immune-deficient mice more potently (da Silva et al., 2009; Hao et al., 1995; Lansdorp et al., 1993; Ueda et al., 2001).

1.1.2 Adult haematopoiesis

1.1.2.1 Haematopoietic stem cells

The study of adult HSPCs took off as a consequence of the atomic age when Jacobson et al. showed that transplantation of BM from a non-irradiated donor could rescue the lethal myeloablation caused by radiation by regenerating and sustaining a chimeric haematopoietic system (Ford et al., 1956; Jacobson et al., 1951). The first multipotent, self-renewing HSPCs were observed in colonies which appeared 9-14 days after BM transplantation along the spleens of the recipient mice, termed colony-forming unit – spleen or CFU-S (Siminovitch et al., 1963; Till and Mc, 1961; Wu et al., 1968). In the following decades, more sensitive ex vivo and in vivo repopulation assays were developed proving the existence of HSC down to the single-cell level (Ito et al., 2002; Osawa et al., 1996; Waskow et al., 2009). This data suggests that under steady-state conditions, HSCs reside in a quiescent, autophagy-dependent, glycolytic state with reduced mitochondrial and protein translation activity compared to its progeny to ensure long-term self-renewal (Laurenti and Gottgens, 2018).
In the mouse, several multi-lineage progenitor populations termed multipotent progenitor cells (MPPs), and short-term HSC (ST-HSC) were characterized down-stream of HSCs. These cell types are capable of multi-lineage repopulation but only spanning over a limited time. To distinguish true HSCs with continuous self-renewal during serial repopulation, the expression long-term HSCs (LT-HSCs) was coined (Doulatov et al., 2012; Morrison and Weissman, 1994). However, even among this stringently selected population heterogeneity exist. When measured under single-cell transplantation settings, LT-HSCs can vary extensively in their lineage output, making them highly biased for lymphoid or myeloid lineages (Oguro et al., 2013). When injected as a pool, the attribution of cells to individual LT-HSCs also shows considerable differences in their overall contribution to haematopoiesis. Interestingly, several studies demonstrated that heterogeneity is not a cause of random differentiation events guided by extrinsic factors because the progeny of those individual LT-HSCs carried the same biased behaviour as their parents (Dykstra et al., 2007; Muller-Sieburg et al., 2002; Yu et al., 2017). Yu et al. suggests that a conserved epigenetic memory in HSCs underlies the heterogenic clonal behaviour (Yu et al., 2017). Still, the origin for the heterogeneity is only partially understood. For instance, myeloid-biased HSCs lack expression of Interleukine-7 receptor (IL7R) making them irresponsive to lymphoid differentiation signals, but the origin and causality of their existence are currently unknown (Muller-Sieburg et al., 2004). A clue may come from the emergence of HSCs at different

locations and times since the pool of those HSCs in the FL already shows heterogeneity (Benz et al., 2012).

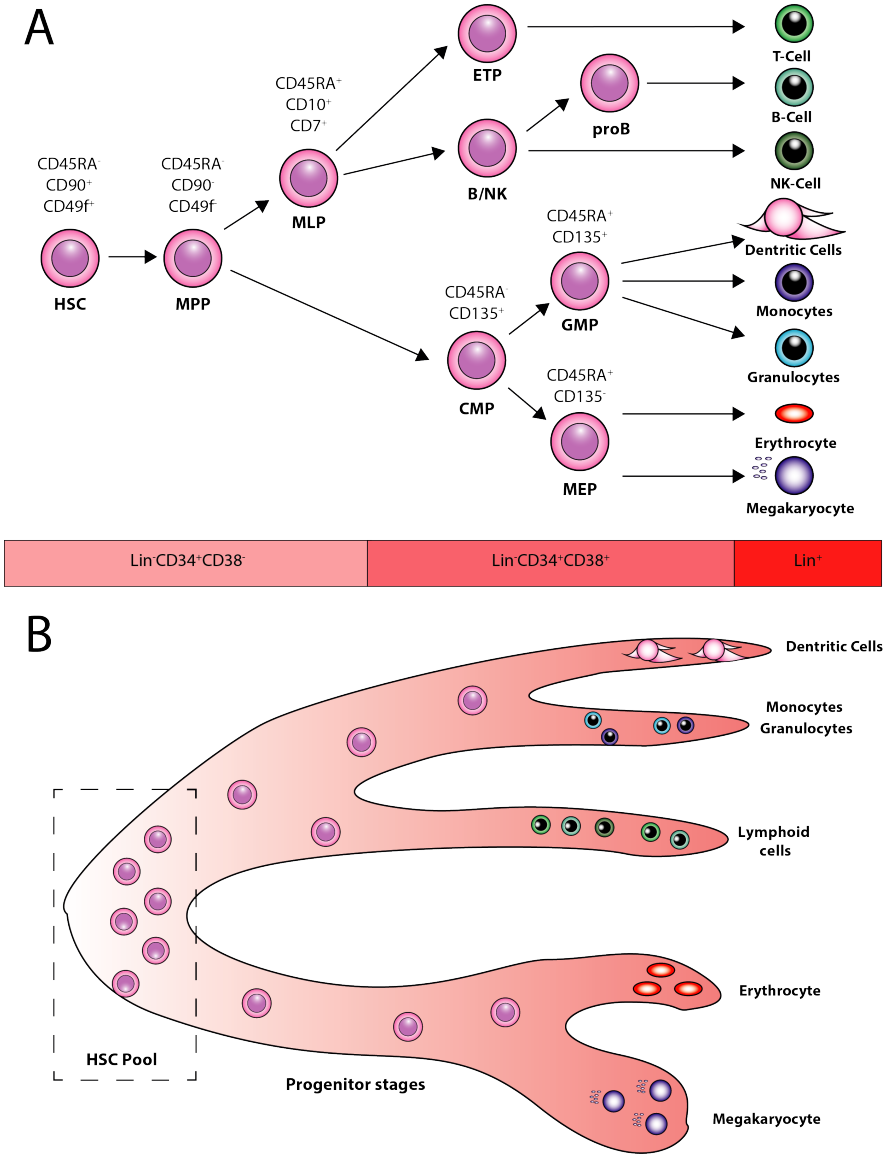


Figure 1. The human haematopoietic hierarchy. Adapted from (Doulatov et al., 2012) and (Laurenti and Gottgens, 2018)
(A) Classical model of haematopoietic lineage commitment and HSPC phenotype **(B)** Current proposed model of continuous differentiation with early lineage commitment

The majority of evidence about adult HSCs is derived from transplantation studies but in a steady-state system HSCs divide every 175-350 days (Catlin et al., 2011; Wilson et al., 2008) and extensive proliferation exhausts HSCs (Baumgartner et al., 2018; Bernitz et al., 2016). Hence the extent to which quiescent HSCs contribute to adult haematopoiesis is still controversial. Several groups have addressed this question in the mouse haematopoietic system with contradicting results by measuring the HSC-specific output through CRE-based fluorescent or genetic barcoding under an HSC-specific promoter like *Krt18*, *Fgd5*, *Pdzk1ip1*

or *Tie2* promoters (Busch et al., 2015; Chapple et al., 2018; Sawai et al., 2016). The fluorescent label from *FGD5*, *Krt18* and *Pdzk1ip1* HSC could be detected after a few weeks and were at equilibrium between HSC and downstream compartments 26 weeks after recombination (Chapple et al., 2018; Sawai et al., 2016). On the contrary, while *Tie2* driven label was found extensively throughout the haematopoietic system when labelled at E10.5, labelling in the adult resulted in far slower equilibration and would have exceeded the lifetime of a mouse (Busch et al., 2015). Tie2 expression marks a subgroup of HSCs with excellent repopulation capacity but which is mainly quiescent in the adult (Ito et al., 2016). Other promoters like *Fgd5* or *Krt18* may label different more active subsets among the heterogeneous LT-HSCs.

Evidence against HSC-driven haematopoiesis also comes from the Camargo lab who clonally traced the fate of HSPCs by tagging randomly integrated transposons (Rodriguez-Fraticelli et al., 2018; Sun et al., 2014). Sun et al. and Rodriguez-Fraticelli et al. suggest that haematopoiesis mainly originates from many transiently active clones of uni- and oligo-lineage potent MPPs while LT-HSCs can bypass the MPP stage and predominantly produce megakaryocytes progenitors (Rodriguez-Fraticelli et al., 2018; Sun et al., 2014). However, one of the most striking observations comes from mice in which the ablation of over 90 % of HSPCs in mice proved insufficient to affect haematopoietic parameters at steady-state. Even though LT-HSCs remained depleted throughout the experiment, progenitors quickly recovered to normal levels. In fact, haematopoietic stress conditions like anaemia and infection but not severe myeloablation with 5-fluorouracil were well tolerated by the mice (Schoedel et al., 2016).

Together these observations show that during steady-state clusters of activated HSCs/MPPs retain extensive self-renewal when unchallenged and form the spearhead of adult haematopoiesis. This allows a subset of HSCs to remain dormant and hence limiting their contribution to naïve haematopoiesis but providing a back-up system when severely challenged.

1.1.2.2 MPPs and downstream progenitors

In the classical haematopoietic hierarchy, differentiation occurs along a progressive loss of self-renewal and multilineage potential from multipotent HSCs to MPPs to oligopotent progenitors. The two major branches, lymphoid and myeloid, diverge very early on and only LT-HSCs and a few downstream progenitors called MPPs, are capable of dual-lineage output

(Pei et al., 2017). Similar to LT-HSCs, MPPs are heterogeneous regarding lineage fate and three subclasses of murine MPPs have been assigned via transplantation experiments. MPP2 and MPP3 comprise a class of myeloid-biased MPPs with additional megakaryocyte potential in MPP2. Lastly, MPP4 can be distinguished from MPP2/3 through Flt3 expression and initially gives rise to mixed lineage output and switches to exclusively lymphoid later on. Interestingly, MPPs do hold some self-renewal potential in transplantation assays but were shown to exhaust after 4-8 weeks (Pietras et al., 2015).

Shortly after MPPs the haematopoietic progenitors ultimately split into lymphoid and myeloid systems. The common lymphoid progenitor is the earliest lymphoid progenitor and further diverges into B- and T- cell-specific progenitor stages. The classical haematopoietic hierarchy model further divides the myeloid side into a common myeloid progenitor (CMP) downstream of MPPs, which branches into megakaryocyte-erythrocyte progenitors (MEP) and granulocyte-monocyte progenitors (GMPs) (Doulatov et al., 2012) (Figure 1A).

However, several reports over recent years have put the classical model into question. Under specific conditions, differentiation pathways outside the classical model may occur, and HSCs can bypass the MPP stages to produce lineage-committed myeloid (Yamamoto et al., 2013), erythroid (Singh et al., 2018) or megakaryocyte progenitors (Rodriguez-Fraticelli et al., 2018). Interestingly, while in steady-state HSCs predominantly generate megakaryocyte/platelet output, but after transplantation Rodriguez-Fraticelli et al. found that HSCs revert to a multilineage output again (Rodriguez-Fraticelli et al., 2018).

Single-cell investigations highlight that not lymphoid-myeloid commitment represents the first lineage commitment step but rather branches into megakaryocyte/erythrocyte and lympho-myeloid differentiation. Myeloid/erythroid/megakaryocyte differentiation was previously believed to originate from a common-myeloid progenitor but also experiments with human HSPCs have shown that mixed-lineage output of single progenitors like CMPs, GMPs and MEPs is merely present during foetal development. In adults multilineage output and megakaryocyte production does not pass the MPP stage and downstream progenitors are a pool of already strictly uni-lineage committed cells (Notta et al., 2016). This implies that linage commitment and choice may already occur upstream of these progenitor populations at very early stages of differentiation (Figure 1B) (Laurenti and Gottgens, 2018).

1.1.2.3 Immunophenotypic HSCs

One problem that HSC research had to overcome was the scarcity of HSCs in the BM. Similar to mature haematopoietic cells, which express different cell surface proteins depending on their lineage, the expression or absence of specific cell surface proteins have been utilised to create marker combinations that detect or at least enrich HSPCs. In humans, cells immunophenotypically characterized as Lineage marker^{-}CD34^{+}CD38^{-}CD45RA^{-} CD90^{+}CD49f^{+} are currently the most HSC enriched fraction with frequency of 1 HSC in 10 cells (Notta et al., 2011). The marker combinations are poorly conserved throughout evolution, and therefore mouse HSCs are isolated with a different combination of Lineage$^{-/low}$Sca-1^{+}c-Kit^{+}CD34^{-}CD150^{+}CD48$^{-/low}$ to a purity of 1 in 2 (Kiel et al., 2005; Yamamoto et al., 2018). Interestingly, many cell surface markers do not contribute to the functional properties of HSCs (Eaves, 2015). In the murine system, HSCs can be studied in special genetic reporter mice that express a fluorescent protein from a genetic locus exclusively expressed in HSCs. This approach drastically expands the repertoire of selection markers to include markers with relevance to HSC functionality. Examples are *Tie2*, *Fgd5* and *Pdzk1ip1, Hoxb5 and Krt18* (Chapple et al., 2018; Chen et al., 2016; Gazit et al., 2014; Ito et al., 2016; Sawai et al., 2016).

1.2 Assays to analyse HSPCs

1.2.1 Mouse models

In order to study HSCs, one needs to determine what defines a stem cell. For HSCs this means to reconstitute all lineage of the blood and show long-term self-renewal. By today's gold standard HSCs must generate myeloid and lymphoid output (multi-lineage potential) in two consecutive transplantations into mice, each 16-week long (long-term self-renewal) (Doulatov et al., 2012; Eaves, 2015). The most sensitive mouse recipient for human normal and malignant HSPCs is the NOD-scid IL2Rγnull (NSG) mouse because its severe immunodeficiency renders it incapable of rejecting non-self-tissue (Ito et al., 2002). The NSG mouse (Table 1) harbours several genetic mutations and polymorphisms and therefore lacks functional T- and B-lymphocytes (*PRKDC^{scid}*), natural killer (NK) cells (*IL2Rγ^{tm1Wjl}*), compromised functionally of the complement system, macrophages and dendritic cells (NOD polygenic background).

In recent years two additional variants of the NSG model have been established and widened its sensitivity. Firstly, the integration of a CMV-promoter driven overexpression of human IL-3, GM-CSF and SCF in the NSG mouse named NSG-SGM3 to drive myeloid engraftment at the expense of long-term self-renewal. This modification has been especially successful in the field of myeloid leukaemias (Wunderlich et al., 2010).
The second variant emerged from the necessity to sub-lethally irradiate recipient mice to remove endogenous HSPCs from their BM niches which facilitates human engraftment but also severely impedes the supportiveness of the niche cells. This trade-off was recently overcome in *Kit* mutant mice, which allow human HSPCs to engraft without the need of conditioning the recipient mice (McIntosh et al., 2015; Waskow et al., 2009).

Table 1. Overview of mutations in commonly used immunodeficient mouse models

Mouse Model	Mutation/ Background	Function	Immunodeficiency
NSG	NOD/Lt	**Polygenic**, Polymorphism in ***Sirpa*** allows binding to human CD47 and inhibition of phagocytosis (Shultz et al., 1995; Takenaka et al., 2007)	Functional deficits of NK and APC, Absence of circulating complement
	Prkdc^{scid}	**Protein kinase, DNA-activated, catalytic subunit**: Defective V(D)J recombination and DNA double-stranded break repair (Blunt et al., 1995; Bosma et al., 1983)	Loss of B and T cells
	Il2rg^{tm1Wjl}	**Interleukine-2 Receptor common γ chain**: critical component for IL-2, IL-4, IL-7, IL-9, IL-15, and IL-21 signalling(Ito et al., 2002)	Loss of B, T, and NK cells
NSG-SGM3	NSG background with *SCF/IL3/GM-CSF* Transgene	CMV promoter driven overexpression of ***human Stem cell factor (SCF), Interleukine-3 (IL-3)*** **and** ***granulocyte-macrophage colony-stimulating factor (GM-CSF)*** **(Feuring-Buske et al., 2003)**	None
NSG-W41/W41	NSG background with *Kit*$^{W-41J}$	**Missense mutation in kinase domain of *CD117* (McIntosh et al., 2015; Waskow et al., 2009)**	Competitive advantage of wild-type HSCs, engraftment without irradiation

1.2.2 *Ex vivo* models

Alongside the *in vivo* models, several ex-vivo assays exist; the long-term cell - initiation cell assay (LTC-IC-Assay) and the colony-forming unit-assay (CFU-assay). In the CFU-assay cells grow in a cytokine supplemented semi-solid media to determine clonal colony-forming potential and lineage distribution along the erythromyelopoietic lineage after 7-14 days (Bradley and Metcalf, 1966). The CFU-assay mainly reveals committed progenitors,

especially during the first plating, but secondary and tertiary plating can determine more immature progenitors. The LTC-IC is a two-part assay consisting of a long-term (> 5 weeks) culture on an irradiated stroma support layer and a subsequent CFU-assay. This allows to determine the frequency of immature progenitors, which, contrary to committed progenitors, retain colony-forming potential even after long culture (Islam et al., 1989).

1.2.3 Humanised niche models

Humanised niche models have been developed to study niche development and interactions with normal and malignant haematopoietic cells. Fresh bone tissue as graft can provide osteogenic cells and osteoinductive signals to support bone-healing processes after injury. Implanted outside of bone, bone structures, comprising mature bone tissue and remarkably BM, are formed. Since the development of these so-called ossicles, several other extramedullary niche versions were proposed and investigated. The most recent versions contain human primary mesenchymal stroma cells (MSCs) alone, or together with endothelial cells (EC). MSCs, undifferentiated or differentiated into osteoblasts, adipocytes or chondrocytes establish a humanised niche to support healthy and malignant haematopoiesis. Furthermore, MSCs induce the formation of sinusoidal vasculature to provide critical niche-derived haematopoietic cytokines like angiopoietin-1, SDF1 and SCF.
Niche cells can either be pre-seeded on an extracellular-matrix carrier-material like collagen, providing a scaffold to grow on and subcutaneously transplanted into immune-deficient mice or co-injected alongside a gelatinous protein mixture generated by mouse sarcoma cells called matrigel. Subsequently, further bone formation can, but not necessarily has to be facilitated by administration of osteoinductive factors like bone-morphogenic protein 2 (BMP2) or parathyroid hormone (PTH). Similarly to mouse bone marrow, the humanised niches provides sufficient support to allow human haematopoiesis and maintain HSPCs capable of secondary engraftment (Abarrategi et al., 2017). Furthermore, malignant haematopoiesis like AML or MDS can also be studied in extramedullary niches. Abarrategi et al. and Reinisch et al. further developed this approach as tools to study AML samples with low or delayed xenotransplantation ability. (Abarrategi et al., 2017; Antonelli et al., 2016; Reinisch et al., 2016). The benefits of the humanised niche compared to the residual murine BM niche is the avoidance of the mouse-human species, which proved to be advantages, especially in cases of poorly engrafting leukaemic samples. Furthermore, the necessity of

specific niche elements at the cellular and molecular levels can be interrogated more quickly compared to knockout mice.

1.3 Acute myeloid leukaemia

Acute myeloid leukaemia (AML) is an aggressive cancer originating in the myeloid compartment and comprises the majority of adult acute leukaemias (Yamamoto and Goodman, 2008). The clinical manifestations of AML like fatigue, anaemia, bleeding disorders and frequent infections are a consequence of the accumulation (>20 %) of a clonal population of myeloid progenitors with abnormal proliferation and differentiation in the bone marrow, blood, spleen and infrequently other non-haematopoietic organs like central nervous system (De Kouchkovsky and Abdul-Hay, 2016; Viadana et al., 1978). Based on aetiology, AML may develop after exposure to chemo-radiotherapy (therapy-related AML), from a pre-existing haematopoietic malignancy like myelodysplastic syndrome (MDS) (secondary AML) or like the majority of AML, de novo (de novo AML) (Saultz and Garzon, 2016). Morbidity rate and adverse outcome are strongly correlated with patient age. While 35-40 % of AML patients with 60 or fewer years are cured, the cure rate in older patients above 60 years remains at a highly unsatisfactory level of 5-10% (Dohner et al., 2015; Saultz and Garzon, 2016).

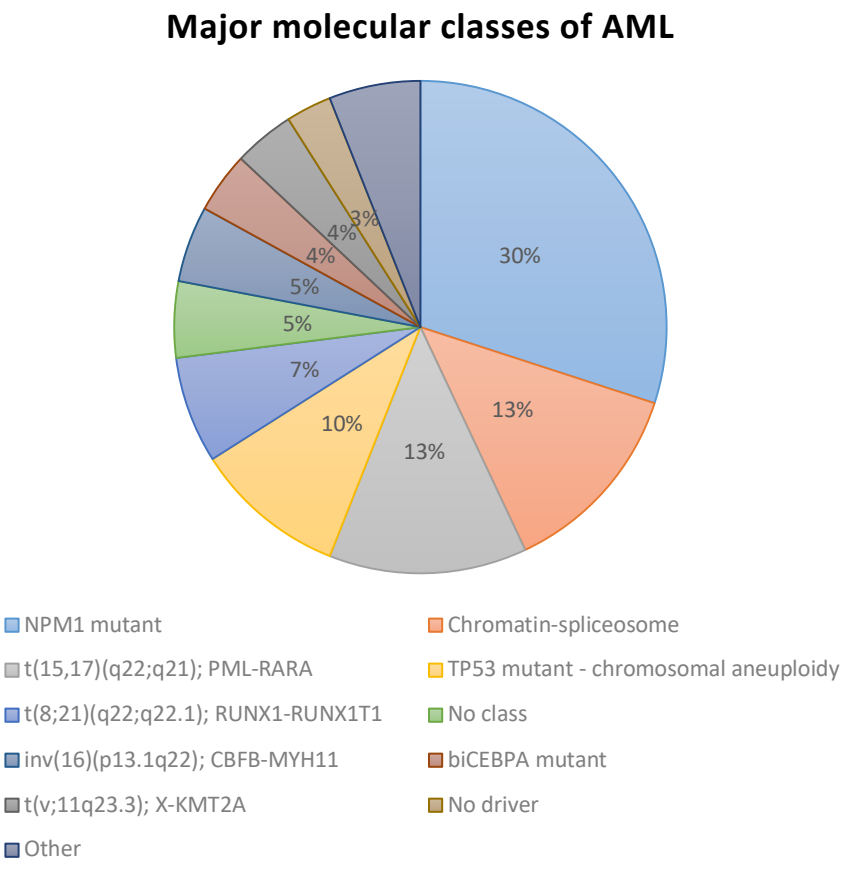


Figure 2. Molecular classes of AML with frequency (>1 %); adapted from (Dohner et al., 2017)

Table 2. Detailed genomic classification of AML proposed by (Papaemmanuil et al., 2016)

Genomic Subgroup	Frequency in the study cohort (%)	Most frequently mutated genes (%)
AML with NPM1 mutation	27	*NPM1* (100), *DNMT3A* (54), *FLT3*^{ITD} (39), *NRAS* (19), *TET2* (16), *PTPN11* (15)
AML with mutated chromatin, RNA-splicing genes, or both	18	*RUNX1* (39), *MLL*^{PTD} (25), *SRSF2* (22), *DNMT3A* (20), *ASXL1* (17), *STAG2* (16), *NRAS* (16), *TET2* (15), *FLT3*^{ITD} (15)
AML with TP53 mutation, chromosomal aneuploidy, or both	13	Complex karyotype (68), *-5/5q* (47), *-7/7q* (44), *TP53* (44), *-17/17p* (31), *-12/12p* (17), *+8/8q* (16)
AML with inv(16)(p13.1q22) or t(16;16)(p13.1;q22); CBFB-MYH11	5	*inv(16)* (100), *NRAS* (53), *+8/8q* (16), +22 (16), *KIT* (15), *FLT3*^{TKD} (15)
AML with biallelic CEBPA mutations	4	*CEBPA*^{biallelic} (100), *NRAS* (30), *WT1* (21), *GATA2* (20)
AML with t(15;17)(q22;q22); RUNX1-RUNX1	4	*t(8;21)* (100), *KIT* (38), *-Y* (33), *-9q* (18)
AML with MLL fusion genes; t(x;11)(x;q23)	3	*t(x;11q23)* (100) *NRAS* (23)

AML with inv(3)(q21q26.2) or t(3;3)(q21;q26.2); GATA2, MECOM(EVI1)	1	*Inv(3)* (100), *-7* (85), *KRAS* (30), *NRAS* (30), *PTPN11* (30), *ETV6* (15), *PHF6* (15), *SF3B1* (15)
AML with IDH2^{R172} mutation and no other class-defining lesions	1	*IDH2^{R172}* (100), *DNMT3A* (67), *+8/8q* (17)
AML with t(6;9)p23;q34); DEK-NUP214	1	*T(6;9)* (100), *FLT3^{ITD}* (80), *KRAS* (20)
AML with driver mutations but no detected class-defining lesions	1	*FLT3^{ITD}* (39=, *DNMT3A* (16)
AML with no detected driver mutations	4	
AML meeting criteria for 2 genomic subgroups	4	

1.3.1 Classification and outcome stratification

Formerly AML was classified based merely on morphology under the French-American-British classification system. More recent classifications like the WHO classification system, incorporate chromosomal and genetic abnormalities with morphology, immunophenotype and clinical presentation of AMLs and related neoplasms. The combination of the cytogenetic profile and molecular abnormalities further guide the stratification of AML patients into favourable, intermediate and adverse prognosis classes and influences therapy decisions (Table 2-3 and Figure 2) (Arber et al., 2016; Dohner et al., 2017; Papaemmanuil et al., 2016). Non-random chromosomal abnormalities account for 52 % of AML cases and were early on attributed as crucial disease initiation and driving factors. Chromosomal translocations or inversions fuse the N- and C-terminal domains, of which one is always a DNA-binding motif, of two independent genes to generate novel hybrid proteins. Inversions on chromosome 16, *AML1/ETO* and *PML/RARA* exemplify chromosomal rearrangements of favourable prognostic value while translocations of 11q and complex karyotypes (>3 chromosomal without genetic abnormalities) largely predicts adverse outcome (Saultz and Garzon, 2016).

Risk Profile	Subset
Favourable	t(8;21)(q22;q22.1); *RUNX1-RUNX1T1*
	inv(16)(p13.1q22) or t(16;16)(p13.1;q22); *CBFB-MYH11*
	Mutated *NPM1* without *FLT3*-ITD or with *FLT3*-ITDlow
	Biallelic mutated *CEBPA*
Intermediate	Mutated *NPM1* and *FLT3*-ITDhigh
	Wild-type *NPM1* without *FLT3*-ITD or with *FLT3*-ITDlow (without adverse-risk genetic lesions)
	t(9;11)(p21.3;q23.3); *MLLT3-KMT2A*

	Cytogenetic abnormalities not classified as favourable or adverse
Adverse	t(6;9)(p23;q34.1); *DEK-NUP214*
	t(v;11q23.3); *KMT2A* rearranged
	t(9;22)(q34.1;q11.2); *BCR-ABL1*
	inv(3)(q21.3q26.2) or t(3;3)(q21.3;q26.2); *GATA2,MECOM(EVI1)*
	−5 or del(5q); −7; −17/abn(17p)
	Complex karyotype, monosomal karyotype
	Wild-type *NPM1* and *FLT3*-ITDhigh
	Mutated *RUNX1*
	Mutated *ASXL1*
	Mutated *TP53*

Table 3. Risk classifications from 2017 European LeukaemiaNet (ELN) based on genetic and molecular abnormalities adapted from (Dohner et al., 2017)

A normal karyotype (CN) is present in nearly half of AML patients, but the advancement of next-generation sequencing led to the discovery of several gene specific abnormalities (Medinger et al., 2016; Tyner et al., 2018). On average, 13 mutations are found in AML with CN, of which merely 5 are recurrent driver mutations (Saultz and Garzon, 2016). Mutations occur in epigenetic regulators (*DMNT3a, TET2, IDH1/2, ASXL1*), nucleophosmin (*NPM1*) signalling transducers (*FLT3, NRAS, KRAS, JAK2, KIT*), myeloid transcription factors (*RUNX1, CEBPA*) and tumour suppressor genes (TP53, WT1) (Arber et al., 2016; Cancer Genome Atlas Research et al., 2013). Furthermore, spliceosome (*SF3B1, U2AF1, SRSF2*) and somatic cohesion complex (*STAG2 and SMC3*) mutations are observed frequently and indicative of a pre-existing haematopoietic disorder like MDS (Saultz and Garzon, 2016).

1.3.2 Clonal haematopoiesis

Clonal haematopoiesis (CH) is an age-related haematopoietic condition which occurs when individual HSCs clonally expand, and a significant proportion of mature haematopoietic cells can be traced back to this single clonal source (Bowman et al., 2018). Often these HSCs carry mutations in AML-related epigenetic regulators like *DMNT3a*, *TET2* or *ASXL1* (Zink et al., 2017). According to the two-hit model, AML develops from at least one mutations in two classes of genes: pro-proliferative (I), haematopoietic regulators (II) or epigenetic regulators (III) but since the mutation in class III is inflicted prior to AML development these HSCs were termed pre-leukaemic HSCs (Gilliland and Griffin, 2002; Shlush et al., 2014). Shlush et al. found pre-leukaemic HSCs to produce multilineage engraftment in NSG recipients and remain in the BM after AML treatment (Shlush et al., 2014). Interestingly, recent evidence

from Zink et al. using microsatellite clonal tracing indicates that CH as an almost inevitable consequence of ageing and can also appears in the absence of AML-related mutations (Zink et al., 2017). Specific selection pressures like ageing-related replication stress or AML-unrelated exposure to chemotherapy allows pre-leukaemic HSCs to outcompete their wild-type counterparts (Bowman et al., 2018; Coombs et al., 2017). In the mouse model, loss-of-function mutations in *TET2* and *DMNT3a* convey increased self-renewal in HSCs during serial transplantation (Challen et al., 2011; Moran-Crusio et al., 2011). Additionally, *DMNT3a* R882, a specific point mutation, and *PPM1D* mutations increase the resistance of murine HSCs to alkylating agents and cisplatin, respectively and are commonly found in therapy-related AML (Guryanova et al., 2016; Hsu et al., 2018).
Individuals with CH only show limited alterations in haematopoietic parameters and often go clinically unnoticed (Buscarlet et al., 2017). Statistically, CH elevates the mortality rate, which includes haematopoietic disorder but with varying degree with respect to the specific mutation (Jaiswal et al., 2014). Mutations in *TP53* or *IDH1/2* are associated with much higher risk than *DMNT3* or *TET2* (Desai et al., 2018). Surprisingly, haematopoietic disorders are still relatively rare occurrences despite CH and cannot account fully for the increased mortality rate (Coombs et al., 2017; Genovese et al., 2014; Jaiswal et al., 2014). Immune cells especially macrophages from CH individuals were found to have deficiencies in anti-inflammatory feedback mechanisms and favour a pro-inflammatory environment may explain the increased morbidity of inflammation-dependent diseases like cardiovascular, pulmonary and type 2 diabetes from CH (Zhang et al., 2015).

1.3.3 Therapeutic options and disease progression

After diagnosis, the treatment options depend on patient-associated factors (age and performance status) and disease-related factors (risk stratification, WHO classification and aetiology). The backbone of AML treatment consists of consecutive cytotoxic regiments. The induction therapy or "7 + 3" regiment is designed to rapidly eliminate the majority of AML cells via three days treatment with anthracyclines (daunorubicine, idarubicine) and seven days treatment with cytarabine (Ara-C). Ultimately 60-80 % of patients will undergo complete remission post-induction therapy (De Kouchkovsky and Abdul-Hay, 2016). Depending on the patient's condition, a consolidation treatment follows, which utilises a smaller dose of cytarabine and is designed to prevent relapse and minimal residual disease.

Younger patients, adverse risk groups and patients in relapse are recommended to receive allogeneic stem cell transplants (ASCT), which remains the most effective long-term therapy. ASCT allows extensive myeloablative preconditioning beyond otherwise dose-limiting bone marrow toxicity. Additionally, slight HLA-mismatching of donor and recipient grants an anti-leukaemic activity of the donor's immune cells against any residual leukaemic cells (graft-versus-leukaemia-effect) (De Kouchkovsky and Abdul-Hay, 2016; Dohner et al., 2015; Saultz and Garzon, 2016).

In particular, the prognosis for patients above 65 is grim due to a higher chance of an adverse cytogenetic risk profile and limited tolerance of the toxicity resulting from extensive cytotoxic therapy and ASCT. Ultimately AML reoccurs in most patients three years post-induction therapy. Genetic and functional studies of clonal evolution show that relapse is triggered by major or minor clones present at diagnosis or from clones with newly acquired mutations (Ding et al., 2012a). Relapse mutations are often enriched for point mutations transforming purine to pyrimidine or vice versa called transversions and are a sign of mutagen exposure most likely as a result of cytotoxic therapy (Shlush et al., 2017).

1.3.4 AML heterogeneity

Over the last few decades, a particular type of AML cells has received increased investigative attention. Work by Lapidot et al. and Bonnet et al.in the 1990s demonstrated that in analogy to normal HSCs only few specialised cells are capable of initiating AML de novo in immune-deficient mice and were termed leukaemia initiating cells (LICs) (Bonnet and Dick, 1997; Lapidot et al., 1994). Despite initially promising results, characterisation of LICs yielded definitive phenotypic markers only with limited success. LICs are present at highly variable frequencies in one or more populations of $CD34^{+}CD38^{-}$ (Bonnet and Dick, 1997), $CD34^{+}CD38^{+}$ (Taussig et al., 2010) or $CD34^{-}$ (Sarry et al., 2011; Taussig et al., 2008). Compared to the AML blast the LICs are different in terms of cell cycle, metabolism, response to intrinsic- and extrinsic signalling pathways and expression of stem-like gene signature (Lagadinou et al., 2013; Ng et al., 2016; Saito et al., 2010). Because cytotoxic therapy relies on active DNA synthesis, any dormant LICs from major or minor clones present before therapy will resist and eventually trigger relapse (Di Tullio et al., 2017).

Indeed, higher abundance of LIC specific genes predicts adverse outcome in AML patients and some instances LIC signature and frequency are increased in relapse samples (Ng et al., 2016; Shlush et al., 2017). Hence, new investigative treatments focused on eradicating LICs like BCL2 inhibitor venetoclax and well-tolerable treatments for the elderly like HDAC inhibitors holds promising potential (Pollyea et al., 2018; Quintas-Cardama et al., 2011).

1.4 The healthy bone marrow microenvironment

In 1978, Raymond Schoefield published a review in which he proposed that the stem cell niche or microenvironment (SCN) forms a regulatory unit to maintain HSC quiescence. Any HSC progeny would differentiate unless it can occupy a similar HSC niche (Schofield, 1978). Over the last 40 years, as numerous non-haematopoietic and haematopoietic components of the SCN have been discovered, the niche hypothesis was validated at its core, but also a more complex reality was revealed (Boulais and Frenette, 2015).

The microenvironment governs HSC behaviour as early as HSC emergence in the AGM region, the FL stage and in the adult bone marrow (Gao et al., 2018). In the adult, at least two distinct SCN may exist (Kiel et al., 2005; Kunisaki et al., 2013) comprising numerous distinct types of niche cells which influence not only HSCs but also their progeny and the SCN itself (Ding and Morrison, 2013). Additionally, the HSC cell cycle is just one aspect of the SCN's regulatory spectrum which now includes recovery and protection from genotoxic or oxidative stresses (Gur-Cohen et al., 2015; Himburg et al., 2017), regulation of inflammatory response (Prendergast et al., 2017), HSC egress and homing (Sugiyama et al., 2006), circadian rhythm (Mendez-Ferrer et al., 2008) and regulation of oxygen and metabolism (Kusumbe et al., 2014). Besides regulating HSCs, specialised niche members display stem cell properties themselves and continuously replenish other post-mitotic cell types (Park et al., 2012). Lastly, niche dynamics and interconnectivity drastically change during ageing, and haematopoietic malignancies to an extent that specific SCN modification alone are sufficient to induce premature ageing or myeloproliferative disorders.

1.4.1 The anatomy of bone marrow

The primary site of adult haematopoiesis is the red bone marrow found in flat bones of the skull, clavicles, vertebrae, ribs, sternum, pelvis and at the ends of long bones. The study of mammalian haematopoiesis mainly focuses on the femur and tibia as examples of long bones and the calvarium and sternum for flat bones. Of note, in non-mammalian vertebrates without bone marrow like zebrafish, the kidney functions as the ultimate site of adult haematopoiesis and contains the SCN (Kapp et al., 2018). In flat bone, the inner area is made of a network of trabecular bone that forms a sponge-like structure called cancellous bone or spongy bone. Compact bone surrounds and protects the inner cancellous bone. Long bones can be divided into three areas with distinct cavity, bone and vascular features. Epiphysis are the rounded ends which connect the bone to adjacent bones via joints. Like flat bones, these areas are

cancellous bone. The bone shaft is called the diaphysis and is made of compact bone that surrounds a large central medullary cavity. Lastly, the transitional zone between epiphysis and diaphysis is the metaphysis. During childhood bone growth is confined to the cartilaginous growth plate in the metaphysis, which ossifies in adulthood into solid bone (Clarke, 2008).

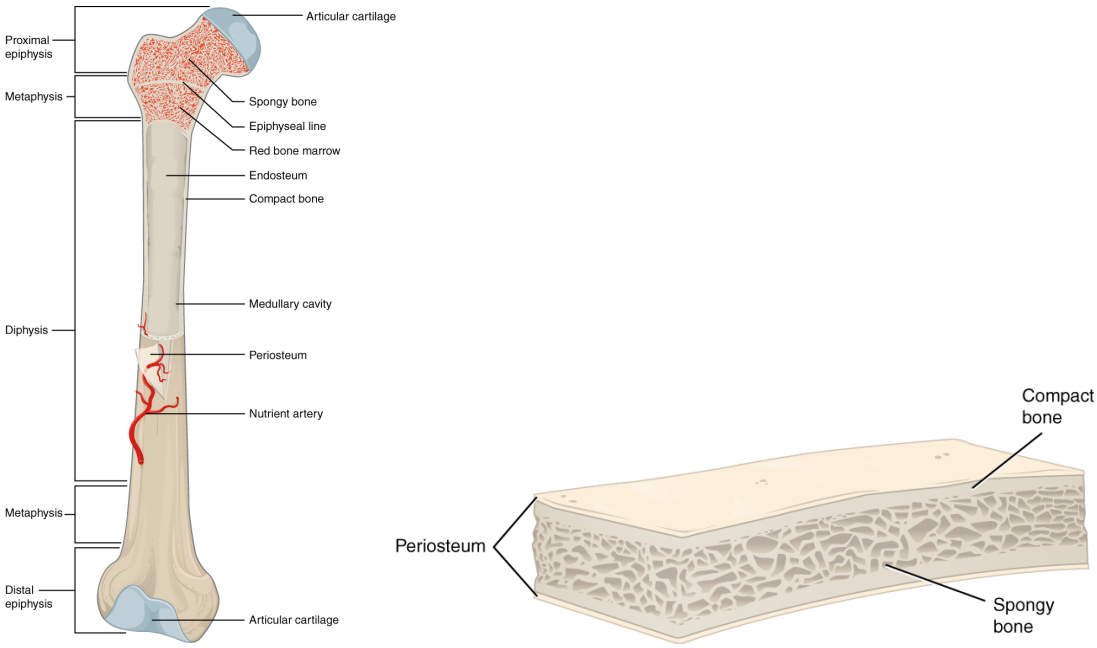


Figure 3. Anatomy of long and flat bones adapted from (Clarke, 2008)

The major non-haematopoietic cell types found in BM are endothelial cells, mesenchymal cells, pericytes, adipocytes and cells of the peripheral nervous system like non-myelinating Schwann cells and sympathetic neurons. Inside the medullary cavity, the bone surface is covered by a membrane called endosteum which also consists of a thin layer of osteoblasts and osteoclasts. Osteoblasts are of mesenchymal origin and form bone by firstly producing an organic collagen matrix into which they deposit a calcium-phosphate mineral called hydroxylapatite (Long, 2011). Osteoclasts, on the other hand derive from haematopoietic cells and secrete acid and collagenases to resorb and remodel bone (Feng and Teitelbaum, 2013).

The BM is traversed by an extensive network of endothelial cells which may at first seem surprising given the hypoxic nature of BM (Spencer et al., 2014). However, the BM vasculature not only supplies nutrients and oxygen but ensures passage of circulating HSPCs to egress and home in the BM (Itkin et al., 2016). The nutrient artery enters the bone marrow

through an opening in the compact bone in the diaphysis or epiphysis. Inside, the arteries run centrally along the diaphysis, emitting smaller branches which run laterally towards the endosteum and gradually decrease in diameter (Nombela-Arrieta et al., 2013). In contrast, Kusumbe et al. observed that arteries preferentially enter long bones relatively unbranched through the epiphysis and are found as highly branched forms in the metaphysis or relatively unbranched close to the endosteum (both termed Type H-capillaries). H-capillaries connect to a vaster sinusoidal network in the medullary cavity called type L-capillaries close to the endosteum in the diaphysis or at the interface of diaphysis and epiphysis. Overall the sinusoidal vasculature covers a much larger volume than arterioles. Eventually, L-capillaries drain into a central vein (Kusumbe et al., 2014; Sivaraj and Adams, 2016).

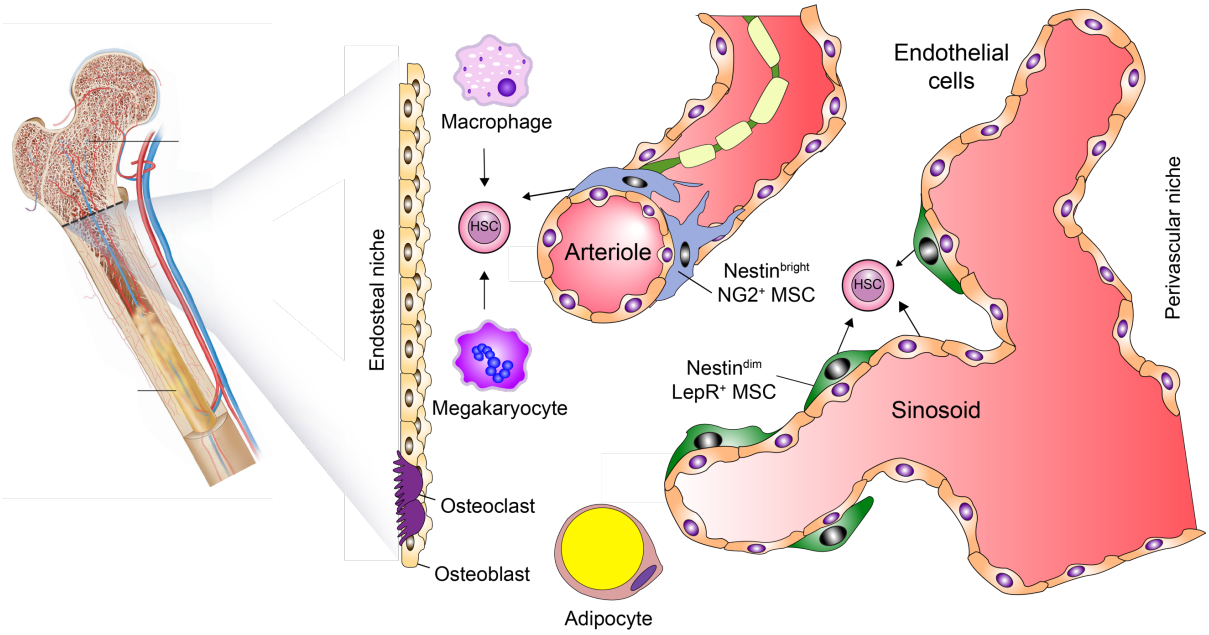


Figure 4 The bone marrow niche for HSCs adapted from (Boulais and Frenette, 2015)

From the inside, blood vessels are composed of endothelial cells surrounded by perivascular cells (pericytes) embedded into the subendothelial basement membrane. Arterial vessels have an additional layer of α-SMA^{+} smooth muscle cells on the outside making them thick-walled but with smaller diameter and higher blood flow than sinusoidal vessel (Sivaraj and Adams, 2016; Spencer et al., 2014).

1.4.1.1 The endosteal niche

HSPCs are not randomly distributed in the BM. HSCs are significantly enriched in the diaphysis compared to epiphysis and metaphysis. Within the medullary cavity of the femur, the frequency of CFU-spleen, a mixture of HSCs and MPPs, steadily increases from the central marrow axis towards the endosteum (Lord et al., 1975). C-kit^{+} cells, mostly progenitors, are equally distributed between metaphysis and diaphysis and CFUs are only marginally enriched 50-200 µm away from the endosteum (Lord et al., 1975; Nombela-Arrieta et al., 2013). Osteoblast, as part of the endosteal lining, were among the first non-haematopoietic cells classified as SCN. A high expression of haematopoietic cytokines and their ability to maintain HSCs *ex vivo* long-term made them an excellent candidate (Taichman and Emerson, 1994). Indeed, an expansion of osteoblastic cells in two independent studies via parathyroid hormone receptor and bone morphogenic protein 2 (BMP2)-signalling drastically increased the HSC pool through Notch signalling and N-cadherin-mediated adhesion, respectively (Calvi et al., 2003; Zhang et al., 2003). However, subsequent studies found that other means of increasing the osteoblast pool like strontium or knockout of N-cadherin showed no immediate effect on HSCs (Kiel et al., 2007; Lymperi et al., 2008). However, osteoblasts may still form a niche since ablation of Col2.3^{+} osteoblasts or deletion of chemokine stroma derived factor 1 (SDF1) severely abrogates lymphopoiesis, especially B-cell development (Ding and Morrison, 2013; Visnjic et al., 2004). Currently, osteoblasts are no longer considered part of the SCN niche but rather a lymphocyte niche capable of indirectly influencing HSCs via the SCN (Morrison and Scadden, 2014).

1.4.1.2 The perivascular niche

Until 2005, detection of HSCs required multiple phenotypic markers, and therefore microscopic detection of the SCN via the HSC location was not possible. SLAM markers CD150^{+} and CD48^{-} together with CD41^{-} and Lin^{-} enriched HSCs to 1 in 2.2 cells, providing microscopy-suitable two-color HSC (CD150 and CD41/CD48/Lin) detection. Approximately 60 % of HSCs were in contact with sinusoidal vasculature while merely 14 % located to the endosteum (Kiel et al., 2005). The introduction of optical bone clearing and 3D deep imaging together with Catenin α like 1 (*Ctnnal1*), as an HSC specific genetic marker (1 in 3 cell frequency), provided further evidence for the sinusoidal niche but also showed that 80 % of randomly distributed cells are in proximity to the extensive sinusoidal vasculature (Acar et

al., 2015). In contrast, Kunisaki et al. located HSCs preferentially in the highly vascularized endosteum near scarcer SCA-1^{+}Nestin^{bright} arterioles (Kunisaki et al., 2013). Of note, in these studies, the endosteal niche spans a region from 0 to 100 µm away from the bone surface. Live-imaging studies in flat and long bones and conventional imaging traced purified HSCs up to 4 days post-injection and found that HSCs located significantly closer to the endosteum than MPPs and progenitors (Lo Celso et al., 2009; Nilsson et al., 2001). One possible explanation could be that in these studies, the irradiation before injection disrupts the sinusoidal vasculature whose recovery is essential for long-term haematopoiesis (Hooper et al., 2009). Indeed, HSCs home closer to the endosteal niche than in non-irradiated murine recipients (Xie et al., 2009). Also, *ex vivo* endothelial cells were demonstrated to maintain LT-HSCs and expand the HSC pool *in vivo* through cell contact-dependent Notch signalling (Butler et al., 2010; Poulos et al., 2015). Currently, both arteriolar and sinusoidal niches are conceived as SCN but potentially with different properties. The arteriolar niche may be home to quiescent ROS^{low} HSCs while the sinusoidal niche regulates HSC mobilisation (Itkin et al., 2016).

1.4.1.3 Mesenchymal stroma cells (MSCs)

Mesenchymal stem cells possess *ex vivo* colony-forming ability and continuously replenish mature osteoblasts and adipocytes (Omatsu et al., 2010; Park et al., 2012). MSCs have a perivascular location but are a heterogeneous population. Arterial H-type vessel are associated with Neuron-glial antigen 2 expressing (NG2^{+}) MSCs, also referred to as pericytes, and express high levels of intermediary filament nestin (NG2^{+}Nestin$^{bright/high}$) (Kunisaki et al., 2013) while L-type sinusoidal vessels co-localise with Leptin-receptor^{+} Nestin$^{low/dim}$ MSCs (Ding et al., 2012b). Despite these markers, pericytes may be a heterogeneous population and a considerable amount of controversy exists regarding the overlap of specific pericyte markers.

A reduction of HSCs accompanied the ablation of all pericyte types, but it remains unclear whether this is a direct, specific consequence or the product of a general BM injury (Beerman et al., 2017). Specific deletion of key haematopoietic chemokine SDF1 (also known as CXCL12) or key haematopoietic cytokine, SCF by the Frenette and Morrison labs again produced conflicting evidence. The Morrison lab found that exclusively SDF1 deletion in LepR^{+} pericytes and SCF deletion in LepR^{+} pericytes and endothelial cells to alter HSC maintenance (Ding and Morrison, 2013). For Frenette and colleagues Nestin expression

labels all pericytes hence, SDF1 and SCF knockout severely impact HSCs, but sinusoidal are the primary providers of SCF while SDF1 is generated predominantly by arteriolar pericytes (Asada et al., 2017).

In humans, perivascular mesenchymal cells expressing high levels of SDF1 have also been identified and isolated from BM (Sacchetti et al., 2007) and labelled initially mesenchymal stem cells. The defining properties are adherence to plastic, multilineage differentiation potential (adipogenic, osteoblastic and chondrogenic differentiation) potential, CFU-F ability and expression of CD105, CD73 and CD90 and lack expression of CD45, CD14, CD11b, CD79, CD19 and HLA-DR (Dominici et al., 2006). Furthermore, marker heterogeneity of MSCs like nestin-GFP and leptin receptor$^+$ MSCs may also exist in the human context. CD146 expression on MSCs has been associated with a perivascular localisation while lack of expression marks an endosteal origin (Tormin et al., 2011).
In recent years the term stem cell was questioned because of extensive inter-donor, inter-clone and intra-clonal heterogeneity. For example, CFU-F ability may be confined to specific sub-fraction like CD271$^+$ (Tormin et al., 2011) or CD146$^+$ cells (Sacchetti et al., 2007) and only ~50 % of MSCs undergo tri-lineage differentiation ability which is also present in fibroblastic non-mesenchymal stem cells. Therefore, the term mesenchymal stroma cells as an umbrella-term seems more appropriate unless specific MSC sub-fractions are studied (Li et al., 2014).
MSCs have been extensively studied to model interactions between normal and malignant HSPCs and the niche. Results from such approaches needs to be interpreted with caution since the fundamental properties of MSCs might be altered by ex vivo culture conditions which do not reflect the complex composition of the bone marrow niche. For example, the properties of the plastic or other extracellular matrices, physiological parameters like oxygen availability or culture dimensions (2D or 3D) and the number of passages impact the behaviour of MSCs (McLeod and Mauck, 2017). To partially overcome these limitations, transplantable 3D culture systems have been introduced in recent years as described in more detailed above. These systems reflect more closely the physiological parameters of BM and allow the generation of partially humanised niche models for the long-term maintenance of HSPCs and AML (Abarrategi et al., 2017). However, these models still rely on the isolation and expansion of BM MSCs, which might impact any potential finding.

1.4.1.4 Other non-haematopoietic SCN members

Adipocytes are present at high numbers, especially in humans occupy increased marrow space in older compared to young individuals. In the mouse, only tail vertebrae house an adipogenic marrow which contains fewer but more quiescent HSCs than non-adipogenic marrow. Blocking adipogenesis after irradiation promotes HSC reconstitution but potentially only indirectly since other BM niche members like osteoblasts are affected as well (Naveiras et al., 2009).

$GFAP^+$ non-myelinating Schwann cells are the primary converter of latent, inactive TGF-β1 to active TGF-β1. TGF-β1 is a potent cell cycle inhibitor of HSCs making these cells important regulators of HSC quiescence (Yamazaki et al., 2011). Other peripheral nervous system cells like β-adrenergic $receptor^+$ nerve extensions directly modulate perivascular mesenchymal cells and control osteogenic differentiation and the rhythmic fluctuations of SDF1. The latter determines the circadian nocturnal egress and daytime homing of HSCs (Mendez-Ferrer et al., 2009).

1.4.1.5 Haematopoietic SCN members

Megakaryocytes localise in close to HSCs in the perivascular niche. Furthermore, by secreting TGF-b and CXCL4 they directly govern HSC behaviour (Bruns et al., 2014; Zhao et al., 2014). Another myeloid niche population are $CD169^+$ macrophages which facilitate SDF1 production from $Nestin^+$ mesenchymal cells and hence, promote HSC retention. G-CSF, a clinically used inducer of HSC mobilisation, functions by reducing SDF1 expression in the SCN, which is counteracted by macrophages (Chow et al., 2011). Lastly, with the recent addition of T-regulatory cells, a lymphoid component was also added to the SCN (Hirata et al., 2018).

1.5 The malignant bone marrow niche

1.5.1 AML interactions with the niche

The difficulty to maintain primary AML cells outside of the BM niche is indicative of non-cell autonomous factors contributing to leukemogenesis. As previously mentioned, non-haematopoietic BM populations like endothelial cells (Liesveld et al., 2005), adipocytes (Shafat et al., 2017) and MSCs (Griessinger et al., 2014; Ito et al., 2015) can provide some of these factors to enhance AML survival, proliferation and protect from chemotherapeutic agents. However, this crosstalk is not unilateral. As haematopoietic malignancies progress, the SCN is reshaped into a chemo-protective niche, which promotes the expansion of malignant clones but suppresses normal haematopoiesis (Korn and Mendez-Ferrer, 2017; Schroeder et al., 2016; Zhang et al., 2012). However, the location of LICs, the affected niche components and the remodelling mechanisms vary among different haematopoietic disorder like CML, AML and MPN (Korn and Mendez-Ferrer, 2017) but also depend within the same haematopoietic disorder on specific leukaemic driver mutations (Jacamo et al., 2017).

Compelling evidence that a dysregulated niche could be a significant driver of haematopoietic malignancies is derived from a series of murine knockout (KO) models with a lethal myeloproliferative neoplasm (MPN) phenotype. Loss of Notch signalling (globally and BM-specific) via *RBPJk* (Wang et al., 2014) and *Mib1* (Kim et al., 2008), over activation of NF-κB via KO of *IkBα* (Rupec et al., 2005) and *RARγ* (Walkley et al., 2007) or mesenchymal cell-specific deletion of *Pnpt11* (Dong et al., 2016), a regulator of RAS signalling, promotes expansion and mobilisation of GMPs, granulocytes and neutrophils. Importantly, when these mice received wildtype BM also MPN of donor origin developed, implying a non-cell autonomous mechanism. Additionally, MDS and AML were reported in osteo-specific ablation of Dicer1 (Raaijmakers et al., 2010) and β-catenin (Kode et al., 2014), respectively. Once exposed to the malignant niche, HSCs developed leukaemic mutations and could propagate the disease upon transplantation into secondary wild type mice (Kode et al., 2014; Raaijmakers et al., 2010). Except Ptpn11 and Dicer1, for which germline mutations have been reported (Slade et al., 2011; Tartaglia et al., 2001), niche-specific mutations are rare and their clinical-importance uncertain. Also, the vast majority of MPN cases harbour JAK2, Calreticulin and MPL mutations in haematopoietic cells (Silvennoinen and Hubbard, 2015) which were absent in these mouse models. However, these studies imply that a dysfunctional niche may be beneficial for haematopoietic mutations to clinically manifest and develop a

malignancy. For example, miR-155, regulated by in RBPJk KO mice, is also upregulated in endothelial cells from MPN patients (Wang et al., 2014) and aberrant nuclear translocation of β-catenin in osteoblasts occurs in 38 % of AML cases (Kode et al., 2014).
A dysregulated niche could also be involved in donor cell leukaemia (DCL), which describes a rarely observed development of leukaemia after ASCT but of donor origin (Wiseman, 2011). Relapse from DCL has a more extended latency period than common relapse which may indicate the necessity for additional leukaemic mutations, but a persistently altered niche environment may select for already existent malignant or pre-malignant donor clones (Gondek et al., 2016; Reichard et al., 2006; Wiseman, 2011).

1.5.2 The location of AML in the niche

Determining the precise location of normal HSCs within the BM cavity facilitated the discovery of the SCN (Kiel et al., 2005; Kunisaki et al., 2013). Similar attempts for AML are limited due to the variability among patient samples concerning the phenotype and frequency of LICs (Sarry et al., 2011). In the murine model of MLL-AF9 driven AML, two GMP-like populations of LICs with distinct disease latencies are well described. Pre-LICs composed of early transduced GMPs, induce AML within 10-30 weeks in primary recipients while LICs of primary leukaemic mice have a latency of 3-5 weeks (Yeung et al., 2010). Lane et al. observed that pre-LICs, like HSCs, localise in close proximity to the endosteum but LICs are located further away resembling the location of wt GMPs (Lane et al., 2011) and in another study, focusing exclusively on AML samples with LICs in the $CD34^{+}CD38^{-}$ compartment, LICs from AML samples injected into sub-lethally irradiated NSG mice also preferentially home to the endosteum where they mostly lack cell cycle activity and hence resist chemotherapy (Ishikawa et al., 2007). Since irradiation significantly affects BM vasculature, other perivascular niches may have been overlooked (Hooper et al., 2009). Indeed, injection of AML into non-irradiated recipients revealed the both the epiphyseal endosteal the perivascular region as sites for homing and proliferation (Ninomiya et al., 2007). Also, in the liver, an under-recognized extramedullary infiltration site in 23 % of AML patients, AML cells localise to the portal vein (Cogle et al., 2014). Residual cells after Ara-C treatment were found with similar frequency in endosteal and perivascular niches in diaphysis and epiphysis (Ninomiya et al., 2007).

A perivascular localisation was also reported for lymphoblastic leukaemias like the B-ALL. B-ALL cell line NALM-6 was observed perivascular on E-selectin^{+}SDF1^{+} endothelium (Sipkins et al., 2005) while T-ALL, murine and patient samples, are highly exploratory and stochastically distributed without a preferential niche (Hawkins et al., 2016).

1.5.3 AML remodels the niche

The infiltration of leukaemia into the SCN results in profound quantitative and qualitative alterations of the niche components. Both acute and chronic haematopoietic malignancies remodel the BM niche with both overlapping and distinct disease-specific mechanisms and consequences for disease progression, chemoprotection and relapse (Boulais and Frenette, 2015; Tabe and Konopleva, 2015).

AML from the MLL-AF9 murine model, cell lines as well as patient samples in NSG induces an expansion of mesenchymal cells (Nestin^{+} (Hanoun et al., 2014) or CD146^{-}CD166^{-}Sca1^{+} (Kumar et al., 2018)) at the expense of mature bone lining osteoblasts (Col2.3^{+} (Duarte et al., 2018) or CD146^{-}CD166^{+} (Kumar et al., 2018)). Using BCR-ABL chronic myeloid leukaemia (CML) as a model for acute leukaemia, Schepers et al. described similar alterations of the mesenchymal-osteoblastic niche (Schepers et al., 2013). In concordance, bone mineralisation, trabecular and cortical bone volume and circulating osteocalcin levels are all compromised (Frisch et al., 2012; Hanoun et al., 2014; Krevvata et al., 2014; Kumar et al., 2018). TRAP^{+} osteoclasts were found increased at an early but decreased at a late disease stage, ruling out bone resorption by osteoclasts as a cause (Frisch et al., 2012; Hanoun et al., 2014; Krevvata et al., 2014). Similarly, AML alone did not resorb bone matrix (Frisch et al., 2012). Duarte et al. suggested that the destruction of specialised endosteal vasculature, capable of regulating osteoblasts and bone formation (Kusumbe et al., 2014), predates and hence initiates osteoblast loss (Duarte et al., 2018). Administration of a serotonin synthesis inhibitor to alleviate the loss of osteoblasts and trabecular volume significantly delayed leukemogenesis (Krevvata et al., 2014). Interestingly, treatment with osteoclast inhibitor zoledronic acid (Frisch et al., 2012) or a selective RANKL inhibitor (Krevvata et al., 2014) also rescued trabecular bone loss but without measurable impact on disease progression and LIC frequency. This indicates that osteoblastic functions other than bone formation are responsible for AML suppression.

Mature osteoblasts are post-mitotic cells which need constant replenishment by Osterix$^+$ osteoprogenitor cells and Mx1$^+$ MSCs (Park et al., 2012). To address the osteogenic dysfunction of AML BM, several studies investigated the MSC differentiation potential with conflicting results. Surprisingly, an increase of osteoblastic differentiation potential was observed by Hanoun et al.in Nestin$^+$ MSCs isolated from AML bearing mice (Hanoun et al., 2014) and by Lokesh Battula et al. and Boyd et al.in AML patient BM-derived MSCs (Battula et al., 2017; Boyd et al., 2017). In contrast, Frisch et al. and Geyh et al. described a dysfunctional osteoblastic differentiation capacity in MSCs from Nup98/HoxA9 driven murine leukaemia and AML patient-derived MSCs, respectively (Frisch et al., 2012; Geyh et al., 2016).

On the other hand, Perilipin$^+$ adipocytes are strongly depleted in number and have reduced lipid content (Boyd et al., 2017; Hanoun et al., 2014), which correlates negatively with patient survival (Lu et al., 2018). MSCs isolated from AML patients have severely impeded adipogenic differentiation potential (Battula et al., 2017; Boyd et al., 2017) but another study with a larger cohort found no significant difference (Geyh et al., 2016). A potential explanation could be increased hypoxia signalling (Boyd et al., 2017) or increased Smad signalling via BMP (Battula et al., 2017) or TGF-β1 (Boyd et al., 2017), all known antagonists of adipogenesis (Zhou et al., 2005). Another explanation could be AML-induced lipolysis. Fatty acid (FA) transporters CD36 (Farge et al., 2017) and FABP4 (Shafat et al., 2017) are generally overexpressed by AML cells to acquire additional fatty acids from the environment. FA driven oxidative metabolism supports AML proliferation and chemoresistance (Shafat et al., 2017). Indeed, chemotherapy-resistant blast crisis CML cells are preferentially located in adipocyte-rich gonadal adipose tissue (Ye et al., 2016).

Increased angiogenesis and expression of angiogenesis promoting factors like VEGF-A have long been recognized in AML (Hussong et al., 2000) and MDS (Korkolopoulou et al., 2001) but recent evidence suggests widespread vascular dysfunction. Accordingly, Hanoun et al. recorded an increased number of CD31$^+$Sca1$^-$ sinusoidal endothelial cells from AML bearing bones (Hanoun et al., 2014). The CD31$^+$Sca1$^+$ arteriolar vasculature, on the other hand, was severely disrupted, especially in the endosteal regions of the metaphysis as opposed to the diaphysis (Duarte et al., 2018). In contrast, Passaro et al. reported an overall increase of arteriolar vessels at the expense of sinusoidal vessels in NSG mice engrafted with AML patient samples (Passaro et al., 2017b).

Not only numerical but also functional perturbations are found in the AML vasculature. Vascular permeability determines nutrient availability, redox state and homing/egress of HSPCs (Itkin et al., 2016). Passaro et al. observed an increased vascular permeability in AML patient-derived xenografts (PDX) and BM biopsy as a consequence of aberrant nitric oxide (NO) signalling. Restoration of arteriolar vasculature or inhibition of NO-signalling improved chemotherapeutic clearing of the bone marrow (Passaro et al., 2017b). Furthermore, an impaired endothelial network may also explain the reduced levels of oxygen in the AML BM (Jensen et al., 2000; Konopleva et al., 2015) and increased hypoxic signalling in AML MSCs (Boyd et al., 2017).

AML progression is also associated with a severe reduction of tyrosine hydroxylase$^+$ (TH) sympathetic nerve fibres. β-adrenergic signalling directly regulates Nestin$^+$ MSC quiescence and HSPC homing via SDF1 (Hanoun et al., 2015). Furthermore, artificial induction of BM neuropathy via ablation with neurotoxic chemotherapeutics or oxidopamine accelerated leukemogenesis and impeded HSPC regeneration in the BM (Hanoun et al., 2014; Lucas et al., 2013).

Besides AML, other haematopoietic malignancies are known to remodel the BM niche as well but with clear distinctions as well as overlaps to the AML niche. In BCR-ABL mutant murine MPN, osteoblastic cells but not MSCs expand under the influence of chemokine CCL3 and inflammatory signalling pathways IL1β and TNF-α (Schepers et al., 2013). In contrast, MPN harbouring JAK2 V617F diminishes Nestin$^+$ MSCs, sympathetic nervous fibres and non-myelinating Schwann cells to escape the tumour-suppressive effect of these niche cells (Arranz et al., 2014). B-ALL disrupts the osteoblastic and vascular niche and in response to chemotherapy rebuilds a chemoprotective microenvironment by attracting Nestin$^+$ MSCs through CCL3. Further release of TGF-β1 transforms the MSCs into FAP$^+$α-SMA$^+$ cancer-associated fibroblast (CAF), which express chemoprotective factor GDF15 (Duan et al., 2014).

1.5.4 The niche remodels AML

Functional interplay between the BM niche and AML is not unilateral. Cell surface and secreted proteins from a naïve or remodelled niche modulate AML metabolism, drug resistance, proliferation, and facilitate niche remodelling (Tabe and Konopleva, 2015). Proteomic interrogation has shown that AML, co-cultured with MSCs, activate MAPK-kinase signalling including ERK1/2, mTOR and AKT, inflammatory response signalling

STAT3 and NF-kB leading to upregulation of pro-survival signalling pathways and increased resistance to Ara-C (Jacamo et al., 2014; Zeng et al., 2012). AML samples extracted from BM aspirates showed higher mTOR and S6K1 phosphorylation as compared to the peripheral blood samples (Braun et al., 2016). Similarly, adhesion of AML cells to stroma-deposited extracellular matrix components like hyaluronic acid and fibronectin enhances survival via CD44 and VLA-4, respectively (Charrad et al., 1999; Matsunaga et al., 2003).

The stroma also overrides the pre-existing metabolic pathways and stimulates increased lactate secretion, oxidative phosphorylation and fatty acid-based β-oxidation, commonly known as Warburg effect (Samudio et al., 2009). Adipocytes (Shafat et al., 2017), BM MSCs and cell lines (Braun et al., 2016; Samudio et al., 2008) and endothelial cells (Nobrega-Pereira et al., 2018) stimulate AML metabolism via distinct pathways. Samudo et al. suggested that through an unknown stimulant AML increases lactate secretion and oxygen consumption rate (OCR). Surprisingly, the OCR was not accompanied by an increase of mitochondrial ATP production due to a transmembrane H+ carrier in the mitochondria called uncoupling protein 2 (UCP2). UCP2 eliminates the mitochondrial proton gradient and therefore, also the gradient dependent adenosine triphosphate (ATP) production via mitochondrial ATP-synthase (Samudio et al., 2008). Of note, similar work by Braun et al. using a human stroma cell line identified an involvement of SDF1 (Braun et al., 2016) and work by Jitschin et al. on chronic lymphoid leukaemia (CLL) suggests a Notch-Myc driven mechanism (Jitschin et al., 2015).
The surge of metabolic activity is not fuelled by glucose since glucose uptake remains unaltered in MSC co-culture. If not glucose, fatty acids (FA) may be the fuel-source. In adipocyte-rich tissue and *ex vivo* AML and blast crisis CML initiate a release of FA from adipocytes. Inhibition leads to reduced proliferation and increased sensitivity to Ara-C (Shafat et al., 2017). Owing to their central role in metabolism and apoptosis, mitochondria have received increased attention. Two recent studies present evidence that functional mitochondria can be transferred from the microenvironment to healthy and malignant haematopoietic progenitors (Moschoi et al., 2016). Mitochondria were transferred to AML via long-ranged plasma membrane protrusions called tunnelling nanotubes (Marlein et al., 2017). This process was shown to contribute the metabolic switch and to chemoresistance of AML.

1.6 Normal haematopoiesis in AML

1.6.1 Clinical perspective

Metastasis, defined as the spread of cancer cell from the primary tumour to surrounding and distant tissues, accounts for 90 % of cancer-inflicted mortality (Chaffer and Weinberg, 2011). In AML, metastasis to non-haematopoietic organs like the liver and central nervous system is relatively uncommon (Viadana et al., 1978). Nonetheless, if left untreated, AML patients quickly succumb to infection, haemorrhage and organ failure (Chang et al., 1976). Severe lack of functional haematopoietic cells (cytopenia) are commonly present in AML (Huck et al., 2015). Clinical manifestations include anaemia from erythrocytopenia, low platelet count and haemorrhage from thrombocytopenia and bacterial, fungal and viral infections due to neutropenia and lymphopenia (Huck et al., 2015; Rauch et al., 2016). Patients with cytopenia are older and often meet cytogenetic criteria for secondary AML (Huck et al., 2015). Intermediary risk group patients with thrombocytopenia and severe neutropenia have significantly worse event-free survival (EFS) and overall survival (OS) independent of treatment approach, age and karyotype risk (Huck et al., 2015; Madiha Iqbal, 2016) and delayed time to neutrophil recovery after chemotherapy (Buckley et al., 2014). Even in complete remission (CR) around 25-34 % of patient do not fully recover neutrophil and platelet counts and are termed complete remission with incomplete blood count (CRi). CRi is a sign of minimal residual disease (MRS) and associated with significantly reduced OS and EFS but also increases non-relapse mortality and early infection after ASCT (Cheng et al., 2018; Walter et al., 2010).

Pancytopenia is often treated as a consequence of the excessive expansion and infiltration of blast cells. However, in other malignancies like CLL cytopenias are less frequent even at blast percentages exceeding 50 % (Rauch et al., 2016). Acute leukaemias and MDS are among the significant causes of pancytopenias (Jalaeikhoo et al., 2017). In AML, cytopenia are reported at less than 50 % blast count, and the severity does not correlate with blast percentage, which argues for additional causes (Rauch et al., 2016). Extensive apoptosis of BM cells resulting in BM necrosis has been reported in AML at diagnosis but with respect to the frequency of pancytopenias very rarely (Paydas et al., 2002).

1.6.2 HSPCs in acute leukaemias

Investigations on human and murine residual HSPCs in acute leukaemias and myeloproliferative neoplasm found extensive loss of differentiated cells and progenitor cells, especially during advanced stages. Several highly related mechanisms have been proposed which involve the destruction and remodelling of the BM niche leading to displacement and egress of HSPCs, reduced SCN support for HSPCs and reduced differentiation and proliferation of HSPCs.
Time-course analysis of AML progression in NSG and murine leukaemia and co-injection of patient AML samples with CB HSPCs highlights three distinct phases with respect to AML infiltration, cytopenia and HSPCs: early (<20 % AML in BM), mid (20 -80 % AML in BM) and late-stage (>80 % AML in BM) (Akinduro et al., 2018; Cheng et al., 2015; Miraki-Moud et al., 2013).

During the early phase, haematopoietic populations and parameters are mostly unaffected. Total leukocyte count, progenitors and HSCs counts remain stable. Spleen weight is not increased yet, and AML infiltration of peripheral blood and spleen is shallow (Cheng et al., 2015). Merely total WBC count in the peripheral blood may be slightly increased already at this stage (Cheng et al., 2015). CFU- and reconstitution potential of HSPCs is also not affected (Cheng et al., 2015; Miraki-Moud et al., 2013).

During the mid-phase, AML engraftment in the bone marrow reaches 20-80 %. AML cells are present in PB, and spleen but compared to BM with delayed kinetics (<20 % of total leukocyte) (Cheng et al., 2015; Miraki-Moud et al., 2013). Total mononucleated cell counts are sharply reduced in the BM and increased in peripheral blood and spleen (Akinduro et al., 2018). Especially mature myeloid lineages are reduced while lymphoid lineages with longer half-life time are not affected (Boyd et al., 2017). Red blood cell count and platelet counts are slightly decreased in PB and the mice may display first disease symptoms (Cheng et al., 2015; Wang et al., 2016). Progenitor cells also decrease in the BM but with distinct kinetics from mature normal CB leukocytes resulting in a relative enrichment of CMPs, stable proportions of GMPs and a reduction of MEPs. Similarly, LT-HSCs, ST-HSCs are relatively enriched among total leukocytes while MPPs proportions remain stable (Akinduro et al., 2018; Boyd et al., 2017; Cheng et al., 2015; Miraki-Moud et al., 2013). When equal numbers of human non-leukaemic HSPCs from AML patients and healthy donors are injected into

primary and secondary mice or plated in methylcellulose, an increased reconstitution and CFU-potential has been reported, respectively. Agreeing, non-leukaemic CD45`cells from MLL-AF9 murine leukaemic mice also generate higher reconstitution and display increased CFU-ability (Cheng et al., 2015; Miraki-Moud et al., 2013). Since all progenitors, MPPs and HSCs contain fewer cells in S-phase before transplantation, the lower proliferation rate has been proposed as cause (Cheng et al., 2015; Jensen et al., 2000; Miraki-Moud et al., 2013). Additionally, the preferential egress/apoptosis of less primitive HSPCs may selectively enrich for quiescent, self-renewing $CD48^-$ HSCs in the non-leukaemic $CD45^+$ cells and could present another non-mutually exclusive explanation (Akinduro et al., 2018).
In the spleen, a surge of HSPCs with increased cell cycle activity is present to compensate for reduced BM output (Cheng et al., 2015). Of note, no increase of apoptosis was reported except for ST-HSCs during late-phase (Akinduro et al., 2018).

The late-stage comprises all engraftment above 80 %. Further loss of MNCs and HSPCs from the bone marrow occurs. AML chimerism in the PB and spleen reaches above 50 %, and MNCs and HSPCs are drastically reduced in the spleen. Red blood cell and especially platelet counts are strongly reduced, and the mice develop splenomegaly (Akinduro et al., 2018; Cheng et al., 2015; Miraki-Moud et al., 2013). Despite further enrichment of HSPCs among MNCs, the CFU- and reconstitution-ability is sharply reduced (Cheng et al., 2015). Accordingly, functional analysis of phenotypic HSCs associated a significantly worse outcome for AML patients with compromised multilineage reconstitution ability of HSCs (Wang et al., 2017).

1.6.3 Mechanistic perspective

1.6.3.1 Displacement of HSPCs from the niche

During mid and late-phase non-malignant MNCs are displaced from the BM and later from the spleen and even within leukaemic BM, HSC localise further away from their arteriolar and endosteal niches compared to non-leukaemic BM (Hanoun et al., 2014; Miraki-Moud et al., 2013). Furthermore, BM homing of HSCs injected into leukaemic mice is significantly impaired (Duarte et al., 2018).
The chemokine SDF1 is the primary regulator of HSPC homing and mainly expressed in BM $Nestin^+$ MSCs, endothelial cells and osteoblastic cells (Asada et al., 2017). The receptor CXCR4 is widely expressed on HSPCs and influences adhesion, BM retention and

proliferation (Sugiyama et al., 2006). Nestin^{+} mesenchymal cells from MLL-AF9 murine AML, JAK2 V617F MPN and BCR-ABL CML express significantly less SDF1 (Arranz et al., 2014; Ge et al., 2011; Hanoun et al., 2014; Zhang et al., 2012). Sympathetic nerve extensions regulate SDF1 expression in the BM during homeostasis. Hence reported loss of sympathetic nerve extensions in AML (Hanoun et al., 2014) and the increased expression of G-CSF (Schepers et al., 2013; Zhang et al., 2012), a clinically used HSPC mobiliser and negative regulator of SDF1, may be a crucial component for the reduced expression of SDF1.

HSPCs migrating towards a CXCL12 gradient must transverse the endothelial barrier. Vascular permeability allows transendothelial migration and HSPC trafficking (Itkin et al., 2016). NO concentrations, a potent agonist of vascular permeability (Gur-Cohen et al., 2015), are increased in murine and patient AML BM. Interestingly, inhibition not only improved cytotoxic clearance of AML but also drastically increased residual HSPCs in BM of leukaemic mice (Passaro et al., 2017b). Besides changes in chemical nature, Akinduro et al. hypothesize that the lack of space in the BM could result in the dislodgment of HSPCs. Indeed, MLL-AF9 AML blasts are significantly more massive than normal HSPCs, but direct evidence has not been reported yet (Akinduro et al., 2018).

1.6.3.2 Cell cycle

The continuous loss of mature haematopoietic cells from apoptosis and resorption in the spleen requires constant replenishment through highly proliferative progenitor cells. Hence severe impairment of HSPC proliferation could rapidly induce cytopenias, especially in myeloid lineages with shorter half-life. The measurement of DNA content with a DNA intercalating dye like DAPI is the simplest form of cell cycle analysis of normal HSPCs. A more dynamic approach is the injection of a thymidine analogue like BrdU or EdU, which will be incorporated into DNA during S phase. A secondary antibody or a click-chemistry reaction will then fluorescently mark any cell which entered S-phase between the time of injection and sacrifice/cell fixation. Ki67 expression, a marker associated with ribosomal RNA transcription, presents another mean of cell cycle analysis. Opposed to S-, G1-, G2- and M-phase, the quiescent cells in G0 phase of the cell cycle do not express Ki67. Normal HSPCs from leukaemic rat (Jensen et al., 2000), mice (Cheng et al., 2015) and humans (Miraki-Moud et al., 2013) contain proportionally fewer BrdU^{+} or EdU^{+} cells indicating a smaller proportion of actively cycling cells. Human CD34^{+}CD38^{-} HSPCs from patients with CD34^{-} AML, strongly associated with NPM1 mutations (Taussig et al., 2010), contain six

times more Ki67^{-}DAPI^{-} quiescent cells (Miraki-Moud et al., 2013). The timely separated injection of BrdU followed by EdU allows to measure the proportion of cells entering S-phase per hour and a proliferation measurement independent of S-phase duration. Data from Akinduro et al. who used this method also suggests decreased proliferation of MPPs and ST-HSCs, especially during mid-late phase, while the proliferation rate of AML remains constant throughout phases. Owing to the short duration between EdU and BrdU injections, the HSC proliferation could not be measured omitting any conclusions (Akinduro et al., 2018).
The precise mechanisms behind the reduction of HSPC proliferation is still mostly unknown. Isolated HSCs from leukaemic mice express higher levels of cell cycle inhibitors *p19^{Cip1}*, *p21* and *Egr1-3* and lower levels of cyclins and cyclin-dependent kinases, essential for initiation and traverse of cell cycle phases, which could explain the reduced proliferation rates. Furthermore, elevated expression of *Hes1* and *Hey1* indicated dysregulated Notch activity but was not further explored (Cheng et al., 2015). A follow-up study by Gong et al. reported Egr3 as a downstream effector of TGF-β1 signalling, a potent secreted HSPC cell cycle inhibitor found at elevated concentrations in AML BM interstitial fluid (Gong et al., 2018).

1.6.3.3 Microenvironment

Several lines of evidence support the hypothesis that niche remodelling facilitates the expansion of malignant cells by reducing niche support for normal HSPCs. Compared to aged-matched healthy donor MSCs (N-MSCs), Leukaemic MSCs have reduced capacity to expand and maintain normal HSCs (Geyh et al., 2016). Interestingly, BCR-ABL expressing CML HSCs preferentially expand on leukaemic MSCs implying niche reprogramming as a strategy for malignant clone selection (Zhang et al., 2012). Secreted factors such as TNF-α and Adiponectin present in BM interstitial fluid mice strongly inhibit the CFU-ability of normal HSPCs directly (Broxmeyer et al., 1978; Hornick et al., 2016; Iversen and Wiig, 2005) and also indirectly via remodelling of N-MSCs (Mead et al., 2017). Conversely, AML patient MSCs express lower levels of haematopoiesis regulating factors such as c-Kit-ligand SCF and Notch-ligand Jagged-1 (Geyh et al., 2016; Kumar et al., 2018). Besides HSPCs support, detailed characterisation by Geyh et al. and Kornblau et al. revealed that AML MSCs contain fewer CFU-F, cycle slower and become senescent faster due to overexpressed p53/p21 axis. In contrast, Diaz de la Guardia et al. found more CFU-F and no significantly altered proliferation but did not culture further than passage 5 (Diaz de la Guardia et al., 2017). Interestingly, MSCs isolated from patients in CR regain HSC maintenance ability

(Geyh et al., 2016), but MSCs expanded over several passages remain dysfunctional owing to altered SMAD signalling (Geyh et al., 2018).

Other signalling pathways affected by AML are inflammatory pathways in particular NF-kB and STAT (TNF-α, IL-1β) (Jacamo et al., 2014; Mead et al., 2017), Smad-pathway (TGF-β1, BMP) (Battula et al., 2017; Geyh et al., 2018) and hypoxia response signalling (HIF-1α) (Boyd et al., 2017). These well-studied pathways play key roles to regulate niche and HSC homeostasis, but dysregulation may give AML a competitive advantage by blocking normal HSPCs. For example, inflammatory signals via TNF-α are often elevated in BM interstitial fluid of AML patients. Recently TNF-α was shown to deplete both wildtype and FLT-ITD knock-in HSCs, but the latter to a less extent (Iversen and Wiig, 2005; Mead et al., 2017). IL1-β induces proliferation in AML but inhibits CFU-potential of normal HSPCs (Carey et al., 2017). Recent work by the Kurre and Chen lab identified vesicular transport, including exosomes as a potent mechanism for AML to transform the BM niche and dysregulate normal haematopoiesis. Exosomes can be either directly up-taken by murine HSPCs or indirectly via the mesenchymal and vascular microenvironment. Mir-150 and Mir-155 overexpressed in AML exosomes or Wnt-pathway inhibitor DKK1 caused dysfunctional HSPC expansion and reprogrammed the BM niche into a leukaemia-permissive environment (Hornick et al., 2016; Kumar et al., 2018). However, in contrast to AML infiltrated mice, AML exosome preconditioning of healthy mice increased HSPC proliferation.

For individual niche elements remodelling may go beyond a regulatory dysregulation. Post-mitotic osteoblasts, adipocytes and arteriolar vessels are greatly diminished from AML BM. Boyd et al. reported that AML abrogates mature adipocytes from BM and inhibits adipogenesis in MSCs. Adipogenic stimulation with PPAR-γ agonist not only restored adipocyte levels but also partially ameliorated the differentiation blockage of HSPCs. Co-culture experiments with healthy HSPCs indicate that mature niche cells like osteoblasts and adipocyte are far more supportive for erythro-myelo differentiation than undifferentiated MSCs (Boyd et al., 2017). Lastly, Duarte et al. observed that in late-phase AML deteriorates mature osteoblasts and arteriolar vessels, especially in the metaphysis. During homeostasis, the metaphysis is well supplied with oxygen and metabolites via highly branched arteriolar vessels and hosts highly proliferative HSPCs. Stimulation of arteriolar angiogenesis via

Notch activation or HIF-1α stabilisation ameliorated loss of vessels and HSCs in the metaphysis (Duarte et al., 2018).

1.7 Hypoxia in BM during normal and malignant haematopoiesis

1.7.1 Oxygen distribution in the BM

Oxidative phosphorylation (OXPHOS) is the most substrate-efficient means of ATP generation. Firstly, electrons are transferred to cofactors like NAD^+ when substrates like glucose or fatty acids are metabolised to lactate or CO_2. Secondly, reduced NAD, called NADH, drives a proton efflux pump system called electron transport chain, in the mitochondria during which O_2 is converted to H_2O. Lastly, the proton gradient literally propels ATP-synthetase to regenerate ATP from ADP (Lodish H, 2000; RN., 2011). Hence oxygen supply via a vascular network is a rate-limiting factor. Tissue oxygenation is dependent on consumption and supply. Oxygen is carried via haemoglobin in erythrocytes and diffuses into tissue from arterial blood supply which drops from 75-100 mmHg in arterial to 30-40 mmHg in venous blood. Oxygen tension in tissues ranges from 27-31 mmHg in muscular tissue, 34-42 mmHg in liver to over 50 mmHg in intestine and cortex (Sharma S, 2018). Despite extensive vascularisation, the BM of flat bones contains a low extravascular and intravascular oxygen tension of 15 mmHg and 20 mmHg (2-3 % O_2), respectively. Furthermore, endosteal arteriolar areas are significantly more oxygenated than central sinusoidal niches which is driven by a lower oxygen consumption rather than differences in oxygen supply (Spencer et al., 2014).

1.7.2 The HIF family of transcription factors

Hypoxia-inducible factors (HIFs) are major regulators of the cellular response to hypoxia. The oxygen-sensitive α subunit heterodimerize with the β subunit HIF-1β via the HLH and PAS domains. While HIF-1β is expressed ubiquitously, the three mammalian α subunits HIF-1α, HIF-2α, HIF-3α are expressed tissue-specific. The complex then binds to hypoxia response elements (HRE) in the genome and regulates the transcription of HIF-target genes. In well-oxygenated environments, the α subunits are constantly degraded. Prolyl hydroxylases (PHDs) utilise a ferrous iron cofactor and oxygen and α-ketoglutarate as substrate to hydroxylate conserved proline residues on HIFs. The hydroxylation is recognized by an E3 ubiquitin ligase called von Hippel-Lindau protein complex (VHL) and initiates proteasomal destruction. Another O_2-dependent regulator is factor-inhibiting HIF-1α (FIH) which disrupts binding to transcriptional coactivators P300/CBP. PHD/FIH-dependent

regulators of HIF include citric-acid metabolites (fumarate, succinate and α-ketoglutarate) and reactive oxygen species (ROS), an umbrella term for oxygen radicals produced as side-products during OXPHOS. PHD/FIH-independent negative regulators are deacetylase Sirtuin1 and aryl hydrocarbon receptor (AhR) while AMP-activated protein kinase (AMPK) activation promotes HIF-1α stabilisation. Many HIF-target genes are involved in angiogenesis (*Vascular endothelial growth factor* (*VEGF*)), anaerobic glycolysis (glucose transporters and glycolytic enzymes/regulators like *GLUT1*, *PDK1* and *LDHA*), redox homeostasis (antioxidant enzyme *SOD2* and *HMOX1*) and cell migration (*SDF1* and its receptor *CXCR4*) (Irigoyen et al., 2017; Majmundar et al., 2010).

1.7.3 Role of hypoxia for normal haematopoiesis

Hypoxia and HIFs are essential regulators of normal and malignant haematopoiesis. *Ex vivo*, culture of both HSPCs and AML under hypoxic conditions improves the long-term maintenance of HSCs and LICs (Danet et al., 2003; Griessinger et al., 2014; Ivanovic et al., 2002; Mantel et al., 2015). Human HSPCs express both HIF-1α and HIF-2α to regulate metabolism and redox state (Rouault-Pierre et al., 2013; Takubo et al., 2010), niche-localisation (Forristal et al., 2015; Miharada et al., 2011) and quiescence (Takubo et al., 2010). HIFs, especially HIF-2α, also play an important role in erythropoiesis. HIF-2α knockout mice lack erythropoiesis stimulation factor erythropoietin (EPO) and develop severe anaemia but can be rescued by EPO administration (Scortegagna et al., 2005). Murine HSCs lacking HIF-1α (Rouault-Pierre et al., 2013; Takubo et al., 2010) or its transcriptional regulator MEIS1 (Kocabas et al., 2012; Unnisa et al., 2012), show diminished self-renewal in a ROS-dependent manner. In human HSCs depletion of HIF-2α and HIF-1β but not HIF-1α compromised reconstitution potential also owing to accumulation of ROS (KEVIN Reference). However, in two recent murine studies abrogating HIF-1α and HIF-2α could not repeat previous results. Since HSPCs were extracted shorter after knockdown than previous studies (2 weeks versus 1-2 months) the authors also speculate that the differences could be due to shorter exposure to a HIF-1α defective microenvironment (Guitart et al., 2013; Vukovic et al., 2016). Indeed, for HIF-2α, a non-cell autonomous role of HIF-2a in the BM microenvironment has been reported (Scortegagna et al., 2003). Another explanation could be that these studies only deleted exon 2 containing the HIF-1β binding domain, but HIF-1β -independent mechanisms have been reported.

1.7.4 Role of hypoxia for malignant haematopoiesis

The role of hypoxia and HIF in AML is also quite disputed. AML and other haematopoietic malignancies decrease oxygen pressure in the bone marrow of rats (Jensen et al., 2000), mice (Passaro et al., 2017b) and humans (Konopleva et al., 2015) especially in close proximity to AML cells (Passaro et al., 2017b). Hypoxia enhances LIC maintenance and Ara-C resistance owing to the quiescence promoting effects of hypoxia but also increased differentiation of AML cells through HIF-1α accumulation have been reported. HIF-1α stabilisation and upregulation of various HIF target genes in AML is associated with an adverse disease progression (Deeb et al., 2011; Song et al., 2014; Xu et al., 2017). Conversely, inhibition of HRE-binding by echinomycine and HIF-1α and HIF-2α knockdown in patient AML samples induces apoptosis and impairs their CFU and serial transplantation ability (Abdul-Aziz et al., 2018; Gao et al., 2015; Rouault-Pierre et al., 2013; Wang et al., 2011). Abdul-Aziz et al. demonstrated that HIF-1α stabilisation in AML induced expression of macrophage inhibitory factor (MIF), which supported AML proliferation via MSC-derived Interleukine-8 (IL-8) (Abdul-Aziz et al., 2018). In contrast, Velasco-Hernandez et al. and Vukovic et al. reported conflicting data. In murine AML1/ETO AML lacking HIF-1α, leukemogenesis was accelerated while for MLL-AF9 and Meis1-Hox9, no significant impact was observed. HIF-2α ablation accelerated leukemogenesis in MLL-AF9 driven AML (Vukovic et al., 2015). Interestingly, HIF-1α ablation resulted in different ROS, apoptosis and mitochondrial biogenesis phenotypes among the three AML models indicating that HIF-1α has a mutation-specific role which may partially explain variations among AML model systems (Velasco-Hernandez et al., 2014).

1.7.5 HIF in the BM microenvironment

Another explanation for the controversy regarding HIFs in AML could stem from the role of HIF-1α in the microenvironment, which is poorly understood. HIF-1α knockout models were mostly Mx1-cre driven, thus deletion of HIF-1α will have occurred in the microenvironment as well (Park et al., 2012; Takubo et al., 2010). Indicative of the hypoxic BM microenvironment, human and murine MSCs also express high levels of both HIF-1α and HIF-2α to promote anaerobic glycolysis, self-renewal and differentiation. Furthermore, MSCs reduce HIF-1α stabilisation to stimulate HSPC expansion both *ex vivo* and *in vivo*

highlighting a non-cell autonomous role of HIFs in HSPC regulation (Guarnerio et al., 2014; Palomaki et al., 2013). Conversely, AML MSCs were reported to be enriched with HIF-1α-target genes compared to N-MSCs (Boyd et al., 2017; Dong-Feng et al., 2012) and AML can induce increased expression of HIF-1α target genes *ex vivo*. HIF-1α knockdown in MSCs reduces AML engraftment in a matrigel-based *in vivo* niche model (Chen et al., 2012) and reduces the chemoprotective ability of MSCs by downregulation of SDF1 (Kojima et al., 2011).

1.8 The Stanniocalcin family of secreted proteins

1.8.1 STC in fish and mammals

Stanniocalcin (STC) is a family of secreted glycoproteins of which STC1 was first described in the corpuscles of stannous (CS) in the kidneys of bony fish. Elevated serum levels of calcium (hypercalcemia) are recognized by the calcium-sensing receptor (CaR) which then stimulates the release of STC1 from the CS to enter the circulation. STC1 or CS extract responds to hypercalcemia by decreasing the environmental net calcium uptake by the branchial arches of the gills and the upper intestine. Phosphate levels, a calcium chelator and regulator of serum calcium, are increased due to elevated net phosphate uptake/reabsorption in the gills and kidney (Wagner and Dimattia, 2006). The corresponding receptor for STC1 and the exact target cells have not been identified but Lu et al. and Tseng et al. suggest that calcium uptake is inhibited via reduced calcium channel mRNA expression owing to active cyclic adenosine monophosphate (cAMP)-Protein Kinase A (PKA) signalling (Lu et al., 1994; Tseng et al., 2009). The fish STC1 gene is unique among known proteins and has only one known relative STC2 with which it shares 39 % homology and potentially a common ancestor (Roch and Sherwood, 2011; Wagner and Dimattia, 2006). STC1 consist of two identical glycosylated 223 kDa polypeptide chains connected through a disulphide bridge (Cys169) to form a homodimer. STC1 has a high content of α-helices and 11 conserved cysteine residues of which 10 form intra-chain disulphide links, however a detailed tertiary structure of STC1 is still missing from the literature (Trindade et al., 2009).

In the 1990s, the two vertebrate orthologs of STC were discovered. STC1 has 61 % and STC2 about 30 % amino acid homology to fish STC1. Cysteine residues, glycosylation sites and exon-intron boundaries are strongly conserved. In mammals STC1 is broadly expressed in heart, lung, liver, adrenal gland, kidney, prostate and ovary and STC2 in pancreas, spleen, kidney and skeletal muscle (Yeung et al., 2012). Secreted STC has been shown to be sequestered by cells lacking STC mRNA like luteal cells (Paciga et al., 2003) and macrophages (Wang et al., 2009). Studies on the subcellular location of STC and its receptors utilising an STC-alkaline phosphatase fusion protein revealed that STC and its receptors are located on mitochondriae, in particular, the inner membrane, and the surface of lipid droplets (McCudden et al., 2002; Paciga et al., 2003).

1.8.2 The roles of STC

The role of STCs for mammalian calcium/phosphate homeostasis is disputed. Injection of human kidney extract containing STC1 into fish mimicked the calcium regulating function of fish STC1 (Wagner et al., 1995). In vitro studies with recombinant human STC1 on swine and rat intestine and initially also supported an involvement in calcium/phosphate transport (Madsen et al., 1998; Wagner et al., 1997). However, *Stc1*$^{-/-}$, *Stc2*$^{-/-}$, *Stc1*$^{-/-}$*Stc2*$^{-/-}$ nor STC2 transgenic mice show any changes in serum phosphate or calcium (Chang et al., 2005; Chang et al., 2008; Johnston et al., 2010). Opposed to fish serum, mammalian serum is entirely devoid of STC, and pharmacokinetic analysis suggests that STC in circulation is quickly modified and losses its reactivity (De Niu et al., 2000). This indicates that in mammals, STCs may instead act as a paracrine/autocrine factor but does not exclude that STCs are involved in cell-intrinsic calcium regulation. *Stc2*$^{-/-}$ mouse embryonic fibroblasts (MEF) accumulate higher levels of cellular calcium following endoplasmic reticulum (ER) Ca^{2+} store depletion. STC2 localises to the ER and interacts with the ER Ca^{2+} sensor STIM1, which activates store-operated Ca^{2+} channels (Zeiger et al., 2011). Similarly, local calcium regulatory functions for STC1 were postulated for macrophages (Kanellis et al., 2004), terminally differentiated neurons (Serlachius et al., 2004) and cardiomyocytes (Sheikh-Hamad et al., 2003).

To date, two STC transgenic mouse models with STC under the control of myosin light chain-2 promoter and metallothionein I minimal promoter have been generated. In both models, STC induces substantial skeletal and muscular defects, dwarfism and altered fertility (Filvaroff et al., 2002; Johnston et al., 2010; Varghese et al., 2002). However, again, *Stc1*$^{-/-}$ mice failed to produce any consistent phenotypes (Chang et al., 2005). On the other hand, *Stc2-/-* are bigger than wild type littermates (Chang et al., 2008). Olsen and colleagues showed that STCs could inhibit the enzyme pregnancy-associated plasma protein – a (PAPP-A) which frees Insulin-like growth factor (IGF) from IGF-binding proteins (IGF-BP) by enzymatically cleaving the latter. Mice expressing a mutant variant of STC2, STC2(C120A), which lacks PAPP-A inhibitory action, reversed the dwarfism phenotype of STC2 transgenic mice (Jepsen et al., 2015).

The high affinity of STC1 to lipid droplets and mitochondria provoked investigations into metabolism-regulating functions. Inhibitory actions of STC1 and STC2 on progesterone

synthesis were reported in rat granulosa and bovine luteal cells. The effect was conducted via the PKA pathway and subsequent downregulation of critical steroidogenic enzymes (Paciga et al., 2003). Furthermore, experiments with isolated mitochondria showed that high concentrations of STC1 (>1µg/mL) increased oxygen consumption at the expense of ATP production. This counterintuitive relation was caused by an uncoupling of ATP generation from oxygen consumption via UCP (McCudden et al., 2002). Ohkouchi et al. showed that the addition of STC1 to epithelial cell line A549 induced stabilisation of UCP2 and replicates the effects observed with isolated mitochondriae. As a consequence of the mitochondrial uncoupling, levels of ROS and mitochondrial superoxide declined (Ohkouchi et al., 2012). In line with an antioxidative function, STC1 transgenic mice are more resilient to kidney and lung injury inflicted by ischemia and bleomycin, in part by downregulation of ROS (Huang et al., 2015; Pan et al., 2015).

1.8.3 STC1 in cancer

STCs are significantly upregulated in various solid tumours and patient serum, making it attractive biomarkers (Chan et al., 2017; Fang et al., 2014). Stratification of STC expression determined an adverse outcome for patients with high expression of either STC1 or STC2 in renal cancer, gastric cancer and head and neck cancer. Additionally, STC1 alone is prognostic in cervical cancer (unfavourable), lung cancer (unfavourable), breast cancer (unfavourable) and glioma (unfavourable) and STC2 alone for liver cancer (unfavourable) and breast cancer (favourable) (Uhlen et al., 2015). In normal and malignant haematopoietic cells STC1 and STC2 are not/low expressed although two reports suggest an adverse outcome in AML patients with high STC1 expression (Abaza et al., 2016) and that the detection of STC1 mRNA in blood predicts relapse (Tohmiya et al., 2004).

STC1 expression can be induced through multiple pathways. A few examples are oxidative stress (Block et al., 2009), IL-1β (Bartosh et al., 2013) , TGF-β (Ono et al., 2015) , HIF-1α (Yang et al., 2015; Yeung et al., 2005) and p53 (Lai et al., 2007). Overexpression of STC1 has a positive role for proliferation and tumorigenesis in cellular models of breast, ovarian, gastric and lung cancer, but cell cycle inhibitory functions in cervical cancer. The adverse effect of STC1 expression in some models may also be due to an altered cancer microenvironment. STC1 promotes angiogenesis when administered to endothelial cells directly (Law and Wong, 2013) or indirectly by promoting VEGF expression from cancer

cells (He et al., 2011). However, not only neoplastic cells express STC1 but also cancer-associated fibroblasts (CAFs) and MSCs. In a model of colorectal cancer, platelet-derived growth factor (PDGF) activated STC1 expression from CAFs to drive migration and lymph node metastasis (Pena et al., 2013) and in MSCs, secreted STC1 remodelled the cancer metabolism which protected from chemotherapeutic agents and irradiation (Block et al., 2009; Ohkouchi et al., 2012). In these reports, several downstream mechanisms of STC1 with well-known implications for cancer were proposed ranging from antioxidative effect via UCP2, to MAP-kinase signalling and anti-apoptotic factors like BCL-2 (Chu et al., 2015; Yeung et al., 2012). However, since the receptor or any direct interaction partners of STC1 have not been identified the causality of these proposed mechanisms remain unknown, and additional discrepancies exist whether these effects are due to intracellular or extracellular STCs.

1.9 Objective of study

The BM microenvironment is an essential regulator of hematopoiesis by controlling the quiescence, homing and maintenance of HSPC in homeostasis and stress. Myeloid malignancies like AML have been shown to disrupt healthy niche architecture on the phenotypic, transcriptomic and functional level. Furthermore, in murine AML models and human AML patients, the residual normal HSPCs are unable to enter the cell cycle and supply sufficient mature hematopoietic cells which coincides with cytopenias as well as an extensive remodelling of the perivascular and endothelial BM niches. I propose that the dissection of the crosstalk between AML, the microenvironment and the normal hematopoietic stem and progenitor system may provide insight into either therapeutically targetable mechanisms or undiscovered regulators of HSPC quiescence and stemness.

Hypothesis

MSCs play a critical role in the remodelling of the BM niche by AML, disrupting normal HSPC proliferation and leading to the development of cytopenias.

Aims

1. To generate a simplistic fully-humanised model system of the bone marrow niche using bone marrow MSCs and HSPCs, which recapitulate the ability of AML to inhibit HSPC cell cycling and preserve stemness in HSPCs.
2. To investigate the secretome of MSCs and how this changes in response to AML, and thereby identify potential proteins that inhibit HSPC proliferation.
3. To examine the impact of AML on MSCs at the transcriptional level.
4. To use the transcriptional data to identify the molecular mechanisms regulating changes in the MSC secretome in response to AML.
5. To perform in vivo experiments to determine whether mechanisms identified in vitro can be recapitulated in vivo.

Chapter 2 Materials and Methods

2.1 Cell culture

All cells were routinely cultured at 37° C and in a humidified atmosphere of 5 % CO_2, 17 % O_2 and 78 % N_2, which is referred to as normoxic culture conditions. Hypoxic culture conditions refer to 5 % CO_2, 1-3 % O_2 and 92-94 % N_2. All media and supplements were purchased from ThermoFisher Scientific. All cell lines were originally obtained from ATCC (distributor LGC standards, UK) and were grown by in-house cell services. All cell lines were routinely mycoplasma tested and STR authenticated prior to commencing experiments. All haematopoietic cytokines were purchased from Peprotech unless when pre-supplemented in methylcellulose medium from Stem Cell Technologies.

AML cell lines were passaged every 3-4 days to maintain them at optimal cell density (0.1-1x10^6/mL). Adherent cell lines and primary cells were passaged by trypsinisation and maintained at sub-confluency.

Table 4. Cell line/Primary cells and culture conditions

Name	Cell Type	Species	Media	Supplement(s)
HL60	AML Cell Line	Human	RPMI 1640	10 % FBS + 100 U/ml P/S
ML1	AML Cell Line	Human	RPMI 1640	10 % FBS + 100 U/ml P/S
U937	AML Cell Line	Human	RPMI 1640	10 % FBS + 100 U/ml P/S
KG1A	AML Cell Line	Human	RPMI 1640	10 % FBS + 100 U/ml P/S
NB4	AML Cell Line	Human	RPMI 1640	10 % FBS + 100 U/ml P/S
MOLM13	AML Cell Line	Human	RPMI 1640	10 % FBS + 100 U/ml P/S
OCI-AML3	AML Cell Line	Human	RPMI 1640	10 % FBS + 100 U/ml P/S

HEK 293	Cell Line	Human	DMEM	10 % FBS + 100 U/ml P/S
HEK 293TX	Cell Line	Human	DMEM	10 % FBS + 100 U/ml P/S
MS5	Stroma Cell Line	Mouse	α-MEM	10 % FBS + 100 U/ml P/S
MSC	Primary	Human	α-MEM	10 % MSC-qualified FBS + 100 U/ml P/S

2.2 Primary Samples

2.2.1 Mesenchymal Stroma Cells

Primary human mesenchymal stroma cells (hMSCs) were purchased (Lonza) obtained from bone marrow aspiration (male, 19-years of age) or kindly provided by Dr. Dosquet (Universite Paris Diderot, Paris) from human bone marrow obtained during orthopaedic surgery from male and female donors above 50 years of age under ethical approval 10-038 from IRB00006477.

MSCs were expanded in α-MEM supplemented with 10 % MSC-qualified FBS and 100 U/mL P/S. All assays were performed with MSCs between passage 3 and 6.

2.2.2 Umbilical Cord Blood Cells

Umbilical cord blood was collected from mothers giving birth at the Royal London Hospital, in accordance with a protocol approved by the East London and Research Ethics Committee. Informed and written consent was obtained prior to collection of samples.

2.2.2.1 Separation of mononuclear cells by Ficoll density centrifugation

Cord blood samples were pooled and diluted with PBS at a 1:2 ratio. Diluted cord blood was slowly transferred onto 15 ml of Ficoll (GE Healthcare), dispensed into 50 ml Falcon tubes. After centrifugation at 1600 RPM for 30 minutes at RT with slow deceleration, the buffy coat

layer of mononuclear (MNC) cells was carefully removed, and remaining erythrocytes were lysed with ammonium chloride (in-house) for 10 minutes at room. Lysis was stopped with FBS, and the MNCs resuspended in 2 % FBS/PBS.

2.2.2.2 CD34 Positive Purification of HSPCs

MNCs were selected for $CD34^+$ cells using EasySep Human CD34 Positive Selection Kit (Stem Cell Technologies) according to manufacturer's instructions. All steps were performed using 2 % FBS/PBS. Briefly, MNCs were first incubated for 15 minutes with EasySep Positive Selection Cocktail at RT, then EasySep Magnetic nanoparticles were added for another round of incubation at RT for 10 minutes. $CD34^+$ cells were immune-magnetically isolated over at least five consecutive selection rounds, and purity was checked using compatible CD34 antibody clones on flow cytometry.

2.2.3 Acute Myeloid Leukaemia Samples

AML cells were obtained after informed consent from patients attending St Bartholomew's Hospital, London, under a protocol approved by the East London and City Research Ethics Committee.

Table 5. Genetic abnormalities in AML patient cohort

AML ID	Karyotype	FAB	NPM	FLT3	Risk Group
AML5	Normal	n.d.	n.d.	ITD	Intermediate
AML1	n.d.	n.d.	n.d.	n.d.	n.d.
AML2	Trisomy 8,21	n.d.	n.d.	n.d.	Poor
AML3	n.d.	M1	Mut	n.d.	n.d.
AML4	n.d.	M5	Mut	WT	n.d.
AML6	Complex	n.d.	n.d.	n.d.	poor
AML7	normal	M2	Mut	WT	intermediate
AML8	Normal	M1	Mut	ITD	intermediate
AML9	n.d.	n.d.	n.d.	n.d.	poor
AML10	Inv(3)(Q21Q26)/t(8;13)(p21)	M0	n.d.	n.d.	n.d.

2.3 Lentivirus production

All lentivirus particles were produced using a 2nd generation lentivirus packaging system obtained from Addgene (originally deposited by Didier Trono)

Day 0 HEK 293TX are plated at $6x10^4/cm^2$ in a 15 cm plate and incubated ON in DMEM supplemented with 10 % FBS and 100 U/mL P/S.

Day 1 At 70 % confluency the media is carefully replaced with 22 mL of fresh media and incubated for another two hours. For each 15 cm plate, 32 µg of plasmid DNA, 20 µg pCMVdR8.74 (contains tet, pol, gag, rev) and 9 µg pMD2.G (contains VSV-G) are mixed with dH_2O to a total of 1125µl. 125 µl of 2.5 M $CaCl_2$ is added dropwise and mixed thoroughly. After 5 min incubation 1250 µl of 2x HEPES (pH 7.2) is added drop by drop while the solution is vortexed at maximum speed. After another 15 min incubation, the solution is added to the 15 cm plate and incubated ON.

Day 2 All media is replaced by 15 ml of fresh media and incubated for 24h.

Day 3 All media is collected and filtered with a 0.45 µm Nalgene syringe filter (ThermoFisher Scientific) and stored ON at 4° C. 15 mL of fresh media are added to the plate and incubated for another final 24h.

Day 4 Again all media is collected and filtered and together with the media from the previous day centrifuged in an ultracentrifuge (Beckman Coultier) on a SW32Ti swinging bucket rotor at 22000 RPM for 2h with deceleration at 7/10. The supernatant is completely discarded and the bucket inserts are incubated on an orbital shaker at 4° C for min 2h. The concentrated virus is pooled, aliquoted and stored at -80° C.

2.3.1 Determination of virus titre

A frozen aliquot of the concentrated virus is diluted 1/400 in fresh media. $2x10^4$ HEK $293TX/cm^2$ are seeded in a 24-Well plate with 500 µl of fresh media and supplemented with a range of the diluted virus between 1-128 µl/well and incubated for 4 days. The GFP^+ population is measured by flow cytometry for each virus dilution and the virion per µl are calculated with the formula:

Virions per µl = (Percentage of GFP^+ Cells/100)*Dilution Factor*(1/µl of diluted virus)*number of 293TX

2.3.2 Lentivirus transduction

2.3.2.1 MSC

MSCs are seeded at 2.5x10^4/cm2 in a 12-well dish in 400 µL of media at a multiplicity of infection (MOI) of 10 and incubated at 37° C. After 16h the virus is removed and the MSCs are trypsinized and seeded. All co-cultured and scaffolds were started 4 days after MSC transduction.

2.3.2.2 HSPCs

$CD34^+$ HSPCs are resuspended at 0.2-0.5x10^6/mL Stem span SFEM II containing SCF 100 ng/ml, Flt3L 100 ng/ml, IL6 10 ng/ml, IL3 10 ng/ml, G-CSF 25 ng/ml (all cytokines from Peprotech, UK) and 100 U/ml P/S and pre-stimulated for 8h before adding lentivirus at MOI of 30. After 16h the cells are washed with PBS containing 2 % FBS and resuspended in Stem span SFEM II containing SCF 300 ng/ml, Flt3L 300 ng/ml and TPO 20 ng/ml. After another 2 days the GFP^+ HSPCs are FACS-sorted.

2.4 In vitro assays

2.4.1 Culture of MSCs with primary CB $CD34^+$HSPCs/AML patient samples and AML cell lines

All culture of HSPCs/AML patient samples was carried out on MSCs unless stated otherwise.
Day 0 Seeding of 2x10^4 MSCs in tissue culture-treated plastics.
Day 2 HSPCs alone or together with AML cell lines are resuspended in Myelocult H5100 (Stem cell technologies) supplemented with 100 U/mL P/S at densities of 0.4-1x10^5 HSPCs/mL or 1-8x10^5 AML patient samples/mL and 2x10^5 AML/mL and a 100 % media top-up is performed after 4 days.

When HSPCs or AML patient samples had to be isolated for functional analysis 0.4 µm polycarbonate transwell inserts (Corning) were used to separate AML cell lines from MSCs and $CD34^+$. Cells in the well were grown in 500 µl media and in the transwell in 200 µl.

For the comparison of direct contact and transwell $CD34^+$ cells were grown in the transwell and MSCs and AML in the well for 4 days.

For neutralisation experiments 1 µg/mL of blocking antibody or equivalent species Immunoglobulin G were added at the beginning of the experiment. STC1 measurements in the media were conducted according to the manufacturer's instructions using the STC1 ELISA kit (R&D Systems).

2.4.2 Culture of MSCs with primary HSPCs and primary AML cells.

Day 0 Seeding of $2x10^4$ MSCs in tissue culture-treated plastics.

Day 2 AML cells are resuspended in Myelocult H5100 (Stem cell technologies) supplemented IL-3, G-CSF and TPO (each 20 ng/mL) and 100 U/mL P/S at densities of $0.5\text{-}2x10^6$ AML/mL.

Day 4 The media is replaced with Myelocult H5100 (Stem cell technologies) containing 20 ng/mL SCF and 100 U/mL P/S. $CD34^+$ HSPCs are seeded at $0.4\text{-}1x10^5$ HSPCs/mL and a 50% media top-up is performed after 4 days.

2.4.3 Culture comparing feeder-free $CD34^+$ with AML and MSC co-cultured $CD34^+$ with AML

$CD34^+$ were cultured for 4 days in feeder-free conditions in stem span SFEM II (stem cell technology) containing SCF, FLT3L and TPO (all from PeproTech) at 100 ng/ml, 100 ng/ml and 20 ng/mL + 10 % FBS + 100 U/ml P/S. AML-HSPCs with MSCs were prepared as described above and cultured in the same media as the feeder-free condition. 50% media top-up is performed after 4 days.

2.5 Cell division tracking

Cells are resuspended at $1x10^6$/mL in PBS with 5 µM CellTrace Violet or CFSE (ThermoFisher Scientific) and incubated for 10 minutes at 37° C. Add 5 times the original staining volume of culture medium and centrifuge. Repeat the washing step 2 times and resuspend the pellet in the desired medium.

2.6 Preconditioning of MSCs

2.6.1 Generation of AML expressing inducible caspase 9 fragment

A plasmid with the MSCV.IRES.GFP retrovirus backbone expressing a product of FKBP1A fused with a Ser-Gly-Gly-Gly-Ser linker to the small and large subunit of the caspase 9 gene (originally deposited by David Spencer) was obtained from Addgene. Retrovirus production was carried out identically to the lentivirus production with the exception that retrovirus packaging constructs pHIT60 (expressing gag-pol) and pVSV-g (expressing VSV-G) were used (both a generous gift from Jonathan Stoye). AML cell lines were transduced at MOI 10 and sorted for GFP^+ cells (named AML iCasp9) 4 days afterwards.

2.6.2 Preconditioning with AML

MSCs were co-cultured for 5 days with AML iCasp9 cell lines then treated with 10 nM of AP1903 (Insight Biotechnology). 24h after the addition of AP1903 all apoptotic and dead AML cells were carefully washed away and $CD34^+$ HSPCs were seeded at $0.04\text{-}0.1x10^5$/ml.

2.6.3 Preconditioning with hypoxia

After 5 days of MSC culture under hypoxic conditions at 3 % O_2 the media was discarded and replaced with Myelocult H5100. $CD34^+$ HSPCs were seeded at $0.04\text{-}0.1x10^5$/ml.

2.7 Analysis of reactive oxygen species and mitochondrial membrane potential

TMRE (mitochondrial membrane potential) or cellrox deep red (reactive oxygen species) (both from ThermoFisher Scientific) were added 30 minutes before cells were harvested at 40 nM and 5 μM, respectively. MMP and ROS were measured via flow cytometry on 561 nm/594 nm and 640 nm/647 nm, respectively.

2.8 Colony-forming assay

2.8.1 Primary CFU-assay

220 $CD34^+$ HSPCs are resuspended in 1.1 mL methylcellulose (Methocult H4434 Stem Cell Technologies) containing SCF, GM-CSF, IL3 and EPO at manufacturer's concentration. 1 mL of the suspension is transferred one of the 6 inner wells a 12-well dish. The outer wells are filled with dH2O to prevent the methylcellulose from drying. Colonies are scored after 14 days by cell morphology, colony shape and colour into CFU-granulocyte (CFU-G), CFU-macrophage (CFU-M), CFU-granulocyte/macrophage (CFU-GM), burst-forming unit - erythrocyte (BFU-E) and CFU-granulocyte, erythrocyte, monocyte, megakaryocyte (CFU-GEMM).

2.8.2 Secondary CFU-assay

After the primary CFU-assay the methylcellulose is diluted with PBS and the colonies are dispersed with a pipette and transferred to a 15 ml falcon tube. After centrifugation at 300G for 7 minutes the supernatant is discarded and the pellet resuspended in 2 % FBS/PBS. $1.1x10^5$ cells are resuspended in 1.1 mL of fresh methylcellulose with cytokines (Methocult H4434, Stem Cell Technologies). 1 mL of the suspension is transferred one of the 6 inner wells a 12-well dish. The outer wells are filled with dH2O to prevent the methylcellulose from drying. Colonies are scored after 14 days. The number of colonies from $1x10^5$ cells is multiplied by the total number of cells obtained after the primary CFU-assay.

2.9 Long term colony initiation cell – Assay (LTC-IC)

2.9.1 Limiting dilution LTC-IC

As a feeder-layer MS-5 are seeded at $2x10^4$/cm2 on day 0 in a 96-Well plate in 8 rows of 5 columns. On day 1 the plate is irradiated at 7.5 grey. $CD34^+$ HSPCs are serially diluted ranging from 640 – 5 cells/well and resuspended Myelocult H5100 (Stem cell technologies). All media is removed from the 96-well plate and the serially-diluted cell suspension is added to the plate. Half medium exchanges are carried out weekly. After 5 or more weeks, the media is carefully removed and the wells are filled with 100 µL of methylcellulose (Methocult H4434 Stem Cell Technologies) containing SCF, GM-CSF, IL3 and EPO at an undisclosed concentration. The

wells are scored for colonies after 14 days. Positive wells contain one or more colonies while negative colonies contain no colonies.

2.9.2 Bulk Culture LTC-IC

Once the number of colonies per LTC-IC is determined with the limiting dilution LTC-IC a bulk culture LTC-IC can be performed.

As a feeder-layer MS-5 are seeded at $2x10^4$/cm2 on day 0 in a 12-well dish. On day 2 the plate is irradiated at 7.5 grey. 4000 $CD34^+$ HSPCs are resuspended in 1 ml of Myelocult H5100 (Stem cell technologies). The media from the irradiated feeder-layer plate is removed and replaced with 1 ml of the HSPC suspension per Well. 500 µl of media is exchanged twice a week. After 5 or more weeks, all cells are collected and FACS sorted using a surface marker staining for human CD45 and murine SCA-1 to discriminate MS-5 ($Sca\text{-}1^+CD45^-$) and haematopoietic cells ($Sca\text{-}1^-CD45^+$). $2.2x10^4$ of haematopoietic cells are resuspended in 1.1 ml of methylcellulose (Methocult H4434 Stem Cell Technologies) containing SCF, GM-CSF, IL3 and EPO at manufacturer's concentration. 1 mL of the suspension is transferred one of the 6 inner wells a 12-well dish. The outer wells are filled with dH2O to prevent the methylcellulose from drying. Colonies are scored after 14 days. The number of colonies from $2x10^4$ cells is used to calculate the total number of colonies from the progeny of 4000 HSPCs. The total colony number is then divided by the average colony output per LTC-IC which determines the number of LTC-IC per 4000 HSPCs.

2.10 *In vivo* assays

2.10.1 Mice

All animal experiments were performed under the project license (PPL 70/8904) approved by the Home Office of UK and in accordance to The Francis Crick institute animal ethics committee guidelines. NOD.Cg-Prkdcscid Il2rgtm1Wjl/SzJ (NOD/SCID/IL2 receptor 2 gamma chain null, NSG) and NOD.Cg-Prkdcscid Il2rgtm1Wjl Tg(CMV-IL3,CSF2,KITLG)1Eav/MloySzJ (NOD/SCID/IL2 receptor 2 gamma chain null –SCF GM-CSF IL3, NSG-SGM3) mice were obtained from Jackson Laboratory (Bar Harbour, Maine, USA) and bred at the Francis Crick Institute.

2.10.2 Human Xenografts

7 days prior to transplantation mice were put on acidified water. 24 hours prior to transplantation 8-12-week-old mice were sublethally irradiated with 3.75 Gy from a ^{137}Caesium source (IBL 637 Gamma Irradiator). The mice were administered prophylactic antibiotics (Baytril 2.5% via drinking water) three times per week for two weeks after irradiation.
In the primary engraftment purified $CD34^+$ cells, 30000 - 45000 cells per mouse, were injected per mouse in a volume of 150 µl 2 % FBS/PBS. For secondary engraftment $4x10^6$ purified $hCD45^+$ cells (Isolated with human/mouse chimaera isolation kit from Stem cell Technologies) in a volume of 150 µl were injected per mouse.

Mice were first warmed in a heat box to 38°C to dilate the tail vein and cells were injected intravenously with a 30 G needle and 0.5 ml syringe.

2.10.2.1 Analysis of human engraftment (12 weeks)

Engraftment of human cells in the murine bone marrow was assessed 12 weeks post-injection. Mice were sacrificed by cervical dislocation and tibia, femur and ilium dissected bilaterally. Bone marrow was harvested by flushing the bone cavity with 2% FBS/PBS using a 30 G needle and 1 ml syringe or by crushing with pestle and mortar, each mouse was processed individually. Remaining erythrocytes were lysed with 2-3 ml of ammonium chloride for 3 minutes at room temperature. The reaction was stopped by addition of an equal volume of FBS and cell were pelleted. The sample was then processed for FACs analysis as described in the next section.

2.10.2.2 Bone marrow aspiration (8 weeks)

Bone marrow cells were sampled from the tibia of anaesthetized mice with a 30 G needle and 0.5 ml syringe 8 weeks post-transplantation. The aspirated cells were resuspended in 0.5 ml of 2% FBS/PBS.

2.11 Scaffold

2.11.1 Scaffold preparation

All the experimental procedures were performed according to aseptic operating conditions. Gelfoam gelatine sponges (2 cm x 6 cm x 7mm) (Pfizer, Kalamazoo, MI, USA) were cut into 24 equally sized squares, washed once with ethanol 70% and two times with PBS. MSCs were resuspended in α-MEM with 10 % FBS at $1x10^6$ cells/ml and 100µl ($1x10^5$ cells) were carefully injected into each scaffold. The scaffolds were cultured in polystyrene ultra-low attachment 24 well plates and MSCs allowed to adhere for 3-5 hours prior to addition of media. Scaffolds were then cultured for 3 to 5 days to allow MSCs to expand. HSPCs ($1x10^5$ $CD34^+$), AML Cell lines ($0.1x10^5$) and AML Patient samples ($1\text{-}5x10^5$ MNC) were injected in these MSC-seeded scaffolds and media was replaced to Myelocult H5100 (Stem Cell Technologies). Myelocult H5100 (Stem Cell Technologies) was supplemented with cytokines (20ng/ml G-CSF, 20ng/ml IL-3 and 20ng/ml TPO from PeproTech, London, UK) when AML patient samples were used.

2.11.2 Surgery and pre- and post-surgery care

All animal experiments were performed in accordance to Home Office and Crick guidelines. Anti-inflammatory and pain-killer drugs Caprofren (Rimadyl, Zoetis) or Metacam (Boehringer Ingelheim) were administrated 24 hours before surgical procedure to each animal in the drinking water or mixed with egg custard, respectively. Anaesthesia was induced with 2-2.5% isoflurane (Abbott Vet Isoflurane) and O_2 at 2-4%. 24h before surgery the fur on the back of the animal was shaved and immediately prior to surgery sterilised with 0.8 % chlorhexidine in H_2O. Along the spine two 0.5 cm incisions spaced 3 cm from each other were made. Subcutaneous pockets along the sides of the animals were formed with scissors and scaffolds placed inside (1 per pocket) and the incision was closed with staples. Up to six scaffolds were implanted per mouse. Buprenorphine (Vetergesic, Alstoe) and Metacam (Boehringer Ingelheim) was subcutaneously injected and animals were allowed to recover from anaesthesia in a prewarmed cage. After surgery, animals were checked frequently for their well-being. Rimadyl in the drinking water or Metacam in baby egg custard was provided daily until 48 hours after surgery. At endpoint, all scaffolds were harvested and then digested in a HBSS digestion solution containing 2% FBS, DNase I (10 µg/ml), Collagenase (1 mg/ml), Dispase II (5 mg/ml) and Heparin (20 U/ml) at 37°C for 1.5h. The reaction was stopped with 3 volumes of MSC media.

2.12 Flow Cytometry

2.12.1 Extracellular Staining and Analysis Parameters

Cells were incubated with antibodies at room temperature for 15 minutes, or 4°C for 30-60 minutes, in the dark in 100 µl 2 % FBS/PBS. Samples were subsequently washed and suspended in DAPI (4', 6'-diamidino-2-phenylindole) at concentration 100 ng/ml in 2 % FBS/PBS and analysed on a flow cytometer (LSR Fortessa or LSRII from BD Biosciences or MACSQuant Analyser 10 from Miltenyi Biotec).
Single colour controls were prepared with OneComp compensation beads (eBiosciences). Gates were set to exclude non-viable cells, debris and doublets during analysis. For absolute quantification, CountBright™ Absolute Count beads (Life Technologies) were used at 5000-10000 beads per sample.

2.12.2 AnnexinV Staining

Cells were resuspended in 100 µL 1x AnnexinV staining buffer (BD Pharmigen, BMS306PE/100) containing 5 µL of anti-AnnexinV antibody together with other cell surface staining antibodies. The suspension was allowed to incubate for 15-30 minutes at RT in the dark and washed and resuspended with AnnexinV staining buffer. 100 ng/mL DAPI was added to label dead cells and debris. Live cells undergoing apoptosis were identified as DAPI negative and AnnexinV positive. DAPI and AnnexinV double-positive cells were classed as dead.

2.12.3 Intracellular Staining

Cells were first stained for extracellular markers, washed with PBS and fixed and permeabilisation using the cytofix/cytoperm kit (BD biosciences) according to the manufacturer's instructions. The cells are fixed with PFA (Para-formaldehyde) containing fixation buffer at 4°C for 20 minutes. Cells were washed in with permeabilisation-wash buffer containing saponin and resuspended in 100 µl staining solution consisting of the antibodies and permeabilisation-wash buffer. Primary and secondary antibody staining was carried out over 1h at 4°C. Cells were washed with permeabilisation-wash buffer and resuspended in DAPI 1 µg/ml with 2% FBS/PBS and analysed.

2.12.4 Ki67 and EdU staining

For cell cycle analysis cells were fixed and permeabilised as described and stained with 2 µl of anti-Ki67- APC. Staining was performed for ON at 4°C. Cells were washed in 2 % FBS/PBS and resuspended in 300 µl 2 % FBS/PBS with DAPI 1 µg/ml.

For EdU analysis 200 µl of 10 mM EdU PBS solution was injected intraperitoneal (IP) 16h before the mice were culled. After scaffold harvest and digestion, the cells were fixed and permeabilised according to Click-it plus EdU Alexa 647 flow cytometry assay kit instructions (Thermo Scientific). After fixation the cells were stored ON at 4°C for any remaining PFA to evaporate. On the next day the cells were stained in Alexa 647 click-it staining cocktail for 30 min at RT and subsequently flow cytometry analysed. As negative control an aliquot of cells was stained with click-it staining cocktail without Alexa 647 picolyl azide.

2.12.5 Cell Sorting

Cells were stained as previously described and as appropriate for the assay. Samples were resuspended in 1 ml DAPI 100 ng/ml in 2% FBS/PBS and filtered through a 40 µm mesh filter (BD Biosciences) to remove clumps and samples kept on ice. Sorting was performed on either MoFlo XDP (Beckman Coulter), BD FACS Aria or BD Influx sorters using a 100 µm nozzle. Collection tubes contained 2% FCS/PBS and purity checks were performed to check sort quality.

2.13 Molecular Biology

2.13.1 RNA Extraction

The direct-zol RNA purification kit (Zymo Research) was used for samples $<1x10^5$ cells and the RNeasy Mini kit (Qiagen RNeasy) for samples between $1x10^5$ - $1x10^7$ cells. RNA was extracted using the according to manufacturer's protocol. RNA was eluted in RNase-free distilled water. The RNA concentration and purity were quantified on the Nanodrop 2000c Spectrophotometer (Thermo Scientific) by measuring absorbance at 230 nm, 260 nm and 280 nm. Samples were stored at -80°C.

2.13.2 Reverse Transcription

RNA was reverse transcribed to cDNA using Superscript III M-MLV reverse transcriptase (Invitrogen), according to manufacturer's protocol. A maximum of 1 µg of total RNA and oligo dT20 primers were used per 20 µl reaction. The reaction was incubated for 30-60 minutes at 50°C, and then inactivated at 70°C for 15 minutes. cDNA was stored at -20°C.

2.13.3 Quantitative real-time PCR

All quantitative PCR (QPCR) was performed with SybrGreen. Reactions were performed in 10 µl reactions in 384-well plates with the following components: 3-20 ng cDNA, forward and reverse primers at 300 nM each, 5 µl of SYBR® Green Mastermix (Applied Biosystems) and distilled water to 10 µl. Reactions were always run at least in duplicate. GAPDH (for HSPCs) and Ribosomal Protein L18A (RPL18A) (MSC) was used as housekeeping gene controls. Thermal cycling was performed on a QuantStudio™ 5/7 (Applied Biosystems) using the standard manufacturer's settings and mRNA expression was quantified with the Comparative CT Method.

2.13.4 Western blotting

Cells were lysed in RIPA buffer containing a protease and phosphatase inhibitor cocktail (all from Sigma). The protein concentration was measured with a Lowry protein assay (DC Protein Assay from BioRad). Total protein extracts (20-30 µg) were mixed with 4x Nupage Loading buffer (ThermoFisher Scientific) and boiled at 96° C for 5 min. The samples were run on a denaturing precast 8-12 % bis-tris Nupage gel (ThermoFisher Scientific) and transferred by wet transfer to nitrocellulose membranes. Primary antibodies were incubated ON at 4° C and secondary antibodies 1h at RT. Protein bands were visualised using an enhanced chemiluminescence visualisation system (ECL Plus, Amersham Life Sciences).

2.14 Statistical Analysis

The results are shown as mean +/- SEM unless stated otherwise. All statistical analyses were performed using GraphPad Prism software. The unpaired or paired Student's t-test was used unless indicated otherwise. A p-value <0.05 was considered significant.

Table 6. Antibodies

Antigen	Species	Clone	Manufacturer	Catalogue number
β–Actin	Human	AC-15	Sigma	A1978
CD135	Human	4G8	BD	583494
CD19	Human	HIB19	BD	555412
CD3	Human	UCHT1	BD	555333
CD33	Human	WM53	BD	551378
CD34	Human	4H11	eBioscience	25-0349-42
CD34	Human	8G12	BD	347222
CD34	Human	581	BD	555824
CD38	Human	HB7	eBioscience	25-0388-42
CD45	Human	HI30	eBioscience	25-0459-42
CD45	Mouse	30-F11	eBioscience	45-0451-82
CD45RA	Human	HI100	eBioscience	47-0458-42
CD49f	Human	GoH3	BD	555736
CD51	Mouse	RMV-7	eBioscience	12-0512-83
CD73	Human	AD2	BD	563199
CD90	Human	eBio5E10	eBioscience	17-0909-42
HIF-1α	Human	54/HIF-1α	BD	610959
HLA-A2	Human	BB7.2	BD	558570
Ki67	Human	20RAJ1	eBioscience	50-5699-82
Lineage cocktail	Human	CD3 (clone SK7), CD16 (clone 3G8), CD19 (clone SJ25C1), CD20 (clone L27), CD14 (clone MφP9), CD56 (clone NCAM16.2)	BD	340546
STC1	Human	N-15	Santa Cruz	sc-14346

Table 7. shRNA sequences

Target	Sequence
shCTL(dsRed)	GCTCCAAGGTGTACGTGAATTCAAGAGATTCACGTACACCTTGGAGC
HIF-1α	GATGTTAGCTCCCTATATCCCTTCAAGAGAGGGATATAGGGAGCTAACATC
shCTL (lacZ)	GTCGGCTTACGGCGGTGATTTCTCGAGAAATCACCGCCGTAAGCCGAC
STC-1 #1	GCATGTCTTAAATGCTCATAACTCGAGTTATGAGCATTTAAGACATGC
STC-1 #2	GTACTGTGCCTGGTTTGATTTCTCGAGAAATCAAACCAGGCACAGTAC

Table 8. RT-PCR primer sequences

Gene	Species	5’ sequence	3’ sequence
STC-1	Human	TGAGGCGGAGCAGAATGACT	CAGGTGGAGTTTTCCAGGCAT
STC-2	Human	GGTGGACAGAACCAAGCTCTC	CGTTTGGGTGGCTCTTGCTA
VEGF-A	Human	ATGAACTTTCTGCTGTCTTGGGT	TGGCCTTGGTGAGGTTTGATCC
RPL18A	Human	GGAGAGCACGCCATGAAG	AAGATTCGCATGCGGTAGAG
IGF-BP1	Human	TCAAAAAATGGAAGGAGCCCT	AATCCATTCTTGTTGCAGTTT
IGF-BP2	Human	CACCGGCACATGGGCAA	GAAGGCGCATGGTGGAGAT
PDK1	Human	CGGATCAGAAACCGACACA	ACTGAACATTCTGGCTGGTGA
GLUT1	Human	AACTCTTCAGCCAGGGTCCAC	CACAGTGAAGATGATGAAGAC
IFN-α	Human	GACTCCATCTTGGCTGTGA	TGATTTCTGCTCTGACAACCT

HIF-1α (mut): (Proline/Asparagine to Alanine conversion)

ATGGAGGGCGCCGGCGGCGCGAACGACAAGAAAAAGATAAGTTCTGAACGTCGAAAAGAAAAGTCTCGAG
ATGCAGCCAGATCTCGGCGAAGTAAAGAATCTGAAGTTTTTTATGAGCTTGCTCATCAGTTGCCACTTCC
ACATAATGTGAGTTCGCATCTTGATAAGGCCTCTGTGATGAGGCTTACCATCAGCTATTTGCGTGTGAGG
AAACTTCTGGATGCTGGTGATTTGGATATTGAAGATGACATGAAAGCACAGATGAATTGCTTTTATTTGA
AAGCCTTGGATGGTTTTGTTATGGTTCTCACAGATGATGGTGACATGATTTACATTTCTGATAATGTGAA
CAAATACATGGGATTAACTCAGTTTGAACTAACTGGACACAGTGTGTTTGATTTTACTCATCCATGTGAC
CATGAGGAAATGAGAGAAATGCTTACACACAGAAATGGCCTTGTGAAAAAGGGTAAAGAACAAAACACAC
AGCGAAGCTTTTTTCTCAGAATGAAGTGTACCCTAACTAGCCGAGGAAGAACTATGAACATAAAGTCTGC
AACATGGAAGGTATTGCACTGCACAGGCCACATTCACGTATATGATACCAACAGTAACCAACCTCAGTGT
GGGTATAAGAAACCACCTATGACCTGCTTGGTGCTGATTTGTGAACCCATTCCTCACCCATCAAATATTG
AAATTCCTTTAGATAGCAAGACTTTCCTCAGTCGACACAGCCTGGATATGAAATTTTCTTATTGTGATGA
AAGAATTACCGAATTGATGGGATATGAGCCAGAAGAACTTTTAGGCCGCTCAATTTATGAATATTATCAT
GCTTTGGACTCTGATCATCTGACCAAAACTCATCATGATATGTTTACTAAAGGACAAGTCACCACAGGAC
AGTACAGGATGCTTGCCAAAAGAGGTGGATATGTCTGGGTTGAAACTCAAGCAACTGTCATATATAACAC
CAAGAATTCTCAACCACAGTGCATTGTATGTGTGAATTACGTTGTGAGTGGTATTATTCAGCACGACTTG
ATTTTCTCCCTTCAACAAACAGAATGTGTCCTTAAACCGGTTGAATCTTCAGATATGAAAATGACTCAGC
TATTCACCAAAGTTGAATCAGAAGATACAAGTAGCCTCTTTGACAAACTTAAGAAGGAACCTGATGCTTT
AACTTTGCTGGCCGCCGCCGCTGGAGACACAATCATATCTTTAGATTTTGGCAGCAACGACACAGAAACT
GATGACCAGCAACTTGAGGAAGTACCATTATATAATGATGTAATGCTCCCCTCACCCAACGAAAAATTAC
AGAATATAAATTTGGCAATGTCTCCATTACCCACCGCTGAAACGCCAAAGCCACTTCGAAGTAGTGCTGA
CCCTGCACTCAATCAAGAAGTTGCATTAAAATTAGAACCAAATCCAGAGTCACTGGAACTTTCTTTTACC
ATGCCCCAGATTCAGGATCAGACACCTAGTCCTTCCGATGGAAGCACTAGACAAAGTTCACCTGAGCCTA
ATAGTCCCAGTGAATATTGTTTTTATGTGGATAGTGATATGGTCAATGAATTCAAGTTGGAATTGGTAGA
AAAACTTTTTGCTGAAGACACAGAAGCAAAGAACCCATTTTCTACTCAGGACACAGATTTAGACTTGGAG
ATGTTAGCTGGCTATATCCCAATGGATGATGACTTCCAGTTACGTTCCTTCGATCAGTTGTCACCATTAG
AAAGCAGTTCCGCAAGCCCTGAAAGCGCAAGTCCTCAAAGCACAGTTACAGTATTCCAGCAGACTCAAAT
ACAAGAACCTACTGCTAATGCCACCACTACCACTGCCACCACTGATGAATTAAAAACAGTGACAAAAGAC

CGTATGGAAGACATTAAAATATTGATTGCATCTCCATCTCCTACCCACATACATAAAGAAACTACTAGTG
CCACATCATCACCATATAGAGATACTCAAAGTCGGACAGCCTCACCAAACAGAGCAGGAAAAGGAGTCAT
AGAACAGACAGAAAAATCTCATCCAAGAAGCCCTAACGTGTTATCTGTCGCTTTGAGTCAAAGAACTACA
GTTCCTGAGGAAGAACTAAATCCAAAGATACTAGCTTTGCAGAATGCTCAGAGAAAGCGAAAAATGGAAC
ATGATGGTTCACTTTTTCAAGCAGTAGGAATTGGAACATTATTACAGCAGCCAGACGATCATGCAGCTAC
TACATCACTTTCTTGGAAACGTGTAAAAGGATGCAAATCTAGTGAACAGAATGGAATGGAGCAAAAGACA
ATTATTTTAATACCCTCTGATTTAGCATGTAGACTGCTGGGGCAATCAATGGATGAAAGTGGATTACCAC
AGCTGACCAGTTATGATTGTGAAGTTGCCGCTCCTATACAAGGCAGCAGAAACCTACTGCAGGGTGAAGA
ATTACTCAGAGCTTTGGATCAAGTTAACTGA

Chapter 3. *Ex vivo* modelling the AML crosstalk with microenvironment and normal haematopoietic HSPCs

3.1 Introduction

The mechanics of how AML utilises and reshapes the BM microenvironment has received increased scientific interest in recent years. In particular, the non-haematopoietic niche components have seen extensive approaches to weight their contribution to the SCN and measure quantitative and qualitative changes during AML. At the same time, normal HSPCs from murine and human AML patients show increased quiescence and egress from the BM niche and several groups successfully implicated the AML niche for this phenotype (Duarte et al., 2018; Gong et al., 2018; Hanoun et al., 2014).

During the progression of AML, mature haematopoietic cells are increasingly replaced by AML blast. HSPCs are also numerically sharply reduced but at different rates, enriching specific populations in the remaining normal haematopoietic compartment. Restricted progenitors (HPCs), like MEPs, are equally lost relative to the number of total normal mononucleated cells (MNCs), but also in absolute numbers. MPPs and HSCs are numerically reduced as well but are more resilient and relatively enriched among MNCs (Cheng et al., 2015; Miraki-Moud et al., 2013).

Precise mechanistic studies, especially involving human specimens, are still rare owing to the complexity of the niche and often scarcity of samples. The current literature covers mostly murine HSPCs from the murine MLL-AF9 fusion gene model (Akinduro et al., 2018; Cheng et al., 2015; Duarte et al., 2018; Gong et al., 2018) and the AML xenotransplant into NSG mice (Miraki-Moud et al., 2013). Human $CD34^{+}$ HSPCs from AML patients have been exclusively studied in $CD34^{-}$ NPM1 mutated AML due to phenotypic distinction between HSPCs and AML (Miraki-Moud et al., 2013). In recent years, aldehyde dehydrogenase activity (ALDH) has emerged as promising new markers to distinguish normal from leukaemic HSPCs. However, selection pressures from pre-existing conditions like MDS or clonal haematopoiesis may complicate a direct comparison of non-leukaemic HSCs from AML patients with aged-matched HSPCs (Hoang et al., 2015; Wang et al., 2017). Lastly, Boyd et al.co-transplanted normal CB HSPCs with AML patient samples in NSG mice and observed a lack of myeloid-erythroid differentiation owing to a deteriorated adipocyte niche. However, it is unclear to what

extent their data reflects an AML-HSPC crosstalk or a competition for the SCN between LICs and HSCs (Boyd et al., 2017).

In summary, the complex non-haematopoietic and haematopoietic BM environment are extensively impacted by AML. The BM niche provides a suitable environment for AML proliferation, but it is not clear to what extent a complex BM niche is necessary to provoke defective HSPC expansion. Our objective was to develop an *ex vivo* and *in vivo* niche system to capture AML – HSPC interactions directly and indirectly via the mesenchymal stroma niche. A fully humanised environment may be of particular importance for AML and allows interactions without species barrier limitations (Abarrategi et al., 2017). In this system, the interactions could be precisely quantified, functionally investigated and modulated.
BM MSCs can be easily isolated, expanded and cultured *ex vivo* and facilitate the maintenance of normal and malignant cells making them excellent representatives of the bone marrow niche (Griessinger et al., 2014; Rouault-Pierre et al., 2017; Walenda et al., 2010). Additionally, MSCs co-cultured with AML or directly isolated from AML patients are distinct from their normal BM MSCs implying extensive remodelling of the mesenchymal niche (Battula et al., 2017; Geyh et al., 2018; Jacamo et al., 2014). CB $CD34^+$ HSPCs cells were chosen as normal haematopoietic component due to availability, higher *ex vivo* performance compared to their adult BM counterparts (da Silva et al., 2009).

3.2 Results

3.2.1 Quantitative analysis of normal CB HSPCs co-cultured of with BM MSCs and AML

The two known impacts of AML on HSPCs are numeric reduction and egress from BM. While homing could be mimicked via an SDF1 migration/homing assay, egress poses difficulties to mimic in a culture dish. Hence, we first measured quantitative changes of phenotypically defined total haematopoietic cells ($CD45^+$), HPCs ($CD34^+CD38^+$ or +/+) and HSPCs ($CD34^+CD38^-$ or +/-) by flow cytometry.

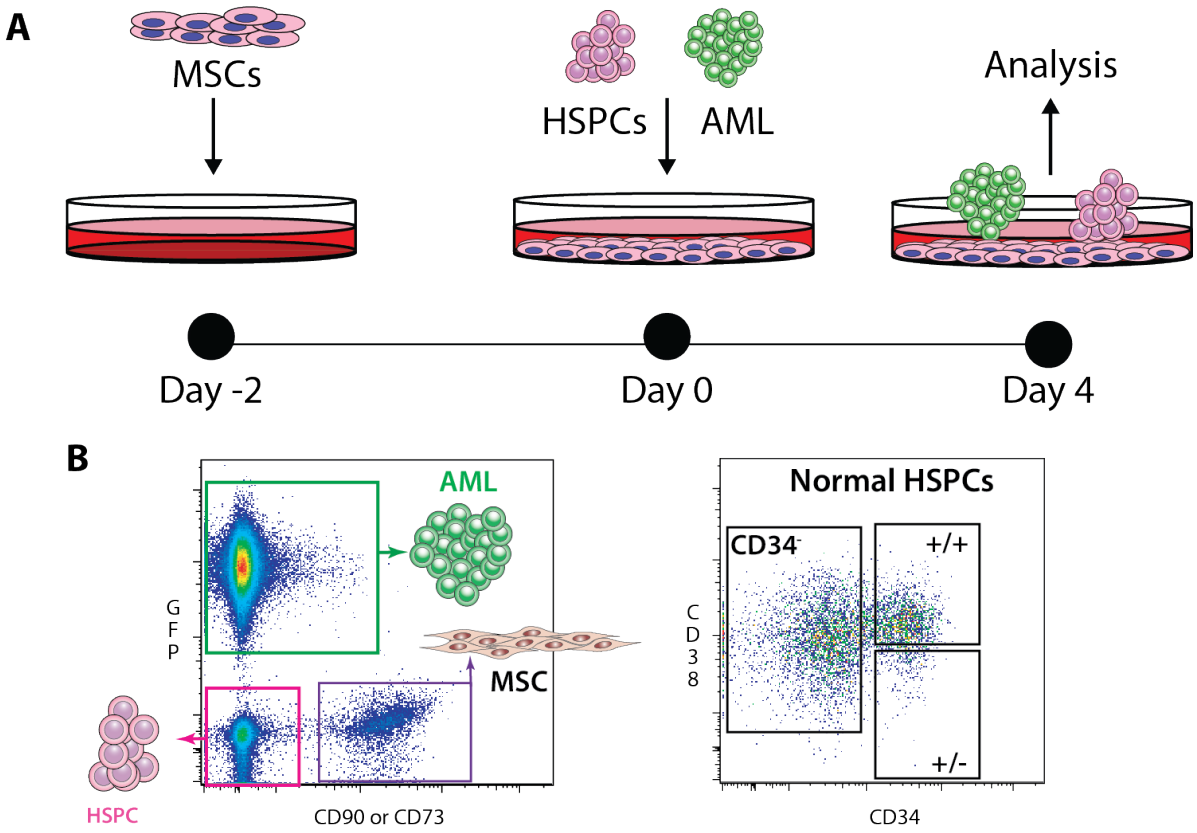


Figure 5. Schematic of in vitro culture protocol and cell separation
(A) MSCs were plated on culture dish 48h prior to seeding of CB HSPCs and AML. After 4 days all cells were collected and processed accordingly for downstream analysis. **(B)** Non-leukaemic HSPCs were separated from AML and MSCs via expression CD45 and absence of GFP, CD73/CD90 expression. Normal HSPCs were further separated into CD34-, HPCs ($CD34^+CD38^+$) and HSPCs ($CD34^+CD38^-$).

Since MSCs highly express CD73 and CD90 and are devoid of CD45, we used these markers to separate haematopoietic cells ($CD90^{-/low}$ or $CD73^-$ and $CD45^+$) from MSCs. AML cell lines were transduced with a lentivirus vector to express green fluorescent protein (GFP) to discriminate normal HSPCs from AML (Figure 5). When AML patient samples were tested,

we used human leukocyte antigen – A2 (HLA-A2) mismatched between AML and normal CB HSPCs to separate the respective cells using an HLA-A2 specific fluorophore-conjugated antibody.

3.2.1.1 Time course analysis with AML cell line

Firstly, we performed a time-course analysis to determine the growth kinetics of HSPC co-cultured with AML cell line U937. As comparison, CB HSPCs cultured without AML under identical culture conditions, termed $CD34^+$ alone, were used as controls throughout all *ex vivo* work. Since cryopreserved CB HSPCs were used, which necessitate a 48h recovery period, no measurements were taken during the first 48h. The ratio of AML:normal HSPCs at day 0 was 3:1 for AML cell lines to mimic extensive BM infiltration.

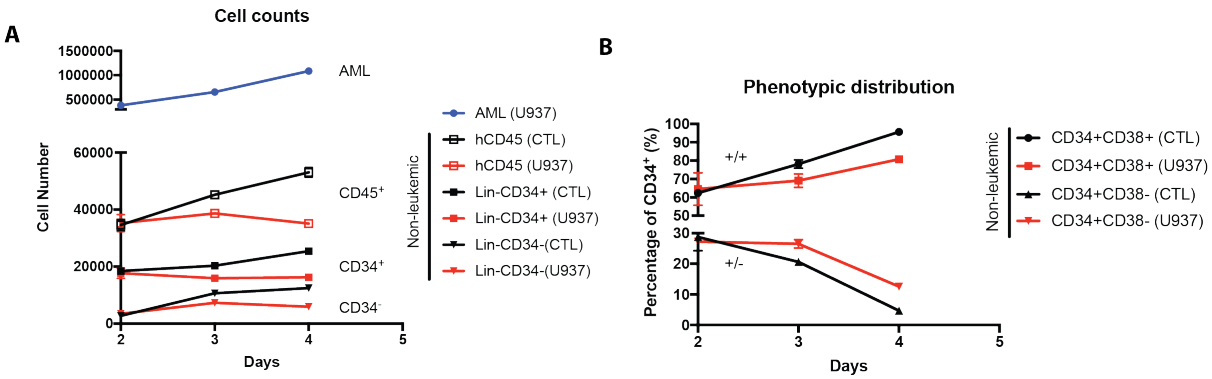


Figure 6. 4-day time course analysis of HSPC cultured with and without AML cell line U937

(A) Cell counts of total non-leukaemic haematopoietic cells (hCD45) and undifferentiated $CD34^+$ (Lin^-CD34^+) and $CD34^-$ (Lin^-CD34^-) from $CD34^+$ alone (black line/CTL) and together with AML cell line U937 (red line/U937) (B) Cell counts of $CD34^+$ sub-fractions HPCs +/+ and HSPCs +/- were divided by total $CD34^+$ cells to obtain the distribution among $CD34^+$; CTL – Control; Error bars are +/- SEM (standard deviation of the mean) (n=2 technical replicates)

Without AML cell line U937, normal HSPCs (black lines) expanded quickly between 2-4 days and a population doubling of total non-leukaemic haematopoietic cells ($CD45^+$) was estimated every 78h. As the $CD34^+$ exit their mostly quiescent state from day 0, the $CD34^+$ cells give rise to more differentiated cells lacking CD34 and yet also distinct lineage marker expression (Figure 5A). Within the remaining $CD34^+$ cells, the +/- fraction progressively acquires CD38 expression and becomes +/+ progenitors (Figure 6B). In the presence of AML cell line U937 (red line), no expansion of total and $CD34^+$ haematopoietic cells were observed at time points

between 2 to 4 days (Figure 6A). Furthermore, +/- HSPCs were proportionally and even numerically enriched among the total haematopoietic cells at the expanse of +/+ progenitors (Figure 6B). Of note, U937 population doubling was estimated at 34h and 36h for day 3 and day 4, respectively, indicating that AML proliferation remained mostly unperturbed (Figure 6A). This data shows that AML cell lines U937 is capable of selectively impeding HSPC expansion *ex vivo*.

3.2.1.2 Screen with AML cell lines and AML patient samples

To make sure that the effect seen was not specific to the cell line used, we carried out a larger screen on HSPCs with a range of AML cell lines (HL60, ML1, U937, KG1A, NB4, MOLM13 and OCI-AML3) and patient samples to cover multiple genetic abnormalities recurrent in AML. Each cell line and patient were assigned a specific symbol which is kept consistent throughout this report (Table 1)

Table 9. AML cell lines and patient samples and their respective symbols in graphs

AML Cell Line	Symbol	*AML Patient Sample* **CD34$^+$ alone**	Symbol
MOLM-13	▼	*AML1*	□
KG1A	○	*AML2*	▲
ML1	⬢	*AML3*	○
U937	◭	*AML4*	◇
KG1	▬	*AML5*	◆
HL60	◒	*AML8*	▼
OCI-AML3	◆	*AML10*	⬢
NB4	★	**CD34$^+$ alone**	●

AML patient samples were given a 48h pre-culture recovery phase and a higher ratio of at least 10:1 to compensate for apoptosis which often initially occurs during AML *ex vivo* cultures. We also added a second control by adding normal CB mononucleated cells at a 3:1 ratio to mimic the conditions of healthy bone marrow, called + normal CB mononucleated cells. Normal CB mononucleated cells consist mainly of $CD3^+$ T-lymphocytes and to a lesser extent $CD33^+$ myeloid and $CD19^+$ B-cells (Figure 7). In comparison, BM mononucleated cells contain comparable compositions consisting of around 22 % $CD3^+$ T-cells, 4 % B-cells and 32 % myeloid cells (Hassan et al., 1996; Yang et al., 2013).

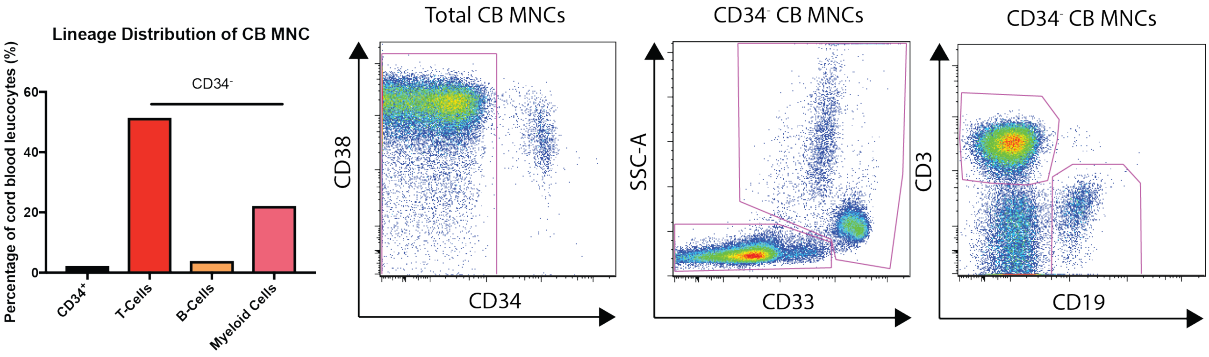


Figure 7. Lineage Distribution of normal CB MNCs
Normal CB mononucleated cells were analysed for expression of B-cell marker CD19, pan-myeloid marker CD33 and T-cell marker CD3. (n=1)

Consistent with the previous results, after 4 days, all cultures containing AML, (+ AML cell lines and + AML patient samples), contained between 24-38 % fewer total haematopoietic cells ($CD45^+$) and 13-60 % less +/+ progenitor than $CD34^+$ alone or + normal CB MNCs controls (Figure 8A). Furthermore, within $CD34^+$ cells, we observed a 2 to 4-fold higher proportion of +/- at the expense of +/+ progenitors (Figure 8B).

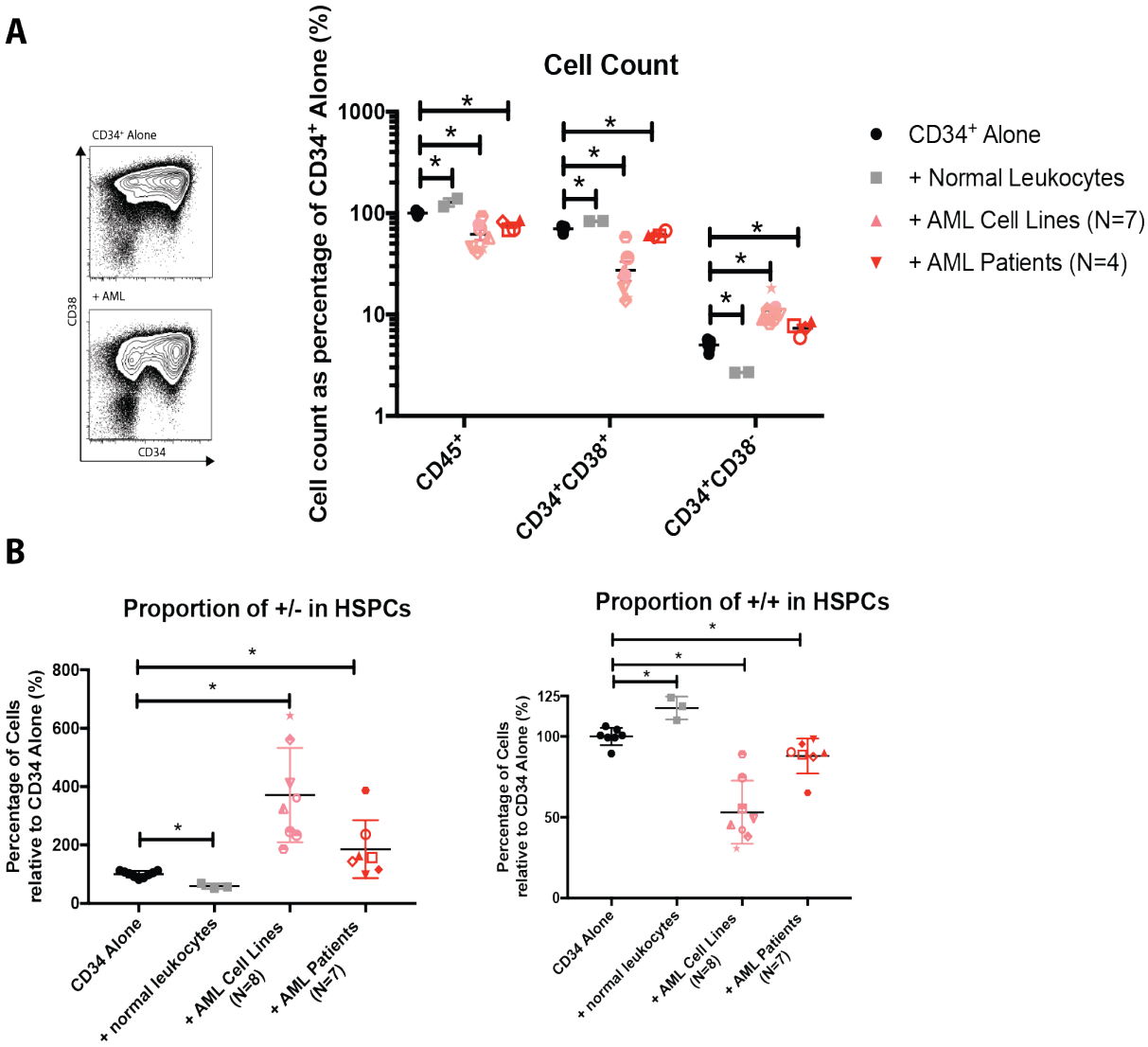


Figure 8. Relative cell counts and phenotypic distributions of non-leukaemic haematopoietic cells after 4 days

(A) Representative flow cytometry plots of non-leukaemic HSPCs and cell counts of total non-leukaemic haematopoietic cells (hCD45) and HPCs +/+ and HSPCs +/- from $CD34^+$ alone, + normal CB MNCs, + AML cell lines and + AML patients. (B) Cell counts of $CD34^+$ sub-fractions were divided by total $CD34^+$ cells to obtain the distribution among $CD34^+$; for + AML cell lines and + AML patients each dot represents a different cell line or patient sample from three different experiments (n = 3). *p<0.05. Error bars are +/- SEM

Interestingly, + normal CB MNCs controls accelerate the expansion of HSPCs as opposed to AML and $CD34^+$ alone ruling out non-specific effects from normal haematopoietic cells (Figure 8A/B). Additionally, the extent by which HSPC expansion was suppressed depended on the AML cell line or patient samples but did not significantly correlate with AML cell numbers (Figure 9). In a separate experiment normal CB MNCs were FACS-sorted into $CD3^+$ T-cells, $CD19^+$ B-Cells and $CD33^+$ myeloid cells and co-cultured with CB HSPCs. Again, the recovery of total and $CD34^+$ haematopoietic cells was not affected by non-malignant B-, T-

and myeloid lineage cells (Figure 10). This indicates that mutationally diverse AML cell lines and patient samples suppress HSPCs and since non-malignant BM cells could not reduce HSPC expansion, this effect is AML-specific.

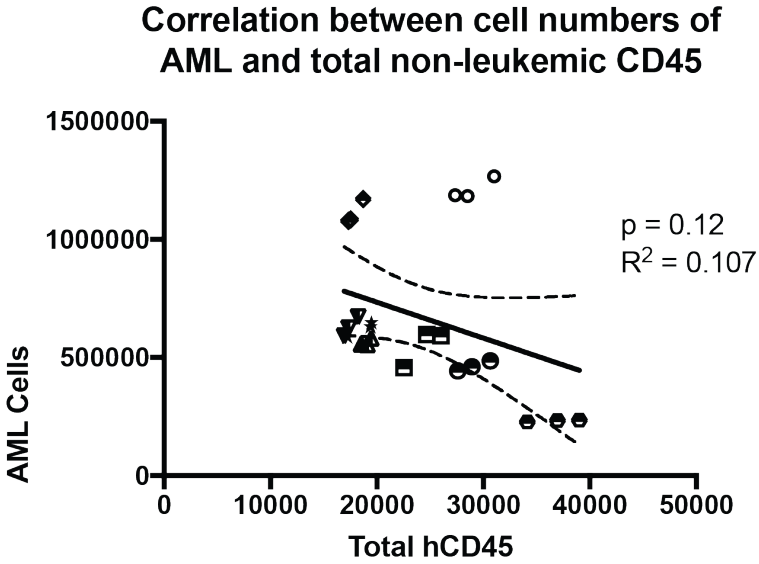


Figure 9. Relationship between numbers of AML cells and total non-leukaemic haematopoietic cells

Best curve fit (solid line) and 95 % confidence intervals (dotted lines) of total non-leukaemic haematopoietic cells and AML cells; representative data from 3 independent experiments.

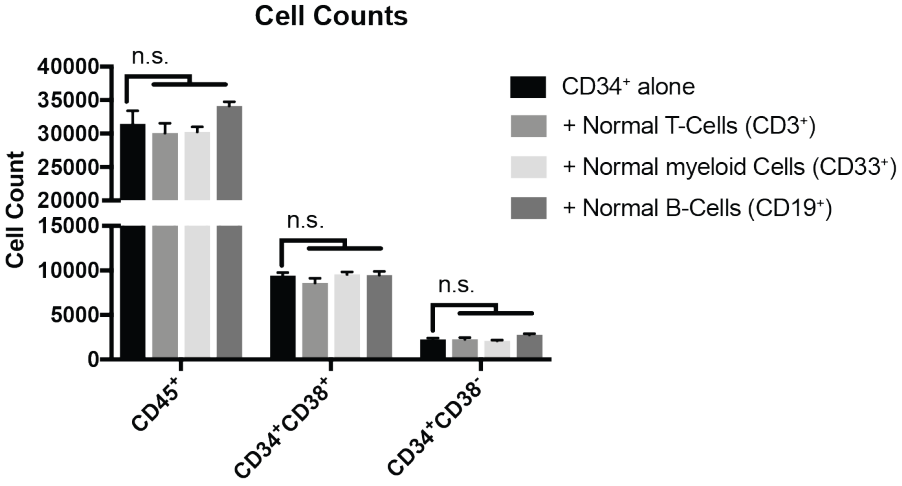


Figure 10. Cell counts of HSPCs and sub-populations after co-culture with purified normal CB MNCs fractions.

B-cells, T-cells and myeloid cells were sorted from normal CB MNCs and co-cultured with HSPCs. After 4 days cell counts of total non-leukaemic haematopoietic cells (hCD45) and HPCs +/+ and HSPCs +/- were taken and compared to $CD34^+$ alone (n=1); Error bars are +/- SEM

3.2.1.3 HSPC Viability

To explain the reduction of HSPC expansion, either cell cycle activity or viability should be reduced. Viability was measured either by absorption of an DNA inter-calleting dye like ′,6-Diamidin-2-phenylindol (DAPI) or propidium iodine (PI) alone or in combination with annexin V, a marker of early apoptosis. Neither approaches revealed a considerable reduction of cell viability of +/+ or +/- which was above 90 % in most cases (Figure 11A-B). Only more mature $CD34^-$ cells were enriched for $AnnexinV^+/DAPI^+$ apoptotic-dead cells (Figure 11C). This indicates that cell death does not account for the reduction of HSPC expansion at least within the $CD34^+$ compartment.

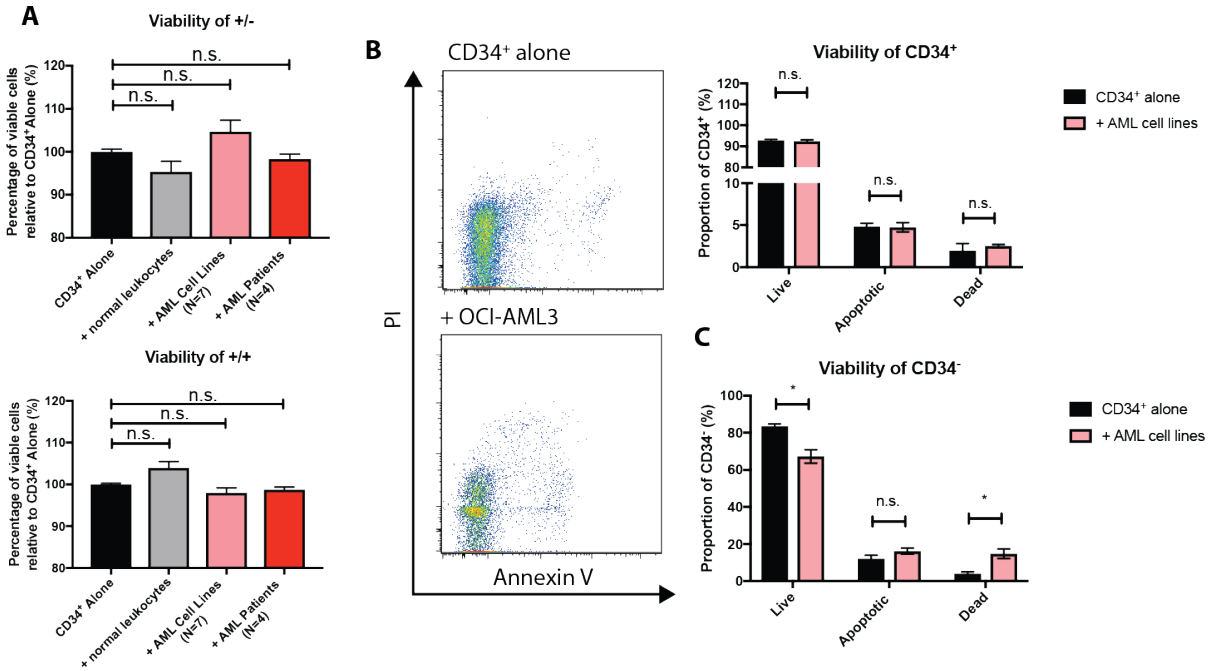


Figure 11. Viability of HSPCs alone or co-cultured with AML
(A) $PI/DAPI^-$ +/+ HPCs or +/- HSPCs normalised to $CD34^+$ alone (n=3) **(B)** Representative plots of $CD34^+$ alone or + AML to measure cell viability using PI for dead cell discrimination and $AnnexinV^+PI^-$ for early apoptotic cells; quantifications of viability of $CD34^+$ cells **(C)** Quantification of viability of $CD34^-$; each dot representing a different cell line or AML patient sample for + AML cell lines or + AML Patients (n=2); *p<0.05, non-significant p > 0.05. Error bars are +/- SEM

3.2.1.4 Cell cycle and proliferation assay

Right after isolation from CB, HSPCs are almost exclusively in G0/G1 phase of the cell cycle. Upon cell cycle activation, HSPCs express Ki67, a component of ribosomal RNA synthesis, in all phases of the cell cycle. Additionally, the cellular DNA content, measured by DNA inter-

calleting dyes increases with the onset of S-phase and throughout G2 and M-phase. Hence quiescent cells are strictly Ki67$^-$DAPI$^-$. To examine the status of cell cycle activation, the fixed and permeabilised HSPCs were analysed for Ki67 expression and DNA replication. In agreement with the reduction of HSPC expansion, total, +/+ and +/- cells from AML cultures were significantly enriched between 1 to 4-fold in Ki67$^-$DAPI$^-$ quiescent cells at the expense of S, G2 and M-phase Ki67$^+$DAPI$^+$ cells (Figure 12A-C). The reduction of cell cycle activation at 48h predates any measurable changes in cell number, which may indicate the lack of HSPC expansion is due to a diminished cell cycle activity (Figure 12B).

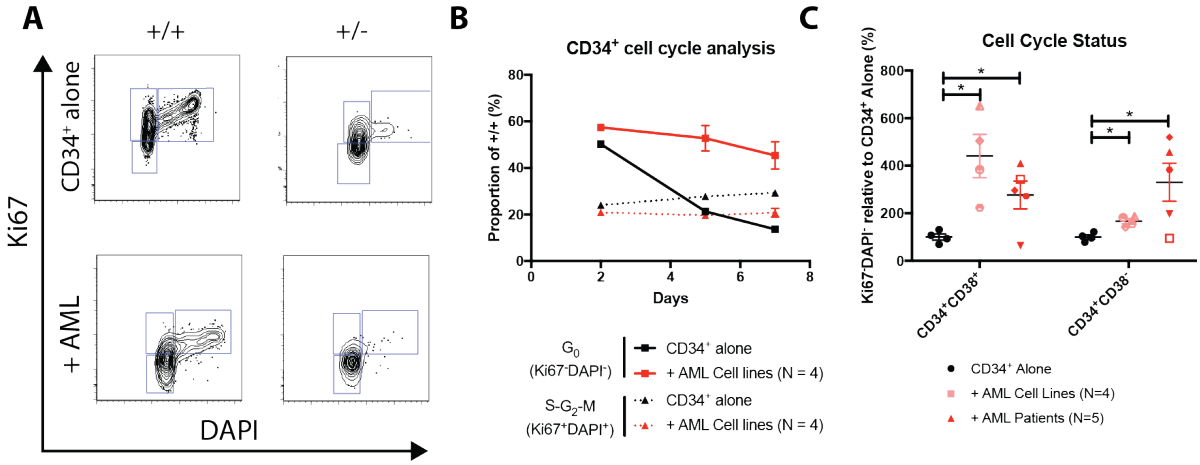


Figure 12. Cell cycle analysis of HSPCs and sub-populations alone or co-cultured with AML

(A) Representative plots displaying the cell cycle analysis based on Ki67 expression and DNA/DAPI content of HPCs +/+ and HSPCs +/- cultured alone or with AML cell line U937 **(B)** 7- day time course analysis of CD34$^+$ showing the proportions of quiescent cells (Ki67-DAPI-) (solid line) and DNA-replicating/dividing cells (Ki67$^+$DAPI$^+$) **(C)** Quantification of proportions of quiescent cells normalised by CD34$^+$ alone cultured with AML cell lines (n=3) or AML patients (n=2), each dot representing a different cell line or AML patient sample for + AML cell lines or + AML Patients; *p<0.05, n.s. p > 0.05. Error bars are +/- SEM

Because the cell cycle status is a static measurement, we opted for a more dynamic approach involving cell division tracking dyes. Cells of interest are shortly stained with cell-permeable fluorescent esters like Carboxyfluorescein succinimidyl ester (CFSE) or derivatives like CellTrace Violet (CTV) which covalently bind to intracellular amine residues and thereafter lose cell permeability. With every division, the signal per cell divides by half and proliferation events can be accumulatively measured over long periods and multiple cell divisions. Over a 4 -day time course differences in retention of proliferation dye between CD34$^+$ alone and + AML commenced after 48h and further intensified on day 3 and 4 as HSPCs failed to expand (Figure 13).

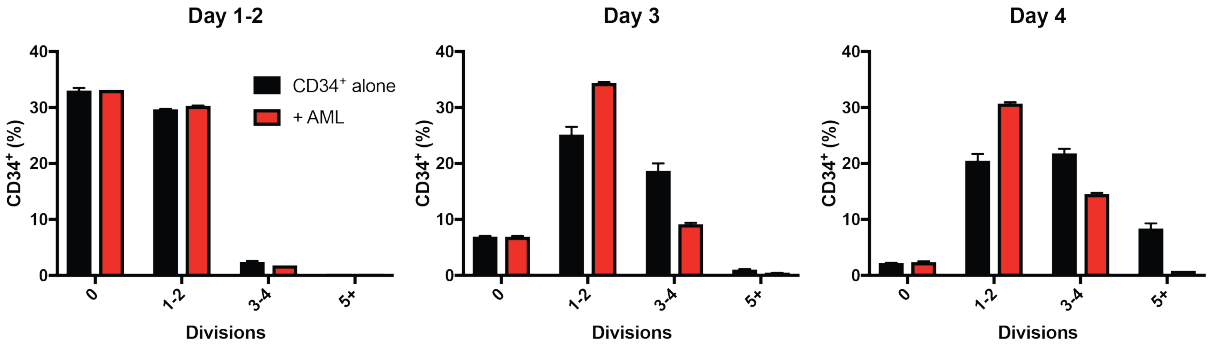


Figure 13. 4-day time course analysis of cell divisions of CD34$^+$
CB CD34$^+$ cells were stained with a semipermeable cell division tracker on day 0 and co-cultured with AML cell line U937 or alone to measure cell divisions over 4 days. Division 1 and 2 (1-2), 3 and 4 (3-4) and 5 or more (5+) were pooled; Error bars are +/- SEM (n=2 technical replicates)

In analogy with Histone H2B-GFP or BrdU pulse-chase experiments, we quantified the percentage of cells with a high concentration of proliferation dye (termed CTV^{hi}) for the HSPCs screened with a range of AML samples. Between 25-50 % and 10-40 % more cells with high concentrations of proliferation dye were observed in the +/+ and +/-, respectively (Figure 14). Furthermore, the percentage of CTV^{hi} and CD34$^+$ cell numbers were strongly inversely correlated. This further consolidates that the lower recovery of HSPCs from AML co-cultures is a consequence of impeded proliferation.

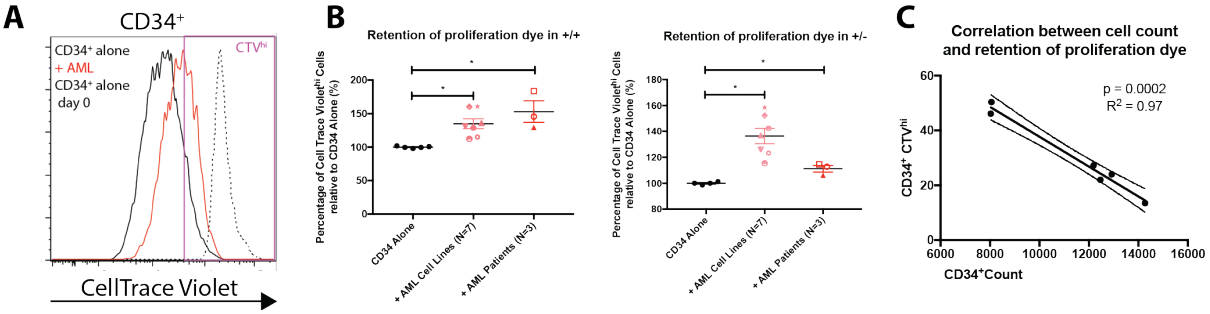


Figure 14. Tracking of HSPC divisions cultured alone or co-cultured with AML
(A) Representative plot showing the CellTrace Violet signal intensity of CD34$^+$ before culture (dotted line), alone (CD34$^+$ alone, black) or cultured with AML cell line NB4 (+AML, red), the purple gate displays the gating strategy to obtain CTV^{hi} population **(B)** Quantification of CTV^{hi} normalised by CD34$^+$ alone of +/+ HPCs and +/- HSPCs (n=3) **(C)** Best curve fit (solid line) and 95 % confidence intervals (dotted lines) of CD34$^+$ cell count and corresponding CTV^{hi} (%) (n=1); each dot representing a different cell line or AML patient sample for + AML cell lines or + AML Patients; *p<0.05, n.s. p > 0.05. Error bars are +/- SEM

3.2.2 Qualitative analysis of normal CB HSPCs co-cultured of with BM MSCs and AML

In agreement with results from Miraki-Moud et al. and Cheng et al., we observed that AML impairs the proliferation but not the survival of normal HSPCs *ex vivo* (Cheng et al., 2015; Miraki-Moud et al., 2013). Next, we addressed whether the reduced proliferation was associated with reduced differentiation and enhanced stemness (Cheng et al., 2015; Miraki-Moud et al., 2013). To test this, we isolated normal $CD34^+$ from AML co-cultures and performed functional *ex vivo* and *in vivo* analysis. $CD34^-$ cells were sorted once but did not produce any CFUs. *Ex vivo* analysis comprised a serial CFU-assay to determine immediate and sustained progenitor cell function and LTC-IC Assay to assess the frequency of long-term colony-forming cells (a mixture of MPPs and HSCs). To specifically address HSC potency, we followed the current gold standard of two sequential 12-week transplantation assay into immune-deficient mice (Figure 15).

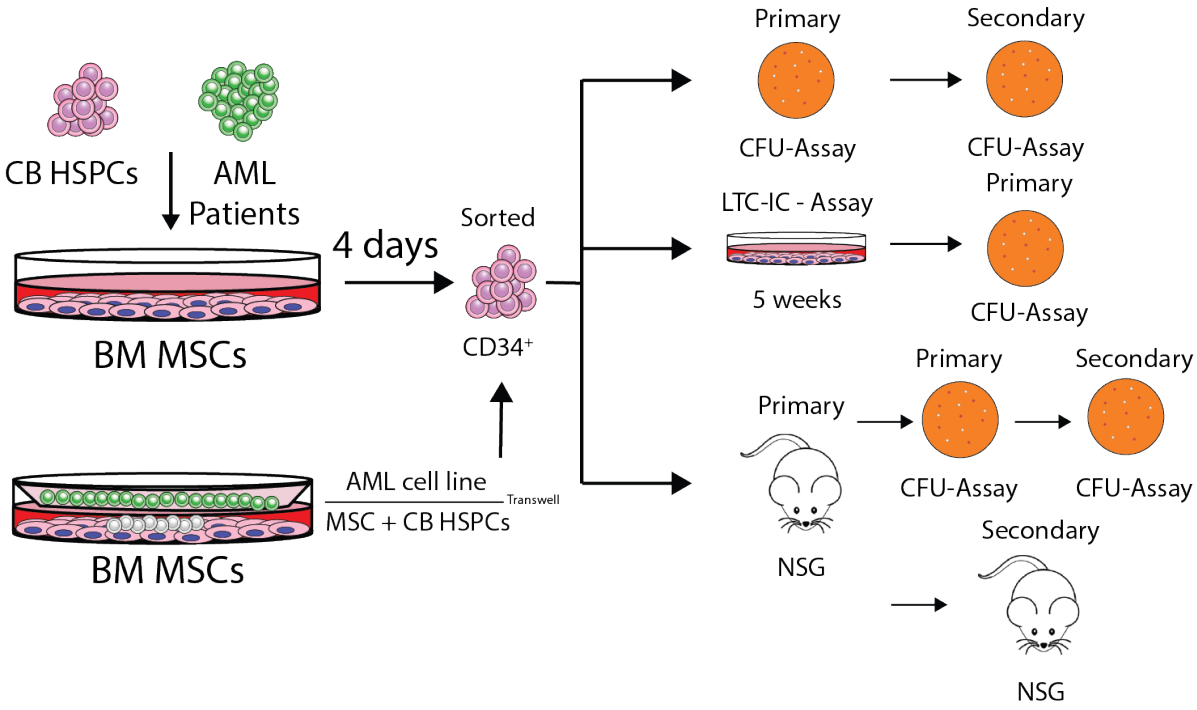


Figure 15. Schematic depicting the functional analysis of $CD34^+$ cells isolated from HSPCs cultured alone or with AML for 4 days
HSPCs were cultured for 4 days alone, with HLA-A2 mismatched AML patients or transwell separated AML cell lines. FACS-sorted $CD34^+$ cells were plated in methylcellulose at 200 cells/ml for primary and 10^5/ml for secondary CFU-assay. Colonies were scored after 14 days. 4000 $CD34^+$ cells were cultured on irradiated MS-5 stroma cells for 5 weeks and CFU-frequency was scored with a primary CFU-assay. 3-4.5x10^4 $CD34^+$ cells were injected into primary NSG mice and after 12 weeks 1-2x10^6 $hCD45^+$ cells were injected into secondary recipients or 5x10^4 $hCD45^+$ cells were cultured and scored for CFU-ability.

Of note, despite employing a strict gating strategy, FACS-sorted HSPCs from AML cell line co-culture were repeatedly contaminated with rare AML cells which over time outcompeted HSPCs in LTC-IC and secondary CFU-assays. Therefore, for all qualitative analysis, AML

cell lines (HL60, ML1, U937, KG1A, NB4, MOLM13 and OCI-AML3) were physically separated from MSCs and HSPCs via a 0.4 µm pore-sized transwell insert (Figure 16A). AML patient samples were cultured in direct contact with HSPCs without any AML contaminations probably owing to LICs being more infrequent. Importantly, AML cell lines in transwell cultures still impaired HSPC proliferation and differentiation. However, to an around 50 % lesser extent regarding phenotypic differentiation blockage than AML in direct contact with HSPCs and MSCs (Figure 16B).

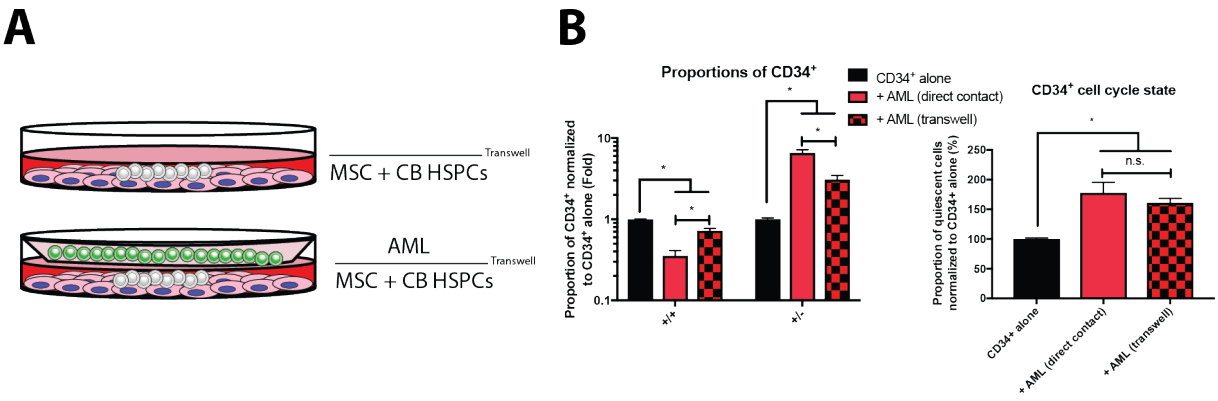


Figure 16. Comparison of transwell versus direct contact exposure of AML to CB HSPCs and MSCs

(A) AML were co-cultured with HSPCs and MSCs as described above or separated from HSPCs and MSCs by 0.4 µm pore-size transwell inserts **(B)** Proportions of HPCs +/+ and HSPCs +/- within $CD34^+$ and quiescent cells ($Ki67^-DAPI^-$)within $CD34^+$ normalised to $CD34^+$ alone from $CD34^+$ alone, + AML cell lines (direct contact) and + AML cell lines (transwell), data for AML was obtained from cell lines NB4, OCI-AML3 and U937 and displays representative data from experiment performed in duplicate; *$p<0.05$, n.s. $p > 0.05$. Error bars are +/- SEM

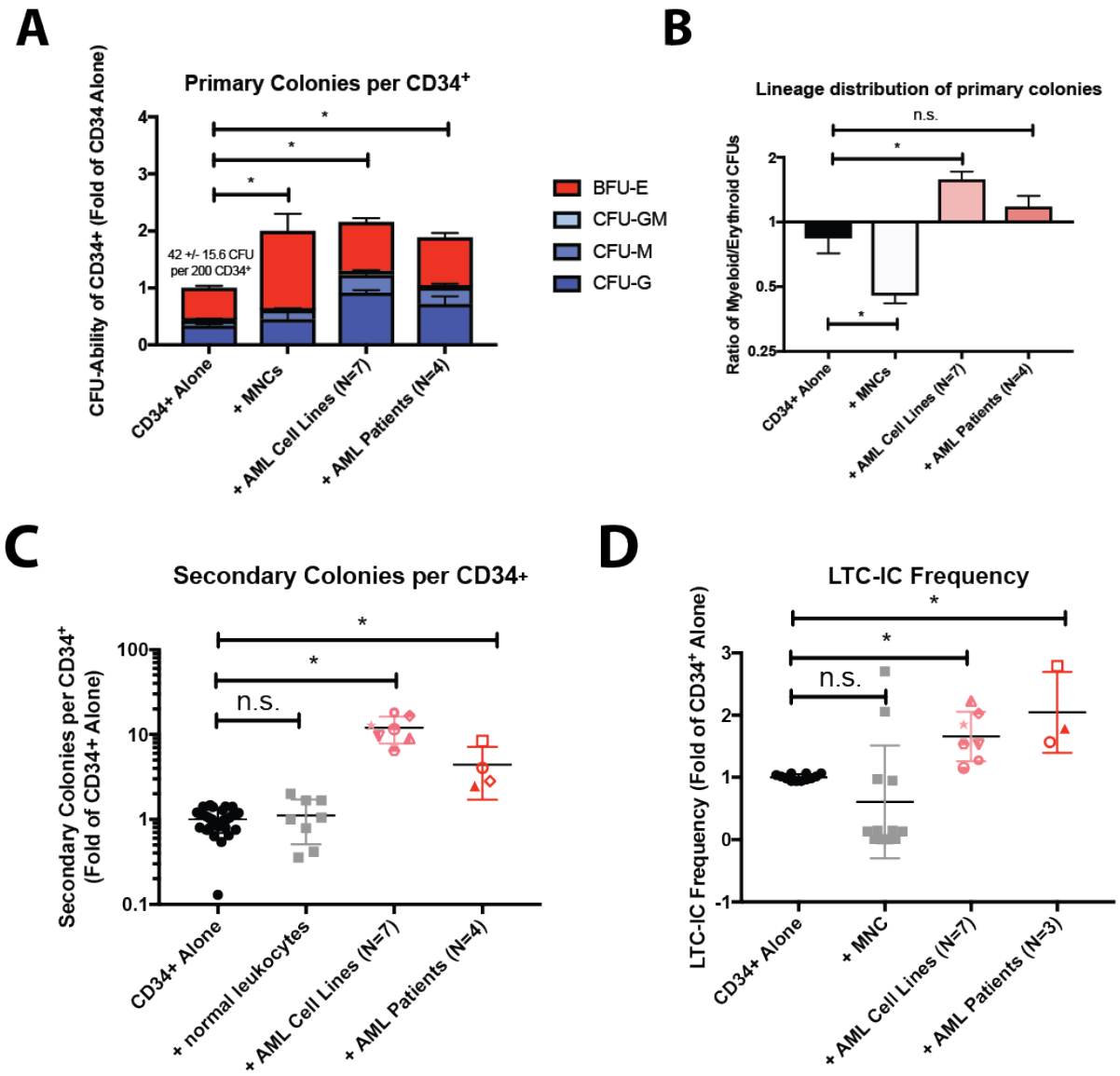


Figure 17. Results from serial CFU-assay and LTC-IC assay of sorted CD34⁺ cells from HSPC-AML co-cultures

(A) CFU-type and CFU-numbers of primary CFU-assay from CD34⁺ cells isolated from HSPCs after 4 days of culture alone or with AML. Results are normalised by numbers of CD34⁺ alone (n=4) **(B)** Ratio of myeloid CFUs (combined CFU-G, CFU-M and CFU-GM) to erythroid CFUs from primary CFU-assay (n=4) **(C)** Total secondary CFUs per primary CD34⁺ cells normalised by values from CD34⁺ alone (n=4) **(D)** LTC-ICs relative to LTC-ICs from CD34⁺ alone, +AML cell lines (n=4), +AML patients (n=2); each dot representing a different cell line or AML patient sample for +AML cell lines or +AML Patients; *p<0.05, n.s. p > 0.05. Error bars are +/- SEM

3.2.2.1 Serial CFU-assay

From the primary CFU-assay we obtained 42 +/- 15.6 colonies from 200 isolated HSPCs from CD34⁺ alone. In comparison + normal CB MNCs, + AML cell lines and + AML patients HSPCs produced a 2-fold increased CFU output (Figure 17A). Interestingly, the increased CFU

output for both + AML were mainly of granulocyte and monocyte lineage morphology in contrast to +normal CB MNCs which preferentially produced erythrocyte colonies. The altered lineage distribution of +normal CB MNCs and +AML HSPCs became clearer when the ratio of myeloid to erythroid cultures was calculated. +AML HSPCs produce between 1.2 and 1.7 CFU-granulocyte (CFU-G), CFU-granulocyte/monocyte (CFU-GM) or CFU-monocyte (CFU-M) for every CFU-erythrocyte (CFU-E). On the other hand, $CD34^+$ alone and +normal CB MNCs HSPCs produced a ratio of 0.7 to 0.4, respectively (Figure 17B).

After re-plating of a fraction of cells from primary CFU-assay, only self-renewing cells can give rise to CFUs, called secondary CFUs. Again, + AML HSPCs contained a 3 to 10-fold higher secondary colony frequency per $CD34^+$ than HSPCs from $CD34^+$ Alone or + normal CB MNCs (Figure 17C).

3.2.2.2 LTC-IC Assay

Lastly, the LTC-IC Assay utilises a 5-week culture on irradiated mouse stroma cell line MS-5 prior to the CFU-assay to eradicate cells with limited self-renewal and distinguish immature progenitors from short-term progenitors. In agreement with the CFU-assay, the LTC-IC frequency of 1 in 22-45 $CD34^+$ from $CD34^+$ alone was elevated by 1.5 – 2-fold from + AML cell lines and + AML patients, respectively (Figure 17D). + normal CB MNCs failed for most replicates to contain any considerable number of LTC-ICs which is consistent with the hypothesis that HSPC expansion and long-term self-renewal are inversely correlated. Together this data from the *ex vivo* assays show that suppression of HSPC expansion results in an enrichment of less differentiated progenitors indicative of a temporary, reversible differentiation blockage in the presence of AML at least on the progenitor level.

3.2.2.3 Serial transplantation Assay

To measure differences in HSC potency around 3-4.5x10^4 $CD34^+$ cells were injected per mouse and engraftment was determined after 12 weeks. Primary recipients showed a human chimerism between 30-80 % of total haematopoietic cells. Lymphoid and myeloid lineage distribution was not significantly affected by AML co-culture (Figure 18A-B). Furthermore, total human engraftment after 12 weeks and the frequency of HSCs between the three groups, $CD34^+$ alone, + AML cell lines and + AML patients, was not significantly different (Figure 19 A-C). Human $CD45^+$ cells from primary mice were isolated for further *in vivo* analysis in

secondary recipients (1-2x10^6/mouse) and *ex vivo* serial CFU-assay. Human $CD45^+$ from + AML patients generated 50-60 % more primary CFUs, but secondary colonies showed no significant difference (Figure 19D). Since the results from the secondary engraftment were not available at this time, the data so far does not support that HSC activity is significantly altered by AML co-culture.

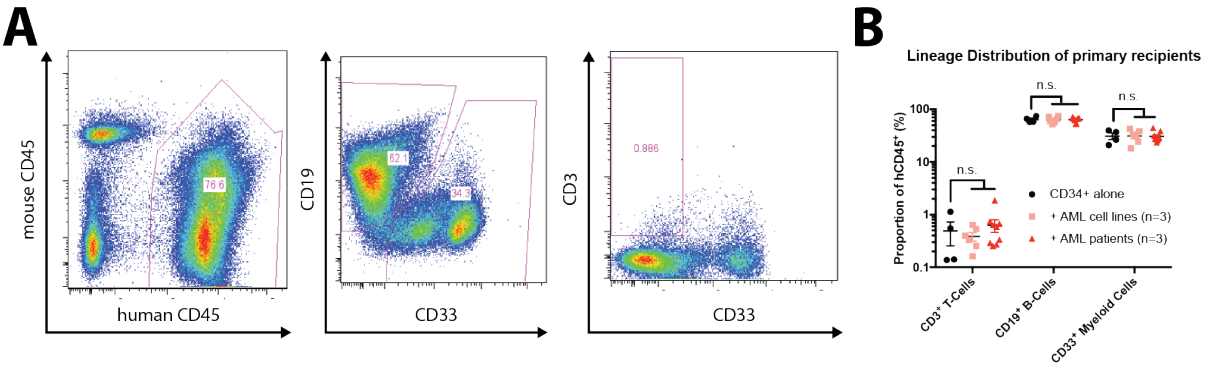


Figure 18. Lymphoid and myeloid lineage distribution of human CD45 from primary recipients

(A) Gating strategy to detect human chimerism in BM of primary recipients and to detect $CD19^+$ B-cells, $CD33^+$ myeloid cells and $CD3^+$ T-cells **(B)** Quantification of lineage distributions from 35 mice from three independent experiments represented as percentage of human $CD45^+$ cells;*$p<0.05$, n.s. $p > 0.05$. Error bars are +/- SEM

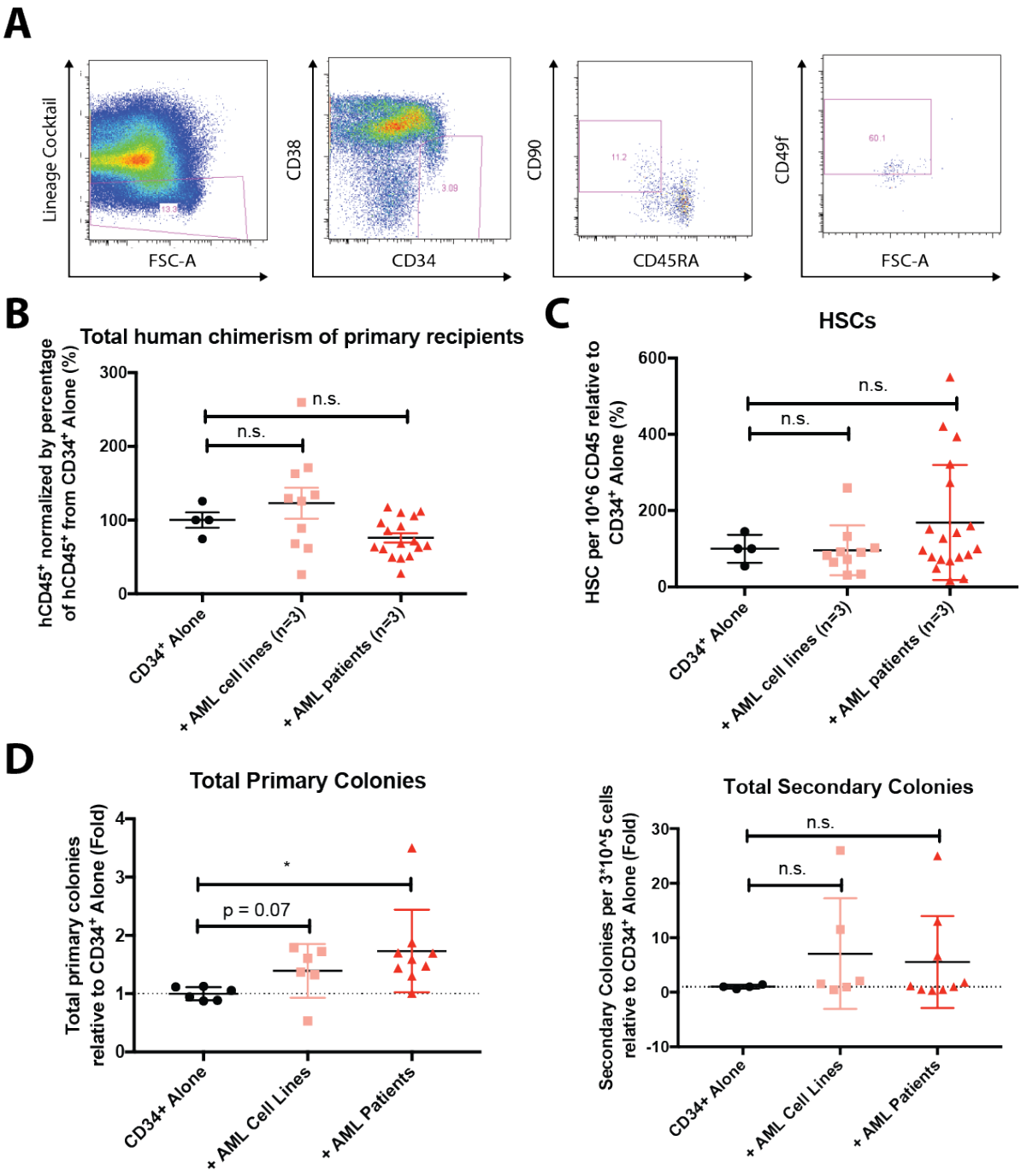


Figure 19. Engraftment and phenotypic HSC frequencies of primary recipients
(A) Gating strategy to measure human chimerism on BM and phenotypic HSCs **(B)** Quantifications of human chimerism in BM after 12 weeks from 35 mice from three independent experiments normalised to engraftment percentages of $CD34^+$ alone **(C)** Frequencies of $hCD45^+CD34^+CD38^-CD45RA^-CD90^+CD49f^+$ among 10^6 $hCD45^+$ cells normalised to proportions of $CD34^+$ alone **(D)** Primary and secondary colonies from 5*10^4 and 10^5 cells, respectively. Total colony counts were normalised by counts from $CD34^+$ alone;*$p<0.05$, n.s. $p > 0.05$. Error bars are +/- SEM

3.2.3 Impact of an AML-remodelled microenvironment on AML proliferation

During the initial 4-day time course the proliferation of the AML cell line remained undisturbed, but from this experiment, no solid conclusions can be drawn about the impact of an AML-remodelled microenvironment on AML proliferation. Therefore, we cultured either AML patient samples or normal HSPCs on MSCs alone or together with AML cell lines separated via transwell (Figure 20A). Surprisingly, when we normalised the cell count alone to + AML we found that AML cells were either affected to a lesser extent than HSPCs or, like in most cases, had proliferated between 1.2 to 3.5-fold more (Figure 20C). To ensure that AML patients samples had proliferated, we stained them with CellTrace violet and measured the retention of dye. Indeed, compared to the mean fluorescence intensity of CTV from uncultured AML (Sample day 0), the cultured AML cells contained considerably less proliferation dye confirming that AML divided. Additionally, AML cells cultured with AML cell lines outperformed their alone culture counterparts indicated by a smaller fraction of CTV^{hi} cells (Figure 20B). After co-culture, FACS-sorted AML plated in methylcellulose generated CFU from two of the three AML samples. + AML samples generated between 2 to 3-fold more CFU than AML cultured alone on MSCs (Figure 20D). This indicates that AML produces an environment which favours the expansion of malignant cells over normal HSPCs without compromising LICs.

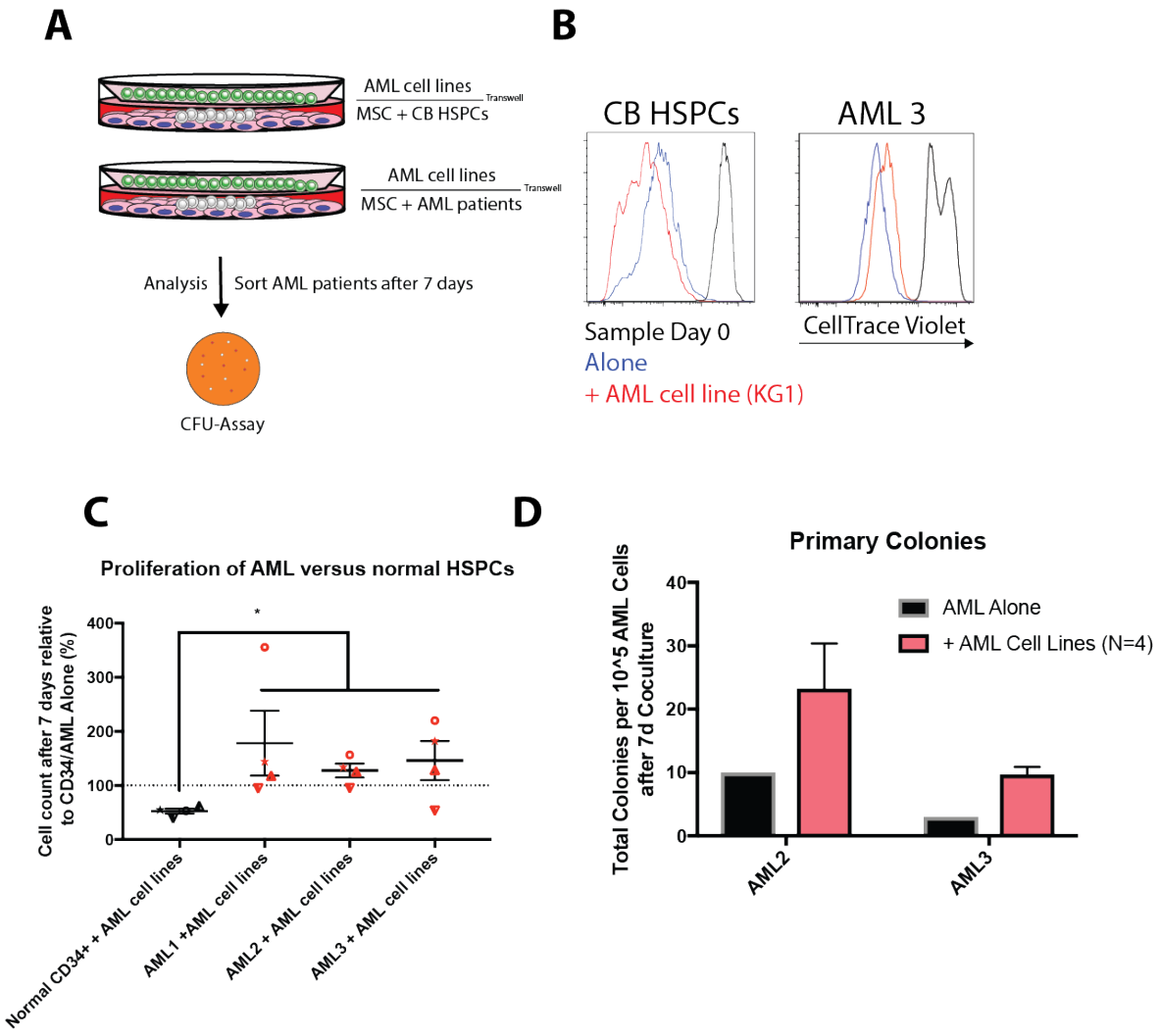


Figure 20. AML patient samples and HSPCs co-cultured with AML cell lines
(A) Schematic representation of experimental setup. CB CD34$^+$ HSPCs or 3 AML patient samples were cultured with AML cell lines (U937, KG1A, NB4 and MOLM-13) separated by a transwell insert. After 7 days cell counts were measured and AML samples sorted for subsequent a CFU-assay **(B)** Representative plots showing the retention of proliferation dye by HSPCs and AML patient samples after 7 days and before conducting culture **(C)** Cell counts after 7 days normalised to cell counts from HSPCs/AML patient samples cultured alone (dotted line) (n=3) **(D)** Representative results of primary CFU-assay of AML patient samples cultured alone or with AML cell lines performed in duplicate; each dot representing a different cell line *p<0.05, n.s. p > 0.05. Error bars are +/- SEM

3.3 Discussion

In a simplified *ex vivo,* niche model AML cell lines and AML patients are capable of suppressing the expansion and phenotypic differentiation of normal CB HSPCs. The time course analysis demonstrated that AML requires around 48h to transform its environment to suppress HSPCs. If we had allowed the MSCs to pre-incubated with AML in order to transform the environment before the HSPCs are added, the HSPC's phenotypic differentiation and proliferation might have been blocked prior to 72h. Additional to timing, the ratio of AML cells to normal HSPCs might also detrimental to generate sufficient cytokine/metabolite concentration. Across the repertoire of AML cell lines used in this study, the cell numbers of AML did not significantly correlate with HSPC inhibition. However, preliminary data has shown that within the same cell line a ratio as small as 1:4 could reduce HSPC expansion in a ratio-dependent manner. Hence, one may speculate that the suppression of HSPC proliferation is a product of AML cell numbers multiplied by each cell's capacity to remodel the environment. A slowly growing AML sample may still impede normal HSPCs proliferation owing to a high remodelling index. This would fit with the observation that cytopenias in AML are not correlated with BM infiltration, but disease progression worsens cytopenia on an individual patient basis (Rauch et al., 2016).

Akinduro et al. observed that ST-HSC underwent apoptosis at an advanced disease state (Akinduro et al., 2018). In contrast, Miraki-Moud et al. and Cheng et al. did not observe any impacts on cell viability of HSPCs but lacked a detailed phenotypic discrimination like Akinduro et al. (Cheng et al., 2015; Miraki-Moud et al., 2013). From a clinical perspective, necrotic BM has been reported in AML but with a much lower prevalence than cytopenias (Badar et al., 2015). In agreement, in our *ex vivo* niche model, HSPCs were not significantly affected by AML as a whole and neither when we discriminated +/+ and +/-. On the other hand, $CD34^-$ cells did contain more apoptotic cells which was particularly pronounced with AML cell lines OCI-AML3. This could be a consequence of the proliferation blockage, lack of specific niche requirements for these cells or an unknown independent effect. HSPCs may be more resilient as cell cycle inhibition represents a natural mechanism to regulate haematopoietic output (Baumgartner et al., 2018). AML, which consist of differentiation inhibited progenitors, may transform the niche into a progenitor propagating niche. On that note, Boyd et al. observed a depletion of adipocytes and osteoblasts in AML BM, which were

more stimulating for haematopoietic cell differentiation than MSCs which themselves might select for more immature HSPCs (Boyd et al., 2017).

Akinduro et al. hypothesized that immature HSPCs are most resilient to AML displacement and that the lack of proliferation and differentiation measured by serial transplantation assays is simply a consequence of selection pressure from displacement (Akinduro et al., 2018). In an *ex vivo* system, egress from the niche does not occur, but the proliferation of HSPCs was reduced. The increased apoptosis of $CD34^-$ cells may slightly select for more immature HSPCs, but even within $CD34^+$ both +/- and +/+ cell cycle activity was significantly reduced. These observations argue against the hypothesis by Akinduro et al.as the differentiation blockage and reduced proliferation single-handedly arise from selective pressure from HSPC displacement, which enriches for quiescent, self-renewing cells. The data instead supports the report from Cheng et al. and Gong et al. that AML creates an anti-proliferative environment for normal HSPCs (Cheng et al., 2015; Gong et al., 2018). However, in an *in vivo* situation, these two scenarios are not mutually exclusive and the displacement selection pressure may contribute additionally.

The expansion of HSPCs is believed to impede their functionality. *In vivo* HSCs which have divided fewer times are more potent in serial transplantation assays (Bernitz et al., 2016). However, cell cycle inhibition may not automatically dictate the preservation of self-renewal potential. For example, treatment of HSCs with the potent cell cycle inhibitor TGF-β1 impedes self-renewal although HSCs remain quiescent. TGF-β1 does not suppress the cell cycle activity of already quiescent cells but rather impedes the divisions of continuously dividing cells (Wang et al., 2018). The proportions of HSPCs which had remained entirely quiescent throughout was not significantly affected during all 4 time points and AML HSPCs were most enriched between division 1-2. HSPCs co-cultured with AML had undergone at least one cell division within the first 48h similar to their $CD34^+$ alone counterparts. Rather the percentage of cells which had undergone at least 2 or more divisions was disproportionately reduced. Therefore, it may not seem so surprising that AML HSPCs were more potent in serial CFU-assay and LTC-IC which provide measurement of progenitors, MPPs and to a lesser extent HSCs, but not during the predominantly HSC challenging serial transplantation assay. Cheng et al. and Gong et al. observed that increased TGF-β1 and the expression of TGF-β1 downstream target Egr3 contribute to HSPC quiescence in leukaemic mice but neither HSC overexpression of Egr3 nor

treatment of TGF-β1 enhanced their engraftment and did not recapitulate the increased reconstitution potential of HSC from leukaemic mice (Cheng et al., 2015; Wang et al., 2018). Potentially, regarding the LT-HSC phenotype, enrichment by selective displacement as suggested by Akinduro et al. may be a better explanation than the suppression of proliferation. Indeed, Wang et al. isolated HSC from leukaemia patients based on ALDH activity and observed that reduced engraftment capacity correlated with adverse survival. Because the reduction of HSCs occurred prior to relapse, it suggests competition of LICs and HSCs for the same niche as cause. Interestingly, while HSCs were defective, the +/+ progenitor cells demonstrated an increased frequency of LTC-ICs, suggesting reduced differentiation of progenitor compartments downstream of LT-HSCs (Wang et al., 2017). LT-HSC are predominantly quiescent at steady-state (Wilson et al., 2008) and in recent years several reports questioned their contribution to unchallenged haematopoiesis. Work from Camargo and colleagues suggests that haematopoiesis is mainly driven by short-lived clones of MPPs and progenitors and selective abrogation of > 90 % of HSCs did not induce lasting haematopoietic effects (Rodriguez-Fraticelli et al., 2018; Sun et al., 2014). Therefore, impairment of proliferation and differentiation of several progenitor types may be sufficient to induce severe cytopenias.

AML patients commonly develop anaemia and haematocrit levels are reduced in leukaemic mice during mid-late phase. A reduced erythrocyte potential of HSPCs has also been reported by Cheng et al, Boyd et al. and Wang et al.(Boyd et al., 2017; Cheng et al., 2015; Wang et al., 2016). We find that HSPCs from + AML displayed a lineage biased toward granulocytes/monocytes in the CFU-assay, however, the absolute numbers of BFU-Es are not changed between + AML and $CD34^+$ alone. Phenotypic analysis of myeloid progenitors, like CMP, GMP and MEP demonstrated that AML HSCPs contained 70 % increased proportions of CMPs while GMP proportions were largely unchanged. On the other hand, MEP proportions were slightly decreased in AML HSPCs. Together this may explain the increased granulocyte/monocyte CFU-output of AML HSPCs. The increased expression of flt3 receptor marking CMPs and GMPs may be a consequence of inflammatory signalling. Increased activation of NF-κB in MSC co-cultured with AML has been reported and in HSPCs flt3 receptor expression is also upregulated by inflammatory signals (Jacamo et al., 2014; Singh et al., 2012).

In summary, the simplified *ex vivo* niche system recapitulates the inhibition of differentiation and proliferation of normal HSPCs establishing that for this phenotype AML cell lines and patient samples do not require a complex *in vivo* niche. Since AML HSPCs have undergone fewer cell divisions, they are more potent than HSPCs cultured alone in terms of CFU- and LTC-IC capacities. The preliminary data on HSCs suggests so far that these mostly quiescent population of cells is not significantly enriched after AML culture. While disadvantageous for non-leukaemic HSPC expansion, the environment created by AML favours the expansion of malignant cells which are either more resilient to proliferation inhibition or proliferate faster. An inhibition of normal versus malignant cells may provide additional space and nutrients for the expansion of AML.

Chapter 4. Development of an *in vivo* fully humanised scaffold model

4.1 Results

To expand the mesenchymal niche model to a more complex environment, we opted to establish a transplantable 3D scaffold model containing the same components, BM MSCs, CB HSPCs and AML. The model was adapted from Abarrategi et al., who used a gelatine sponge as scaffold for healthy BM MSCs to adhere and form an extramedullary niche (Abarrategi et al., 2017). BM MSCs have previously been shown to establish an extramedullary BM niche alone or supported by extracellular matrix-based scaffold (Antonelli et al., 2016; Sacchetti et al., 2007). Abarrategi et al. established this model in our lab and proved the feasibility to maintain either CB HSPCs or a wide range of patient AML samples. The benefits of this model are that it recapitulates a complex niche environment with a stable murine vascular and human mesenchymal niche. The latter is derived from BM MSCs which can easily be manipulated by lentivirus-mediated delivery of overexpression of knockdown plasmids. Recipients for these scaffolds need to be immuno-deficient NSG or NSG-SGM3 mice. The latter overexpress human SCF, IL-3 and GM-CSF under the CMV promoter allowing enhanced normal myeloid and AML engraftment (Nicolini et al., 2004; Wunderlich et al., 2010). The cytokine driven myeloid differentiation exhaust HSPCs and therefore presents an ideal model to test whether AML blocks differentiation and proliferation of normal HSPCs to delay exhaustion.

The process to develop a humanised niche starts by cutting the gelatine sponge into sterile 4 mm^3 cubes (Figure 21A). These cubes are incubated with a concentrated suspension of BM MSCs, which quickly adhere to the scaffolds within 24h (Figure 21B). These scaffolds are allowed to recover for 48h-5 days after seeding with MSCs. Subsequently, a mixture of HSPCs and AML cell are directly injected into the scaffolds and cultured for another 24h *ex vivo* prior to subcutaneous transplantation. For AML cell lines (called +AML cell lines) a ratio of AML:HSCPs of 1:10 was chosen to compensate for the faster proliferation of AML to normal HSPCs. AML patients proliferated much slower than AML cell lines and contained proportionally fewer LICs. Therefore, a ratio of 10-4:1 was chosen, and the mixture was termed + AML patients. Scaffolds with AML cell lines were analysed between 2-3 weeks after transplantation and scaffolds with AML patients 6-8 weeks. To distinguish AML and normal HSPCs, the HSPCs or, in case of experiments with cell lines, the AML cell lines were transduced with lentivirus vector containing GFP as selection marker.

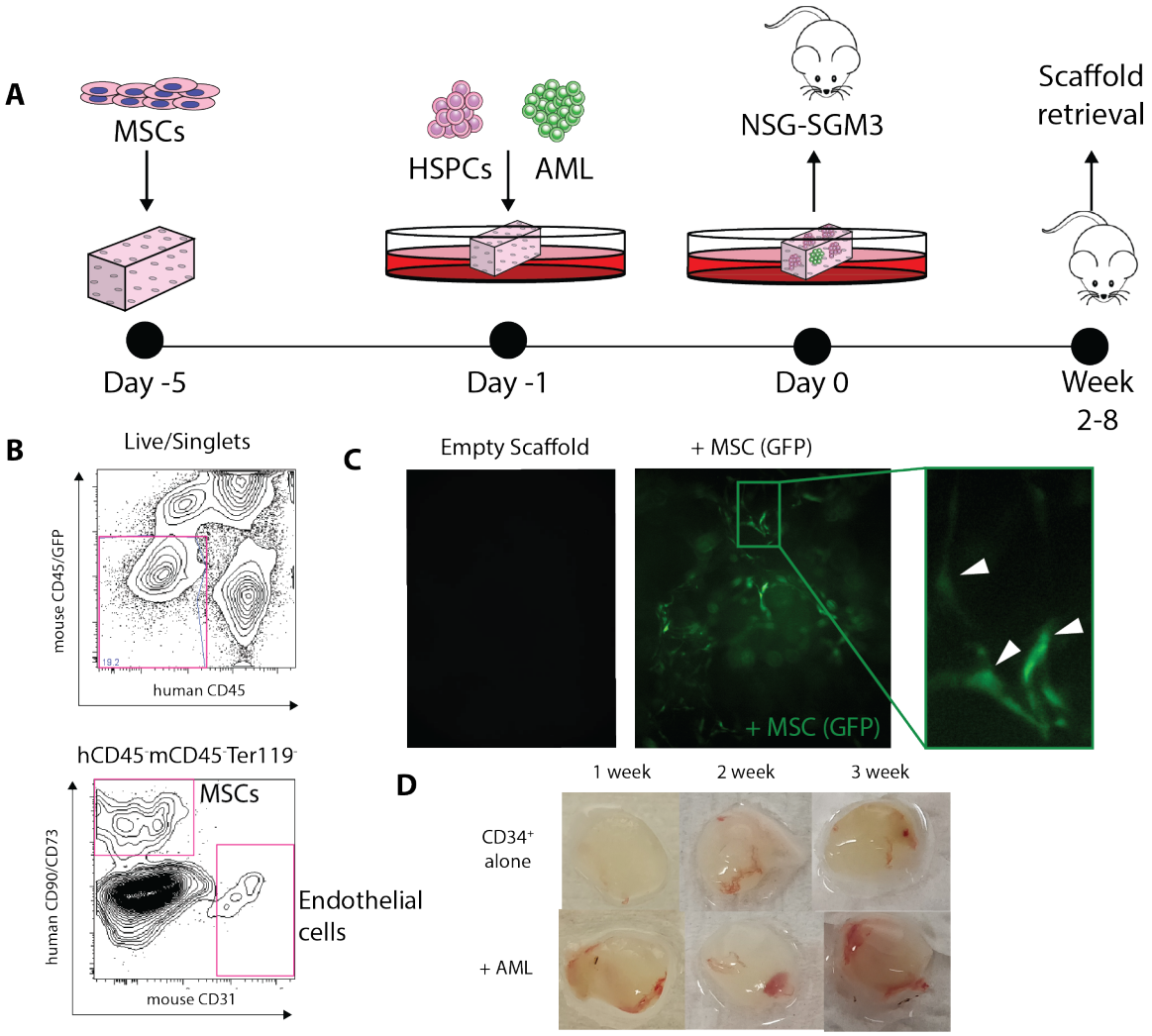


Figure 21. Schematic presentation of experimental design and fundamental scaffold properties

(A) Experimental design outline (B) After dead cell and duplet exclusion mCD45$^-$hCD45$^-$Ter119$^-$ cells were plotted for human CD90/CD73 and mouse CD31 which delineate human MSCs and murine endothelial cells, respectively. (C) Images of scaffolds seeded with and without lentiviral transduced MSCs to express GFP showing dense MSC adherence (white arrows) along the scaffold surface (D) Representative images of scaffolds retrieved after at various time points initially seeded with CD34$^+$ alone or together with AML cell line U937

4.1.1 Time course analysis

Abarrategi et al. retrieved the scaffolds 8-12 weeks after transplantation. AML cell lines proliferate quicker than AML patient samples, and some cell lines like U937 can generate myeloid sarcomas. Therefore, we performed another time course analysis similar to our *ex vivo* culture to develop an understanding of the system. We retrieved the scaffolds weekly up to 3 weeks after transplantation. Already after 1 week both CD34$^+$ alone and + AML scaffolds showed vascularisation in proximity to the scaffold and from another experiment flow

cytometry analysis of the non-haematopoietic fraction ($CD45^-$ cells) established the presence of $CD45^-mCD31^+$ phenotypic endothelial cells already after 1 week (Figure 21B and 1D). In $CD34^+$ alone scaffolds total human haematopoietic cells (hCD45/black line), identified by expression of human CD45 (hCD45), doubled weekly from around $7*10^4$ at week 1 to $1.4x10^5$ and $2.8x10^5$ at week 2 and week 3, respectively. The transplanted $CD34^+$ HSPCs ($CD34^+$/black line) quickly downregulated CD34 expression by a magnitude of 10 per week, starting at 20% at week 1 and then dropping to 1 % and 0.1 % at week 2 and week 3, respectively (Figure 22B). In scaffolds co-transplanted with AML cell line U937, the total normal engraftment, absolute (Figure 22A) or expressed as chimerism among total non-leukaemic cells (Figure 22B), were reduced by 4-fold (hCD45/red line) at 2-week and 3-week time points, respectively. Based on the cell numbers, we estimated the doubling time of total normal haematopoietic cells between week 2 and 3 at 16.5 days as opposed to 7 days for total $hCD45^+$ from $CD34^+$ alone. $CD34^+$ HSPCs ($CD34^+$/red line) were reduced in absolute numbers per scaffold but proportionally enriched among non-leukaemic $CD45^+$ by 2 to 3-fold compared to $CD34^+$ alone after 2 and 3 weeks, respectively (Figure 22B).

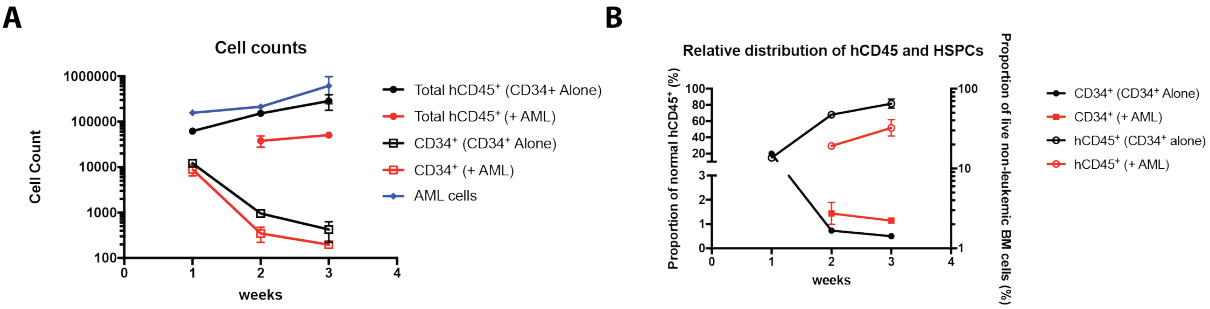


Figure 22. Kinetics of AML and normal haematopoietic cells over a 3-week time course

(A) Cell numbers per scaffold of total non-leukaemic human haematopoietic (Total $hCD45^+$), non-leukaemic HSPCs ($CD34^+$) and AML cells over a 3-week time course of $CD34^+$ alone scaffolds (black line) or + AML cell line U937 (red line/blue line for AML); at the 1-week time point only $CD34^+$ cell of + AML were analysed but total $hCD45^+$ could not be distinguished from AML (n=1) **(B)** Percentage of normal $CD34^+$ among non-leukaemic $CD45^+$ ($CD34^+$) in scaffolds with $CD34^+$ alone or +AML cell line U937; percentage of total non-leukaemic $CD45^+$ among all non-leukaemic cell (including mouse haematopoietic and mouse stroma cells) (n=1); Error bars are +/- SEM

4.1.2 Screen of AML cell lines and AML patient samples

To consolidate our observation with AML cell line U937, we again expanded our AML repertoire to cover several AML recurrent mutations with AML cell lines and AML patient

samples. Since not all experiments were performed at the same time and slight variations regarding scaffold retrieval occurred, we homogenized the results by normalising to CD34$^+$ alone control which was part of every experiment. Additionally, to homogenize the heterogeneous engraftment of the AML patient samples we stratified into a low (>20 % engraftment) (AML2, AML5 and AML3a) and a high engrafting patient group (20-80 % engraftment) (AML1, AML4 and AML3b) (Figure 23A-C). AML patient 3 generated ambivalent engraftment (owing to different numbers injected into the scaffolds) and was therefore placed in both groups depending on the engraftment levels. The cause may be that initially a re-frozen AML sample was used and during the second attempt, a different previously un-used cryovial was used. AML cell lines always generated an engraftment of at least 75 % despite the injection of much fewer AML cells per scaffold.

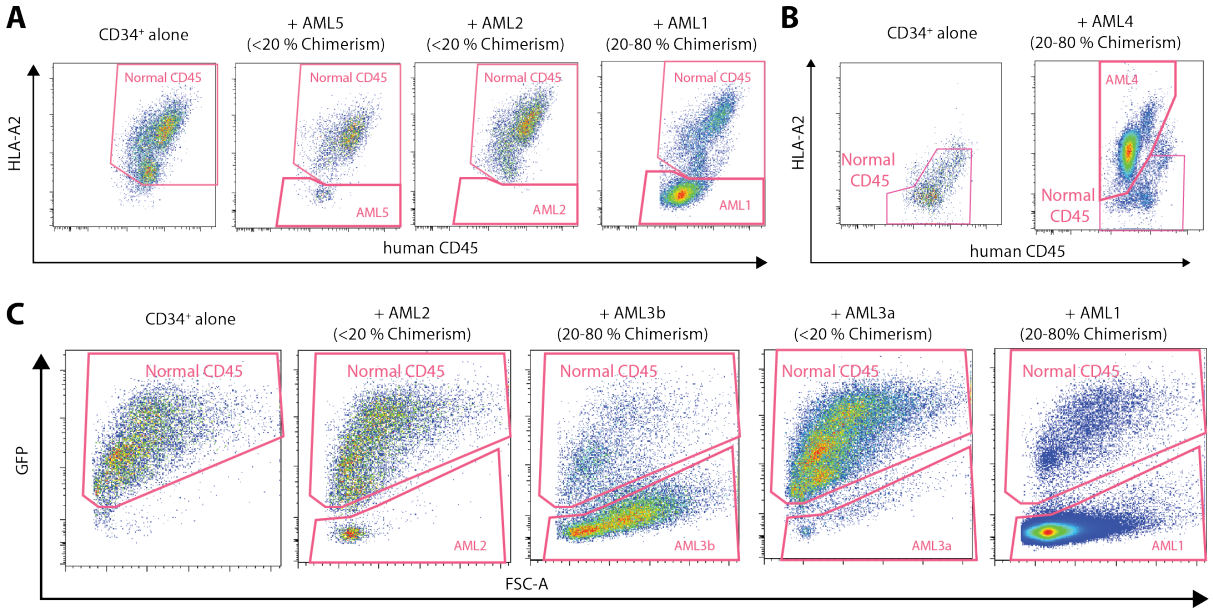


Figure 23. Engraftment of AML patient samples + normal CB CD34$^+$ in scaffolds
(A-B) Normal human CD45 were HLA-A2 mismatched with AML prior to injection into scaffolds and could be separated based on HLA-A2 staining after 5-8 weeks, HLA-A2 intensity was not homogeneous within the normal CD45 population owing to the high autofluorescence of granulocytes **(A)** Normal CB HSPCs were HLA-A2$^+$ and matched with HLA-A2$^-$ AML **(B)** HLA-A2$^-$ HSPCs were matched with HLA-A2$^+$ AML **(C)** Prior to scaffold injection CB HSPCs were transduced with a lentivirus vector to establish GFP expression and distinguish normal CD45 (GFP$^+$) from AML (GFP$^-$)

Around 40-50 % fewer total non-leukaemic human haematopoietic cells from scaffolds with high engraftment AML patients (+AML high) or AML cell lines were retrieved as compared to CD34$^+$ alone controls. In contrast, cell counts from low engrafting AML patients (+ AML low) were not significantly altered. In addition, we also quantified the engraftment as chimerism among all non-leukaemic scaffold cells. With this method, we observed less intra-

group variation among scaffolds because it normalises small variations of scaffold size and HSPC seeding numbers. In CD34$^+$ alone, scaffolds normal hCD45$^+$ cells account for around 50 % of all cells. + AML high and +AML cell lines suppressed normal engraftment from 50 % to 30 % and from 30 % to 10 %, respectively. Similar to the absolute quantifications, the +AML low patients had no significant impact on chimerism (Figure 24C).

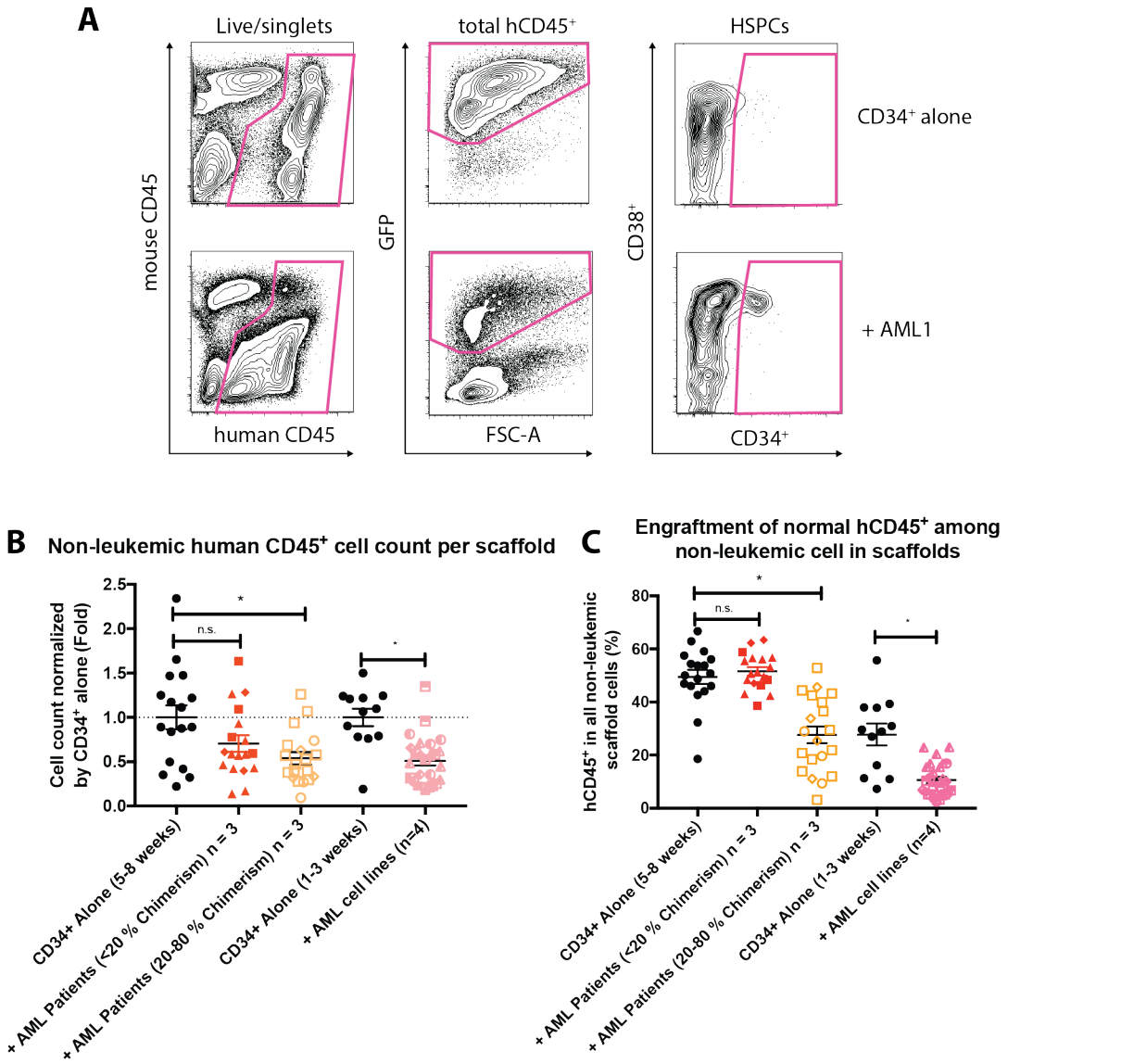


Figure 24. Engraftment of normal HSPCs alone or + AML patient samples/cell lines **(A)** Representative plots regarding the gating strategy to identify human CD45$^+$ (left), non-leukaemic CD45$^+$ (mid) and CD34$^+$ HSPCs (right) **(B)** Quantification of total non-leukaemic human haematopoietic cells per scaffold normalised by cell counts from CD34$^+$ alone scaffolds (+AML cell lines n=5, +AML patients n=4) **(C)** Engraftment of non-leukaemic human CD45+ quantified as percentage of all non-leukaemic mouse and human cells (+AML cell lines n=5, +AML patients n=4); each dot represents a scaffolds and symbols represent the specific AML patient samples/cell line; *p<0.05, n.s p > 0.05. Error bars are +/- SEM

In a few cases the engraftment of AML and normal human haematopoietic cells was analysed in the BM and spleen but in the majority of experiments either no haematopoietic cells were observed (N/D), or the engraftment was below the threshold of 0.1 % (Figure 25A-B). Only AML4 migrated to the spleen to generate a smaller engraftment (<2 %) (Figure 25B).

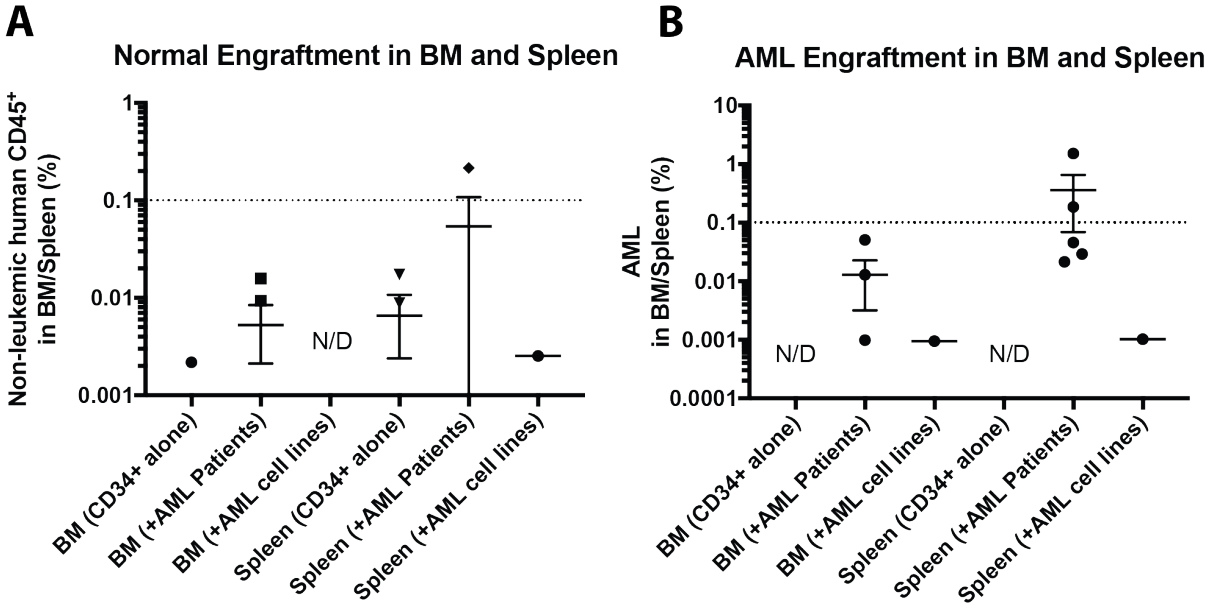


Figure 25. Engraftment of non-leukaemic and leukaemic human CD45 in spleen and BM of mice

(A) Quantification of engraftment of non-leukaemic human haematopoietic cells in BM and spleen of $CD34^+$ alone scaffolds or + AML patients/cell lines **(B)** Quantification of engraftment of AML cells in BM and spleen of $CD34^+$ alone scaffolds or + AML patients/cell lines; Error bars are +/- SEM; dotted line at 0.1 % presents the minimum percentage to be considered engraftment; non-detected (N/D)

4.1.3 Viability of non-leukaemic haematopoietic cells in scaffolds

Similar to the *ex vivo* human niche model, we first excluded the possibility that suppression of HSPC expansion in the scaffolds was a consequence of apoptosis. Viable cells from total non-leukaemic human $CD45^+$ cells and $CD34^+$ HSPCs were quantified owing to the excretion of DNA intercalating substances DAPI or PI. On average more than 85 % in both population from $CD34^+$ alone, +AML patients and + AML cell lines were viable. Paired statistical analysis confirms no consistent impact on viability except $CD34^+$ HSPCs from AML patients which

were marginally reduced between 2 to 5 % (Figure 26B).

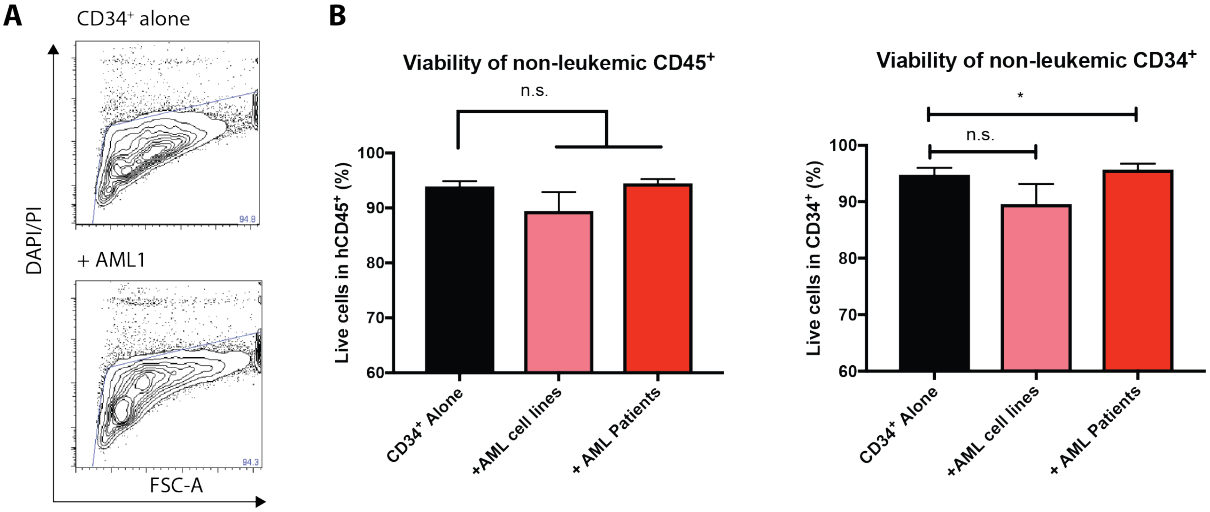


Figure 26. Viability of non-leukaemic human haematopoietic cells
(A) Representative plots of gating strategy to distinguish viable from dead cells using DAPI/PI exclusion **(B)** Quantification of viability of all non-leukaemic human haematopoietic cells ($CD45^+$) and $CD34^+$ HSPCs from 3 independent experiments; n=*p<0.05, n.s. p > 0.05 determined using paired student T-test. Error bars are +/- SEM

4.1.4 Proliferation of non-leukaemic haematopoietic cells

The proliferation of HSPCs *in vivo* was measured utilising two independent techniques. The first technique is based on the injection of the thymidine analogue EdU 16h prior to scaffold retrieval and digest. EdU is incorporated in the replicating DNA strands by cells in S-phase, and the proportion of EdU^+ cells determine the percentage of cells in S-phase at any point during the 16h between injection and retrieval. For scaffolds devoid of AML around 15-25 % of non-leukaemic $hCD45^+$ cells contained EdU but +AML high and + AML cell lines showed on average 50 % fewer EdU^+ cells (Representative example: Figure 27A). Surprisingly, normal $hCD45^+$ from +AML low scaffold also contained 25 % fewer EdU^+ cells (Figure 27B). EdU analysis requires fixation and permeabilisation after staining for surface antigens. This and the relatively small number of $CD34^+$ cells prevented a meaningful analysis of EdU incorporation in $CD34^+$ HSPCs in + AML patient scaffold. +AML cell lines scaffold were retrieved 2-5 weeks earlier, allowing an analysis of Edu incorporation in HSPCs. In agreement with total haematopoietic cells, also the proportion of EdU^+ cells were reduced to a similar extent in +

AML cell lines scaffolds (mean decrease: 50 %) (Figure 27C).

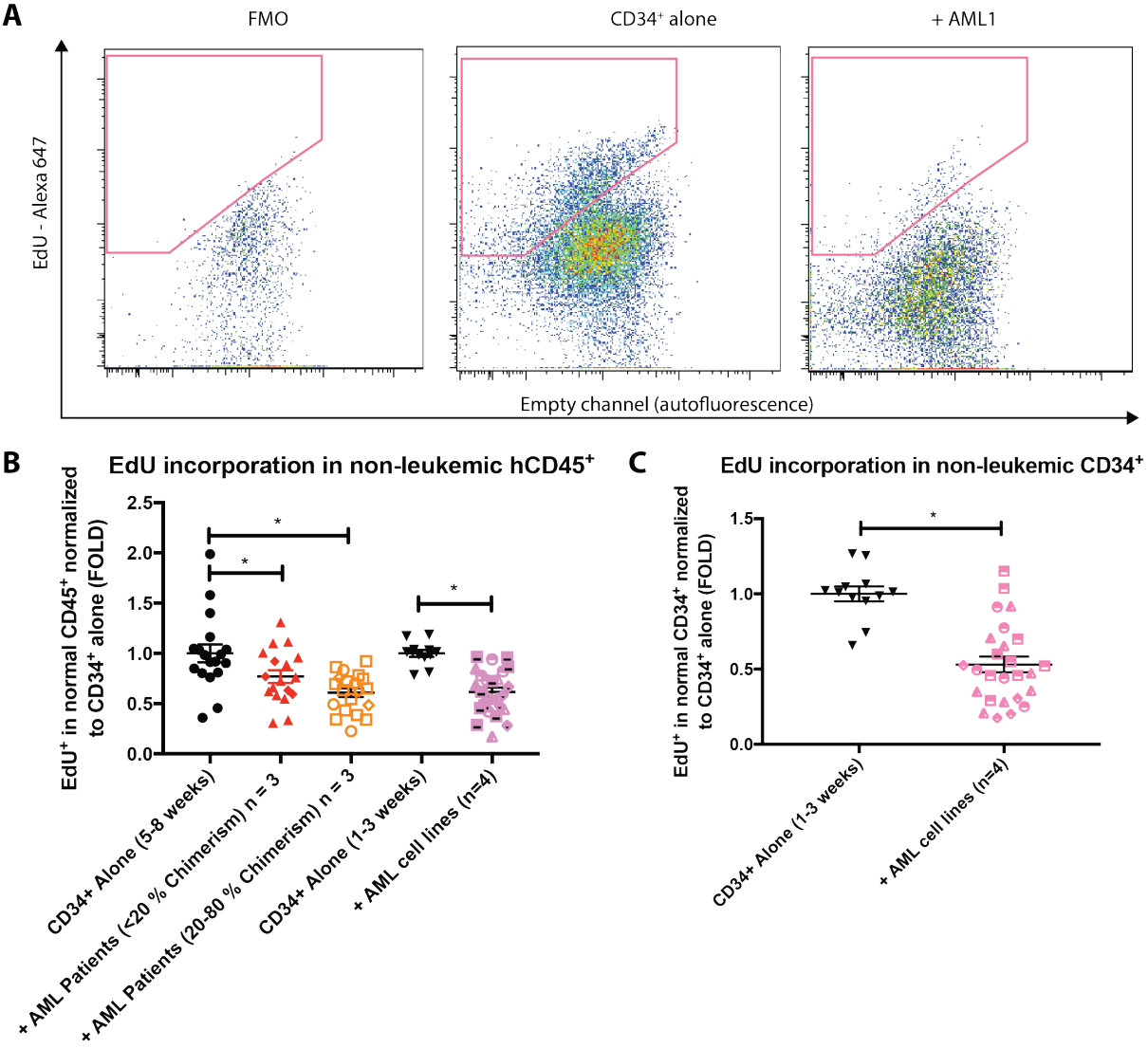


Figure 27. Analysis of cycling non-leukaemic human haematopoietic cells via EdU incorporation

EdU was injected 16h prior to scaffold retrieval interperitoneally (IP) **(A)** Representative plots showing the gating strategy to determine EdU-Alexa647$^+$ cells from CD34$^+$ alone (mid) and + AML1 (right) using an Alexa647 negative control (left) **(B)** Quantifications of EdU$^+$ non-leukaemic human haematopoietic cells relative to CD34$^+$ alone (n= min. 3) **(C)** Quantifications of EdU$^+$ non-leukaemic human CD34$^+$ HSPCs from + AML cell lines relative to CD34$^+$ alone (n=5); each dot represents a scaffolds and symbols represent the specific AML patient samples/cell line *p<0.05, n.s p > 0.05; Error bars are +/- SEM

For the second technique to compare proliferation, we performed another pulse-chase experiment with normal HSPCs stained with CellTrace Violet shortly before injection into scaffolds. Because cells containing CellTrace Violet were found up to 2 weeks post-transplantation, we conducted only experiments with AML cell lines (Figure 28A). In CD34$^+$ alone scaffolds the CellTrace Violet$^+$ population (termed CTV^{hi} in analogue with the *ex vivo*

model) was enriched with CD34$^+$ cells highlighting the generally more quiescent state of haematopoietic HSPCs compared to more differentiated CD34$^-$ progenitors (Figure 28B left). In + AML cell line scaffolds both normal hCD45$^+$ and CD34$^+$ HSPCs were on average 2.1-fold more enriched with CTV^{hi} cells which confirms the suppression of HSPC proliferation (Figure 28C).

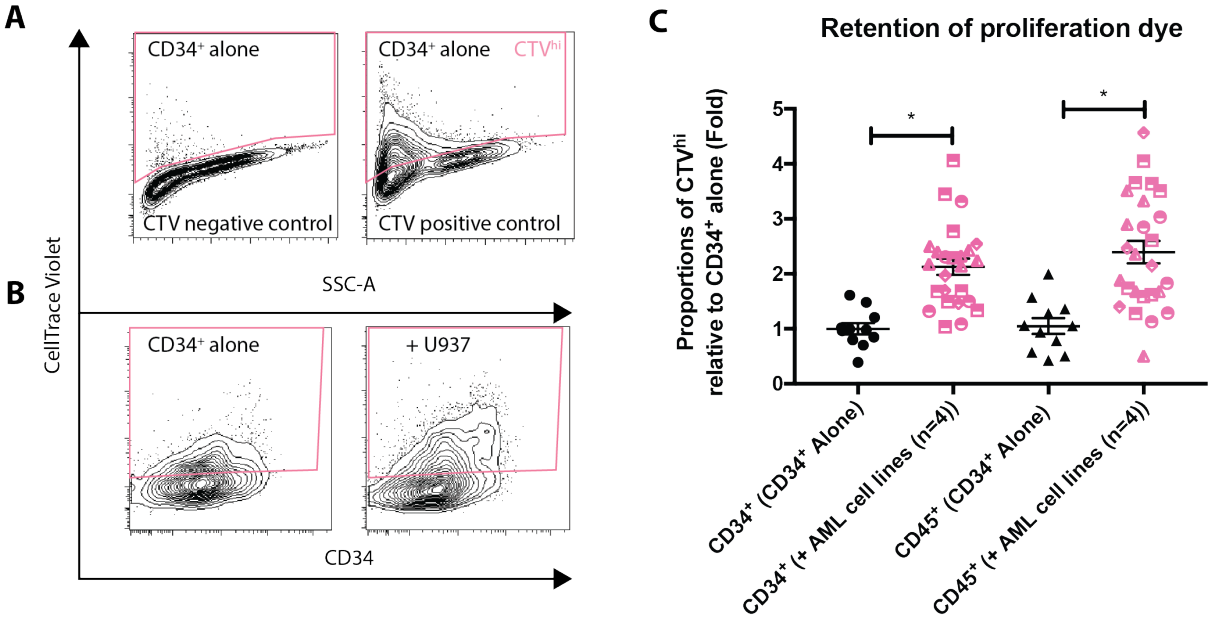


Figure 28. Tracking of proliferation using pulse-chase cell tracer experiments
(A) Representative plots showing the retention of CellTrace violet after 7 days in human non-leukaemic CD45$^+$ cells (right) compared to an unstained control (left) **(B)** Representative plots showing the gating strategy to obtain CTV^{hi} populations of non-leukaemic human CD45$^+$ cells from scaffolds retrieved after 10 days with CD34$^+$ alone (left) or +AML cell line U937 (right) **(C)** Quantification of CTV^{hi} population relative to CD34$^+$ alone (n=5); each dot represents a scaffolds and symbols represent the specific cell line*$p<0.05$, n.s $p > 0.05$; Error bars are +/- SEM

Lastly, we quantified the proportions of CD34$^+$ among normal hCD45$^+$ to establish whether the lack of proliferation also delays the differentiation of CD34$^+$. Indeed, the addition of AML patients or AML cell lines in scaffolds, induced an enrichment of CD34$^+$ HSPCs between 1.5 to 2-fold (Figure 29A). To test the functionally of the HSPCs at least as CFU-generating progenitors 10^5 FACS-sorted normal hCD45$^+$ was plated in methylcellulose supplemented with haematopoietic cytokines. After 21 days, wells with hCD45$^+$ cells from + AML high and + AML cell lines scaffolds had generated between 3 and 1.8-fold more CFUs (Figure 29B).

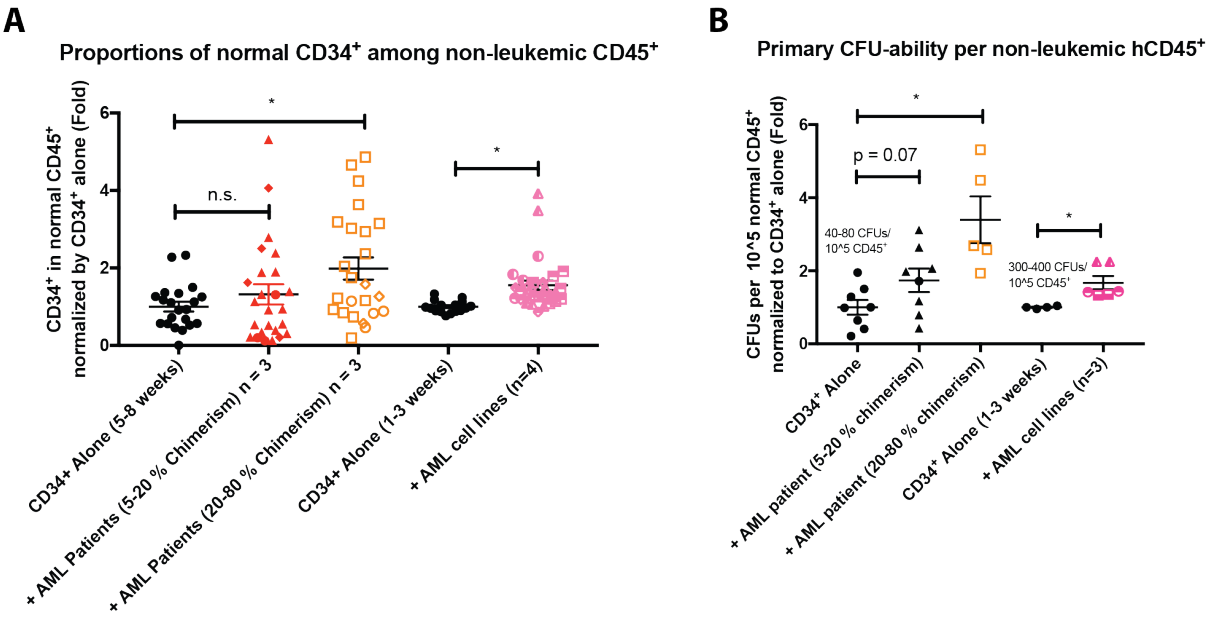


Figure 29. Proportions of CD34$^+$ among total non-leukaemic human haematopoietic cells

(A) Quantifications of CD34$^+$ relative to total non-leukaemic hCD45$^+$ normalised by values from CD34$^+$ alone (n= min 3) **(B)** CFU ability of human non-leukaemic CD45$^+$ cells from CD34$^+$ alone or + AML patients/cell line scaffolds normalised by mean number of CFUs from CD34$^+$ alone (n = 2); each dot represents a scaffolds and symbols represent the specific AML patient sample/cell line*$p<0.05$, n.s $p > 0.05$; Error bars are +/- SEM

4.2 Discussion

In order to compromise between an *in vivo* environment and a fully humanised model system we opted for the MSC-based scaffold system, with pre-seeded haematopoietic cells previously developed in our lab (Abarrategi et al., 2017). Other models developed by Churinga, Majesty and Andreeff and colleagues injected MSCs with an extracellular matrix carrier like Matrigel or directly adhered to a ceramic scaffold. Importantly, these reports showed that these scaffolds (untreated or treated with human parathyroid hormone (PTH), allowed the development of extramedullary haematopoiesis for up to 10 weeks post-transplantation (Antonelli et al., 2016; Chen et al., 2012; Reinisch et al., 2016). Subsequently, AML cells were injected intravenously (I.V.) or directly into the scaffolds and engrafted at higher levels in the humanised niche than the mouse bone marrow niche. Another non-scaffold model developed by Boyd et al. and Passaro et al.is the co-injection of normal HSPCs with AML into immunodeficient mice. While this model may present the most complex niche, it is also difficult to specifically modify niche elements and very early competition for the SCN could influence engraftment outcome (Boyd et al., 2017; Passaro et al., 2017b). Indeed, co-injections of murine HSPCs together with MLL-AF9 transformed leukaemia cells significantly delay leukemogenesis in an HSPC dose-dependent manner as fewer AML cells reach the SCN (Glait-Santar et al., 2015).

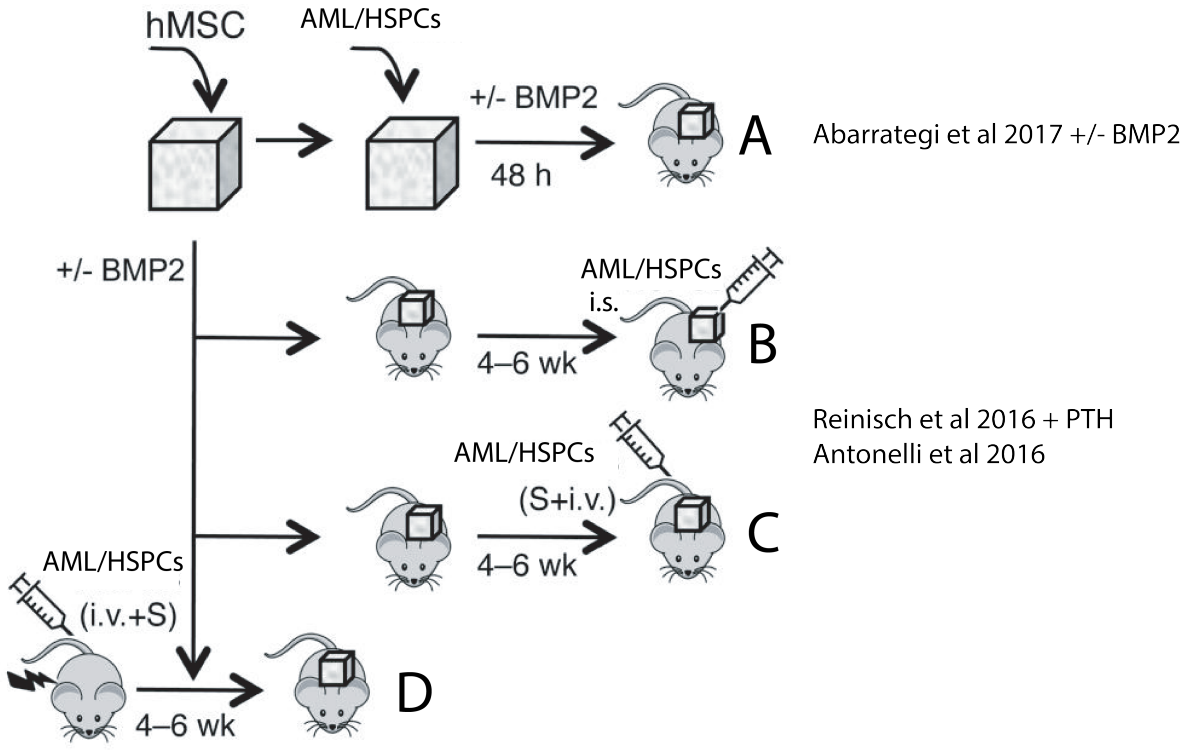


Figure 30. Schematic overview of different MSC scaffold models (adapted from (Abarrategi et al., 2017))
Comparison of potential routes of HSPC/AML administration from published MSC scaffold models. Intravenous injections (i.v.), intra-scaffold (i.s.)

The collagen-scaffold system from the Bonnet lab facilitates engraftment of normal HSPCs and AML patient samples even for samples with inferior murine BM engraftment capabilities. As part of the optimisation, Abarrategi et al. compared MSC scaffold pre-injected with CB HSPCs to MSC-scaffolds transplanted without HSCPs which either had received HSPCs I.V. 4-6 weeks before or after implantation I.V. or directly via intra-scaffold (I.S.) injections. The pre-seeding technique achieved similar human engraftment as the pre-engrafted mice (Figure 30A/D) but the engraftment in scaffold injected with HSPCs 4-6 weeks after transplantation was significantly lower (Figure 30B/C) (Abarrategi et al., 2017). Despite a rapid vascularisation of the collagen-matrix scaffolds, even without the support of pre-seeded endothelial cells (Passaro et al., 2017a), single injections of HSPCs do not deliver enough HSPCs to the scaffold to ensure high engraftment. Scaffolds in HSPC pre-implanted mice are continuously seeded with circulating HSPCs over a longer period and therefore achieve similar engraftment as pre-seeded scaffolds (Abarrategi et al., 2017).

To faithfully compare the engraftment of normal HSPCs in the absence or presence of AML equal numbers of HSPCs at the beginning of the experiments in all scaffolds is pivotal. Other options than pre-seeding of haematopoietic cells prior to transplantation would have been I.V. or I.S. Injections of cells (Figure 30 B/C) or implantation of scaffolds into mice pre-transplanted with AML or normal HSPCs (Figure 30D).
For the first option to generate similar engraftment as pre-seeded scaffolds, higher number of precious human HSPCs or continuous injections would have been required. Furthermore, this option grants less control over precise cell numbers per scaffold than pre-seeding techniques. In particular, I.S. injections are difficult because *in vivo,* the previously spongy scaffolds transformed into a rubber-like consistency and compared to BM do not provide a cavity for injection.
The second option would be to pre-engrafted mice with normal HSPCs and implant CB HSPC, as control, or pre-seeded AML scaffolds. Over time the HSPC from the BM would home to scaffold and generate a human engraftment. In this model, to compare control and + AML scaffolds equal homing of HSPCs from the BM to empty or AML engrafted scaffolds would be required. AML has been shown to affect the homing of HSPCs via down-regulation of

SDF1, which would impede to distinguish between homing and proliferation on the outcome of normal engraftment. Pre-engrafting mice with HSPC instead of AML would solve the homing bias and ensure an equal number of HSPCs per scaffold at the start of the experiments, but AML cells usually do not enter circulation before high chimerism is achieved. Additionally, AML cell lines usually lead to fatal outcome within 3 weeks which may be too short to allow AML engraftment into the scaffolds, and systemic effects of AML like cytopenia and cachexia would also influence the experiments.

In consideration of the experimental data from Abarrategi et al. and the available options to ensure a fair comparison between AML and control scaffold, the pre-seeding model provides the best advantage/disadvantage ratio. The apparent disadvantage being that the MSCs and endothelial cells may not have enough time to generate a normal niche before AML engraftment.

In agreement with the *ex vivo* data, AML cell lines and AML patients with high engraftment potential reduced normal engraftment. In the study, only AML patients capable of engraftment in murine NSG recipient were used, but certain patients failed to generate significant AML engraftment. Surprisingly, when these AML patients were transplanted without CB HSPCs, the engraftment percentage and retrieved AML cell numbers were significantly higher. This implies that also in our model HSPCs delayed AML engraftment in certain AML cases. Of note, the high engrafting AML sample, AML1, also produced around 100-fold more CFU *ex vivo* than AML patient samples with low *in vivo* engraftment hence the frequency of LICs may be a decisive factor.

Normal human haematopoietic cells showed less proliferation measured by two independent techniques. The pulse-chase technique is a powerful tool to record all cell cycle event over an intermediate period of time (up to two weeks). For experiments with AML patients, at least 5 weeks were necessary to generate proper AML engraftment. Therefore, we opted to measure proliferation with EdU incorporation. Ki67/DAPI expression would have been another possibility but EdU provides a more direct measurement since it is incorporated in DNA during replication. Other causes than proliferation which could diminish normal haematopoietic engraftment were also considered like cell death and egress. Cell death as the root cause was eliminated since no significant changes in the proportions of viable cells among normal $hCD45^+$ cells was observed. Egress of normal HSPCs from the scaffolds may provide another explanation for the reduced engraftment of normal HSPCs. In contrast to Abarrategi et al. who observed engraftment of HSPCs in the BM of scaffold implanted mice, we observed neither

normal nor AML engraftment in the BM or extramedullary haematopoietic sites like the spleen. However, our model was on average 6 weeks shorter and the BM was not cleared of residual HSPCs by irradiation. Therefore, we may have missed any significant scaffold egress, which is not mutually exclusive with the proliferation hypothesis and may present an additional factor.

Lastly, HSPCs differentiation measured by the down-regulation of $CD34^+$ was delayed in AML co-transplanted scaffolds. In both control and AML scaffolds, HSPCs differentiated rapidly, especially during the first 10 days dropping from exclusively $CD34^+$ cells to 20 % and 1 %, respectively. This rapid expansion of HSPCs agrees with the cell cycle promoting effects of SCF, IL3 and GM-CSF expressed by the NSG-SGM3 mice (Wunderlich et al., 2010). The low leukemogenesis from the patients AML cells or the few AML cell line cells during scaffold initiation phase may allow some initial differentiation/proliferation similar to the first 48h of the *ex vivo* model. Additionally, the lack of proliferation from $CD34^-$ cells may initiate further differentiation from HSPCs to compensate. Importantly, our *ex vivo* CFU-assay revealed a higher frequency of primary CFU-forming cells per normal human $CD45^+$. Unfortunately, more stringent HSC-oriented validations could not be performed because normal HSPCs from scaffolds did not engraft when injected intravenously into secondary recipients.

In summary, the *in vivo* humanised niche model supports the hypothesis that AML suppresses reduces HSPC expansion by preventing differentiation and proliferation of immature progenitors. Like the *ex vivo* model, apoptosis does not seem to be involved in suppressing the engraftment of normal $hCD45^+$ cells. AML patient samples generated two different phenotypes depending on the AML engraftment level. Aggressive patient samples actively suppress HSPC expansion much like cells lines, but low engraftment does not seem to inhibit HSPC proliferation significantly. This seems to be reminiscent of the *ex vivo* system with AML cell lines which displayed individual differences regarding the ability to induce HSPC suppression *ex vivo*.

Chapter 5. An AML remodelled mesenchymal niche suppresses normal HSPCs

5.1 Introduction

The BM microenvironment, including the SCF is subject to vast transcriptional and proteomic remodelling (Geyh et al., 2018; Kornblau et al., 2018; Reikvam et al., 2015). A transformation into a niche that exclusively favours AML proliferation occurs (Xiao et al., 2018; Zhang et al., 2012). Like the haematopoietic system, the post-mitotic nature of osteoblastic/adipocytic niche elements makes them dependent on undifferentiated mesenchymal cells like MSCs to replenish cell loss due to injury or inflammation (Park et al., 2012; Zhou et al., 2014). Both adipocytes and mature osteoblasts are depleted from AML BM since either AML harnesses their lipid content or directly induces apoptosis (Boyd et al., 2017; Duarte et al., 2018; Shafat et al., 2017). Loss of the osteoblastic niche stimulates lymphocyte egress from the BM and provides AML with additional space and nutrients to expand (Bowers et al., 2015). On the other hand, MSCs are more numerous in AML BM and enter cell cycle partly due to the defective and/or disappearance of the sympathetic nervous system extensions which in steady-state control MSC quiescence (Hanoun et al., 2014; Mendez-Ferrer et al., 2010). In turn, this leads to exhaustion and p16/p21 mediated senescence of MSCs (Abdul-Aziz et al., 2019). However, the MSCs are unable to differentiate properly, an inhibitory effect of AML on MSC-adipocyte differentiation has been reported repeatedly (Battula et al., 2017; Boyd et al., 2017). More disputed are the effects on MSC-osteoblast differentiation since AML poises MSCs for osteogenic differentiation by up-regulation of key early osteoblastic transcription factors like RUNX2 but also inhibit complete differentiation towards functional osteoblasts (Battula et al., 2017; Geyh et al., 2016; Kumar et al., 2018).

Often AML MSCs are cultured over several weeks in multiple passages, and only self-driven molecular alterations will persist in the absence of AML. For example, TGF-β1 activation is a potent inhibitor of osteoblastic differentiation, and AML MSCs display a TGF- β 1 response signature and secrete abnormal quantities of TGF-β 1 (Geyh et al., 2016). Furthermore, p16 activation and senescence is often observed in MSCs from AML patients which expand over fewer passages than their healthy donor counterparts and is associated with an increased inflammatory cytokine release called the senescence-associated secretory phenotype (SASP). SASP and many SASP-related cytokines like Interleukine-8 (IL-8) or Interleukine-6 (IL-6) facilitate AML proliferation (Abdul-Aziz et al., 2019). Specific cytokines with positive

feedback-loops like TGF-β 1 or the SASP are attractive candidate to explore common haematopoietic defects after complete remission like CRi or AML relapse. Indeed, TGF-β 1 participates in the cell cycle suppression of normal HSPCs in leukaemic mice and AML MSCs are less supportive for HSC over long-term culture (Geyh et al., 2016; Gong et al., 2018). Other transcriptional modifications lacking positive feedback-loops and therefore depend on the presence of AML. Examples include NF-kB, which is activated by VLA-1/VCAM-1 or IL-1β or hypoxia-response genes (Jacamo et al., 2014).

Hypoxia regulates several pathways, but the most studied is the HIF-pathways. Comparable to the regulation of p53, the alpha units are constitutively expressed but under normoxia post-translationally modified and degraded. Modifying enzymes rely on oxygen or other oxygen-related metabolites and hence are unable to induce the degradation under hypoxia. Stable alpha units interact with the beta unit and bind to HRE sequences in the genome and recruit histone acetyltransferase P300 to regulate neighbouring genes (Majmundar et al., 2010). The non-malignant BM already contains a limited oxygen pressure which is further reduced in AML (Passaro et al., 2017b; Spencer et al., 2014). Hypoxia is particularly pronounced around AML occupied BM, which may be explained by the oxidative metabolic requirement of unregulated expansion compared to normal BM cells and a dysfunctional vasculature (Passaro et al., 2017b). In solid cancers and the normal BM oxygen concentrations gradually drops along the mean distance from the tumour surface or vasculature (Spencer et al., 2014). In addition to diffusion gradients of oxygen, cancer cell respiration in 2D and 3D cultures diminishes oxygen pressure even in normoxic culture conditions implying cell autonomous (respiration) and non-cell-autonomous(diffusion/vasculature) causes (Russell et al., 2017; Weise et al., 2013).
Apart from HSPCs, the α units, HIF-1α and HIF-2α are expressed in human and murine MSCs and negatively regulate the proliferation of MSCs and HSPCs *ex vivo* (Guarnerio et al., 2014; Palomaki et al., 2013). However, the importance of hypoxia-regulated genes and HIF α subunits for AML cells themselves and their potential roles in regulating HSPCs during AML is mostly unknown.

5.2 Results

5.2.1 The impact of AML on the MSC transcriptome

As part of a related project we observed that culture of MSCs in intermediate hypoxia (3% O_2) activated the transcription of several well-established hypoxia response genes by several-fold like *glucose transporter 1* (*GLUT1)*, *pyruvate dehydrogenase kinase 1* (*PDK1), transforming growth factor -β2 (TGF-β2) and Interferon-alpha (IFN-a)* and *vascular endothelial growth factor 1* (*VEGF1)*. Additionally, we found that the transcription of secreted glycoprotein *stanniocalcin 1* (*STC1*) and several *IGFBPs* were affected (Figure 31B, white column). Surprisingly, we observed that many of the same genes were up- or down-regulated in FACS isolated MSCs co-cultured in normoxia with AML cell lines and patient samples (Figure 31A-B). This indicates that AML induces a hypoxia-like gene expression signature in MSCs even under normoxic conditions.

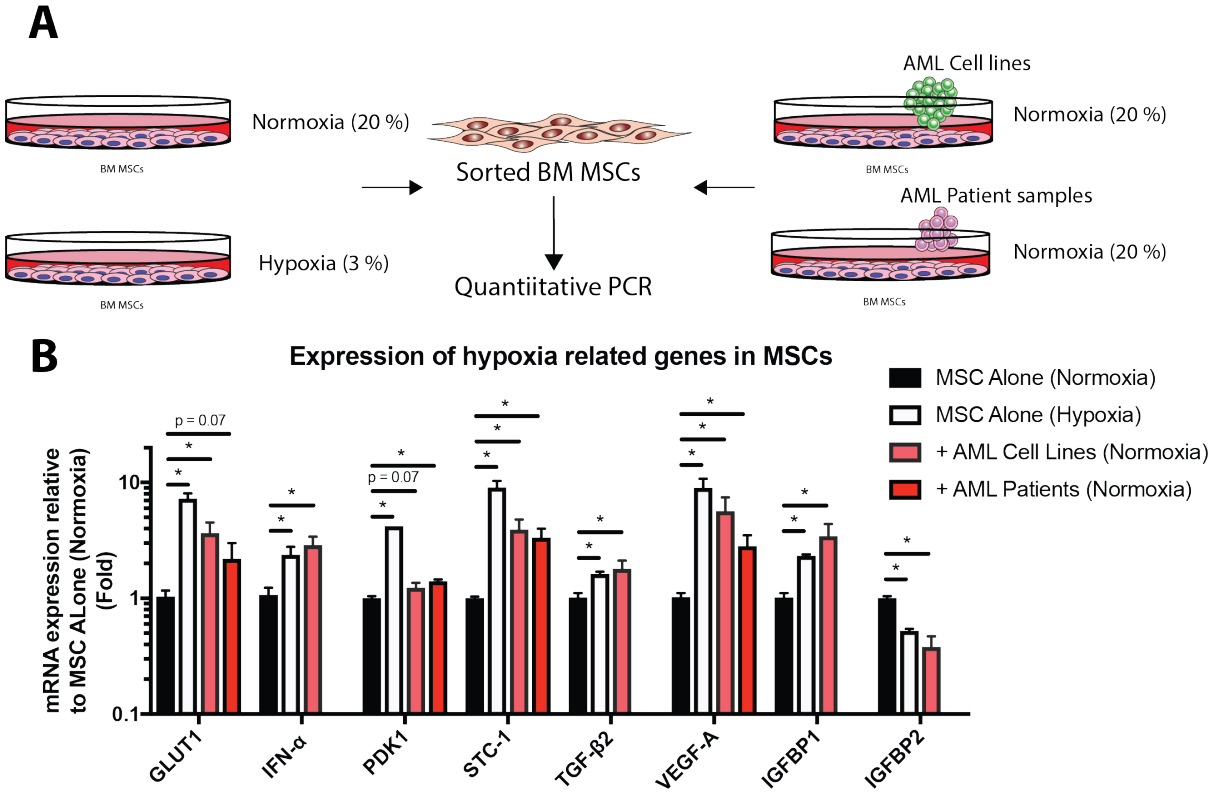


Figure 31. Expression of hypoxia-regulated genes in MSCs co-cultured with AML in normoxia

(A) Schematic representation of experimental approach to dissect the impact of AML on the MSC transcriptome, MSCs were cultured for 5 days with AML cell lines/patient samples or alone in normoxia and hypoxia **(B)** Expression of several hypoxia regulated genes representative of 3 independent experiments from 3 AML cell lines (HL60, ML1 and U937) and 3 AML Patients (AML6, AML8 and AML9). RNA was measured with comparative CT Method using RPL18A as housekeeping gene; *p<0.05, n.s. p > 0.05; Error bars are +/- SEM

5.2.2 Impact of mesenchymal microenvironment on HSPC repression

The *ex vivo* system consist of a niche mimicking MSC part, normal human HSPCs and malignant AML cells. The latter suppresses the proliferation of HSPCs, but whether AML remodelled microenvironment is required or suppression occurs per se cannot be discriminated at this point. Therefore, we adapted the culture conditions to support feeder-free expansion of normal HSPCs by replacing the standard culture medium with feeder-free media supplemented with a supportive cytokine cocktail (SCF, TPO, FLT3L). This enables a direct comparison of HSPC proliferation alone and with AML in the presence or absence of MSCs. Since AML patient samples grow poorly without supporting stroma, we carried out all experiments with AML cell lines (Figure 32A).

After 4 days culture the proliferation of $CD34^+$ HSPC was measured by pulse-chase CTV retention and normalised by the proportions of CTV^{hi} from $CD34^+$ alone for both MSC feeder (+ MSC) and feeder-free conditions (-MSC). Both + AML (-MSC) and + AML (+MSC) affected the proliferation of HSPCs, however, + MSCs HSPCs displayed a more profound retention of CTV (+AML (+MSC) 4-fold versus + AML (-MSC) 2-fold). In agreement, we recovered significantly fewer $CD34^+$ HSPCs from +AML (+MSC) than +AML (-MSC) cultures which further indicates that MSCs amplify the HSPC suppressive effect of AML (Figure 32C). AML cell numbers between +MSCs and -MSCs were comparable which excludes differences in AML proliferation as confounding factor.

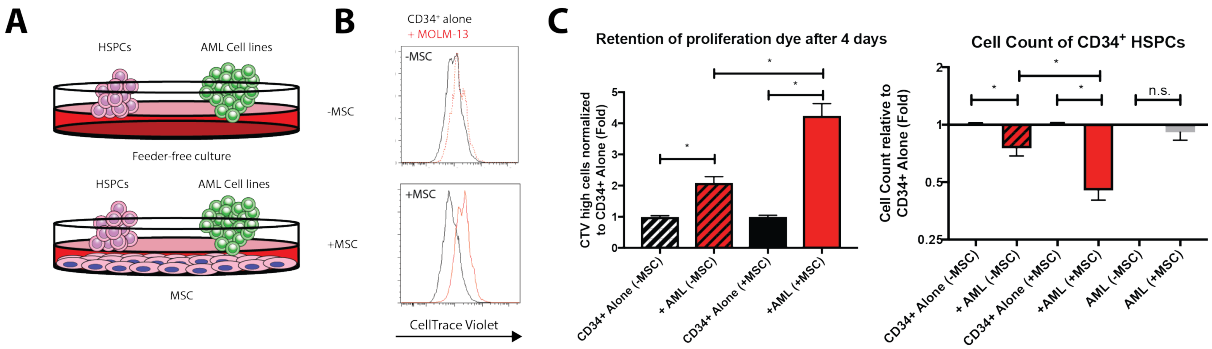


Figure 32. Comparison of HSPC suppression by AML on feeder-free and MSC supported conditions

(A) Schematic representation of culture conditions to assess the impact of the microenvironment on HSPC repression **(B)** Representative plots to measure retention of CellTrace Violet from $CD34^+$ alone (black line) and + AML cell line MOLM-13 (red line) in feeder-free (top) and MSC-based (bottom) conditions **(C)** Quantification of CTV^{hi} population (left) and $CD34^+$ HSPCs cell counts (right) from feeder-free (black stripped) or MSC-based (solid) conditions normalised by $CD34^+$ alone CTV^{hi} and cell count (n=3), respectively; *$p<0.05$, n.s $p > 0.05$; Error bars are +/- SEM

5.2.3 AML pre-conditioned MSCs suppress HSPC expansion

Co-cultures of AML and MSCs have a profound impact on differentiation, proliferation and transcription in both cell types. The stromal niche accelerates the impairment of normal HSPC expansion, but it is not clear whether this effect occurred because AML remodelled the MSCs or vis versa. To prove the concept that HSPC suppression is a consequence of mesenchymal niche remodelling, we pre-conditioned the MSCs with AML cell lines expressing an inducible apoptosis switch under the control of caspase 9 (Figure 33B) (the plasmid was obtained from Addgene and deposited by David Spencer). Once the MSCs were pre-conditioned, we added the chemical dimerizer (AP1903), which bind to the FK503 domains of Caspase 9, efficiently induces apoptosis within 24h and allows the complete removal of AML (Figure 33C). Afterwards, normal HSPCs in fresh media were added and cultured for 48h (Figure 33A). The efficacy of the apoptosis switch was tested on several AML cell lines and compared to their non-transduced parental relatives. Proliferation of AML over 72h was reduced between 90 to 99.9 % in relation to untreated or the parental cell lines (Figure 33D).

Firstly, to confirm that hypoxia-inducible genes remain upregulated at least during the initial 48h after AML removal we analysed the expression of several genes (*VEGF-A*, *STC1*, *GLUT1* and *PDK1*) from MSC alone or AML pre-conditioned MSCs after 24h and 48h. While expression of moderately upregulated genes like *GLUT1* and *PDK1* reverted to levels similar to the MSC alone control, the highly upregulated *STC1* and *VEGF-A* remained at least 1.5-fold upregulated up to 48h after AML pre-conditioning (Figure 34A). STC1 concentrations in HSPC media from AML pre-conditioned MSCs was found 10-45 % elevated compared to MSC alone supernatant for 4 out of 5 AML cell lines which indicates that MSC retain a hypoxia response signature on mRNA and protein level for at least 48h after AML co-culture (Figure 34B).

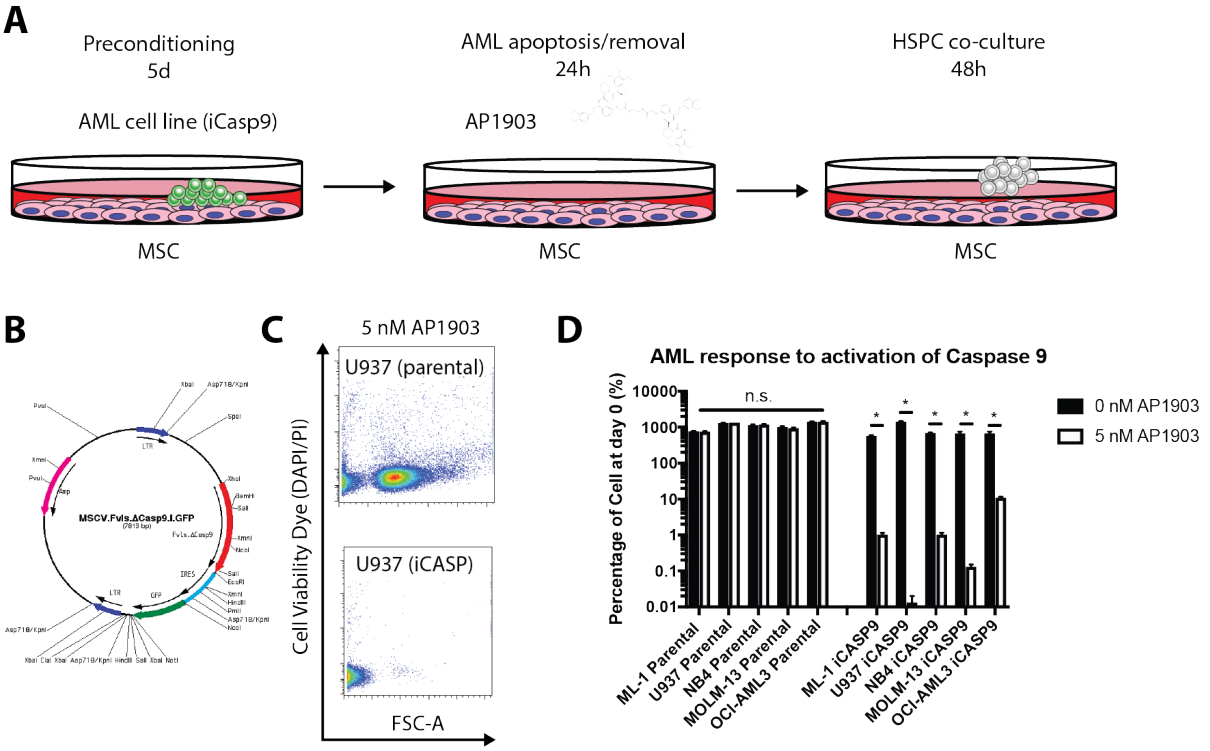


Figure 33. Experimental setup for pre-conditioning MSCs with AML (iCASP)
(A) Experimental setup to precondition MSCs for 5 days with AML (CASP) and removal of AML by induction of apoptosis and subsequent co-culture with normal HSPCs for 48h **(B)** Retroviral CASP expression vector with restriction enzyme sites, open reading frame (ORF), selection markers and long terminal repeats (LTR): Ampicillin selection marker (Amp), Caspase 9 polypeptide – FK503 fusion gene (Fvls.ΔCasp9), internal ribosomal entry site (IRES) **(C)** Representative plot of U937 parental cell line and U937 transduced with iCASP vector treated 24h with 5 nM AP1903 **(D)** Quantifications of cell numbers after 72h treatment relative to seeding cell count; *p<0.05, n.s p > 0.05; Error bars are +/- SEM

After establishing that hypoxia-regulated genes are expressed shortly after AML pre-conditioning, we determined the proliferation of normal HSCPs after 48h co-culture with pre-conditioned MSCs. The CTV^{hi} population in total ($hCD45^{+}$) or $CD34^{+}CD38^{-}$ fraction + AML-preconditioned MSCs was on average increased by 12 % and 19 %, respectively. A similar trend (10 % increased CTV^{hi}) for +/+ HPCs was also observed but did not turn out significant after statistical analysis (Figure 34C). As shown before, the degree of HSPC suppression greatly varies among AML cell lines. Interestingly, when we plotted the percentage of CTV^{hi} cells in both $hCD45^{+}$ and $CD34^{+}CD38^{-}$ (+/-) against the relative concentrations of STC1, we observed a significant positive correlation further ping that the degree of MSC remodelling plays an important role in the proliferation suppression of HSPCs (Figure 34D).

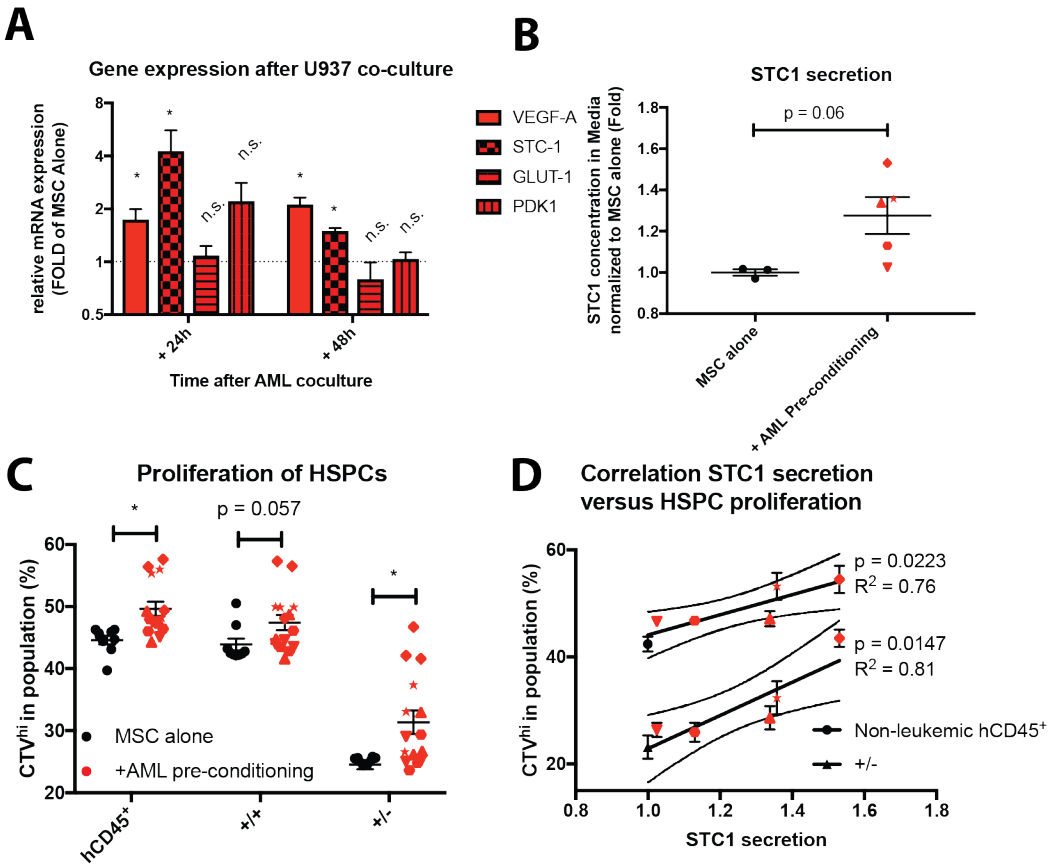


Figure 34. Results of HSPC co-culture with AML-preconditioned MSCs
(A) Representative plot from one out of two experiments of hypoxia response gene expression relative to expression in MSCs alone in MSCs 24h and 48h after AML pre-conditioning, apoptosis and media renewal (B) Relative concentration of STC1 in media supernatant from AML pre-conditioned MSCs after 48h post-AML removal (normalised by STC1 concentrations from MSC alone) (n=1) (C) Percentages of CTV^{hi} in total non-leukaemic $hCD45^{+}$ cells, HPCs +/+ and HSPCs +/- after 48h on MSCs alone or AML pre-conditioned MSCs (n=3) (D) Correlation between relative STC1 concentration in media and CTV^{hi} population after 48h (n=1); each symbol represents data from a specific cell line obtained from an independent experiment *p<0.05, n.s p > 0.05; Error bars are +/- SEM

5.2.4 Hypoxia and hypoxia-regulated genes from MSCs promote HSPC quiescence

Lastly, to confirm that hypoxia and MSC expressing hypoxia-response genes could negatively regulate the proliferation of normal HSPCs, a 7-day co-culture of HSPCs and MSCs was performed at atmospheric oxygen concentrations of 20 %, 3 % and 1 % O_2. The latter two are considered as hypoxia while 20 % acted as a normoxia control. Cell cycle analysis of the HSPCs revealed that both 3 % and 1 % O_2 were sufficient to increase the proportions of quiescent cells in total CD45, HPCs $^{+/+}$ and HSPCs $^{+/-}$ by up to 2.25 to 2.8-fold at an almost equal expense (2.44 and 4.67-fold) of cells in S-M-G2 phase, respectively (Figure 35A). This indicates that O_2 concentration regulates HSPC proliferation in a dose-dependent manner but

does not delineate between cell-autonomous and indirect-MSC cell non-autonomous contributions. Identically to the pre-conditioning of the MSCs with AML, we cultured MSCs for 5 days at 3 % or 20 % O_2 after which HSPCs were added to the cultured with the respective MSCs. Additionally, the expression of hypoxia-regulated genes *STC1*, *VEGF-A* and *GLUT1* was analysed every day following the re-exposure to 20 % O_2. Real-time PCR analysis revealed that all three inspected hypoxia-regulated genes remained significantly upregulated for up to 3 days but with a considerable decay (Figure 35B). The HSPCs co-cultured on hypoxia pre-conditioned MSCs contained on average 12 % more quiescent cells in each HSPC sub-population analysed which indicates that hypoxia-response genes in MSCs reduce the proliferation of HSPCs (Figure 35C).

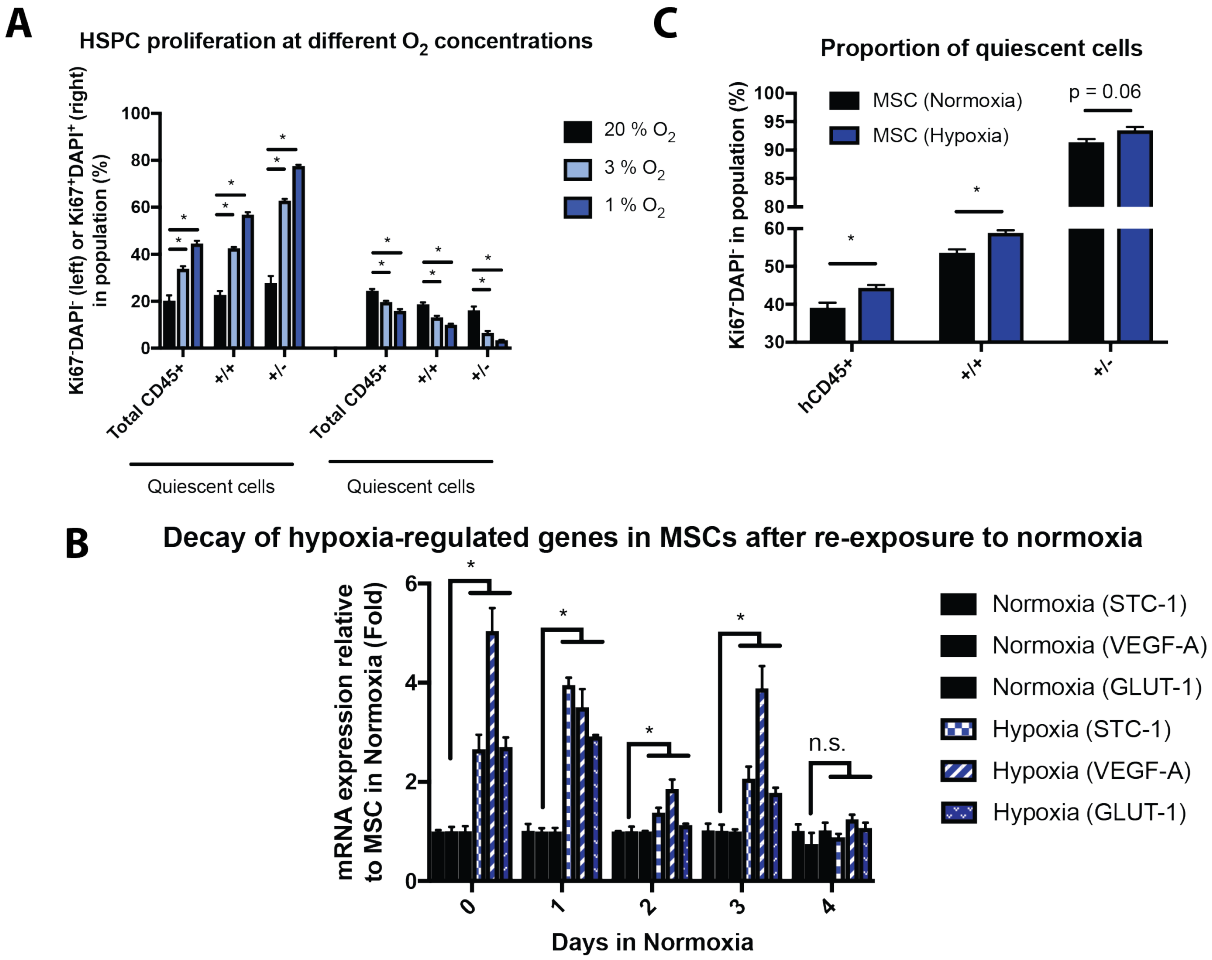


Figure 35. Regulation of HSPC proliferation by hypoxia and hypoxia-regulated genes from MSCs

(A) CB HSPCs were co-cultured with MSCs at different atmospheric O_2 pressure and after 7 days the cell cycle distribution of total haematopoietic (Total $CD45^+$), HPCs +/+ and HSPCs +/- was analysed by Ki67 expression and DNA content (DAPI), representative results from two independent experiments (B) MSCs were pre-conditioned for 5 days at 3 % O_2 or 20 % O_2. Subsequently, the mRNA expression of hypoxia response genes STC1, GLUT1 and VEGF-A was measured and normalised to the expression of 20 % MSCs each day following the re-

exposure to 20 % O_2, representative results from two independent experiments (C) MSCs were preconditioned at 3 % O_2 and 20 % O_2 and followed by HSPC co-culture for 48h. The proportion of quiescent cells among different sub-populations of HSPCs was measured via Ki67 expression and DNA content (DAPI), representative results from three independent experiments; *$p<0.05$, n.s $p > 0.05$; Error bars are +/- SEM

5.3 Discussion

The mesenchymal niche in AML is of particular importance owing to vast cellular, transcriptional and proteomic remodelling. Deficiencies of MSC-downstream osteoblastic and adipocytic cell types further imply that the mesenchymal niche is of crucial importance for haematopoietic homeostasis. From a transcriptional perspective, MSCs isolated from AML patients exhibit aberrant inflammatory NF-kB/IL-1b, TGF-β1 and p16/p21 SASP signalling leading to the downregulation of several essential haematopoietic genes like SCF, Angiopoietin-1 and SDF1 (Abdul-Aziz et al., 2019; Geyh et al., 2018; Jacamo et al., 2014). *Ex vivo* co-cultures of MSCs and AML have mainly been utilised to recapitulate certain transcriptional features of expanded AML MSCs, but less is known about more volatile pathways like the hypoxia-response pathway (Battula et al., 2017). The time-course analysis of hypoxia-regulated genes from hypoxia and AML pre-conditioned MSCs demonstrated that once re-exposed to a control-like environment, the mRNA reverts to control levels within 48h-72h. Obviously, other stimuli than hypoxia may regulate these genes and apart from HIF transcriptional factors, pathways like NF-kB were reportedly involved in the mesenchymal hypoxia response (Crisostomo et al., 2008). A detailed interrogation will follow in chapter 6.

The importance of the mesenchymal microenvironment regarding the response to AML was highlighted by the comparison of feeder-free versus MSC-supported AML-HSPC co-cultures. Interestingly, the proliferation of HSPCs was suppressed in both conditions, but MSCs exacerbated the highest HSPC suppression. This implies that AML is capable of directly suppressing HSPCs, but the majority stems from AML-microenvironmental interactions. From a related project, we reported that lactate, the metabolic end-product of anaerobic glycolysis, induces a dose-dependent suppression of HSPCs proliferation. In comparison to normal MNCs or HSPCs, AML secrete more lactate per cell, indicating that an altered metabolism of AML cells may be part of an MSC-independent mechanism.

Several reports investigated the impact of the mesenchymal microenvironment on AML. Several anti-apoptotic regulators including BCL2 are induced via MAPK-signalling (PI3K, AKT, mTOR) and activation of mitochondrial uncoupling protein UCP2 and beta-oxidation of fatty acids reprograms AML metabolism (Samudio et al., 2008; Samudio et al., 2010; Zhou et al., 2016). Since the perspective of these studies has been on chemoresistance and AML proliferation, little is known regarding the impact of these pathways on HSPC proliferation. Cell counts of AML between feeder-free and MSC-supported cultures were not significantly

different, which at least excludes that differences in AML proliferation affected the HSPC proliferation. However, considering the effects of metabolic end-product lactate, the proliferation-independent rewiring of AML affecting metabolism may impact HSPC expansion and should be further investigated.

Considering the profound impact of AML on MSC hypoxia-response gene expression, at least on the mRNA level, one might speculate that this may impair HSPC proliferation. Interestingly, MSC-supported HSPCs without AML expanded greater than their feeder-free counterparts which implies that normally MSCs do not interfere with HSPC proliferation and provide additional support for haematopoietic cells. Indeed, Xiao et al. postulated that healthy MSCs act as AML suppressors and that by transcriptional reprogramming, the AML transforms them into an AML-exclusively supporting niche (Xiao et al., 2018; Zhang et al., 2012).
Therefore, to rule out that HSPC suppression was merely a result of AML responding to the mesenchymal microenvironment and to elaborate the hypothesis that the hypoxia-response genes in MSCs participate in HSPC suppression, MSCs were pre-conditioned with AML or hypoxia. Indeed, the reduction of HSPC proliferation by pre-conditioned MSCs in a "remodelling-dose"-dependent manner, indicated by the correlation between STC1 secretion and HSPC suppression, supports this hypothesis. Hypoxia-regulated genes, although still upregulated at the protein and mRNA level when compared to normoxia control MSCs, decayed rapidly once the MSCs were re-exposed to a normoxic or AML-free environment. This may underestimate the real contribution of these genes to HSPC suppression but establishes the validity of the concept.

Chapter 6. The MSC secreted factor STC1 suppresses normal HSPCs

6.1 Introduction

Mesenchymal stroma cells are an integral part of the BM microenvironment. In humans, MSCs include 0.001 % - 0.01 % of the nucleated cells in BM but have also been isolated from other sources like liver, dental pulp, spleen, lung, umbilical cord and peripheral blood (Aqmasheh et al., 2017). However, owing to a unique DNA-methylation profile allowing chondrogenic transcription and osteogenic priming, only BM MSCs are capable of generating a bone marrow cavity and sustain haematopoiesis *in vivo* (Reinisch et al., 2015). Apart from humanised *in vivo* niches, BM MSCs are very versatile and have a high clinical potential. MSC secrete anti-inflammatory factors and alleviate inflammatory symptoms of graft-versus-host disease when injected into ASCT patients and myelofibrosis. Furthermore, co-injection of MSCs with HSPCs can improve recovery of haematopoiesis after irradiation (Bader et al., 2018; Liu et al., 2018). MSCs or their murine *in vivo* $LepR^{+}$/$nestin^{+}$ counterparts secrete factor and express surface antigens responsible for HSPC homing (SDF1, VCAM1), maintenance of HSC (SDF), cell cycle (TGF-β1) and immune-response (IL6, IL8) (Aqmasheh et al., 2017; Asada et al., 2017). Additionally, micro-vesicles and exosomes are released in large quantities from MSCs containing miRNA and protein cargo which can promote myeloid progenitor expansion (Goloviznina et al., 2016). As described previously, AML influences the expression of several MSC-derived haematopoietic factors to promote AML proliferation and chemoresistance (Abdul-Aziz et al., 2019; Jacamo et al., 2014) but the effect on normal haematopoiesis is largely unexplored. However, based on the bandwidth of MSC-derived HSPC regulators, it could be predicted that individual modulator could alter HSPC behaviour functions.

The stanniocalcin family of protein was first described in bony fish as regulators of calcium/phosphate homeostasis. In the 1990s, two vertebrae orthologs were discovered: Stanniocalcin-1 and Stanniocalcin-2 but knockout mouse models ruled out involvement in mammalian ion metabolism (Yeung et al., 2012). Both STC1 and STC2 are overexpressed in several solid cancers and convey adverse outcome (Uhlen et al., 2015). Overexpression murine models induce dwarfism mediated via an inhibition of the IGF pathway but further mechanistic analysis of the role of STC1 in cancer is often exacerbated by the lack of knowledge regarding the receptor (Jepsen et al., 2015). Indeed, a conserved signalling response to STC1 has not been demonstrated in different cancer models. Putative modes of action include redox-signalling (Huang et al., 2015; Pan et al., 2015)., MAPK-signalling, BCL2 (Chu et al., 2015; Yeung et

al., 2012) and metabolic reprogramming (Block et al., 2009; Ohkouchi et al., 2012). Furthermore, often, studies do not discriminate between intracellular and extracellular roles of STC1. As an extracellular secreted factor, STC1 has been detected in supernatant from MSCs and endothelial cells. In particular, for MSCs, several STC1 regulating pathways including hypoxia (HIF-1α) (Yang et al., 2015; Yeung et al., 2005), inflammation (IL1α/β) (Bartosh et al., 2013) and TGF-β1 (Ono et al., 2015) have been discovered. For example, irradiated fibroblasts and adenocarcinoma cell line A549 trigger STC1 release from MSCs to improve chemoresistance through UCP2-mediated mitochondrial uncoupling reducing ROS production (Block et al., 2009; Ohkouchi et al., 2012) and in endothelial cells, STC1/2 promotes angiogenesis (Law and Wong, 2013).

In AML, two reports link STC1 measured by mRNA expression in the peripheral blood to adverse outcome (Abaza et al., 2016) and as an early prediction of relapse (Tohmiya et al., 2004). However, when compared to MSCs, AML patients, cell lines and normal HSPCs express several-fold less STC1 mRNA and do not secrete ELISA-detectable amounts into supernatant. On the other hand, MSC-derived STC1 was detected as one of several upregulated MSC genes in response to AML and B-ALL (dos Santos et al., 2011; Reikvam et al., 2015). Nonetheless, the role of STC1 in normal and malignant haematopoiesis is currently unknown.

6.2 Results

6.2.1 AML suppresses is partially dependent on direct contact

Previously, it was already established that direct contact between AML and MSCs accelerates HSPC suppression and transcriptional reprogramming of MSCs, but it is unknown whether direct contact between HSPCs and AML/MSCs is required or secreted factors are responsible. To further dissect this, we compared the HSPC proliferation between HSPCs in direct contact with AML and MSCs to HSPCs separated via a 0.4 µm pore size transwell (Figure 36A). In control conditions of $CD34^+$ alone, no significant difference between HSPCs cultured in direct contact or transwell inserts were detected regarding cell viability or proliferation, confirming the feasibility to compare these two conditions. Firstly, we measured proliferation via retention of CTV and observed in both direct contact and transwell conditions an increased CTV^{hi} population among $CD34^+$ cells but around 50 % less in the transwell (Figure 36B-C). This difference did not prevail when cell counts of total non-leukaemic $hCD45^+$, HPCs and HSPCs was compared (Figure 36D). Of note, normal HSPCs in transwell AML cultures were 10-75 % less viable, explaining why CTV retention, differed but cell counts remained unchanged (Figure 36E). In conclusion, HSPC suppression is mediated by cell-cell interactions and secreted factors, even though HSPCs in close contact with MSCs may be exposed quicker to higher concentrations of secreted factors than HSPCs from transwell inserts which would underestimate the impact of secreted factors.

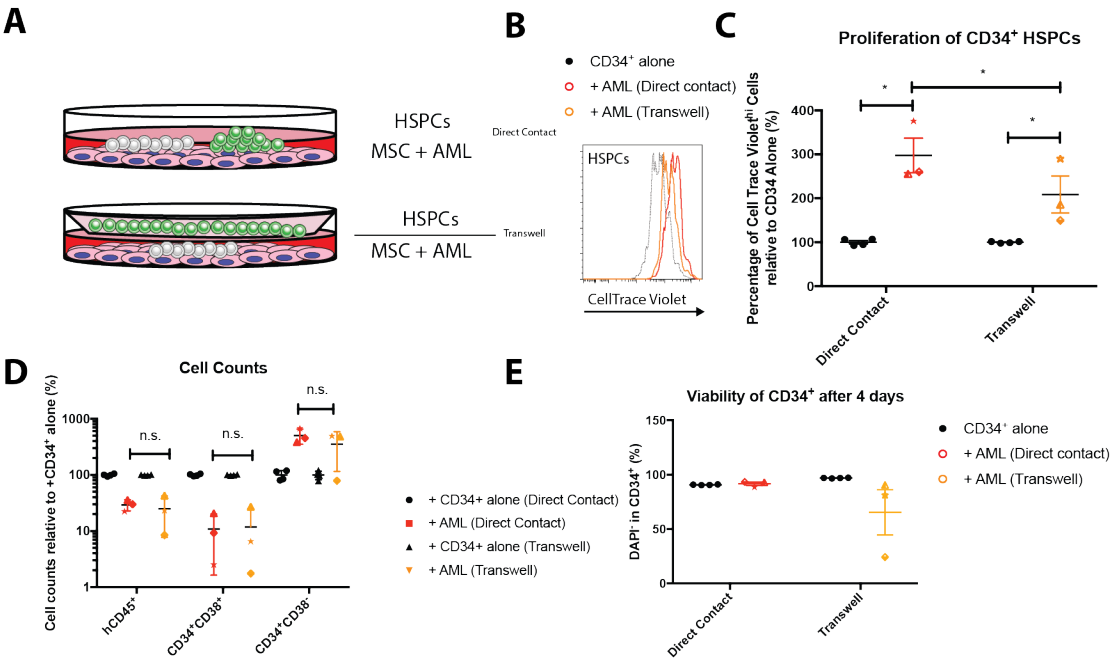


Figure 36. Comparison of HSPCs proliferation in direct contact or in transwell inserts

(A) Schematic representation of experiments design with MSC and AML adhered or in suspension at the dish surface supplemented with HSPCs directly or separated via a transwell insert **(B)** Representative plot of CTV retention in $CD34^+$ HSPCs from $CD34^+$ alone (black), + AML cell line NB4 (direct contact) (red) or + AML cell line NB4 (transwell) (orange) **(C)** Proportions of CTV^{hi} in $CD34^+$ HSPCs normalised to $CD34^+$ alone **(D)** Cell counts of total non-leukaemic haematopoietic cells ($hCD45^+$), HPCs ($CD34^+CD38^+$) and HSPCs ($CD34^+CD38^-$) normalised to cell counts of $CD34^+$ alone **(E)** Percentages of viable ($DAPI^-$) cells among $CD34^+$ HSPCs; each dot represents data from two independent experiments and each symbol represents a specific cell line *p<0.05, n.s p > 0.05; Error bars are +/- SEM

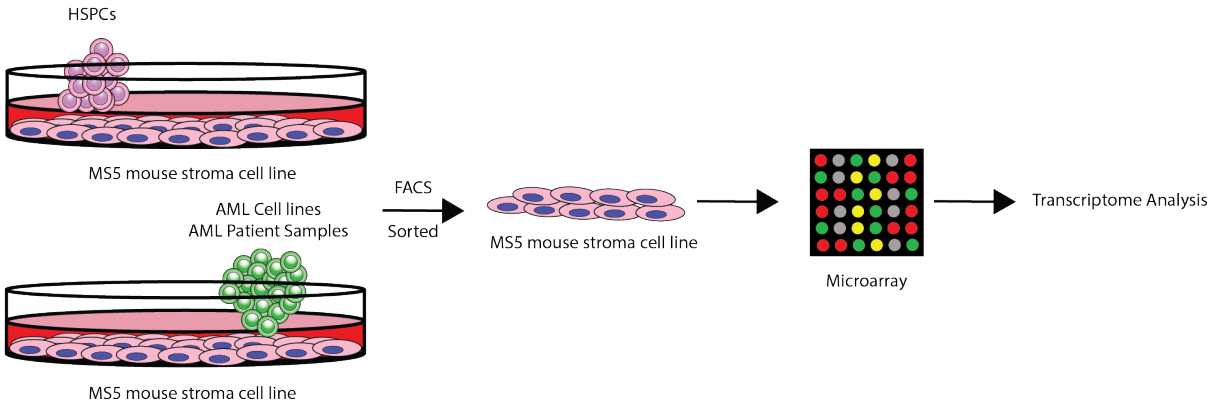


Figure 37. Schematic of transcriptome analysis of MS5 exposed to AML

Microarray performed by Dr. Ashley Hamilton: MS5 mouse stroma cell line was either cultured alone or co-cultured with either normal $CD34^+$ HSPCs, AML cell lines or AML patients. After 5 days, MS5 cell were FACS-sorted to extract RNA for microarray analysis of the transcriptome. MS5 cultured alone were compared to MS5 with AML cell lines and MS5 co-cultured with normal HSPCs were compared with MS5 co-cultured with AML7 and AML8

6.2.2 Investigation of stromal secretome after AML culture

Dr Ashley Hamilton, a previous member of the lab, had setup a microarray to compare the transcriptome of a mouse stromal cell line MS-5 co-cultured AML patient samples (AML7 and AML8) and AML cell lines (KG1, U937, Fujioka-1, Kasumi-1, NB4, HL60 and TH19), respectively. MS-5 cultured alone or co-cultured with CB HSPCs served as controls to detect changes in the MS5 transcriptome (Figure 37). Differentially expressed gene sets from MS5 from AML patients and AML cell lines, shared 69 upregulated genes and 59 down-regulated genes with an adjusted p-value of < 0.05 and with logarithmic fold change (LogFC) of >1 and <-1, respectively. The list was screened for secreted factors utilising the MetazSecKB database from Meinken J, Walker G, Cooper CR, Min XJ containing 1819 putative secreted murine proteins. The differentially expressed genes contained 11 secreted factors (10 upregulated and 1 down-regulated) (Table 10-11). GAS6 and KIRRE3 have been reported as stromal derived

secreted factors regulating HSPC maintenance. IGF1 and IGF2 are well-defined promoters of normal and malignant haematopoietic proliferation and survival. The other 7 secreted protein have not been previously annotated with AML or normal haematopoiesis. Interestingly, STC1 has been reported as an MSC-secreted factor regulating fibroblast and lung adenocarcinoma metabolism and regulating chemo-resistance. In solid cancer, STC1 was described as novel biomarkers and conveyed adverse prognosis in several different cancer models.

Table 10. Commonly up-and down-regulated putative secreted genes in MS5 exposed to AML

	MS5 (Alone) versus MS5 (AML cell line)		**MS5 ($CD34^+$) versus MS5 (AML cell line)**	
Gene Name	**LogFC**	**Adjusted p-value**	**LogFC**	**Adjusted p-value**
LYZ6	3.473279526	1.06E-07	2.414773876	9.66E-05
GAS6	2.433432052	1.80E-09	1.66256347	5.48E-06
STC1	**2.19419962**	**0.00974067**	**2.361545323**	**0.01414398**
SEMAC3	1.61006986	5.87E-05	1.247412434	0.00251425
AMY1A	1.582087648	6.67E-05	1.758626323	7.63E-05
KIRRE3	1.480718522	0.00014821	1.222699085	0.00325633
IGF1	1.371770146	0.00030726	3.615091082	8.00E-09
KNG3	1.245225986	0.00202444	1.116900863	0.01223174
IGF2	1.132262855	0.04557032	3.531109599	8.94E-07
HP	1.065585857	0.00405382	2.770054106	1.49E-07
CCBE1	-1.96783893	1.23E-10	-1.837471329	9.23E-06

Table 11. Gene name, associated protein product and function obtained from Uniprot database

Gene Name	**Protein Name**	**Function**
LYZ6	Lysozyme C-1	Bacteriolytic protein expressed by macrophages and some HSCs
GAS6	Growth arrest-specific protein 6	Ligand for AXL, Tyro3 and Mer receptors, expression in stroma cells supports HSPC maintenance and AXL supports AML growth (Ben-Batalla et al., 2013; Jin et al., 2017; Whitman et al., 2014)
STC1	**Stanniocalcin-1**	Glycoprotein with important roles in solid tumours for MAPK, oxidative stress and metabolism
SEMAC3	Semaphorin-3C	Cardiac development and axon guidance during development

AMY1A	Alpha-amylase 1	Hydrolase of alpha-linked polysaccharides
KIRRE3	Kin of IRRE-like protein 3	Guides target-specific synapses as adhesion molecule and supports HSPCs as secreted factor (Ueno et al., 2003)
IGF1	Insulin-like growth factor I	Promotes AML and HSPC proliferation via IGF-receptors 1/2 activated AKT and MAPK signalling (Cheng et al., 2014; Doepfner et al., 2007)
KNG3	Kininogen-1	Blood coagulation and kinin-kallikrein system
IGF2	Insulin-like growth factor II	Promotes AML and HSPC proliferation via IGF-receptors 1/2 activated AKT and MAPK signalling (Cheng et al., 2014; Doepfner et al., 2007)
HP	Haptoglobin	Plasma protein binding free haemoglobin
CCBE1	Collagen and calcium-binding EGF domain-containing protein 1	Required for lymphangioblast budding and angiogenic sprouting from venous endothelium during embryogenesis

6.2.3 AML triggers STC1 secretion from MSCs

Due to STC1's published roles as MSC-secreted factor, the important implications in solid tumour biology and the lack of annotation regarding normal or malignant haematopoiesis, we analysed its role in more detail. To validate the data from the MS5 mouse stroma cell line, healthy human MSCs were co-cultured with AML cell lines, and AML patient samples, FACS-sorted and STC1 mRNA expression and protein expression analysed in comparison to MSC cultured alone by real-time PCR and western blot, respectively. Relative to MSC cultured alone in normoxia, both AML patients and cell lines as well as hypoxia triggered STC1 up-regulation of approximately 3-fold (Figure 38A) but, surprisingly, on the protein level, no accumulation was found (Figure 38B). STC1 is a secreted protein; hence the supernatant of the *ex vivo* humanised niche system was collected and STC1 concentrations measured by enzyme-linked immunosorbent assay (ELISA). In line with the levels of mRNA expression, STC1 concentrations in the supernatant increased between 2 to 30 fold in + AML cell line cultures as compared to $CD34^+$ alone controls (0.035-0.2 ng/mL of STC1 versus 0.5 – 1.15 ng/mL). Also

+ AML patient culture supernatant contained 2 to 5 fold elevated concentrations of STC1 (0.2-0.4 ng/mL versus 0.75 – 1 ng/mL) (Figure 38C). Since the STC1 in the supernatant could theoretically also be derived from AML, we compared the STC1 mRNA expression relative to a ubiquitously expressed housekeeping gene (ribosomal protein 18S (RPS18)) in MSCs, CB HSPCs and AML cell lines. MSCs cultured in normoxia and hypoxia contained 0.1-0.01 copies of STC1 cDNA per copy of RPS18 compared to around 0.00001 copies in AML cell lines and normal HSPCs indicating that AML and normal HSPCs do not express meaningful quantities of STC1 (Figure 38D). Additionally, STC1 was never detected by western blot in normal HSPCs or AML cell lines.

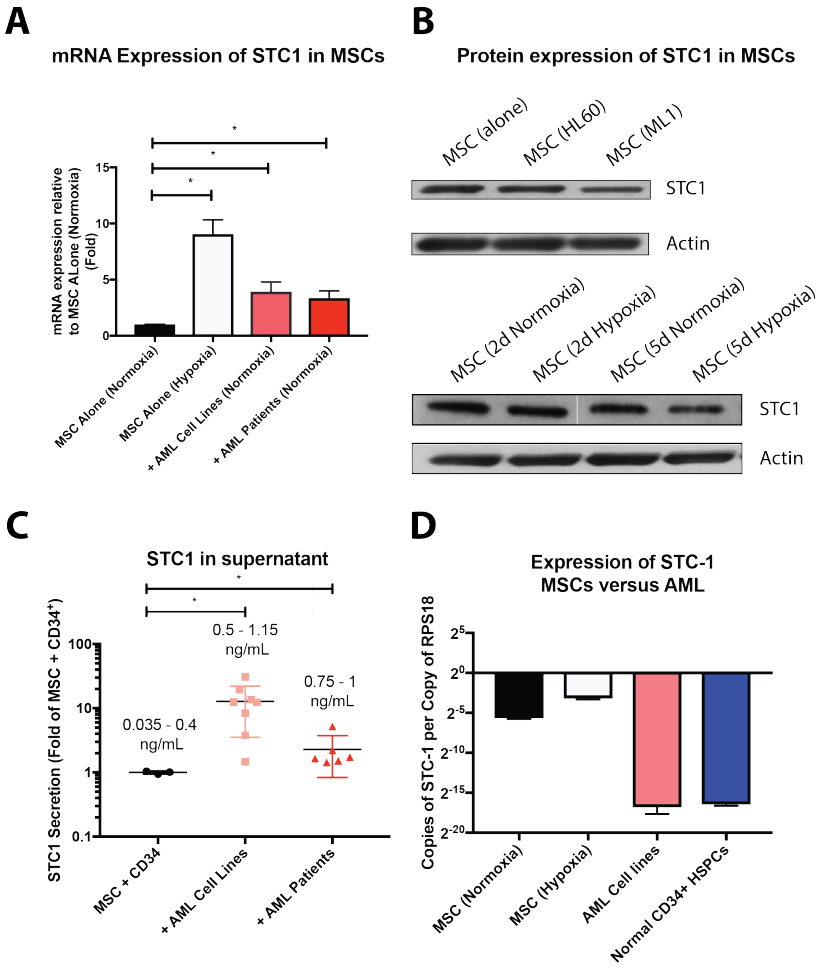


Figure 38. Expression of STC1 in MSCs
(A) STC1 mRNA expression of MSCs cultured alone in either normoxia or hypoxia or co-culture with AML cell lines (HL60, ML1, U937) or AML patient samples (AML7, AML8, AML9) in normoxia (n=2) **(B)** Immunoblot of STC1 protein levels in whole cell extract of MSCs cultured alone or co-cultured with AML cell lines (HL60, ML1) in normoxia (top) and MSCs cultured alone in normoxia and hypoxia for 2 and 5 days, respectively (bottom). Membranes were stripped and re-plotted for actin as loading control (n=1) **(C)** Relative concentrations of STC1 in supernatant from MSCs co-cultured with either normal $CD34^+$ HSPCs, HSPCs + AML cell lines and HSPCs + AML patient samples (n=3) measured by ELISA, absolute concentration ranges are mentioned above the respective bar **(D)** Average

mRNA expression of STC1 relative to housekeeping gene 40S ribosomal protein S18 (RPS18) in MSCs cultured in normoxia and hypoxia (n=3) or AML cell lines and normal $CD34^+$ HSPCs (n=2); *p<0.05, n.s p > 0.05; Error bars are +/- SEM

6.2.4 STC1 as biomarker to measure HSPC suppression

Next, we compared the secretion of STC1 with the suppression of HSPCs. The total numbers of non-leukaemic haematopoietic cells and $CD34^+$ HSCPs and CTV^{hi} $CD34^+$ cells from + AML cell lines and $CD34^+$ alone was plotted against the STC1 expression, expressed as fold-change from $CD34^+$ alone. Statistical analysis of lineage correlation demonstrated a significant inverse relationship between the total numbers of haematopoietic cells and STC1 concentrations (Figure 39A left). For the total numbers of $CD34^+$ HSPCs, a relationship was apparent but did not reach statistical significance (Figure 39A right). Similarly, the proportions of CTV^{hi} cells within total $CD45^+$ cells but not $CD34^+$ were significantly correlated (Figure 39B). This further confirms that MSC transcriptional remodelling is a crucial determinant of HSPCs suppression and indicates that STC1 could be an exciting novel biomarker for these processes.

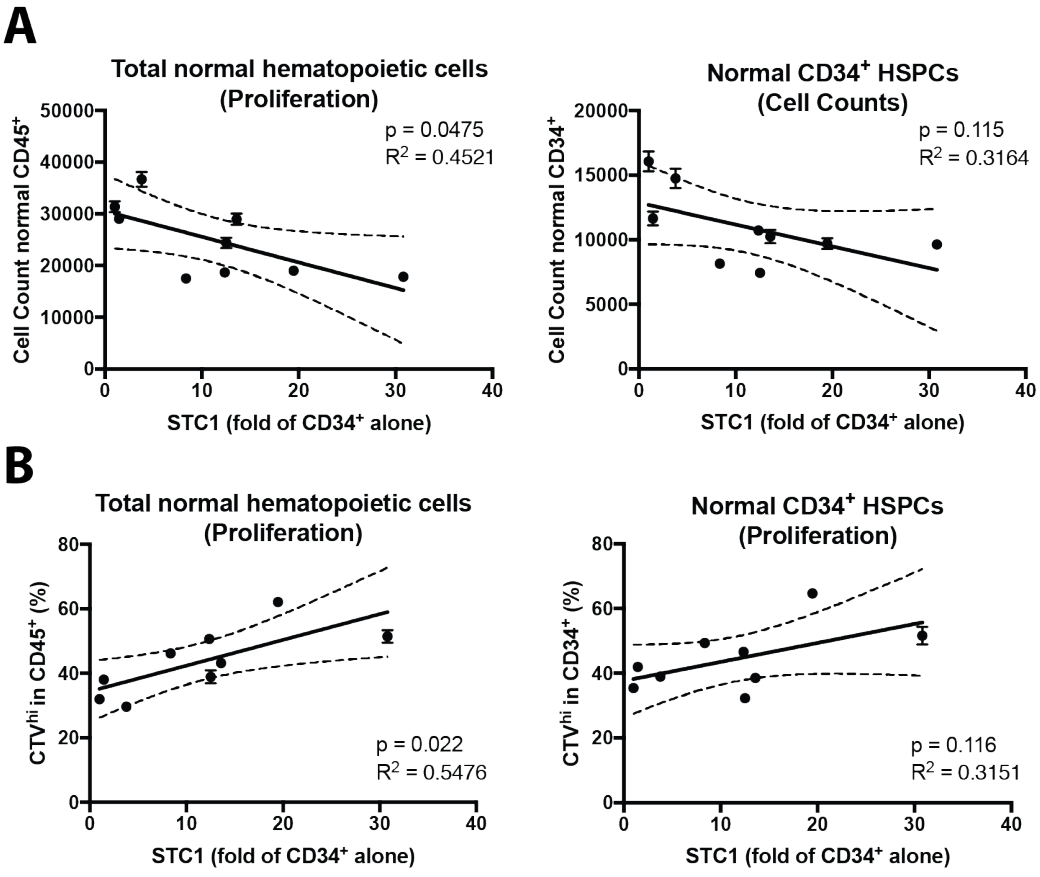


Figure 39. Correlation between normal haematopoietic cells and STC1 concentration in supernatant of HSPC-AML co-cultures

(A) Absolute counts of total normal CD45$^+$ haematopoietic cells (left) and CD34$^+$ HSPCs (right) and the respective STC1 fold-increase relative to CD34+ alone **(B)** Percentage of CTV^{hi} in total normal CD45$^+$ haematopoietic cells (left) and CD34$^+$ HSPCs (right) and the respective STC1 fold-increase relative to CD34+ alone; each dot symbolises a HSPCs wo-cultured with an AML cell lines; lineage regression statistical analysis was performed with thick line representing the lineage relationship and dotted lines representing the 95 % confidence interval

6.2.5 STC1 suppresses normal HSPCs expansion and differentiation

6.2.5.1 Phenotypic and functional characterisation of STC1-treated HSPCs *ex vivo*

To test whether secreted STC1 could be directly involved in the suppression of normal HSPCs by AML, normal CD34$^+$ HSPCs were co-cultured with MSCs and treated with STC1 or vehicle. Most publications use between 50-200 ng/mL of STC1, therefore an intermediate dose of 100 ng/mL was chosen. After 5 days, HSPCs were phenotypically analysed to compare viability, proliferation and cell cycle to vehicle-treated controls. Furthermore, HSPCs were FACS-sorted and functionally analysed in a serial-replating CFU-assay and LTC-IC assay.

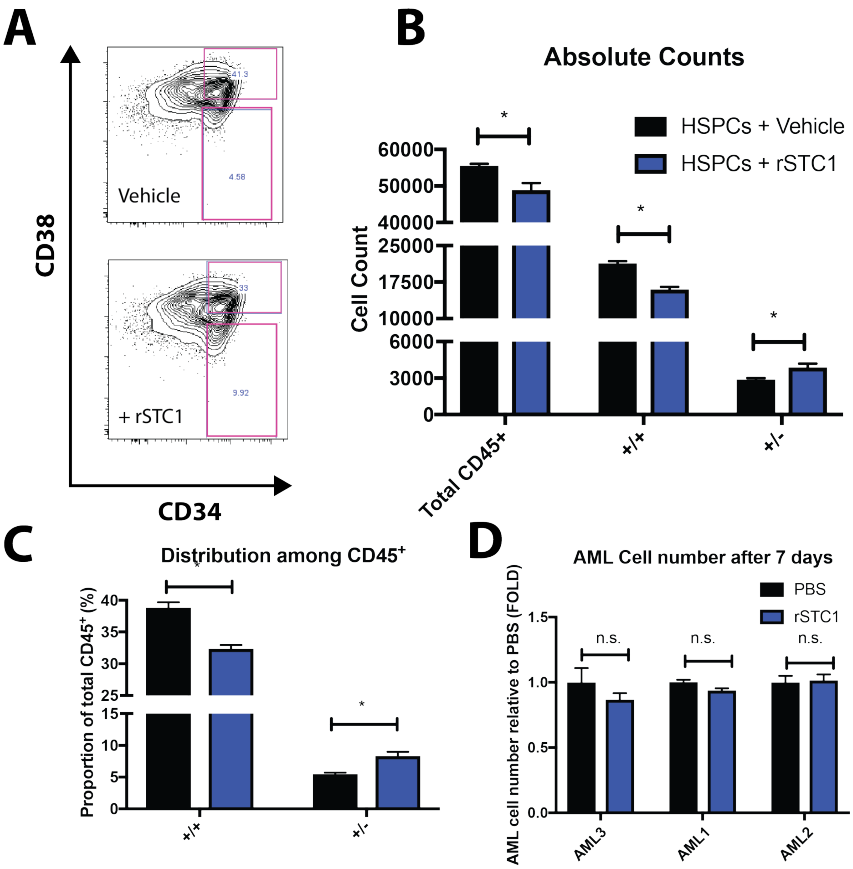


Figure 40. Correlation between normal haematopoietic cells and STC1 concentration in supernatant of HSPC-AML co-cultures
(A) Representative flow cytometry plots of HSPCs co-cultured with normal CD34+ HSPCs treated with vehicle (phosphate buffered saline (PBS)) (top) or recombinant human STC1 for

5 days (bottom) **(B)** Quantification of total haematopoietic cells (Total $CD45^+$), $CD34^+CD38^+$ HPCs (+/+) and $CD34^+CD38^-$ HSPCs (+/-) (n=3) **(C)** Relative distribution of HPCs (+/+) and HSPCs (+/-) among total CD45+ cells (n=3) **(D)** Quantification of cell count of AML patient samples co-cultured with MSCs and treated with vehicle or STC1 for 7 days and normalised to vehicle (n=3); *p<0.05, n.s p > 0.05; Error bars are +/- SEM

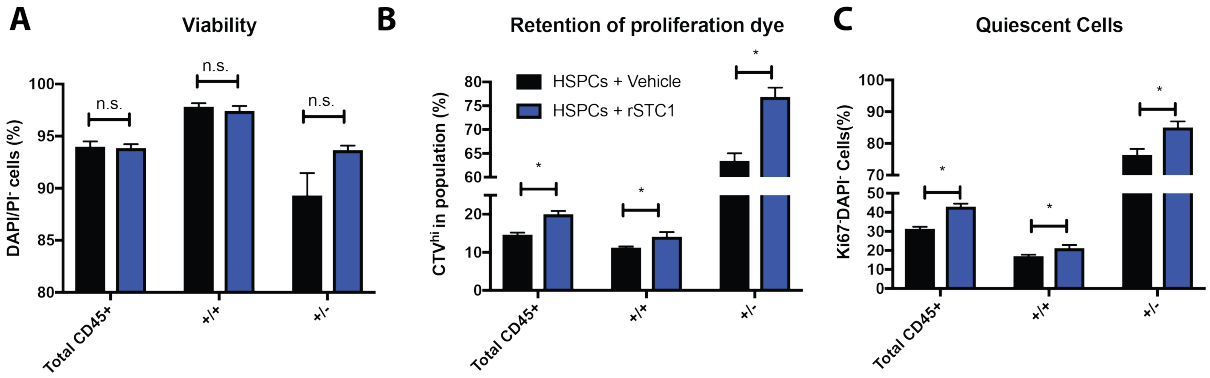


Figure 41. Comparative analysis of viability and proliferation of HSPCs treated with vehicle or STC1

(A) Quantification of viable cells (DAPI or PI negative) among total haematopoietic cells (Total $CD45^+$), $CD34^+CD38^+$ HPCs (+/+) and $CD34^+CD38^-$ HSPCs (+/-) (n=3) **(B)** Quantification of proliferation dye retaining cells after pulse-chase experiment with CTV among total haematopoietic cells (Total $CD45^+$), $CD34^+CD38^+$ HPCs (+/+) and $CD34^+CD38^-$ HSPCs (+/-) (n=3) **(C)** Quantification of quiescent cells ($Ki67^-DAPI^-$) among total haematopoietic cells (Total $CD45^+$), $CD34^+CD38^+$ HPCs (+/+) and $CD34^+CD38^-$ HSPCs (+/-) (n=2); *p<0.05, n.s p > 0.05; Error bars are +/- SEM

After 5 days co-culture STC1-treated cultures contained significantly fewer total haematopoietic cells (Figure 40B) but were proportionally and absolutely enriched for $CD34^+CD38^-$ HSPCs (Figures 40A-C). Similar to +AML co-cultures, viability of vehicle and STC1 treated HSPCs was not significantly different (Figure 41A). Cell cycle analysis showed a significant enrichment of quiescent cells among +/+ HPCs and +/- HSPCs (Figure 41C) which was also confirmed by pulse-chase retention of CTV (Figure 41B). In contrast, AML cell lines or AML patients treated with STC1 for 4-7 days were not significantly increased compared to vehicle controls (Figure 40D). This implies that STC1 can act directly on HSPCs to suppress their proliferation.

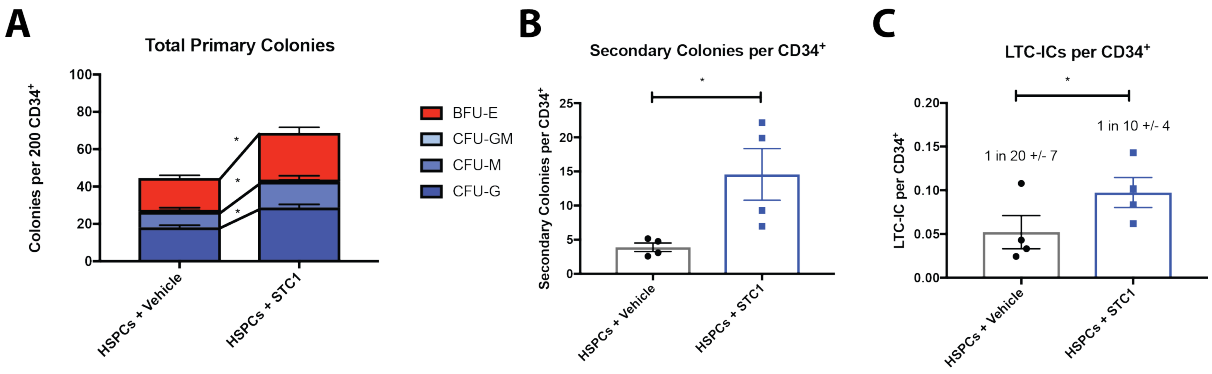


Figure 42. Functional analysis of FACS-sorted CD34$^+$ HSPCs treated with vehicle or STC1

(A) HSPCs were co-cultured with MSCs and treated with vehicle or 100 ng/mL STC1. After 5 days the CD34$^+$ cells were FACS-sorted and seeded at 200 cells/mL into cytokine supplemented methylcellulose (n=4) **(B)** After 14 days in methylcellulose, the primary colonies were homogenized and re-plated at 10^5/mL into fresh methylcellulose, secondary CFUs are expressed as secondary CFU per CD34$^+$ (n=4) **(C)** FACS-sorted CD34$^+$ were first co-cultured with irradiated MS5 for 5 weeks and then plated in methylcellulose to detect LTC-ICs (n=4); *p<0.05, n.s p > 0.05; Error bars are +/- SEM

To dig into the functional aspects of STC1-treated HSPCs, CD34$^+$ cells were first co-cultured with MSCs supplemented with vehicle or STC1 and then FACS-sorted CD34$^+$ were either seeded in a serial-replating CFU-assay or further cultured for 5 weeks on irradiated MS5 stroma cells to dissect whether the reduction of proliferation would preserve immature progenitors. STC1 treated CD34$^+$ HSPCs, demonstrated an increased CFU output in both primary (44 versus 68 total CFUs) (Figure 42A) and secondary plating (3 versus 14 total CFUs) (Figure 42B) as well as increased frequency of LTC-IC frequency by 2-fold (Figure 42C). This confirms that STC1 treatment of normal HSPCs mimics phenotypically and functionally + AML co-cultures.

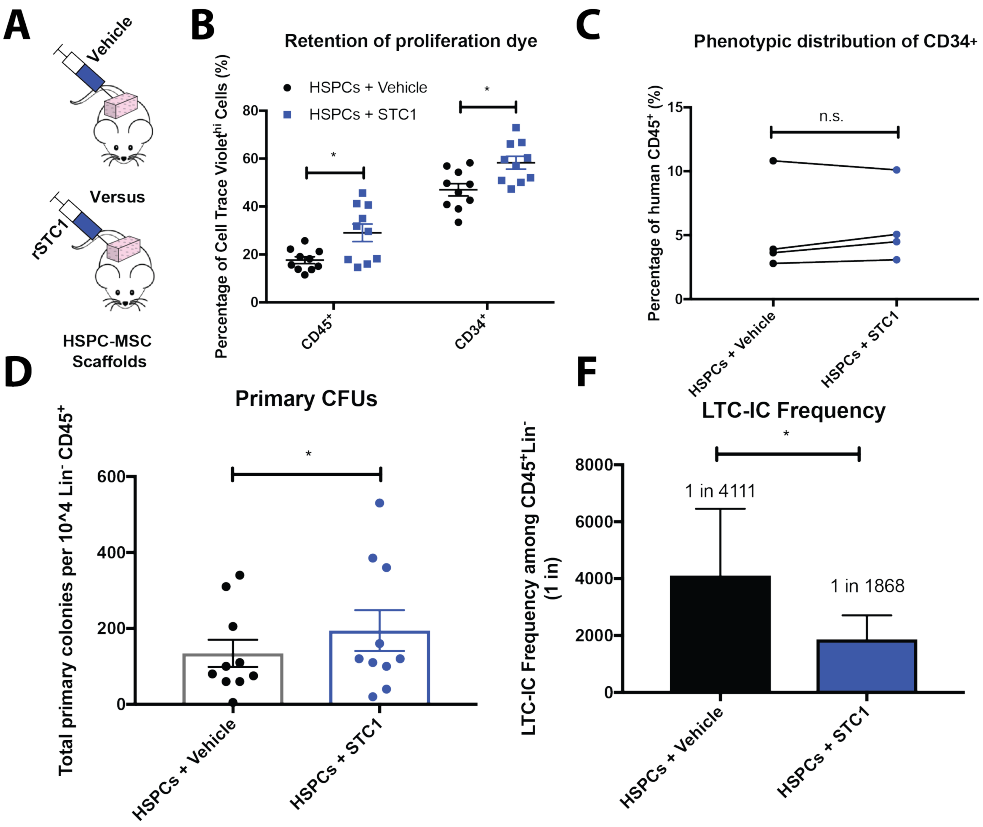


Figure 43. Investigation of HSPCs treated with vehicle or STC1 in scaffold model
(A) MSC-CD34+ HSPCs scaffolds were implanted and treated with 1 µg of STC1/scaffold every 72h for 10-14 days **(B)** Quantification of pulse-chase tracing of total human haematopoietic cell and $CD34^+$ HSPC proliferation with CTV (n=4) **(C)** Proportions of CD34+ HSPCs among total human haematopoietic cells ($hCD45^+$) per mouse **(D)** Quantifications of CFU-ability of FACS-sorted lineage-$CD45^+$ from scaffolds (n=4) **(F)** LTC-IC frequency of FACS-sorted lineage-$CD45^+$ cultured for 5 weeks on irradiated MS5 and analysed for CFU-ability (n=3) ; *p<0.05, n.s p > 0.05; Error bars are +/- SEM

6.2.5.2 Phenotypic and functional characterisation of STC1-treated HSPCs *in vivo*

To validate that STC1 could also suppress the expansion of HSPCs *in vivo*, we first tried administrating STC1 intravenously to study the role on normal HSPCs in the BM. However, even with 7.5 µg of STC1, the concentrations of STC1 in interstitial fluid of the BM was not significantly elevated. The efficacy of the STC1 ELISA assay was not responsible since STC1 was detected in peripheral blood in a dose-dependent manner. This problem was circumvented by establishing MSC-normal HSPC scaffolds and treating them with repeated injections (every 3 days) of STC1 or PBS vehicle (Figure 43A). After 10-14 days the scaffolds were harvested to allow pulse-chase retention of CTV. STC1-treated scaffolds showed a 23 % and 65 % increase of CTV^{hi} cells in both total hCD45 and $CD34^+$, respectively (Figure 43B). In contrast to the +AML scaffolds, phenotypic $CD34^+$ HSPCs were not enriched (Figure 43C) nonetheless

the frequency of CFU-forming HSPCs and LTC-ICs was significantly enriched as compared to PBS-treated controls (Figure 43D-E). This data confirms STC1 as proliferation suppressing factors *in vivo*.

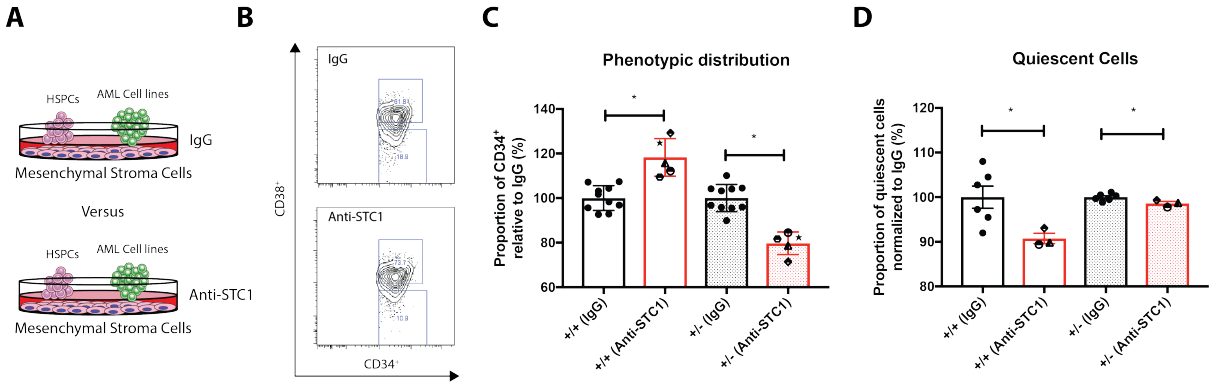


Figure 44. STC1 neutralisation in AML-HSPC co-cultures *ex vivo*
(A) Schematic of experimental setup to neutralise STC1 from *ex vivo* culture of HSPCs with AML cell lines (HL60, ML1, U937, NB4, OCI-AML3) **(B)** Representative plot of phenotypic distribution of HPCs +/+ and HSPCs +/- **(C)** Quantification of phenotypic distribution comparing IgG and anti-STC1 supplemented AML-HSPCs cultures (n=4) **(D)** Quantification of proportions of quiescent cells in HPCs +/+ and HSPCs +/- normalised to IgG (n=2); each dot symbolises an AML cell line, *p<0.05, n.s p > 0.05; Error bars are +/- SEM

6.2.6 Antibody neutralisation of STC1 ameliorates HSPC differentiation blockage *ex vivo*

STC1 is mainly expressed in MSCs, hence MSC-specific knockdown was the first attempt to diminish STC1 secretion and accumulation in the extracellular space. Two independent short hairpin RNA sequences targeted STC1 and knockdown was confirmed by qPCR. Before we attempted culture STC1 knockdown MSCS with HSPCs and AML, we observed that compared to lentivirus transduction controls the viability of MSCs, and the proliferation was reduced, potentially consequential of 3-fold higher ROS levels in shSTC1 MSCs. Since STC1 in the media but not intracellular STC1 was drastically altered between MSCs alone and AML MSCs, an STC1 specific antibody was used to neutralise STC1 (Figure 44A). *Ex vivo,* HSPC + AML cell lines cultures supplemented with anti-STC1 at 1 µg/mL facilitated phenotypic HSPC differentiation from +/- HSPCs to +/+ HPCs as compared to IgG controls (Figure 44B-C). Cell cycle analysis showed that HSPCs were proportionally less quiescent when treated with STC1 neutralising antibody (Figure 44D). This implies that STC1 participates in the *ex vivo* suppression of HSPCs by AML.

6.2.7 Antibody neutralisation of STC1 ameliorates HSPC differentiation blockage *in vivo*

First, the expression of STC1 in the AML scaffold system was analysed. FACS-sorted $CD45^-CD90^+CD73^+$ MSCs from + AML cell line scaffolds expressed around 50 % higher levels of STC1 than their CD34+ alone counterparts (Figure 45B). Surprisingly, we also observed a drastic up-regulation of STC1 in murine $CD45^-mCD51^+$ fibroblasts which had migrated into the $CD34^+$ alone and + AML scaffolds, but total STC1 expression in terms of STC1 copies per copy of housekeeping gene in fibroblasts was still relatively low as compared MSCs (Figure 45C).

Like the STC1-treated protocol, $CD34^+$ alone control scaffolds and + AML cell line (U937) scaffolds were treated every 3 days with 2 μg of IgG or STC1 antibody (Figure 45A). After 2 weeks, the scaffolds were harvested and proliferation was assessed by pulse-chase retention of CTV. In agreement with the proposed quiescence promoting role of STC1, the treatment with neutralising antibody significantly reduced the proportions of CTV^{hi} cells in both non-leukaemic $CD45^+$ cells and $CD34^+$ HSPCs (Figure 45F). Furthermore, the absolute number of non-leukaemic human haematopoietic cells was elevated but did not reach statistical significance. On the other hand, AML counts did not show any significant difference nor trend between IgG and anti-STC1 treated scaffolds (Figure 45D). Together, this data confirms that STC1 accumulation in the interstitial fluid of scaffolds or the supernatant of HSPC-AML co-cultures delays the cell cycle entry of normal HSPCs but surprisingly not AML cell.

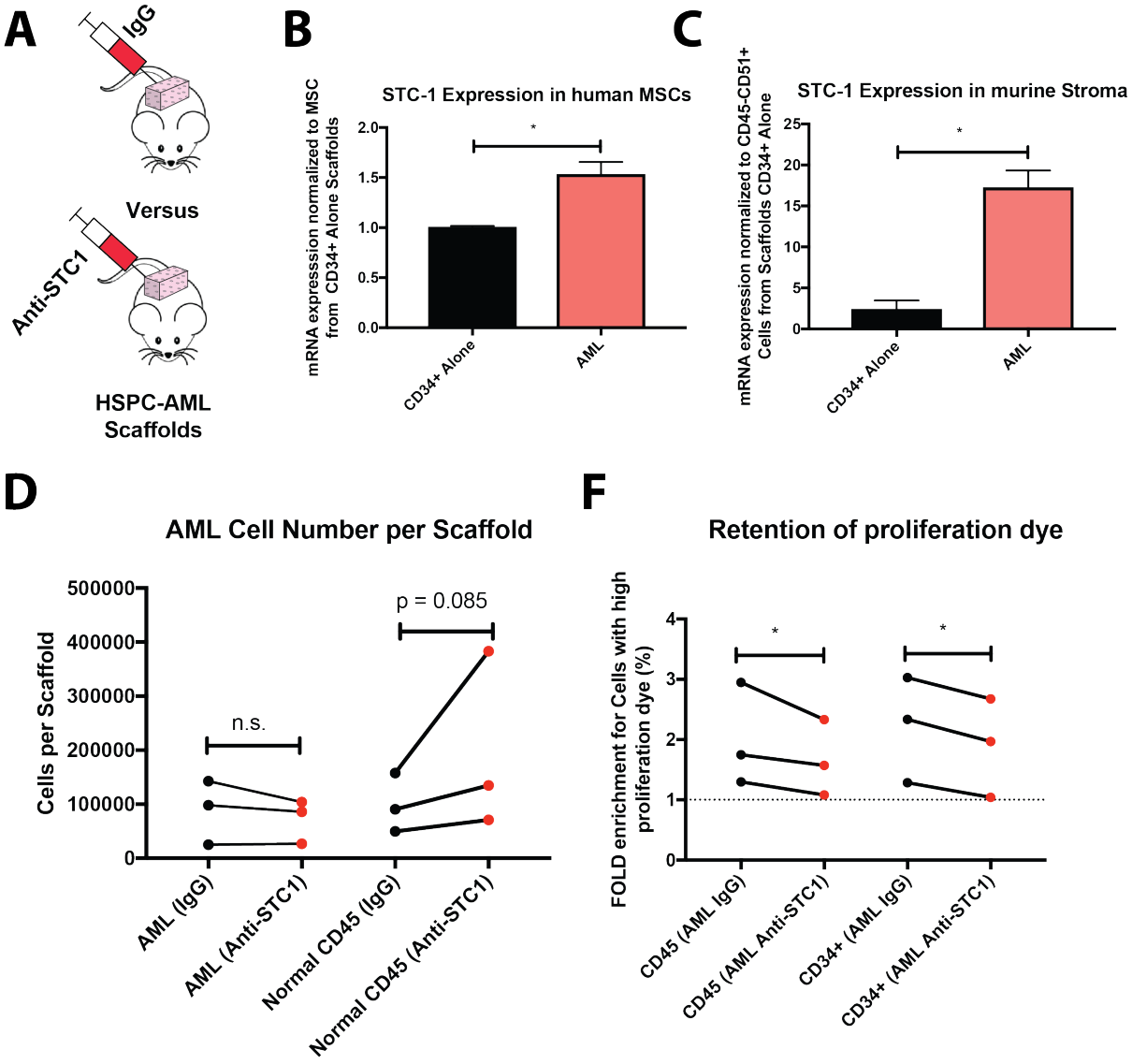


Figure 45. STC1 expression and neutralisation of STC1 in AML-HSPC scaffold model

(A) Schematic of experimental setup to neutralise STC1 in AML-HSPC scaffold model with AML cell line U937 and injections of 2 µg/scaffold every 72h. Scaffolds were harvested after 10 days **(B-C)** mRNA STC1 expression in $CD45^{-}CD73^{+}CD90+$ human MSCs **(B)** and $CD45^{-}mCD51^{+}$ mouse stroma **(C)** in AML-HSPC scaffold normalised to CD34+ alone scaffolds (n=2) **(D)** Quantifications of AML and normal total human haematopoietic cells (Normal CD45) per mouse (n=3) **(CF)** Quantifications of proliferation using pulse-chase retention of CTV per mouse normalised by IgG treated $CD34^{+}$ alone scaffolds (dotted line) (n=3); *p<0.05, n.s p > 0.05; Error bars are +/- SEM

6.2.8 Mechanistic analysis of STC1 on normal HSPCs and MSCs

STC1 has been annotated as oxidative stress response gene to resolve ROS levels by mitigating the mitochondrial proton gradient via UCP2. STC1 knockdown in MSCs drastically reduced MSC homeostasis, preventing MSC expansion and accumulated ROS (Figure 46A-B). ROS

levels in STC1 overexpressing MSCs was measured by ROS specific probe CellROX deep red and mitochondrial membrane potential (MPP) probe by TMRE. Lentivirus-mediated overexpression of STC1 significantly reduced the mitochondrial membrane potential and ROS in MSCs (Figure 46C). HSPCs were co-cultured with MSCs overexpressing STC1 for 5 days, but with the exception of HSPCs +/-, no significant alterations of MMP and ROS levels were observed (Figure 46D).

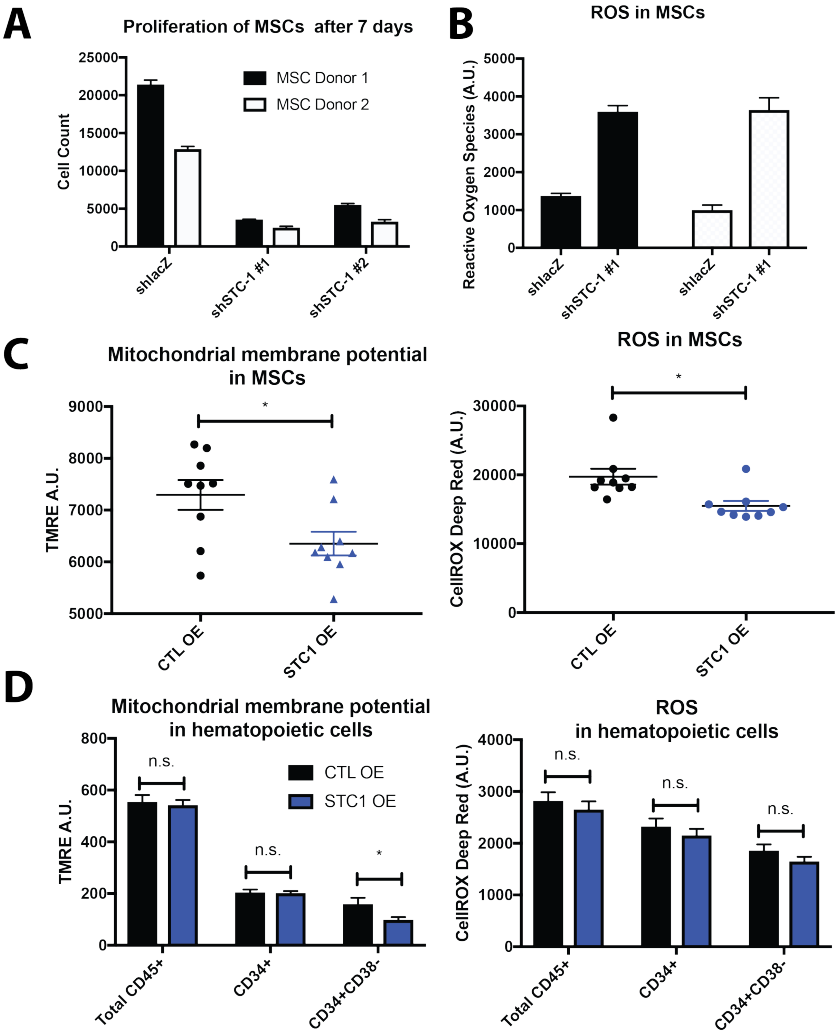


Figure 46. Role of STC1 for ROS and mitochondrial membrane potential in MSCs
(A) Cell numbers of MSCs from two independent donors transduced with lentivirus vector against STC1 after 7 days (n=2) **(B)** ROS levels in MSCs after STC1-knockdown and culture for 7 days measured with CellROX deep red probe (n=2) **(C-D)** Mitochondrial membrane potential measured by TMRE probe and ROS levels in STC1 overexpressing MSCs **(C)** and co-cultured normal HSPCs **(D)** (n=3); *p<0.05, n.s p > 0.05; Error bars are +/- SEM

6.3 Discussion:

The suppression of normal HSPCs is a multifactorial process. As demonstrated in the previous chapter, MSCs potentiate the suppression of HSPCs and the separation between AML-MSCs and HSPCs with a transwell insert demonstrates that secreted factors and direct contact are mediators. However, a reliable comparison between direct and humoral factors is exacerbated by specific physical parameters. In particular, diffusion could artificially shift the results towards direct contact but since we did not anticipate these factors, the STC1 concentration in the transwell inserts and the well supernatant, which would allow a more profound interpretation, was not measured. Molecules diffuse along a concentration gradient from the MSC to the transwell in a 3-dimensional space. An approximation formula to measure the time this process requires is given by

$$Time = \frac{Distance^2}{2 * Diffusion\ coefficient}$$

With the diffusion coefficient for small proteins like STC1 is 10^{-6} a molecule of STC1 would require approximately 15 hours to migrate 1 cm (Brune and Kim, 1993). To mitigate diffusion effects the bottom of the transwell almost touches the bottom of the dish hence, 1 cm is an exaggeration of the distance between MSCs-AML and the HSPCs. However, the small molecules need to diffuse through 0.4 µm pores creating a bottle-neck feature which would further delay the arrival of STC1 in the transwell. A larger pore size like 3 µm would facilitate a faster concentration equalisation but add the risk of AML or HSPCs migration through the pores.

Of note, a similar effect was observed when AML was separated from HSPCs-MSCs via a transwell insert or MSCs cultured in media from AML. In these settings, MSCs significantly upregulated hypoxia-response genes but to a diminished extent than MSCs in direct contact with AML. Again, these results could be explained by a requirement for direct contact. Alternatively, a concentration-dependent effect of the secreted molecules together with a diffusion gradient would also cause an up-regulation of hypoxia-response genes, but due to the diffusion delay, the concentration at the MSC surface is lower, the expression would also be lower. To conclude, the results of the transwell experiment prove that secreted factors are participants in the suppression of HSPCs by AML. Direct contact between AML-MSCs and normal HSPCs may be required as well, but definitive quantifications of the impact of direct

contact versus secreted factors is impossible owing to the physical parameter introduced by transwell inserts. Another alternative to prove that secreted factors are involved are experiments using conditioned media, but this strategy also comes with certain caveats like the half-life of proteins and the diffusion/concentration effects described above. We attempted this approach and observed more quiescent HSPCs in conditioned media from AML, but the effects were more truncated than the transwell culture. In the BM, diffusion and concentration gradients might also play an important role for the clonal growth clusters of AML cells (Herault et al., 2017). For example, hypoxia in the BM of leukaemic mice is highest in close proximity to AML cells implying that the oxygen diffusion from outside the AML clone is slower than oxygen consumption of AML resulting in a concentration gradient (Passaro et al., 2017b).

Another interesting observation from the transwell experiments was the difference in viability between HSPCs in direct contact with MSCs or separated via a transwell insert. Without AML the viability between HSPCs from direct contact and transwell did not differ, but in the AML environment, the cell-cell contact between MSCs and/or AML clearly mediated an anti-apoptotic effect on the HSPCs in particularly with the AML cell line OCI-AML3. Interestingly, this cell line firmly adheres to MSCs and sometimes induces MSC displacement from plastic and apoptosis. On the other hand, separation of AML from MSCs via a transwell insert only marginally reduces AML viability, indicating that AML cell lines are more fit and selected to survive under environmental stress. A similar phenotype was observed when normal HSPCs were cultured with lactate, the main end-product of anaerobic glycolysis. Without stromal support by MS5 mouse stroma cell line, the HSPC's viability was severely diminished even with MS5 conditioned media in a lactate dose-dependent manner. However, the presence of a stromal monolayer completely abrogated the toxicity from lactate. The molecular causality for anti-apoptotic effect of the mesenchymal niche was not further investigated but cell surface proteins like the notch ligand/receptor family or integrin-mediated attachment of HSPCs to the extracellular matrix produced by niche cells have been shown to improve survival of HSPCs under stress conditions like irradiation (Kim et al., 2018; Krater et al., 2017).

The secreted factors mediating HSPC suppression could be derived by the mesenchymal niche or AML. Lactate was previously mentioned as a directly suppressive secreted molecule which could certainly contribute to the pool of secreted factors suppressing HSPCs in the transwell setting. Compared to CB $CD34^+$ HSPCs or mononucleated cells, AML patient samples and AML cell lines generate more lactate even when differences in proliferation were considered

by normalising to lactate secretion per cells. Published data from Andreeff and colleagues, as well as our comparisons of lactate secretion by AML patient cells cultured alone or on supportive MSCs, suggests that the mesenchymal niche promotes anaerobic glycolysis (Samudio et al., 2008). HSPCs could be suppressed by lactate, even when cultured without mesenchymal cells, however when HSPCs were co-cultured with MSCs, the suppression became very irregular and truncated as compared to co-cultures with mouse stromal cell line MS5. Differences regarding the metabolic activity between MSCs and MS5 might be a potential explanation since MSC secrete much higher concentrations of lactate than MS5.

Regarding the secreted factors deriving from MSCs, we compared the transcriptome of MS5 co-cultured with normal HSPCs and AML and specially selected secreted factors upregulated by AML cell lines and AML patient samples. Apart from STC1, several other factors with haematopoietic potential were observed. GAS6 and its receptor tyrosine kinase AXL have been reported to promote the proliferation of AML and CML and secretion of GAS6 is essential for the maintenance of stroma cells to support HSPCs (Jin et al., 2017). Furthermore, GAS6 is expressed by AML in an autocrine manner and high expression stratifies AML patients with adverse prognosis (Whitman et al., 2014). Kirre3 is expressed on the surface of OP9 murine stroma cells and cleaved by metalloproteases. In HSPC-OP9 co-cultures, cobblestone area formation, an indicator of HSPC self-renewal, colocalised with Kirre3 expression by OP9 cells. Supplementation with the extracellular cleaved Kirre3 mitigated HSPC migration and adversely affected LTC-IC frequency (Ueno et al., 2003). Lastly, IGF1/2 were significantly upregulated, but these factors and the IGF receptor – MAPK pathway are associated with HSPC and AML cell cycle entry.

Most likely, multiple factors are involved in the suppression of HSPCs by AML and a better understanding could lead to the discovery of novel HSPC cell cycle regulators. Cheng and colleagues discovered that normal HSCs from leukaemic mice upregulate Egr3, Hey1 and Maff expression, which were subsequently confirmed as HSC cell cycle regulators in murine and zebrafish HSCs (Cheng et al., 2015; Cheng et al., 2016). STC1 had not been annotated as an HSC regulator, but stratification of patients with solid cancer, based on STC1 expression, consistently predicts adverse outcome. Additionally, work by Prockop and colleagues on MSC co-cultures with irradiated fibroblasts and adenocarcinoma cell line A549 demonstrated that oxidative stress upregulates STC1 in MSCs. STC1 was demonstrated to act in an anti-apoptotic

and ROS resolving manner on the irradiated fibroblasts or A549 cells treated under oxidative stress (Block et al., 2009; Ohkouchi et al., 2012).

Our data suggests that STC1 selectively decreases HSPC proliferation but not the proliferation of AML patient samples or cell lines. In ovarian cancer, overexpression of STC1 was shown to lead to increased proliferation, but work on macrophages exposed to secreted STC1 also indicates an anti-proliferative role (Liu et al., 2010; Wang et al., 2009). Similar to our data, this implies that STC1 may provoke different phenotypes dependent on cell type and intra/extracellular localisation. Further, in line with an anti-proliferative/differentiation impact of STC1, HSPCs exposed to STC1 *in vivo* and *ex vivo* performed significantly better in CFU-replating Assays and LTC-IC assays. We attempted to also assess the performance of HSPCs from AML scaffolds exposed to the blocking antibody, but AML contaminations of FACS-sorted HSPCs prevented further analysis.

Published work on macrophages suggests STC1 to be sequestered by macrophages, where it localises to the surface of mitochondria, a previously identified binding site of STC1 (Wang et al., 2009). STC1 supposedly stabilises the putative mitochondrial uncoupler UCP2 but in recent years, the initial annotation of UCP2 as an uncoupling protein has been disputed (Ohkouchi et al., 2012). This data was mainly based on work using the mitochondrial potential dye JC-1, which are usually used to measure mitochondrial membrane potential loss to measure apoptosis. JC-1 forms orange-fluorescent J-aggregate in polarised mitochondria and the mitochondrial potential can be measured by the fluorescence intensity of the aggregates. However, JC-1 has a very low solubility in water and in our hand's supplementation to the media-generated insoluble aggregates in the media. The rhodamine123 and tetramethylrhodamine, ethyl ester (TMRE) are other often used dyes to measure mitochondrial potential (Sakamuru et al., 2016). In our hands, only the latter responded accordingly to the small molecule mitochondrial uncoupler Trifluoromethoxy carbonylcyanide phenylhydrazone (FCCP). In line with a role of STC1 in redox-regulation, we observed that MSCs overexpressing STC1 reduced mitochondrial membrane potential and ROS levels. More dramatically, knockdown of STC1 completely abrogated MSC homeostasis and drastically increased ROS levels. On normal HSPC, the effect was less pronounced, and only +/- HSPCs had significantly reduced mitochondrial membrane potential which did not translate into a reduction of ROS. Compared to HSPCs, the average intensity from mitochondrial membrane potential and ROS probes was much higher in MSC which may be another explanation, besides exposure to lower STC1 concentrations, for a more dramatic effect in MSCs.

In summary, secreted factors mediate a significant proportion of HSPC suppression. Transcriptomic analysis of the mesenchymal niche identified STC1 as glycoprotein whose secretion is triggered by AML *in vitro* and *in vivo*. STC1 concentrations correlate significantly with the suppression of HSPCs and *ex vivo* and *in vivo* exposure of HSPCs to recombinant extracellular STC1 impedes proliferation. Conversely, blockage of STC1 ameliorated the HSPC suppression and improving the expansion of HSPCs in the presence of AML and without acting on AML directly. In line with the proliferation and differentiation impeding effects of STC1, immature HSPCs, measured by CFU-assay and LTC-ICs were increased from STC1 exposed HSPCs. Lastly, STC1 overexpression and supplementation resulted in a marked reduction of ROS in MSCs and mitochondrial membrane potential in MSCs and +/- HSPCs.

Chapter 7. HIF-1α regulates STC1 expression in AML MSCs and suppresses HSPCs

7.1 Introduction

In the previous chapter, we presented correlative and causative evidence for the involvement of STC1 in HSPC suppression by the leukaemic microenvironment. Under normal healthy conditions, STC1 expression in normal and malignant haematopoietic cells is mainly absence and in normal MSCs relatively low, which changes in the presence of AML. By a yet undefined mechanism, AML induces the expression of genes mimicking hypoxia culture conditions termed "hypoxia-response genes". STC1, may therefore, be an interesting read-out to determine signalling pathways in MSCs that are influenced by AML. Furthermore, since these signalling pathways may control more secreted factors with HSPC suppressive effect like STC1, a potent amelioration of HSPC suppression could be achieved.

STC1 regulation at the transcriptional level has been reported by TGF-β1 (Ono et al., 2015), IL1α/β (Bartosh et al., 2013), PDGF (Pena et al., 2013), oxidative stress (Ohkouchi et al., 2012), hypoxia (Yeung et al., 2005), DNA-damage (Block et al., 2009) histone acetyltransferase inhibitors (Ching et al., 2012) and DNA demethylase JMJD3 (Park et al., 2016). Indeed, an interconnection between these pathways exists but considering the importance and recurrence of these pathways in solid cancer development, it is unsurprising that STC1 expression predicts an adverse outcome in several solid-cancer models. For example, hypoxia induces the stabilisation of the α-subunits of HIFs, which in turn can induce IL-1α/β or vis versa (Gorlach and Bonello, 2008; Jung et al., 2003). Activation of NF-κB and TGF-β1 can either induce the transcription of HIF-1α or down-regulate PHD enzyme expression (McMahon et al., 2006; Tannahill et al., 2013).

Hypoxia-inducible factors (HIFs) are major regulators of the transcriptional response of cells to hypoxia and HIF-1α alone regulates more than 40 % of hypoxia-response genes (Benita et al., 2009). HIF transcription factors consist of an oxygen-sensitive α subunit which heterodimerize with the β subunit HIF-1β via the HLH and PAS domains. Three mammalian α subunits, HIF-1α, HIF-2α, HIF-3α exist and are expressed in a tissue-specific manner. The complex of α and β subunits translocate to the nucleus and bind to specific consensus sequences called hypoxia response elements (HRE) in the genome which regulates the

transcription of HIF-target genes. In well-oxygenated environments, the alpha subunits are constantly degraded by PHD enzymes which utilise a $Fe2^{+}$, O_2 and α-ketoglutarate as substrate to hydroxylate HIF at conserved proline residues (Schofield and Ratcliffe, 2004). These hydroxylations induces ubiquitination by VHL and initiates proteasomal destruction. Also, FIH hydroxylates HIFs at the C-terminus, which disrupts binding to transcriptional coactivators P300/CBP (Majmundar et al., 2010).

In haematopoietic system, all three α subunits and the β subunit are expressed but HIF-1α, HIF-2α are mainly expressed in HSPCs and regulate self-renewal of mouse (Takubo et al., 2010) and human HSCs (Rouault-Pierre et al., 2013). On the other hand, MSCs express high levels of HIF-1α and HIF-2α, which are stabilised upon culture in hypoxia conditions (Guarnerio et al., 2014; Palomaki et al., 2013). The role of HIF transcription factors in the SCN has been addressed by Guarnerio et al. in murine MSCs and Kusumbe et al. in endothelial cells, highlighting the importance of HIF-transcriptional programs for niche cell maintenance and homeostasis (Guarnerio et al., 2014; Kusumbe et al., 2014; Palomaki et al., 2013). However, how HIF-target genes influence normal haematopoiesis is largely unknown. Guarnerio et al., reported that HIF stabilisation by murine MSCs is required to maintain mouse HSPC at an undifferentiated state and limit their proliferation (Guarnerio et al., 2014; Palomaki et al., 2013). Nonetheless, the implications for the leukaemic niche and HSPC regulation in a human setting remain unknown.

7.2 Results

7.2.1 Expression of STC1 and other hypoxia-response genes in hypoxia is mediated by HIF-1α stabilisation

The α-subunits of the HIF-family accumulate intracellularly under low oxygen pressure in MSCs as exemplified for HIF-1α (Figure 47A). Several glycolytic genes like *GLUT1*, *PDK1* or the secreted angiogenic factor *VEGF-A* and *STC1* have been associated with HIF-1α as a regulator. HIF-1α stabilisation and accumulation were mitigated by shRNA-mediated knockdown (shHIF-1α) and compared against the same plasmid expressing shRNA against dsRed as control (shCTL). Lentiviral transduction of MSCs with the shHIF-1α expressing plasmid prevented the accumulation of HIF-1α under hypoxia (Figure 47A) and reduced the expression of *GLUT1*, *STC1* and *VEGF-A* in hypoxia by 2 to 5-fold. Hence, without HIF-1α the expression of hypoxia-response genes was normalised to normoxia level (Figure 47B*)*.
On the other hand, overexpression of a stable version of HIF-1α (HIF-1α mut) in MSCs, triggered a 2 to 5-fold increased expression of hypoxia-response genes under normoxic culture conditions (Figure 47D). For HIF-1α mut, the proline residues at position 402 and 564 and asparagine at position 803 were converted to alanine to block hydroxylation, preventing degradation in normoxia conditions.

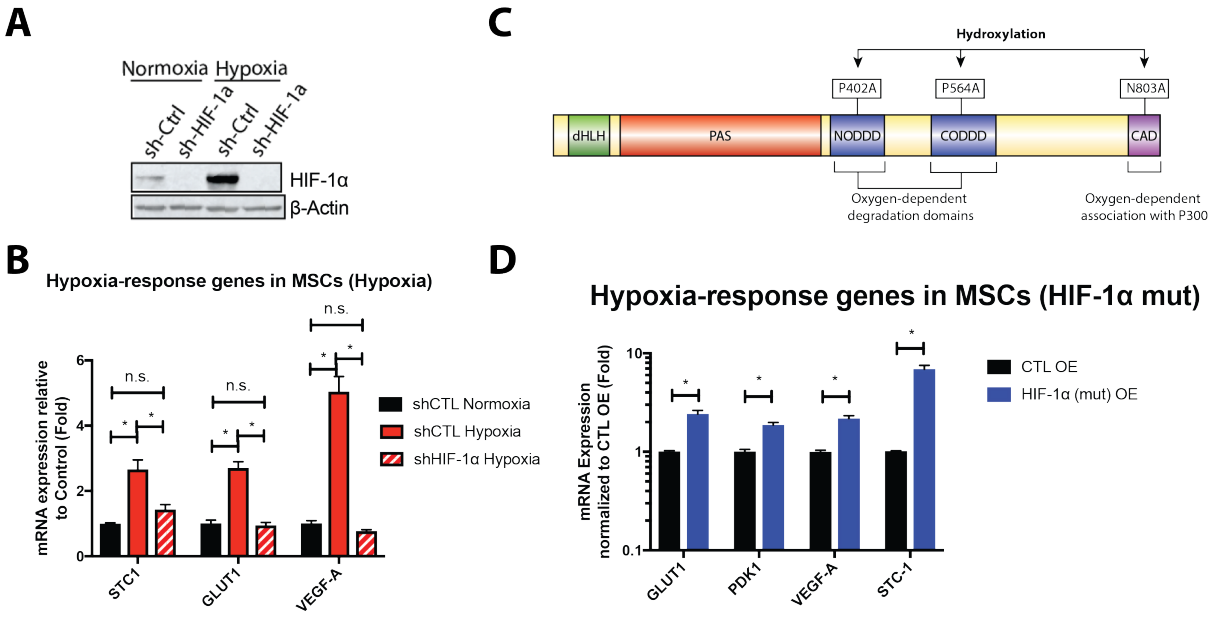


Figure 47. Expression of STC1 and other hypoxia-response genes is mediated by HIF-1α stabilisation.
(A) Western blot analysis of HIF-1α protein in MSCs in normoxia and after 10h in hypoxia and efficacy of shRNA mediated knockdown of HIF-1α. β-Actin protein levels were measured

to ensure equal loading **(B)** mRNA expression of hypoxia-response genes in MSCs transduced with a shRNA control construct (shCTL) or HIF-1α abrogating shRNA (shHIF) cultured in either normoxia or hypoxia (n=2) **(C)** Schematic of HIF-1α protein with domains for DNA-binding domain helix-loop-helix (dHLH), HIF-1β interacting domain Per-Arnt-Sim (PAS) and oxygen-dependent degradation domains (N-terminal and C-terminal oxygen-dependent degradation domains (NODDD and CODDD)) and oxygen-dependent p300 association domain (C-terminal activating domain (CAD)), Prolines at position 402 and 564 and asparagine at position 803 were converted to alanine to mitigate hydroxylation preventing degradation in normoxia conditions **(D)** mRNA expression of hypoxia-response genes in MSCs transduced with lentivirus construct overexpressing the normoxia-stable HIF-1α construct (HIF1a (mut)) (n=2)

7.2.2 AML stabilises HIF-1α triggering expression of STC1 and other hypoxia-response genes

Similar to hypoxia, MSCs co-cultured with AML express several hypoxia-response genes. Hence, the whole cell extract of MSCs co-cultured with AML patient samples was plotted for HIF-1α expression and compared to MSCs cultured alone. Much like the results of HIF-1α stabilisation in hypoxia, AML triggered the accumulation of HIF-1α in MSCs (Figure 48A). Next, we addressed whether similar to hypoxia, HIF-1α downregulation by shRNA could impede the expression of STC1 and other hypoxia-response genes. MSCs expressing shCTL/shHIF-1α shRNA were co-cultured with normal HSPCs or AML cell line U937 for 4 days in normoxia, FACS-sorted and mRNA expression of *STC1*, *VEGF-A* and *GLUT1* analysed (Figure 48B). In line with previous results, AML cell line U937, induced a 0.5 to 1.5-fold increase expression of STC1, VEGF-A and GLUT1 in shCTL MSCs but HIF-1α knockdown normalised the expression of STC-1 and GLUT1 but not VEGF-A to shCTL levels (Figure 48C). Similarly, knockdown of HIF-1α in MSCs, significantly diminished the accumulation of secreted STC1 in the supernatant of MSCs co-cultured with normal HSPCs + AML cell lines (Figure 48D). This data indicates that AML triggers the stabilisation of HIF-1α in MSCs, which contributes to the up-regulation of hypoxia-response genes and STC1 secretion.

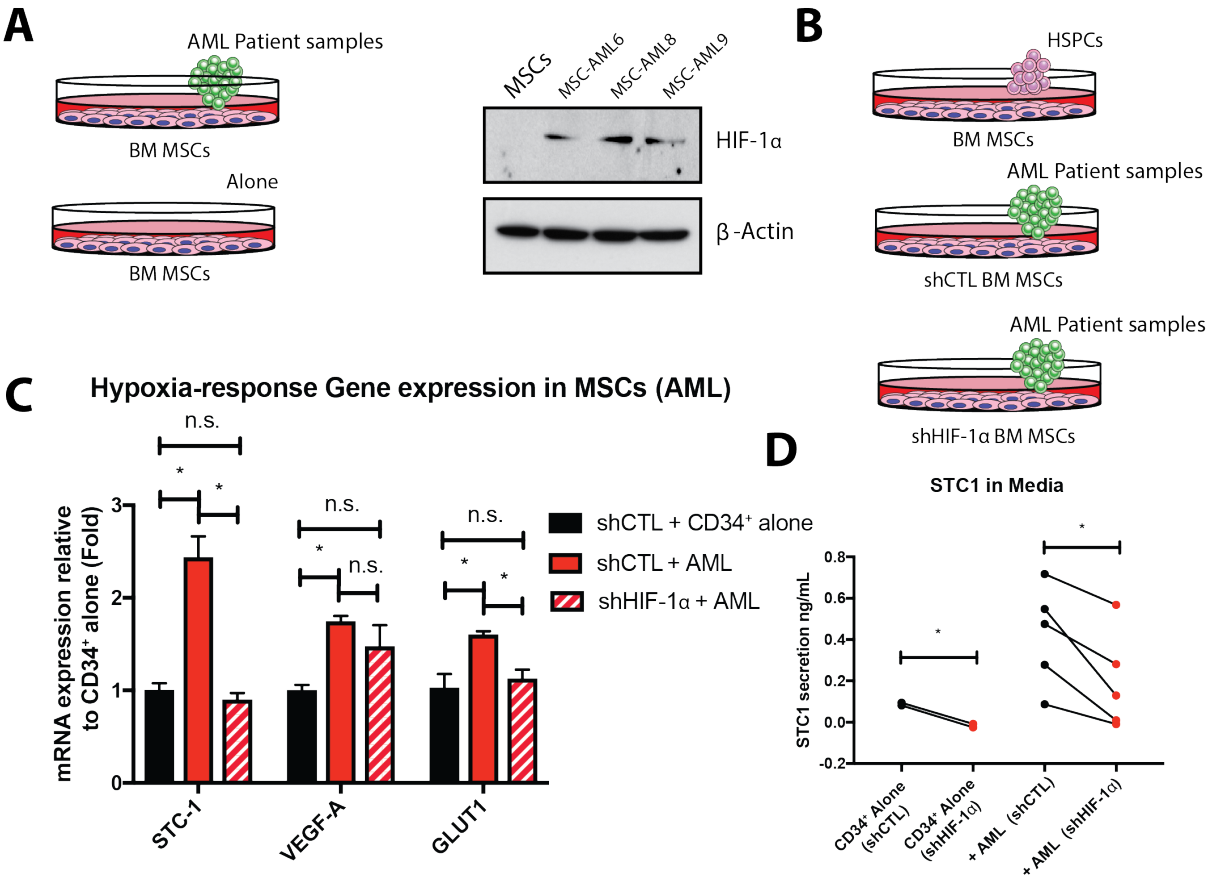


Figure 48. Hypoxia-response gene expression in MSCs is caused by HIF-1α stabilisation

(A) Western blot analysis of HIF-1α protein in MSCs either co-cultured with AML patient samples (AML 6, AML 8 and AML 9) or cultured alone. β-Actin protein levels were measured to ensure equal loading **(B-C)** mRNA expression of hypoxia-response genes STC1, VEGF-A and GLUT1 normalised to $CD34^+$ co-cultured with shCTL -MSC compared to Sh-Control MSC or Sh-HIF1-MSC co-cultured with AML cell line U937 (n=3) and **(D)** STC1 concentration in supernatant (n=2) in shCTL and shHIF-1α MSCs cultured with either normal HSPCs or + AML cell line tested HL60, KG1A, NB4, MOLM-13, OCI-AML3 ; *p<0.05, n.s. p > 0.05; Error bars are +/- SEM

7.2.3 Investigation of other STC1 regulators

HIF-1α knockdown reduced but did not abolish completely STC-1 accumulation in the supernatant of AML-MSC co-cultures and other reported activators of STC1 expression like IL-1α/β and TGF-β1 have been associated with AML. Hence, MSCs were cultured with several AML implicated cytokines available in the lab at 10 ng/mL and mRNA expression of hypoxia-response genes and STC1 accumulation in the supernatant was measured after 72h. However, apart from confirming the reported STC1 regulatory activity of IL-1α/β, TGF-β1 and hypoxia in MSCs, we could not detect increased STC1 secretion for any other cytokines

tested (Figure 49A). Furthermore, while IL-1α/β, TGF-β1 and hypoxia all induced *STC1* expression, only hypoxia culture conditions could upregulate the other hypoxia-response genes *GLUT1* and *PDK1* by 2-fold (Figure 49B). Lastly, the individual contribution of the three confirmed STC1 regulators, IL-1α/β, TGF-β1 and HIF-1α was measured to determine the best strategy to inhibit STC1 secretion. STC1 mRNA expression was analysed in MSC-AML co-cultures supplemented with either TGF-β1 and IL-1α/β neutralising antibody or expressing shRNA against HIF-1α. While HIF-1α normalises STC1 expression to shCTL levels, neutralisation of IL-1α/β and TGF-β1 slightly diminished STC1 expression but without p-values reaching statistical significance (Figure 49C). This data implies that several documented STC1 regulators trigger STC1 expression in AML-MSC co-cultures but highlights HIF-1α as the primary contributor and prime target to alleviate MSC transcriptional reprogramming.

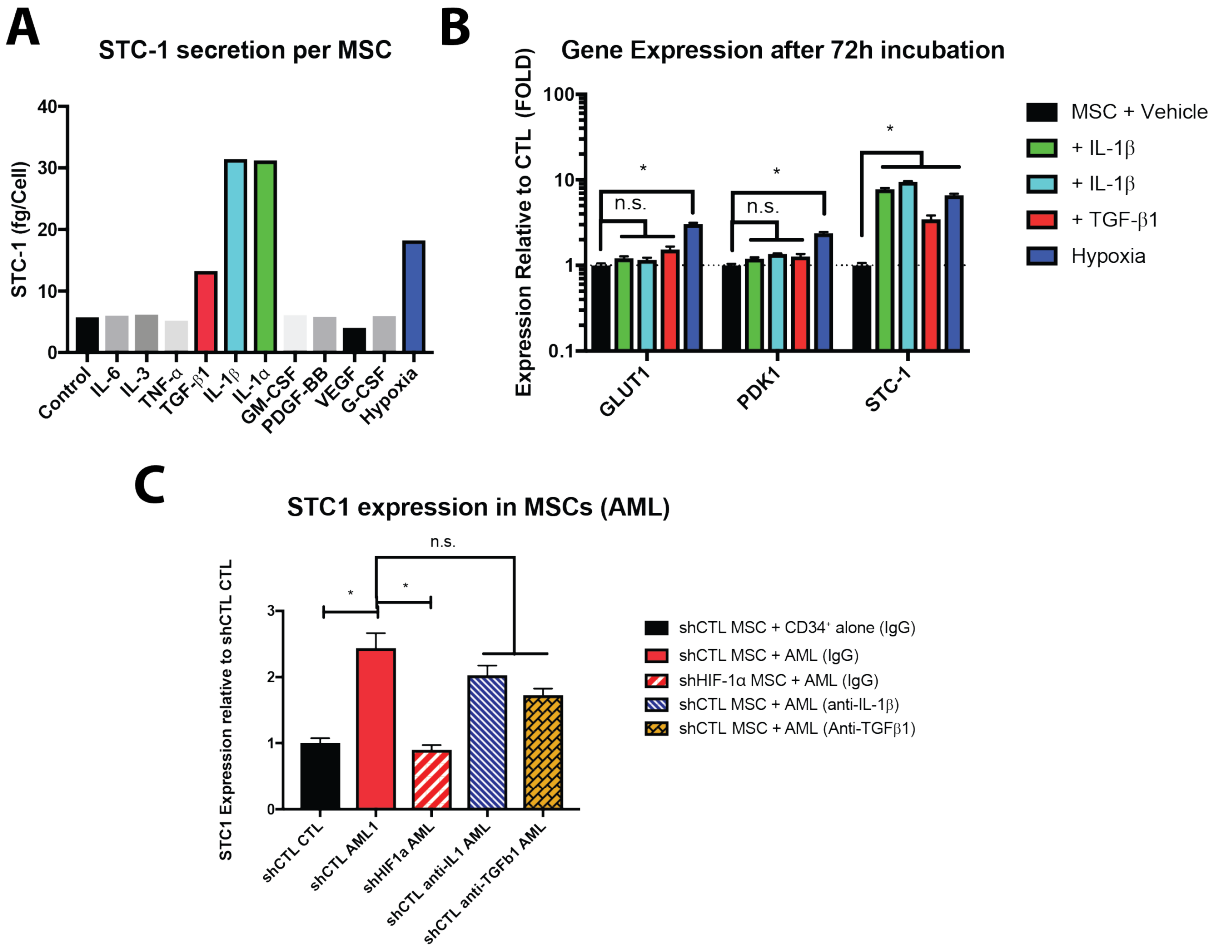


Figure 49. HIF-1α knockdown abrogates STC1 accumulation in supernatant
(A) Secretion of STC1 after 72h culture by MSCs treated with a small screen of different AML-associated cytokines and published STC1 regulators (10 ng/mL) (n=1) **(B)** mRNA expression of hypoxia-response genes STC1, VEGF-A and GLUT1 normalised to vehicle control of MSCs treated with either 10 ng/mL IL-1α, IL-1β, TGF-β1 or cultured under hypoxia **(C)** mRNA expression of STC1 in shCTL MSCs treated with either 1 µg/mL anti-TGF-β1 or IL-1β

neutralising antibody and shHIF-1α MSCs co-cultured with $CD34^+$ alone or +AML (n=3); *p<0.05, n.s. p > 0.05; Error bars are +/- SEM

7.2.4 HIF-1α overexpression in MSCs suppresses expansion of normal HSPCs in co-culture

To confirm that HIF-1α stabilisation in MSCs influences HSPCs proliferation in co-culture, MSCs were lentivirally transduced to express HIF-1α (mut) (HIF-1α OE) or an empty control plasmid (CTL OE) and co-cultured with normal HSPCs for 5 days. Afterwards, HSPCs were analysed for proliferation and FACS-sorted to determine CFU-ability and LTC-IC frequency (Figure 50A). HSPCs co-cultured with HIF-1α (mut) MSCs expanded 30 % less (Figure 50B) but were significantly proportionally enriched for +/- HSPCs by 50 % compared to CTL OE MSCs (Figure 50C). Conversely, pulse-chase retention of proliferation dye in total haematopoietic cells ($CD45^+$) and $CD34^+$ HSPCs was significantly elevated in HPSCs from HIF-1α OE MSCs (Figure 50D).

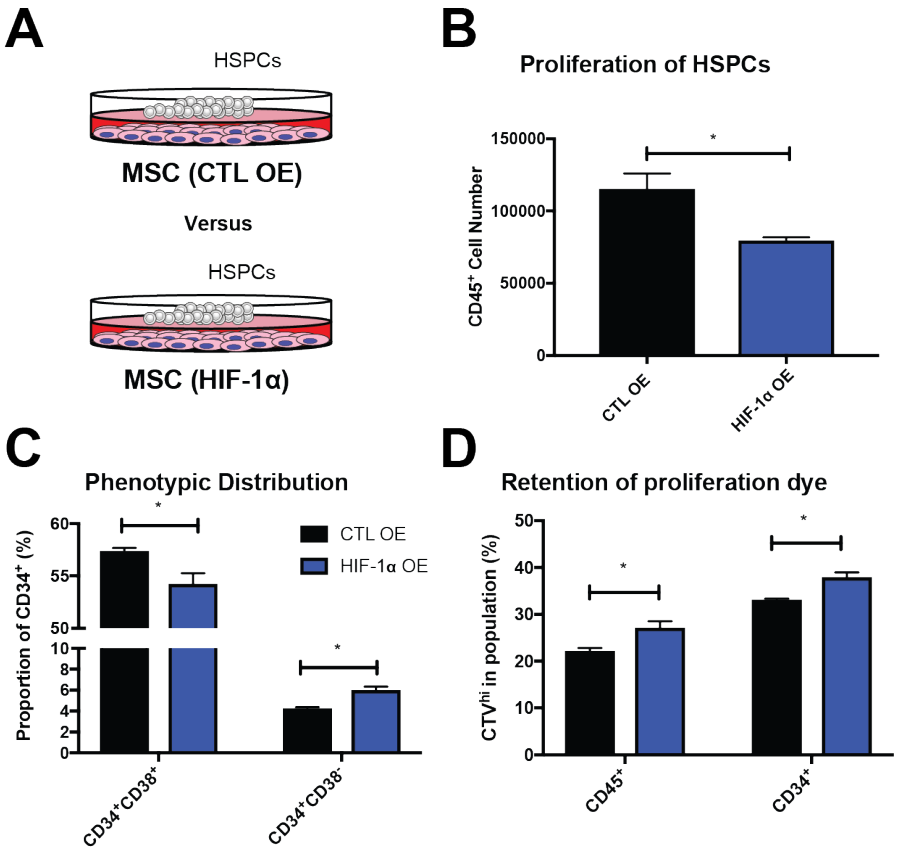


Figure 50. HIF-1α stabilisation in MSCs suppresses HSPC expansion in co-culture
(A) Schematic of experimental setup, MSCs were transduced with lentivirus construct to overexpress HIF-1α (mut) and co-cultured with HSPCs **(B)** Cell count, **(C)** Phenotypic

distribution and (C) pulse-chase retention of proliferation CTV in HSPCs (n=3); *p<0.05, n.s. p > 0.05; Error bars are +/- SEM

We had previously determined that HSPCs co-cultured with AML are enriched with CFU-forming cells and LTC-ICs. In agreement, FACS-sorted HSPCs contained 60 – 70 % more primary and secondary CFU-forming cells (Figure 51A/B) and an enrichment of LTC-ICs of a comparable extent (Figure 51C). This data implies that HIF-1α stabilisation mimics the suppression of HSPC proliferation and differentiation observed in HSPC-AML co-cultures.

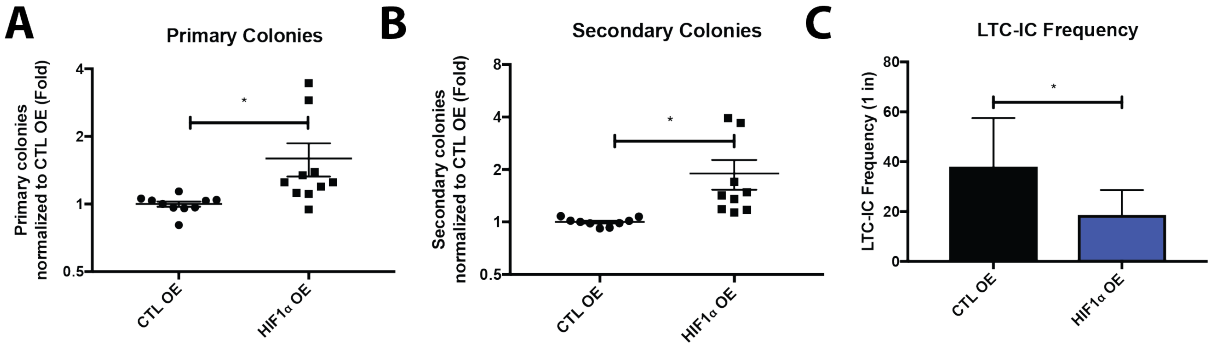


Figure 51. HIF-1α stabilisation in MSCs suppresses HSPC expansion in co-culture
(A) Primary CFU-potential per CD34+, **(B)** secondary CFU-potential and **(C)** LTC-IC frequency from FACS-sorted HSPCs co-cultured for 5 days with MSCs overexpressing GFP (CTL OE) or HIF-1α (mut) (HIF-1α OE) (n=3); *p<0.05, n.s. p > 0.05; Error bars are +/- SEM

7.2.5 HIF-1α knockdown ameliorates HSPC suppression *ex vivo*

HIF-1α knockdown reduced STC-1 and other hypoxia-response genes induced by AML in MSCs. We determined the proliferation of HSPCs co-cultured with shHIF-1α MSCs to evaluate to impact of AML-induced HIF-1α stabilisation in MSCs on the suppression of normal HSPCs. Additionally, to confirm that STC-1 is a downstream mediator of HIF-1α stabilisation, the shHIF-1α MSCs were supplemented with vehicle or STC1 (Figure 52A). $CD34^+$ HSPCs exposed to AML cell lines (+ AML) on shHIF-1α MSCs still contained around 0.55-fold more CTV^{hi} than $CD34^+$ alone (dotted line) but compared to shCTL MSCs (1.55-fold) HSPCs suppression was significantly less. shHIF-1α MSCs supplemented with STC1 partially re-established the HSPC cell cycle inhibition (shCTL 2.4 versus shHIF-1α vehicle 1.61 versus shHIF-1α STC1 1.87) (Figure 52B). Similarly, the blockage of HSPCs differentiation, measured by +/- accumulation within $CD34^+$ cells normalised by $CD34^+$ alone, was alleviated in shHIF-1α MSCs + AML which was again partially re-established by STC1

supplementation (shCTL 4.1 versus shHIF-1α vehicle 2.8 versus shHIF-1α STC1 3.2) (Figure 52C).

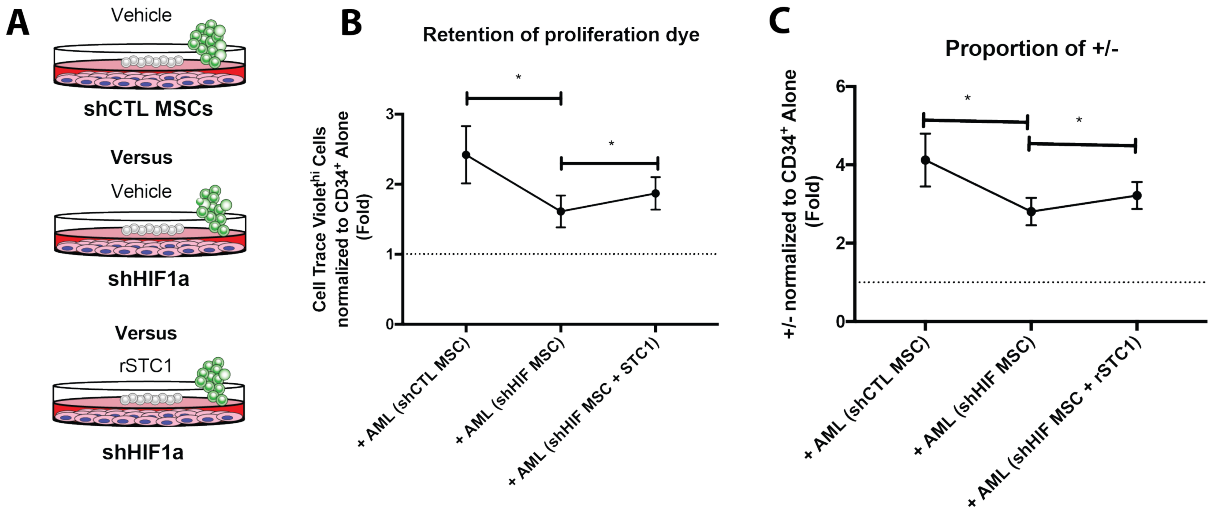


Figure 52. HIF-1α knockdown in MSCs ameliorates the HSPC suppression *ex vivo*
(A) MSCs were transduced with shCTL and shHIF-1α lentivirus vectors and co-culture with $CD34^+$ alone or + AML cell lines (KG1A, U937, OCI-AML3, NB4, MOLM13, ML1). Additionally, the cultures were supplemented with vehicle or STC1 **(B)** Quantification of relative proportions of CTV^{hi} population within $CD34^+$ HSPCs normalised to $CD34^+$ alone (n=3) and **(C)** proportions of phenotypic HSPCs (+/-) among $CD34^+$ normalised to $CD34^+$ alone (n=3); *p<0.05, n.s. p > 0.05; Error bars are +/- SEM

7.2.6 HIF-1α knockdown ameliorates HSPC suppression *in vivo*

Lastly, to establish whether HIF-1α was responsible for HSPC suppression *in vivo*, MSCs expressing shCTL/shHIF-1α were seeded in scaffolds with normal HSPCs and AML cell line U937 and implanted into NSG-SGM3 mice (Figure 53A). In line with previous results, shCTL + AML scaffolds contained 50 % fewer human non-leukaemic haematopoietic cells (Total $CD45^+$) which were enriched for Lin^- (+40 %) and $CD34^+$ cells (+70 %). In comparison, shHIF-1α MSCs were not enriched for Lin^- and $CD34^+$ cells. Furthermore, total $CD45^+$ counts were increased in shHIF-1α scaffolds, but the difference with shCTL scaffold was not significant (Figure 53B). Similar to STC1 neutralisation, AML cell numbers were not significantly different between shHIF-1α and shCTL control scaffolds establishing that the differences in normal haematopoiesis are not merely a consequence of varying AML engraftment (Figure 53B). Additionally, cell cycle activity, represented by EdU incorporation normalised to $CD34^+$ alone, was significantly higher in shHIF-1α scaffolds (shCTL 0.71 versus shHIF-1α 0.87) (Figure 53 C). Lastly, functional HSPCs, determined by CFU-ability, was enriched in non-

leukaemic CD45$^+$ from shCTL MSCs (1.18-fold enrichment) but not shHIF-1α MSC scaffold (Figure 53D). This data confirms that also *in vivo* shHIF-1α accumulation in MSCs is essential for the HSPC suppression by AML.

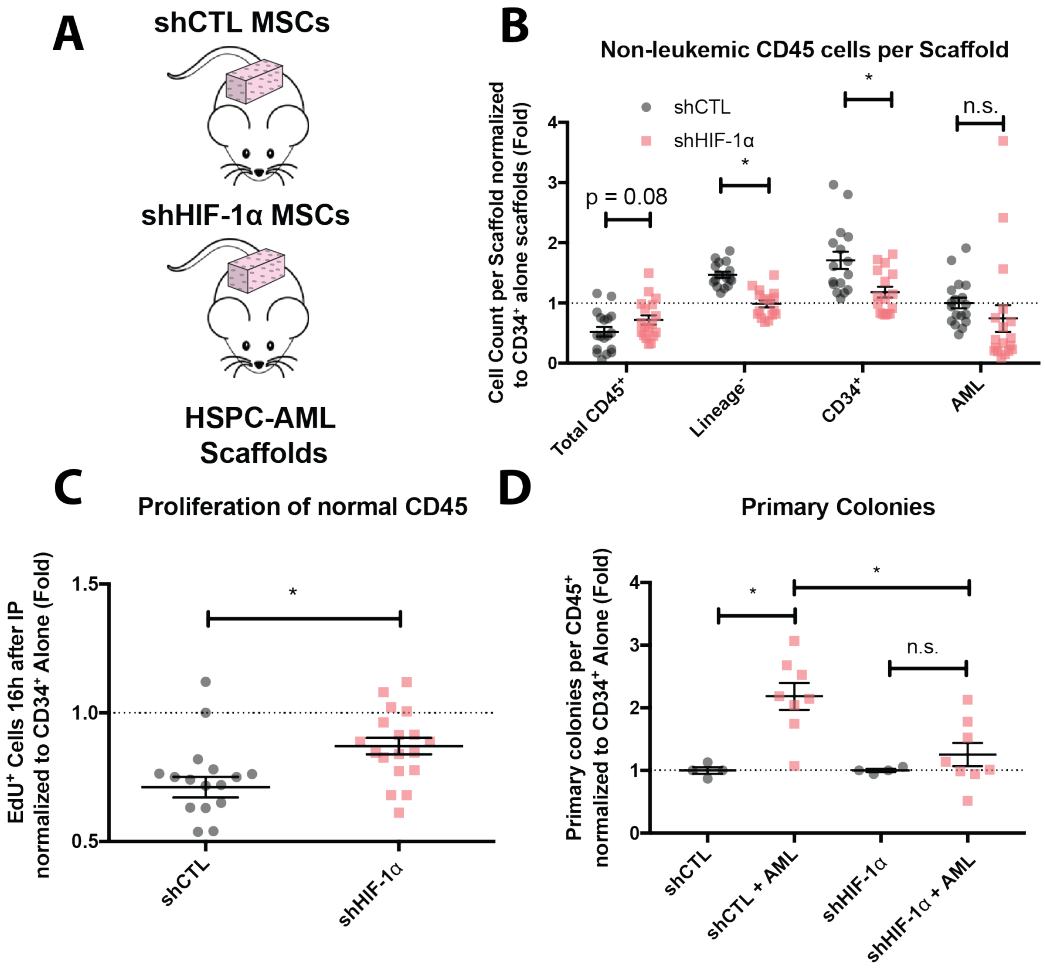


Figure 53. HIF-1α knockdown in MSCs ameliorates the HSPC suppression *in vivo*
(A) MSCs were transduced with shCTL and shHIF-1α lentivirus vectors and pre-seeded in scaffolds with HSPCs and AML cell line U937 **(B)** Cell count per scaffold relative to CD34+ alone (dotted line) from +AML scaffolds (C) Proliferation measured by incorporation of EdU in normal CD45+ cells normalised to CD34+ alone (dotted line) (D) CFU potential of FACS-sorted non-leukaemic CD45$^+$Lineage$^-$ cells normalised to CD34$^+$ alone (dotted line); *p<0.05, n.s. p > 0.05; Error bars are +/- SEM

7.3 Discussion

Over the last decade, numerous regulators of STC1 expression have been identified. Broadly these can be categorised as cellular response to cytokines (TGF-β1 (Ono et al., 2015), IL1α/β (Bartosh et al., 2013)) and or stress (oxidative (Ohkouchi et al., 2012), hypoxia (Yeung et al., 2005), DNA-damage (Block et al., 2009) and histone acetyltransferase inhibitors (Ching et al., 2012)). Indeed, these regulators are interconnected or may even rely on the same downstream effector. For examples, hypoxia induces the stabilisation of the α-subunits of HIFs which in turn can induce IL-1α/β or vice versa (Gorlach and Bonello, 2008; Jung et al., 2003) or even more direct activation of NF-κB and TGF-β1 can either activate the transcription of HIF-1α or induce stabilisation through PDH2 down-regulation (McMahon et al., 2006; Tannahill et al., 2013). Considering the pathway crosstalk, it might seem less surprising that these pathways share common downstream targets. Indeed, analysis of the STC1 promoter region (3 kb upstream and 1 kb downstream of transcription start site) using GPminer (Lee et al., 2012) for consensus sequences for the binding of several transcriptional factors showed binding sites for HIF (HIF-1α and p300), NF-kB (c-Rel and Rel-A), activator protein 1 (AP1), TGF-β1 (SMAD1) and STAT signalling. Being involved in so many solid cancer and AML associated pathways would theoretically make STC1 an interesting biomarker for either solid-cancer or AML-induced reprogramming of the microenvironment. However, while STC1 has been identified in several mammalian organs like lung, kidney and liver, detection of STC1 in the serum has been controversial. James et al. demonstrated that STC1 is quickly metabolised in serum and binds to an undefined erythrocyte surface protein (James et al., 2005). Nonetheless, Fang et al. proved the feasibility of STC1 and STC2 as biomarkers by identifying elevated concentrations in the serum of gastric cancer patients compared to benign controls or post-surgery patients. Compared to conventional biomarkers carcinoembryonic antigen (CEA) and Carbohydrate antigen (CA19-9), STC1 and STC2 demonstrated superior prognostic value (Fang et al., 2014).

Our screen with several AML associated cytokines generally confirmed TGF-β1, IL-1α/β and hypoxia/HIF-1α as STC1 activators in MSCs. Despite several STAT consensus motifs, the STAT3/5 activating interleukins IL6 and IL3, G-CSF and GM-CSF (Callus and Mathey-Prevot, 1998; Sansone and Bromberg, 2012; Yamaguchi et al., 1999) did not induce STC1 secretion. MAP-kinase activating PDGF-BB (Wu et al., 2008), which activates STC1 expression in CAFs (Pena et al., 2013), and VEGF-A (Koch and Claesson-Welsh, 2012) also

did not trigger STC1 secretion. Of note, PDGF-BB cultured contained slightly elevated concentrations which were caused by increased proliferation of MSCs since normalisation by cell numbers showed no more elevated secretion of STC1. Surprisingly, TNF-α, a well-known induces of NF-kB signalling (Schutze et al., 1995), did not trigger STC1 secretion either which could be a technical error. ELISA-analysis of TNF-α in the supernatant of MSC-AML co-cultured showed concentrations between 0.1-15 pg/mL while undetectable in $CD34^+$ alone cultures contained. Despite these minimal concentrations in the supernatant, elevated TNF-α has been detected in the BM interstitial fluid of AML patients, and further investigations should be carried out.

Comparative analysis of STC1 expression in AML-MSC co-cultured determined that HIF-1α is the main activator of *STC1* and *GLUT1*. Neutralisation of either IL-1α/β and TGF-β1 showed a downward trend regarding STC1 but was not significant. Furthermore, VEGF-A expression was not affected by HIF-1α knockdown, but neutralisation of IL-1α/β could ameliorated VEGF-A expression. However, it needs to be stressed that this detailed mRNA-based analysis was only performed with AML cell line U937 even though ELISA analysis of STC1 with other cell lines generally confirms these observations regarding STC1 regulation. Nonetheless, other cell lines or patient samples might shift the individual contribution to STC1 expression and the expression of other hypoxia-response genes might be more dependent on other mechanisms as exemplified by VEGF-A.

The other STC1 regulators IL-1α/β and TGF-β1 have been linked either to leukaemogenesis (Carey et al., 2017), MSC transcriptional response to AML (Jacamo et al., 2014) or to suppression of normal HSPCs (Gong et al., 2018). In our hands, TGF-β1 was highly expressed by MSCs cultures alone and we did not observe increased secretion of TGF-β1 in MSC-AML co-cultures even though mRNA expression showed a slight up-regulation in MSC co-cultured with AML. But other factors than just secretion could affect TGF-β1 signalling since activation of TGF-β1 requires conversion from the latent form into the activated form which can be catalysed enzymatically or by acidic pH conditions (Shi et al., 2011). Gong et al. showed that in MLL-AF9 murine leukaemia models, activated TGF-β1 is elevated in interstitial fluid of the BM and analysis of the main cellular contributors highlighted megakaryocytes as potential source (Gong et al., 2018). Similarly, attempted to neutralise TGF-β1 or IL-1β *ex vivo* in + AML cultures, only TGF-β1 neutralisation, mediated a partial rescue of HSPC suppression in

line with a more pronounced downregulation of secreted STC1 compared to IL-1β neutralisation.

NF-kB activation in ALL and AML mediated through IL-1β and VCAM-1/VLA-4 signalling between MSCs and AML has been shown to mediate drug resistance (Carey et al., 2017; Jacamo et al., 2014). Co-cultures of OCI-AML3 with MSCs showed that the expression of *IL6, IL8, VCAM-1* and *CLL2* in MSCs was strongly dependent on NF-kB activation by IL-1β (Jacamo et al., 2014). We did not analyse expression of *IL8*, *VCAM-1* and *CCL2* but *IL6* expression was determined in MSCs cultured in normoxic and hypoxic conditions and did not show significant differences implying that at least *IL6* in our hands is not a hypoxia-response gene. Like TGF-β1, neutralisation of IL-1β mediated a slight downward trend in STC-1 expression but did not translate into a significant reduced of HSPC suppression.

HIF-1α overexpression in MSCs suppressed the expansion of co-cultured HSPCs and maintained HSPCs in a more immature state than overexpression controls. HIF-1α and HIF-2α are both highly expressed in MSCs, highlighting the hypoxic origin of MSCs from the BM (Palomaki et al., 2013). Prolonged HIF-1α knockdown in MSCs inhibited proliferation which may involve increased cellular ROS levels. Other reports like Jiang and colleagues described that knockdown of HIF-1α in MSCs induces reduced BCL-2 levels causing an upregulation of total p53 and p53 phosphorylation which induces apoptosis in MSCs (Lv et al., 2017). Furthermore, HIF-1α and HIF-2α deficient MSCs show severely reduced differentiation capacity towards adipo-, osteo- and chondrogenic lineages independent of cell viability (Guarnerio et al., 2014). Since HIF-1α is especially important for the cellular adaptation to hypoxia, our *ex vivo* cultures were performed in normoxia and over a relatively short period: in this condition, HIF-1α knockdown did not severely affect MSCs. Also *in vivo*, MSCs counts per scaffold showed a downward trend in shHIF-1α MSCs suggesting that similar to *ex vivo*, HIF-1α also mediates MSC homeostasis in the scaffold conditions. Potentially a longer duration of the scaffold experiments would have generated a more pronounced difference regarding MSC cell number. This implies that even though MSC viability was not severely affected at the time of analysis, it cannot be ruled out completely that our results were partially affected by increased oxidative or hypoxic stressed experienced by MSCs. Like MSCs, HIF-1α plays a crucial role in BM ECs maintenance, especially H-type vessels and osteogenesis (Kusumbe et al., 2014). To protect HSCs in leukaemic mice, Duarte et al. used a clinically-

approved PHD inhibitor to rescue to loss of H-Type vessels in leukaemic bones implying a potential dual role for HIF-1α to protect and maintain HSPC quiescence and homeostasis of niche cells.

Andreeff and colleagues found that HIF-1α in MSCs acts as AML suppressor even though MSC viability could have been involved since shHIF-1α MSCs were cultured for 2 weeks *ex vivo* and for several weeks *in vivo* prior to AML engraftment (Chen et al., 2012). Similarly, in solid cancers, HIF-1α expression in CAFs is associated with increased metastasis and angiogenesis and therefore acts as an oncogene (Chiavarina et al., 2010). During the 2-week *in vivo* period, we did observe a non-significant downward trend regarding AML engraftment which is generally in agreement with Andreeff and colleagues, however, technical differences regarding duration and scaffold system could explain the differences.

HIF-1α stabilisation does not only affect MSC homeostasis and differentiation but also has been shown to regulates the proliferation of normal mouse HSPCs. Guarnerio et al. demonstrated that HIF-1α and HIF-2α overexpression in murine MSCs suppressed HSPC expansion and conversely, knockdown favoured lineage differentiation of HSPCs. From a mechanistic perspective, HIF-1α and HIF-2α suppressed the activation of STAT1 signalling which provokes inflammatory signalling and the expansion and differentiation of normal HSPCs (Guarnerio et al., 2014). In our system, overexpression induced a similar enrichment of immature HSPCs with enhanced *ex vivo* CFU- and LTC-IC ability. However, knockdown of HIF-1α in MSCs in the absence of AML generated varying results. In some experiments, we observed an increased and others decreased expansion, however *in vivo*, total $CD45^+$ counts were not significantly different between shCTL and shHIF-1α. Importantly, all results of the *ex vivo* + AML system were normalised to $CD34^+$ alone values of the respective shCTL or shHIF-1α MSCs which normalises for proliferation differences between HSPCs co-cultured with shCTL and shHIF-1α MSC. HIF-1α reduced HSPC suppression by AML but did not fully rescue, which agrees considering the presence of other identified pathways like TGF-β1 and IL-1β as well as the previously demonstrated direct inhibition of HSPC proliferation mediated an altered leukaemic metabolism. STC-1 partially rescues the HIF-1α mediated alleviation of HSPC suppression by AML which finally establish STC1 as downstream effector of HIF-1α stabilisation. The fact that we did not see a complete rescue was not surprising. HIF-1α

regulates several hundred genes accounting for more than 40 % of transcriptional changes in hypoxia (Benita et al., 2009).

Lastly, an outstanding question remains regarding how AML induces HIF-1α stabilisation. One explanation could be the extensive proliferation and oxygen-consumption of AML. Even a monolayer of cells can reduce the oxygen pressure in cell culture supernatant *ex vivo*. The extensive proliferation of AML, especially cell lines, requires a rapid energy production through all available means. We have observed that lactate secretion and glycolysis are elevated in AML but cancer metabolism has been described to utilise also mitochondrial oxidative phosphorylation for maximum anabolic effect (Samudio et al., 2009). Furthermore, oxygen consumption is an important indicator of drug resistance in AML (Henkenius et al., 2017) and Samudio et al., demonstrated that MSCs provoke further oxygen-consumption and lactate secretion in AML fuelled by FA-oxidation, which may further initiate HIF-1α stabilisation (Samudio et al., 2010). *In vivo*, AML and also B-ALL reduce oxygen pressure especially in close proximity around AML clonal colonies (Konopleva et al., 2015; Passaro et al., 2017b).

Apart from oxygen, other metabolic products can inhibit the degradation by interfering with HIF hydroxylating enzymes called PHDs. PHD's hydroxylase activity depends on co-factors like $Fe2^{+}$, α-ketoglutarate and vitamin C (Yang et al., 2014). High α-ketoglutarate to succinate ratios (Tannahill et al., 2013), Vitamin C deficiency (Kuiper et al., 2010) or iron chelators (Jones and Harris, 2006) all interfere with PHD and induce HIF-1α stabilisation. Similarly, the glycolysis end-product lactate can pass through the cell membrane via specific lactate transporters called MCT and inhibit PHDs, especially in oxidative phosphorylation-dependent cells (De Saedeleer et al., 2012). Tricarboxylic acid cycle products fumarate and succinate are structural analogues of α-ketoglutarate and can inhibit α-ketoglutarate-dependent enzymatic processes at high concentrations (Schofield and Ratcliffe, 2004). HIF-1α can also be induced as a response to elevated ROS levels which trigger stabilisation via an AMPK-dependent non-fully understood pathway involving AP1 factors c-Jun N-terminal kinase and Janus kinase 2 pathways (Jung et al., 2008).

Even though HIF-α is mainly regulated at the protein stabilisation level, AML-involved factors like TGF-β1 can either repress transcription of PHD enzymes or IL-1α/β and NF-κB can upregulate HIF-1α transcription (McMahon et al., 2006; Tannahill et al., 2013). However,

according to our data, we did not see an up-regulation of HIF-1α transcription however, PHD expression was not investigated.

To conclude the last results chapter, we observed that STC-1 is regulated by several AML-involved pathways including hypoxia/HIF-1α, IL-1α/β and TGF-β1. HIF-1α proved most effective to downregulate STC-1 secretion by MSCs. MSC-based overexpression of a normoxia-stable version of HIF-1α down-regulated HSPC cell cycle activity and preserved immature functional HSPCs. Conversely, HIF-1α knockdown in MSCs partially rescued HSPC suppression by AML, which was ameliorated by re-supplementation of STC1 *ex vivo*. *In vivo*, HIF-1α knockdown significantly improved HSPC proliferation and promoted differentiation of normal HSPCs in the presence of AML. Therapeutically, HIF-1α inhibition may be an interesting opportunity to inhibit niche remodelling. However, efficacy may be hindered due to its importance in also maintaining niche homeostasis and putative tumour-suppressive role in at least mouse malignant haematopoiesis (Guarnerio et al., 2014; Vukovic et al., 2015).

Summary and discussion

Examination of HSPCs from AML patients and in leukaemic mouse models uniformly demonstrated that HSCs are resilient to AML infiltration up until the very late stages of disease when a drastic loss occurs (Akinduro et al., 2018; Cheng et al., 2015; Gong et al., 2018; Miraki-Moud et al., 2013). Within the total non-malignant haematopoietic cells, the population of residual HSPCs becomes proportionally enriched which was demonstrated by higher engraftment potential of either total murine haematopoietic or human HSPCs into secondary mouse recipients (Cheng et al., 2015; Miraki-Moud et al., 2013). This enrichment was attributed to a higher proportion of quiescent cells and potentially a selective displacement of more mature cells (Akinduro et al., 2018). Both phenomena may contribute to the cytopenic manifestation of AML including anaemia, haemorrhage and leukopenia increasing treatment and non-treatment related complications and mortality (Chang et al., 1976; Huck et al., 2015).

From a mechanistic perspective, the interactions between AML and the niche are far better understood than between AML and HSPCs, however this most likely also involves a modified microenvironment. The loss of HSCs during very late stages of disease was associated with a collapse of BM vasculature especially endosteal vessels, which is also connected to the loss of osteoblastic cells (Duarte et al., 2018; Passaro et al., 2017b). Before the final stage, non-malignant HSCs express increased levels of cell cycle inhibiting regulators and quiescence promoting transcription factors Egr 1-3 and notch-downstream effectors Hes1 and Hey1 (Cheng et al., 2015). The former is triggered by a surge of megakaryocyte release of TGF-β1 (Gong et al., 2018).

Many recent studies have examined the healthy and malignant BM niche in great detail. In murine MLL-AF9 driven mouse model and MSCs extracted from AML patients, AML remodels the microenvironment to produce fewer haematopoietic maintenance factors like SCF, Angiopoietin-1 and CXCL12 (Geyh et al., 2016; Geyh et al., 2018; Kumar et al., 2018; Xiao et al., 2018). Furthermore, Boyd et al. proposed that loss of adipocytes and adipo-differentiation from MSCs impedes the maturation of normal-haematopoietic cells and transforms the niche into a progenitor cells propagating environment (Boyd et al., 2017). Overall these changes may shift the competition between normal HSPCs and AML towards the expansion of malignant clones which may have acquired mutations like FLT-3 ITD, making them less dependent on the BM niche (Mizuki et al., 2000).

The aim of this study was to examine HSPC interactions in a fully humanised environment *ex vivo* and *in vivo*. The former represented a model with minimal interaction partners to observe in a simplified system how AML interacts with a healthy BM niche. The mesenchymal niche is a particularly powerful *ex vivo* model because MSCs are easily extracted, expanded, express key haematopoietic support factors to maintain HSPCs *ex vivo* and MSC genes can be targeted by lentiviral delivered shRNA. Furthermore, AML provokes an expansion of MSCs in the murine BM (Hanoun et al., 2014) and transcriptional analysis of human AML patient isolated and expanded MSCs demonstrated extensive remodelling of the mesenchymal niche (Geyh et al., 2018). Luckily MSCs can also be utilised to generate an *in vivo* extramedullary BM niche providing us with the necessary cellular tool to generate a humanised leukaemic niche in which normal implanted HSPCs can be studied (Abarrategi et al., 2017; Antonelli et al., 2016; Reinisch et al., 2016).

On the other hand, our results need to be interpreted considering that our models are relying on the expansion of human mesenchymal niche cells which may alter their behaviour compared to their in vivo counterparts or select for a specific population. Especially ex vivo the physiological parameter or bone marrow in particular nutrient and oxygen availability, cytokines and cell-cell interactions cannot be completely mimicked.

Both *ex vivo* and *in vivo* models showed that AML cell lines and patient samples strongly suppresses the proliferation of normal HSPCs without negatively affecting viability in agreement with recent studies on human and murine HSPCs. With the defective expansion, a phenotypic inhibition of differentiation occurred enriching AML exposed HSPCs with phenotypic HSPCs *ex vivo* at the expense of HPCs. Similarly, *in vivo,* an enrichment of $CD34^+$ HSPCs among non-leukaemic haematopoietic cells was observed. Functionally, FACS-sorted HSPCs displayed more potent CFU-potential and LTC-IC frequency indicative of an enrichment of immature HSPCs at the expense of more differentiated HPCs. Similar to Cheng et al. who observed an enrichment of functional murine HSCs within non-leukaemic haematopoietic cells owing to decreased cell cycle activity (Cheng et al., 2015), we speculate that the enrichment of CFU and LTC-IC forming cells is due to more quiescence. Furthermore, since displacement does not occur at least in the *ex vivo* setting, we confirm that the enrichment of quiescent, immature HSPCs is not just a selection process driven by displacement but rather actively induced by AML. One may further speculate that an HSPC-selective cell cycle suppression could provide an advantage to malignant clones, a concept

proposed by Bhatia and colleagues for another myeloid malignancy, CML (Zhang et al., 2012). Consolidating this hypothesis, AML patients showed either unaltered or even accelerated proliferation when cultured in an AML cell line induced leukaemic environment. Surprisingly, injection into immunodeficient NSG primary recipients did not show an increase of HSCs at least in the primary recipients. In case the secondary recipients also do not accommodate a higher human chimerism, we speculate that a co-culture duration of 4 days may be insufficient to promote conservation of stemness. Experiments with TGF-β1, a potent cell cycle inhibitor, showed that TGF-β1 mainly suppresses transiently cycling cells but does not shift the ratio of quiescent cells (Wang et al., 2018). HSCs are the most primitive haematopoietic cells and reside mainly in a quiescent state, especially in CB and BM (Wilson et al., 2008). Therefore, after 4 days, the reduction of cell cycle activity in HSCs may not have been extensive enough to implement functional differences. Of note, neither TGF-β1 nor Egr3 actually raises the frequency of HSCs but rather reduce engraftment of HSCs after exposure (Cheng et al., 2015). Akinduro et al. reported that ST-HSCs are highly apoptotic under AML infiltration and hence, an enrichment of LT-HSCs could be achieved through other means than cell cycle inhibition (Akinduro et al., 2018).

The *ex vivo* model showed extensive remodelling of the MSCs raising the expression of genes whose expression is affected by oxygen pressure and hence mimicking a low oxygen/hypoxic environment. These so-called 'hypoxia-response genes' were indicative of the suppression of HSPC proliferation and an involvement of mesenchymal transcription response to AML was further validated by comparison of feeder-free and stroma-supported AML-HSPCs co-cultures as well as by pre-conditioning the MSCs with fully-removable AML cell lines. Similarly, MSCs pre-conditioned in hypoxia express higher levels of hypoxia-response genes even after several hours in normoxia and promote quiescence in HSPCs. The investigation concerning the primary regulator of these hypoxia-response genes showed that HIF-1α knockdown abolished the expression of several genes and conversely HIF-1α was stabilised in MSCs after AML co-cultured. In agreement with other published work, HIF-1α abrogation did not normalise the expression of all hypoxia-response genes. Indeed, inflammatory or TGF-β1 could also be involved exemplifying the complexity of the AML microenvironment and the difficulty to target individual factors (Abdul-Aziz et al., 2018; Abdul-Aziz et al., 2019; Geyh et al., 2018; Jacamo et al., 2014). However, for the

expression of STC1, HIF-1α knockdown consistently reduced the secretion in AML-MSC co-cultured prompting further investigation as a potential target.

The proliferative response of HSPCs to AML was replicated in direct contact and transwell conditions implying that secreted proteins in the media were at least partially responsible. Secretome analysis of AML-stroma interactions yielded STC1 as secreted factor with a history as MSC-derived regulator of cancer metabolism (Ohkouchi et al., 2012) and a potent predictor of adverse outcome in several solid neoplasms (Chu et al., 2015). Previously a role for STC1 in normal and malignant haematopoiesis has not been defined with the exception of as a potential indicator of relapse/outcome in AML when mRNA expression was measured in AML cells (Abaza et al., 2016; Tohmiya et al., 2004). In contrast, we did not detect meaningful expression of STC1 in haematopoietic cells but instead identified MSCs as the only source of STC1 at least *ex vivo*. *In vivo* STC1 expression was also upregulated in MSCs and murine stroma in leukaemic scaffolds. Interestingly, a recent unpublished report by Scadden and colleagues observed aberrant STC1 expression in sinusoidal and arteriolar vasculature implying a potential role for STC1 in angiogenesis (Ninib Baryawno, 2019)

From a functional perspective HSPCs exposed to recombinant STC1 *in vivo* and *ex vivo* were enriched in CFU- and LTC-IC forming cells and also replicated the proliferation and differentiation inhibition observed in AML-HSPCs. Conversely, neutralisation of STC1 by antibody promoted the differentiation and proliferation of HSPCs. In line with a multifactorial origin for HSPC-AML interactions, STC1 neutralisation did not completely rescue the AML phenotype, but still, it proves the involvement of STC1. The mechanism how STC1 interferes with differentiation and proliferation remains a major unanswered questions which requires further investigation. Preliminary results obtained shortly before thesis submission from RNA-sequencing of HSPCs cultured with STC1, confirm an involvement in cell cycle regulation. Genset-enrichment analysis showed a significant depletion of E2F-target genes and other cell cycle promoting pathways like MYC and mTORC1. However, confirmation by qPCR of differentially expressed genes is remaining. Generally, compared to the murine system, human HSPCs are a problematic system to explore mechanisms since experiments are always limited by HSPC yield and availability and the relatively low numbers of cells complicate standard molecular techniques.

To further alleviate the AML-HSPC phenotype, we investigated the regulators of STC1 with the assumption that up-stream factors may promote the expression of other known as well as un-identified HSPC regulators. As explained above, HIF-1α knockdown produced the strongest amelioration of STC1 secretion, which prompted further investigation. Despite HIF-1α established role in MSCs (Guarnerio et al., 2014), HSPCs (Rouault-Pierre et al., 2013; Takubo et al., 2010) and AML maintenance (Wang et al., 2011), a stabilisation of HIF-1α and an involvement in HSPC regulation in AML has not been addressed in literature. Overexpression of a modified HIF-1α which resists degradation by PHDs and VHL under normoxic conditions (Guarnerio et al., 2014) again mimicked the AML-HSPCs phenotype functionally and regarding cell cycle activity. Conversely, HSPC suppression was significantly reduced in a HIF-1α deficient mesenchymal environment regarding both proliferation and differentiation. Additionally, *in vivo* AML-HSPCs scaffolds with HIF-1α replicated the amelioration of HSPC suppression observed *ex vivo*. Importantly, HSPC suppression could be re-initiated by supplementation of STC1 further consolidating that STC1 is a downstream effector of HIF-1α signalling in MSCs.

From a therapeutic perspective, HIF-1α as novel target to interfere with AML-microenvironment comes with the caveat that prolonged HIF-1α ablation diminishes the viability of the microenvironment and the maintenance of HSPCs (Guarnerio et al., 2014; Rouault-Pierre et al., 2013). STC1 knockdown but not neutralisation affect MSC viability and hence the latter may be an interesting therapeutic target or biomarker although requiring further investigation using BM aspirations of AML patients. However, increased cell cycle activity of normal HSPCs may even be counterproductive to treatment of AML owing to increased toxicity from myeloablative chemotherapeutic treatment which mainly targets actively cycling cells. Hence STC1 would be best targeted after completion of treatment even though our time-course analysis of STC1 expression demonstrated a rapid decline of STC1 expression in MSCs after AML removal. A risky but interesting approach could be to harness the selective inhibition of normal HSPCs by AML and specifically suppress HSPC cell cycle activity allowing more intensive chemotherapy and sparing normal HSPCs which can repopulate the empty BM more effectively. Nonetheless, more knowledge how HSPC interact with AML and the leukaemic microenvironment are required to develop therapeutic strategies which incorporate the ablation of AML while at the same time promote normal haematopoiesis.

Lastly, it needs to be highlighted that all results need to be interpreted with consideration that our system is a model system composed of expanded plastic adherent MSCs which has profound impact on their behaviour. Furthermore, all experiments were performed with CB $CD34^+$ cells which also may differ from BM aged HSPCs.

References

Abarrategi, A., Foster, K., Hamilton, A., Mian, S.A., Passaro, D., Gribben, J., Mufti, G., and Bonnet, D. (2017). Versatile humanised niche model enables study of normal and malignant human hematopoiesis. J Clin Invest *127*, 543-548.

Abaza, H.M., Elmougy, M.I., El Maraghy, H.M., and Mahmoud, H.M. (2016). Stanniocalcin1 gene expression in patients with acute leukemia: impact on response to therapy and disease outcome. Int J Lab Hematol *38*, 81-89.

Abdul-Aziz, A.M., Shafat, M.S., Sun, Y., Marlein, C.R., Piddock, R.E., Robinson, S.D., Edwards, D.R., Zhou, Z., Collins, A., Bowles, K.M.*, et al.* (2018). HIF1alpha drives chemokine factor pro-tumoural signaling pathways in acute myeloid leukemia. Oncogene *37*, 2676-2686.

Abdul-Aziz, A.M., Sun, Y., Hellmich, C., Marlein, C.R., Mistry, J., Forde, E., Piddock, R.E., Shafat, M.S., Morfakis, A., Mehta, T.*, et al.* (2019). Acute myeloid leukemia induces protumoural p16INK4a-driven senescence in the bone marrow microenvironment. Blood *133*, 446-456.

Acar, M., Kocherlakota, K.S., Murphy, M.M., Peyer, J.G., Oguro, H., Inra, C.N., Jaiyeola, C., Zhao, Z., Luby-Phelps, K., and Morrison, S.J. (2015). Deep imageing of bone marrow shows non-dividing stem cells are mainly perisinusoidal. Nature *526*, 126-130.

Akinduro, O., Weber, T.S., Ang, H., Haltalli, M.L.R., Ruivo, N., Duarte, D., Rashidi, N.M., Hawkins, E.D., Duffy, K.R., and Lo Celso, C. (2018). Proliferation dynamics of acute myeloid leukaemia and haematopoietic progenitors competing for bone marrow space. Nat Commun *9*, 519.

Antonelli, A., Noort, W.A., Jaques, J., de Boer, B., de Jong-Korlaar, R., Brouwers-Vos, A.Z., Lubbers-Aalders, L., van Velzen, J.F., Bloem, A.C., Yuan, H.*, et al.* (2016). Establishing human leukemia xenograft mouse models by implanting human bone marrow-like scaffold-based niches. Blood *128*, 2949-2959.

Aqmasheh, S., Shamsasanjan, K., Akbarzadehlaleh, P., Pashoutan Sarvar, D., and Timari, H. (2017). Effects of Mesenchymal Stem Cell Derivatives on Hematopoiesis and Hematopoietic Stem Cells. Adv Pharm Bull *7*, 165-177.

Arber, D.A., Orazi, A., Hasserjian, R., Thiele, J., Borowitz, M.J., Le Beau, M.M., Bloomfield, C.D., Cazzola, M., and Vardiman, J.W. (2016). The 2016 revision to the World Health Organisation classification of myeloid neoplasms and acute leukemia. Blood *127*, 2391-2405.

Arranz, L., Sanchez-Aguilera, A., Martin-Perez, D., Isern, J., Langa, X., Tzankov, A., Lundberg, P., Muntion, S., Tzeng, Y.S., Lai, D.M.*, et al.* (2014). Neuropathy of haematopoietic stem cell niche is essential for myeloproliferative neoplasms. Nature *512*, 78-81.

Asada, N., Kunisaki, Y., Pierce, H., Wang, Z., Fernandez, N.F., Birbrair, A., Ma'ayan, A., and Frenette, P.S. (2017). Differential cytokine contributions of perivascular haematopoietic stem cell niches. Nat Cell Biol *19*, 214-223.

Athens, J.W., Haab, O.P., Raab, S.O., Mauer, A.M., Ashenbrucker, H., Cartwright, G.E., and Wintrobe, M.M. (1961). Leukokinetic studies. IV. The total blood, circulating and marginal

granulocyte pools and the granulocyte turnover rate in normal subjects. J Clin Invest *40*, 989-995.
Badar, T., Shetty, A., Bueso-Ramos, C., Cortes, J., Konopleva, M., Borthakur, G., Pierce, S., Huang, X., Chen, H.C., Kadia, T.*, et al.* (2015). Bone marrow necrosis in acute leukemia: Clinical characteristic and outcome. Am J Hematol *90*, 769-773.
Bader, P., Kuci, Z., Bakhtiar, S., Basu, O., Bug, G., Dennis, M., Greil, J., Barta, A., Kallay, K.M., Lang, P.*, et al.* (2018). Effective treatment of steroid and therapy-refractory acute graft-versus-host disease with a novel mesenchymal stromal cell product (MSC-FFM). Bone Marrow Transplant *53*, 852-862.
Bartosh, T.J., Ylostalo, J.H., Bazhanov, N., Kuhlman, J., and Prockop, D.J. (2013). Dynamic compaction of human mesenchymal stem/precursor cells into spheres self-activates caspase-dependent IL1 signaling to enhance secretion of modulators of inflammation and immunity (PGE2, TSG6, and STC1). Stem Cells *31*, 2443-2456.
Battula, V.L., Le, P.M., Sun, J.C., Nguyen, K., Yuan, B., Zhou, X., Sonnylal, S., McQueen, T., Ruvolo, V., Michel, K.A.*, et al.* (2017). AML-induced osteogenic differentiation in mesenchymal stromal cells supports leukemia growth. JCI Insight *2*.
Baumgartner, C., Toifl, S., Farlik, M., Halbritter, F., Scheicher, R., Fischer, I., Sexl, V., Bock, C., and Baccarini, M. (2018). An ERK-Dependent Feedback Mechanism Prevents Hematopoietic Stem Cell Exhaustion. Cell Stem Cell *22*, 879-892 e876.
Beerman, I., Luis, T.C., Singbrant, S., Lo Celso, C., and Mendez-Ferrer, S. (2017). The evolving view of the hematopoietic stem cell niche. Exp Hematol *50*, 22-26.
Ben-Batalla, I., Schultze, A., Wroblewski, M., Erdmann, R., Heuser, M., Waizenegger, J.S., Riecken, K., Binder, M., Schewe, D., Sawall, S.*, et al.* (2013). Axl, a prognostic and therapeutic target in acute myeloid leukemia mediates paracrine crosstalk of leukemia cells with bone marrow stroma. Blood *122*, 2443-2452.
Benita, Y., Kikuchi, H., Smith, A.D., Zhang, M.Q., Chung, D.C., and Xavier, R.J. (2009). An integrative genomics approach identifies Hypoxia Inducible Factor-1 (HIF-1)-target genes that form the core response to hypoxia. Nucleic Acids Res *37*, 4587-4602.
Benz, C., Copley, M.R., Kent, D.G., Wohrer, S., Cortes, A., Aghaeepour, N., Ma, E., Mader, H., Rowe, K., Day, C.*, et al.* (2012). Hematopoietic stem cell subtypes expand differentially during development and display distinct lymphopoietic programs. Cell Stem Cell *10*, 273-283.
Bernitz, J.M., Kim, H.S., MacArthur, B., Sieburg, H., and Moore, K. (2016). Hematopoietic Stem Cells Count and Remember Self-Renewal Divisions. Cell *167*, 1296-1309 e1210.
Bhatia, M., Bonnet, D., Murdoch, B., Gan, O.I., and Dick, J.E. (1998). A newly discovered class of human hematopoietic cells with SCID-repopulating activity. Nat Med *4*, 1038-1045.
Block, G.J., Ohkouchi, S., Fung, F., Frenkel, J., Gregory, C., Pochampally, R., DiMattia, G., Sullivan, D.E., and Prockop, D.J. (2009). Multipotent stromal cells are activated to reduce apoptosis in part by upregulation and secretion of stanniocalcin-1. Stem Cells *27*, 670-681.
Blunt, T., Finnie, N.J., Taccioli, G.E., Smith, G.C., Demengeot, J., Gottlieb, T.M., Mizuta, R., Varghese, A.J., Alt, F.W., Jeggo, P.A.*, et al.* (1995). Defective DNA-dependent protein kinase activity is linked to V(D)J recombination and DNA repair defects associated with the murine scid mutation. Cell *80*, 813-823.
Bonnet, D., and Dick, J.E. (1997). Human acute myeloid leukemia is organized as a hierarchy that originates from a primitive hematopoietic cell. Nat Med *3*, 730-737.
Bosma, G.C., Custer, R.P., and Bosma, M.J. (1983). A severe combined immunodeficiency mutation in the mouse. Nature *301*, 527-530.
Boulais, P.E., and Frenette, P.S. (2015). Making sense of hematopoietic stem cell niches. Blood *125*, 2621-2629.

Bowers, M., Zhang, B., Ho, Y., Agarwal, P., Chen, C.C., and Bhatia, R. (2015). Osteoblast ablation reduces normal long-term hematopoietic stem cell self-renewal but accelerates leukemia development. Blood *125*, 2678-2688.
Bowie, M.B., Kent, D.G., Dykstra, B., McKnight, K.D., McCaffrey, L., Hoodless, P.A., and Eaves, C.J. (2007). Identification of a new intrinsically timed developmental checkpoint that reprograms key hematopoietic stem cell properties. Proc Natl Acad Sci U S A *104*, 5878-5882.
Bowman, R.L., Busque, L., and Levine, R.L. (2018). Clonal Hematopoiesis and Evolution to Hematopoietic Malignancies. Cell Stem Cell *22*, 157-170.
Boyd, A.L., Reid, J.C., Salci, K.R., Aslostovar, L., Benoit, Y.D., Shapovalova, Z., Nakanishi, M., Porras, D.P., Almakadi, M., Campbell, C.J.V.*, et al.* (2017). Acute myeloid leukaemia disrupts endogenous myelo-erythropoiesis by compromising the adipocyte bone marrow niche. Nat Cell Biol *19*, 1336-1347.
Bradley, T.R., and Metcalf, D. (1966). The growth of mouse bone marrow cells in vitro. Aust J Exp Biol Med Sci *44*, 287-299.
Braun, M., Qorraj, M., Buttner, M., Klein, F.A., Saul, D., Aigner, M., Huber, W., Mackensen, A., Jitschin, R., and Mougiakakos, D. (2016). CXCL12 promotes glycolytic reprogramming in acute myeloid leukemia cells via the CXCR4/mTOR axis. Leukemia *30*, 1788-1792.
Broxmeyer, H.E., Jacobsen, N., Kurland, J., Mendelsohn, N., and Moore, A.S. (1978). In vitro suppression of normal granulocytic stem cells by inhibitory activity derived from human leukemia cells. J Natl Cancer Inst *60*, 497-511.
Brune, D., and Kim, S. (1993). Predicting protein diffusion coefficients. Proc Natl Acad Sci U S A *90*, 3835-3839.
Bruns, I., Lucas, D., Pinho, S., Ahmed, J., Lambert, M.P., Kunisaki, Y., Scheiermann, C., Schiff, L., Poncz, M., Bergman, A.*, et al.* (2014). Megakaryocytes regulate hematopoietic stem cell quiescence through CXCL4 secretion. Nat Med *20*, 1315-1320.
Buckley, S.A., Othus, M., Vainstein, V., Abkowitz, J.L., Estey, E.H., and Walter, R.B. (2014). Prediction of adverse events during intensive induction chemotherapy for acute myeloid leukemia or high-grade myelodysplastic syndromes. Am J Hematol *89*, 423-428.
Buscarlet, M., Provost, S., Zada, Y.F., Barhdadi, A., Bourgoin, V., Lepine, G., Mollica, L., Szuber, N., Dube, M.P., and Busque, L. (2017). DNMT3A and TET2 dominate clonal hematopoiesis and demonstrate benign phenotypes and different genetic predispositions. Blood *130*, 753-762.
Busch, K., Klapproth, K., Barile, M., Flossdorf, M., Holland-Letz, T., Schlenner, S.M., Reth, M., Hofer, T., and Rodewald, H.R. (2015). Fundamental properties of unperturbed haematopoiesis from stem cells in vivo. Nature *518*, 542-546.
Butler, J.M., Nolan, D.J., Vertes, E.L., Varnum-Finney, B., Kobayashi, H., Hooper, A.T., Seandel, M., Shido, K., White, I.A., Kobayashi, M.*, et al.* (2010). Endothelial cells are essential for the self-renewal and repopulation of Notch-dependent hematopoietic stem cells. Cell Stem Cell *6*, 251-264.
Callus, B.A., and Mathey-Prevot, B. (1998). Interleukin-3-induced activation of the JAK/STAT pathway is prolonged by proteasome inhibitors. Blood *91*, 3182-3192.
Calvi, L.M., Adams, G.B., Weibrecht, K.W., Weber, J.M., Olson, D.P., Knight, M.C., Martin, R.P., Schipani, E., Divieti, P., Bringhurst, F.R.*, et al.* (2003). Osteoblastic cells regulate the haematopoietic stem cell niche. Nature *425*, 841-846.
Cancer Genome Atlas Research, N., Ley, T.J., Miller, C., Ding, L., Raphael, B.J., Mungall, A.J., Robertson, A., Hoadley, K., Triche, T.J., Jr., Laird, P.W.*, et al.* (2013). Genomic and epigenomic landscapes of adult de novo acute myeloid leukemia. N Engl J Med *368*, 2059-2074.

Carey, A., Edwards, D.K.t., Eide, C.A., Newell, L., Traer, E., Medeiros, B.C., Pollyea, D.A., Deininger, M.W., Collins, R.H., Tyner, J.W., *et al.* (2017). Identification of Interleukin-1 by Functional Screening as a Key Mediator of Cellular Expansion and Disease Progression in Acute Myeloid Leukemia. Cell Rep *18*, 3204-3218.
Catlin, S.N., Busque, L., Gale, R.E., Guttorp, P., and Abkowitz, J.L. (2011). The replication rate of human hematopoietic stem cells in vivo. Blood *117*, 4460-4466.
Chaffer, C.L., and Weinberg, R.A. (2011). A perspective on cancer cell metastasis. Science *331*, 1559-1564.
Challen, G.A., Sun, D., Jeong, M., Luo, M., Jelinek, J., Berg, J.S., Bock, C., Vasanthakumar, A., Gu, H., Xi, Y., *et al.* (2011). Dnmt3a is essential for hematopoietic stem cell differentiation. Nat Genet *44*, 23-31.
Chan, K.K., Leung, C.O., Wong, C.C., Ho, D.W., Chok, K.S., Lai, C.L., Ng, I.O., and Lo, R.C. (2017). Secretory Stanniocalcin 1 promotes metastasis of hepatocellular carcinoma through activation of JNK signaling pathway. Cancer Lett *403*, 330-338.
Chang, A.C., Cha, J., Koentgen, F., and Reddel, R.R. (2005). The murine stanniocalcin 1 gene is not essential for growth and development. Mol Cell Biol *25*, 10604-10610.
Chang, A.C., Hook, J., Lemckert, F.A., McDonald, M.M., Nguyen, M.A., Hardeman, E.C., Little, D.G., Gunning, P.W., and Reddel, R.R. (2008). The murine stanniocalcin 2 gene is a negative regulator of postnatal growth. Endocrinology *149*, 2403-2410.
Chang, H.Y., Rodriguez, V., Narboni, G., Bodey, G.P., Luna, M.A., and Freireich, E.J. (1976). Causes of death in adults with acute leukemia. Medicine (Baltimore) *55*, 259-268.
Chapple, R.H., Tseng, Y.J., Hu, T., Kitano, A., Takeichi, M., Hoegenauer, K.A., and Nakada, D. (2018). Lineage tracing of murine adult hematopoietic stem cells reveals active contribution to steady-state hematopoiesis. Blood Adv *2*, 1220-1228.
Charrad, R.S., Li, Y., Delpech, B., Balitrand, N., Clay, D., Jasmin, C., Chomienne, C., and Smadja-Joffe, F. (1999). Ligation of the CD44 adhesion molecule reverses blockage of differentiation in human acute myeloid leukemia. Nat Med *5*, 669-676.
Chen, J.Y., Miyanishi, M., Wang, S.K., Yamazaki, S., Sinha, R., Kao, K.S., Seita, J., Sahoo, D., Nakauchi, H., and Weissman, I.L. (2016). Hoxb5 marks long-term haematopoietic stem cells and reveals a homogenous perivascular niche. Nature *530*, 223-227.
Chen, Y., Jacamo, R., Shi, Y.X., Wang, R.Y., Battula, V.L., Konoplev, S., Strunk, D., Hofmann, N.A., Reinisch, A., Konopleva, M., *et al.* (2012). Human extramedullary bone marrow in mice: a novel in vivo model of genetically controlled hematopoietic microenvironment. Blood *119*, 4971-4980.
Cheng, C.W., Adams, G.B., Perin, L., Wei, M., Zhou, X., Lam, B.S., Da Sacco, S., Mirisola, M., Quinn, D.I., Dorff, T.B., *et al.* (2014). Prolonged fasting reduces IGF-1/PKA to promote hematopoietic-stem-cell-based regeneration and reverse immunosuppression. Cell Stem Cell *14*, 810-823.
Cheng, H., Hao, S., Liu, Y., Pang, Y., Ma, S., Dong, F., Xu, J., Zheng, G., Li, S., Yuan, W., *et al.* (2015). Leukemic marrow infiltration reveals a novel role for Egr3 as a potent inhibitor of normal hematopoietic stem cell proliferation. Blood *126*, 1302-1313.
Cheng, H., Liu, Y., Jia, Q., Ma, S., Yuan, W., Jia, H., and Cheng, T. (2016). Novel regulators in hematopoietic stem cells can be revealed by a functional approach under leukemic condition. Leukemia *30*, 2074-2077.
Cheng, W.Y., Zhu, Y.M., Liu, Z., Weng, X.Q., Sui, J.N., Chen, Y.S., Wang, S.Y., and Shen, Y. (2018). Impact of blood count recovery on outcomes of acute myeloid leukemia patients achieving morphologic leukemia-free state. Blood Cancer J *8*, 53.
Chiavarina, B., Whitaker-Menezes, D., Migneco, G., Martinez-Outschoorn, U.E., Pavlides, S., Howell, A., Tanowitz, H.B., Casimiro, M.C., Wang, C., Pestell, R.G., *et al.* (2010). HIF1-alpha functions as a tumour promoter in cancer associated fibroblasts, and as a tumour

suppressor in breast cancer cells: Autophagy drives compartment-specific oncogenesis. Cell Cycle *9*, 3534-3551.
Ching, L.Y., Yeung, B.H., and Wong, C.K. (2012). Synergistic effect of p53 on TSA-induced stanniocalcin 1 expression in human nasopharyngeal carcinoma cells, CNE2. J Mol Endocrinol *48*, 241-250.
Chow, A., Lucas, D., Hidalgo, A., Mendez-Ferrer, S., Hashimoto, D., Scheiermann, C., Battista, M., Leboeuf, M., Prophete, C., van Rooijen, N.*, et al.* (2011). Bone marrow CD169+ macrophages promote the retention of hematopoietic stem and progenitor cells in the mesenchymal stem cell niche. J Exp Med *208*, 261-271.
Chu, S.J., Zhang, J., Zhang, R., Lu, W.W., and Zhu, J.S. (2015). Evolution and functions of stanniocalcins in cancer. Int J Immunopathol Pharmacol *28*, 14-20.
Clarke, B. (2008). Normal bone anatomy and physiology. Clin J Am Soc Nephrol *3 Suppl 3*, S131-139.
Cogle, C.R., Goldman, D.C., Madlambayan, G.J., Leon, R.P., Masri, A.A., Clark, H.A., Asbaghi, S.A., Tyner, J.W., Dunlap, J., Fan, G.*, et al.* (2014). Functional integration of acute myeloid leukemia into the vascular niche. Leukemia *28*, 1978-1987.
Coombs, C.C., Zehir, A., Devlin, S.M., Kishtagari, A., Syed, A., Jonsson, P., Hyman, D.M., Solit, D.B., Robson, M.E., Baselga, J.*, et al.* (2017). Therapy-Related Clonal Hematopoiesis in Patients with Non-hematologic Cancers Is Common and Associated with Adverse Clinical Outcomes. Cell Stem Cell *21*, 374-382 e374.
Crisostomo, P.R., Wang, Y., Markel, T.A., Wang, M., Lahm, T., and Meldrum, D.R. (2008). Human mesenchymal stem cells stimulated by TNF-alpha, LPS, or hypoxia produce growth factors by an NF kappa B- but not JNK-dependent mechanism. Am J Physiol Cell Physiol *294*, C675-682.
da Silva, C.L., Goncalves, R., Porada, C.D., Ascensao, J.L., Zanjani, E.D., Cabral, J.M., and Almeida-Porada, G. (2009). Differences amid bone marrow and cord blood hematopoietic stem/progenitor cell division kinetics. J Cell Physiol *220*, 102-111.
Danet, G.H., Pan, Y., Luongo, J.L., Bonnet, D.A., and Simon, M.C. (2003). Expansion of human SCID-repopulating cells under hypoxic conditions. J Clin Invest *112*, 126-135.
De Kouchkovsky, I., and Abdul-Hay, M. (2016). 'Acute myeloid leukemia: a comprehensive review and 2016 update'. Blood Cancer J *6*, e441.
De Niu, P., Radman, D.P., Jaworski, E.M., Deol, H., Gentz, R., Su, J., Olsen, H.S., and Wagner, G.F. (2000). Development of a human stanniocalcin radioimmunoassay: serum and tissue hormone levels and pharmacokinetics in the rat. Mol Cell Endocrinol *162*, 131-144.
De Saedeleer, C.J., Copetti, T., Porporato, P.E., Verrax, J., Feron, O., and Sonveaux, P. (2012). Lactate activates HIF-1 in oxidative but not in Warburg-phenotype human tumour cells. PLoS One *7*, e46571.
Dean, L. (2005). Blood Groups and Red Cell Antigens Blood Groups and Red Cell Antigens [Internet] Bethesda (MD): National Center for Biotechnology Information (US); 2005 Table 1, Complete blood count Available from: https://wwwncbinlmnihgov/books/NBK2263/table/ch1T1/
.
Deeb, G., Vaughan, M.M., McInnis, I., Ford, L.A., Sait, S.N., Starostik, P., Wetzler, M., Mashtare, T., and Wang, E.S. (2011). Hypoxia-inducible factor-1alpha protein expression is associated with poor survival in normal karyotype adult acute myeloid leukemia. Leuk Res *35*, 579-584.
Desai, P., Mencia-Trinchant, N., Savenkov, O., Simon, M.S., Cheang, G., Lee, S., Samuel, M., Ritchie, E.K., Guzman, M.L., Ballman, K.V.*, et al.* (2018). Somatic mutations precede acute myeloid leukemia years before diagnosis. Nat Med *24*, 1015-1023.

Di Tullio, A., Rouault-Pierre, K., Abarrategi, A., Mian, S., Grey, W., Gribben, J., Stewart, A., Blackwood, E., and Bonnet, D. (2017). The combination of CHK1 inhibitor with G-CSF overrides cytarabine resistance in human acute myeloid leukemia. Nat Commun *8*, 1679.
Diaz de la Guardia, R., Lopez-Millan, B., Lavoie, J.R., Bueno, C., Castano, J., Gomez-Casares, M., Vives, S., Palomo, L., Juan, M., Delgado, J.*, et al.* (2017). Detailed Characterisation of Mesenchymal Stem/Stromal Cells from a Large Cohort of AML Patients Demonstrates a Definitive Link to Treatment Outcomes. Stem Cell Reports *8*, 1573-1586.
Ding, L., Ley, T.J., Larson, D.E., Miller, C.A., Koboldt, D.C., Welch, J.S., Ritchey, J.K., Young, M.A., Lamprecht, T., McLellan, M.D.*, et al.* (2012a). Clonal evolution in relapsed acute myeloid leukaemia revealed by whole-genome sequencing. Nature *481*, 506-510.
Ding, L., and Morrison, S.J. (2013). Haematopoietic stem cells and early lymphoid progenitors occupy distinct bone marrow niches. Nature *495*, 231-235.
Ding, L., Saunders, T.L., Enikolopov, G., and Morrison, S.J. (2012b). Endothelial and perivascular cells maintain haematopoietic stem cells. Nature *481*, 457-462.
Doepfner, K.T., Spertini, O., and Arcaro, A. (2007). Autocrine insulin-like growth factor-I signaling promotes growth and survival of human acute myeloid leukemia cells via the phosphoinositide 3-kinase/Akt pathway. Leukemia *21*, 1921-1930.
Dohner, H., Estey, E., Grimwade, D., Amadori, S., Appelbaum, F.R., Buchner, T., Dombret, H., Ebert, B.L., Fenaux, P., Larson, R.A.*, et al.* (2017). Diagnosis and management of AML in adults: 2017 ELN recommendations from an international expert panel. Blood *129*, 424-447.
Dohner, H., Weisdorf, D.J., and Bloomfield, C.D. (2015). Acute Myeloid Leukemia. N Engl J Med *373*, 1136-1152.
Dominici, M., Le Blanc, K., Mueller, I., Slaper-Cortenbach, I., Marini, F., Krause, D., Deans, R., Keating, A., Prockop, D., and Horwitz, E. (2006). Minimal criteria for defining multipotent mesenchymal stromal cells. The International Society for Cellular Therapy position statement. Cytotherapy *8*, 315-317.
Dong, L., Yu, W.M., Zheng, H., Loh, M.L., Bunting, S.T., Pauly, M., Huang, G., Zhou, M., Broxmeyer, H.E., Scadden, D.T.*, et al.* (2016). Leukaemogenic effects of Ptpn11 activating mutations in the stem cell microenvironment. Nature *539*, 304-308.
Dong-Feng, Z., Ting, L., Cheng, C., Xi, Z., Xue, L., Xing-Hua, C., and Pei-Yan, K. (2012). Silencing HIF-1αlpha reduces the adhesion and secretion functions of acute leukemia hBMSCs. Braz J Med Biol Res *45*, 906-912.
dos Santos, M.T., Trindade, D.M., Goncalves Kde, A., Bressan, G.C., Anastassopoulos, F., Yunes, J.A., and Kobarg, J. (2011). Human stanniocalcin-1 interacts with nuclear and cytoplasmic proteins and acts as a SUMO E3 ligase. Mol Biosyst *7*, 180-193.
Doulatov, S., Notta, F., Laurenti, E., and Dick, J.E. (2012). Hematopoiesis: a human perspective. Cell Stem Cell *10*, 120-136.
Duan, C.W., Shi, J., Chen, J., Wang, B., Yu, Y.H., Qin, X., Zhou, X.C., Cai, Y.J., Li, Z.Q., Zhang, F.*, et al.* (2014). Leukemia propagating cells rebuild an evolving niche in response to therapy. Cancer Cell *25*, 778-793.
Duarte, D., Hawkins, E.D., Akinduro, O., Ang, H., De Filippo, K., Kong, I.Y., Haltalli, M., Ruivo, N., Straszkowski, L., Vervoort, S.J.*, et al.* (2018). Inhibition of Endosteal Vascular Niche Remodeling Rescues Hematopoietic Stem Cell Loss in AML. Cell Stem Cell *22*, 64-77 e66.
Dykstra, B., Kent, D., Bowie, M., McCaffrey, L., Hamilton, M., Lyons, K., Lee, S.J., Brinkman, R., and Eaves, C. (2007). Long-term propagation of distinct hematopoietic differentiation programs in vivo. Cell Stem Cell *1*, 218-229.
Dzierzak, E., and Bigas, A. (2018). Blood Development: Hematopoietic Stem Cell Dependence and Independence. Cell Stem Cell *22*, 639-651.

Eaves, C.J. (2015). Hematopoietic stem cells: concepts, definitions, and the new reality. Blood *125*, 2605-2613.
Fang, Z., Tian, Z., Luo, K., Song, H., and Yi, J. (2014). Clinical significance of stanniocalcin expression in tissue and serum of gastric cancer patients. Chin J Cancer Res *26*, 602-610.
Farge, T., Saland, E., de Toni, F., Aroua, N., Hosseini, M., Perry, R., Bosc, C., Sugita, M., Stuani, L., Fraisse, M.*, et al.* (2017). Chemotherapy-Resistant Human Acute Myeloid Leukemia Cells Are Not Enriched for Leukemic Stem Cells but Require Oxidative Metabolism. Cancer Discov *7*, 716-735.
Feng, X., and Teitelbaum, S.L. (2013). Osteoclasts: New Insights. Bone Res *1*, 11-26.
Feuring-Buske, M., Gerhard, B., Cashman, J., Humphries, R.K., Eaves, C.J., and Hogge, D.E. (2003). Improved engraftment of human acute myeloid leukemia progenitor cells in beta 2-microglobulin-deficient NOD/SCID mice and in NOD/SCID mice transgenic for human growth factors. Leukemia *17*, 760-763.
Filvaroff, E.H., Guillet, S., Zlot, C., Bao, M., Ingle, G., Steinmetz, H., Hoeffel, J., Bunting, S., Ross, J., Carano, R.A.*, et al.* (2002). Stanniocalcin 1 alters muscle and bone structure and function in transgenic mice. Endocrinology *143*, 3681-3690.
Ford, C.E., Hamerton, J.L., Barnes, D.W., and Loutit, J.F. (1956). Cytological identification of radiation-chimaeras. Nature *177*, 452-454.
Forristal, C.E., Nowlan, B., Jacobsen, R.N., Barbier, V., Walkinshaw, G., Walkley, C.R., Winkler, I.G., and Levesque, J.P. (2015). HIF-1αlpha is required for hematopoietic stem cell mobilisation and 4-prolyl hydroxylase inhibitors enhance mobilisation by stabilising HIF-1αlpha. Leukemia *29*, 1366-1378.
Franco, R.S. (2012). Measurement of red cell lifespan and ageing. Transfus Med Hemother *39*, 302-307.
Frisch, B.J., Ashton, J.M., Xing, L., Becker, M.W., Jordan, C.T., and Calvi, L.M. (2012). Functional inhibition of osteoblastic cells in an in vivo mouse model of myeloid leukemia. Blood *119*, 540-550.
Fulcher, D.A., and Basten, A. (1997). B cell life span: a review. Immunol Cell Biol *75*, 446-455.
Gao, X., Xu, C., Asada, N., and Frenette, P.S. (2018). The hematopoietic stem cell niche: from embryo to adult. Development *145*.
Gao, X.N., Yan, F., Lin, J., Gao, L., Lu, X.L., Wei, S.C., Shen, N., Pang, J.X., Ning, Q.Y., Komeno, Y.*, et al.* (2015). AML1/ETO cooperates with HIF1alpha to promote leukemogenesis through DNMT3a transactivation. Leukemia *29*, 1730-1740.
Gazit, R., Mandal, P.K., Ebina, W., Ben-Zvi, A., Nombela-Arrieta, C., Silberstein, L.E., and Rossi, D.J. (2014). Fgd5 identifies hematopoietic stem cells in the murine bone marrow. J Exp Med *211*, 1315-1331.
Ge, J., Hou, R., Liu, Q., Zhu, R., and Liu, K. (2011). Stromal-derived factor-1 deficiency in the bone marrow of acute myeloid leukemia. Int J Hematol *93*, 750-759.
Gekas, C., and Graf, T. (2013). CD41 expression marks myeloid-biased adult hematopoietic stem cells and increases with age. Blood *121*, 4463-4472.
Genovese, G., Kahler, A.K., Handsaker, R.E., Lindberg, J., Rose, S.A., Bakhoum, S.F., Chambert, K., Mick, E., Neale, B.M., Fromer, M.*, et al.* (2014). Clonal hematopoiesis and blood-cancer risk inferred from blood DNA sequence. N Engl J Med *371*, 2477-2487.
Geyh, S., Rodriguez-Paredes, M., Jager, P., Khandanpour, C., Cadeddu, R.P., Gutekunst, J., Wilk, C.M., Fenk, R., Zilkens, C., Hermsen, D.*, et al.* (2016). Functional inhibition of mesenchymal stromal cells in acute myeloid leukemia. Leukemia *30*, 683-691.
Geyh, S., Rodriguez-Paredes, M., Jager, P., Koch, A., Bormann, F., Gutekunst, J., Zilkens, C., Germing, U., Kobbe, G., Lyko, F.*, et al.* (2018). Transforming growth factor beta1-

mediated functional inhibition of mesenchymal stromal cells in myelodysplastic syndromes and acute myeloid leukemia. Haematologica *103*, 1462-1471.
Gilliland, D.G., and Griffin, J.D. (2002). The roles of FLT3 in hematopoiesis and leukemia. Blood *100*, 1532-1542.
Glait-Santar, C., Desmond, R., Feng, X., Bat, T., Chen, J., Heuston, E., Mizukawa, B., Mulloy, J.C., Bodine, D.M., Larochelle, A.*, et al.* (2015). Functional Niche Competition Between Normal Hematopoietic Stem and Progenitor Cells and Myeloid Leukemia Cells. Stem Cells *33*, 3635-3642.
Goloviznina, N.A., Verghese, S.C., Yoon, Y.M., Taratula, O., Marks, D.L., and Kurre, P. (2016). Mesenchymal Stromal Cell-derived Extracellular Vesicles Promote Myeloid-biased Multipotent Hematopoietic Progenitor Expansion via Toll-Like Receptor Engagement. J Biol Chem *291*, 24607-24617.
Gomez Perdiguero, E., Klapproth, K., Schulz, C., Busch, K., Azzoni, E., Crozet, L., Garner, H., Trouillet, C., de Bruijn, M.F., Geissmann, F.*, et al.* (2015). Tissue-resident macrophages originate from yolk-sac-derived erythro-myeloid progenitors. Nature *518*, 547-551.
Gondek, L.P., Zheng, G., Ghiaur, G., DeZern, A.E., Matsui, W., Yegnasubramanian, S., Lin, M.T., Levis, M., Eshleman, J.R., Varadhan, R.*, et al.* (2016). Donor cell leukemia arising from clonal hematopoiesis after bone marrow transplantation. Leukemia *30*, 1916-1920.
Gong, Y., Zhao, M., Yang, W., Gao, A., Yin, X., Hu, L., Wang, X., Xu, J., Hao, S., Cheng, T.*, et al.* (2018). Megakaryocyte-derived excessive transforming growth factor beta1 inhibits proliferation of normal hematopoietic stem cells in acute myeloid leukemia. Exp Hematol *60*, 40-46 e42.
Gorlach, A., and Bonello, S. (2008). The cross-talk between NF-kappaB and HIF-1: further evidence for a significant liaison. Biochem J *412*, e17-19.
Griessinger, E., Anjos-Afonso, F., Pizzitola, I., Rouault-Pierre, K., Vargaftig, J., Taussig, D., Gribben, J., Lassailly, F., and Bonnet, D. (2014). A niche-like culture system allowing the maintenance of primary human acute myeloid leukemia-initiating cells: a new tool to decipher their chemoresistance and self-renewal mechanisms. Stem Cells Transl Med *3*, 520-529.
Guarnerio, J., Coltella, N., Ala, U., Tonon, G., Pandolfi, P.P., and Bernardi, R. (2014). Bone marrow endosteal mesenchymal progenitors depend on HIF factors for maintenance and regulation of hematopoiesis. Stem Cell Reports *2*, 794-809.
Guitart, A.V., Subramani, C., Armesilla-Diaz, A., Smith, G., Sepulveda, C., Gezer, D., Vukovic, M., Dunn, K., Pollard, P., Holyoake, T.L.*, et al.* (2013). Hif-2alpha is not essential for cell-autonomous hematopoietic stem cell maintenance. Blood *122*, 1741-1745.
Gur-Cohen, S., Itkin, T., Chakrabarty, S., Graf, C., Kollet, O., Ludin, A., Golan, K., Kalinkovich, A., Ledergor, G., Wong, E.*, et al.* (2015). PAR1 signaling regulates the retention and recruitment of EPCR-expressing bone marrow hematopoietic stem cells. Nat Med *21*, 1307-1317.
Guryanova, O.A., Shank, K., Spitzer, B., Luciani, L., Koche, R.P., Garrett-Bakelman, F.E., Ganzel, C., Durham, B.H., Mohanty, A., Hoermann, G.*, et al.* (2016). DNMT3A mutations promote anthracycline resistance in acute myeloid leukemia via impaired nucleosome remodeling. Nat Med *22*, 1488-1495.
Hanoun, M., Maryanovich, M., Arnal-Estape, A., and Frenette, P.S. (2015). Neural regulation of hematopoiesis, inflammation, and cancer. Neuron *86*, 360-373.
Hanoun, M., Zhang, D., Mizoguchi, T., Pinho, S., Pierce, H., Kunisaki, Y., Lacombe, J., Armstrong, S.A., Duhrsen, U., and Frenette, P.S. (2014). Acute myelogenous leukemia-induced sympathetic neuropathy promotes malignancy in an altered hematopoietic stem cell niche. Cell Stem Cell *15*, 365-375.

Hao, Q.L., Shah, A.J., Thiemann, F.T., Smogorzewska, E.M., and Crooks, G.M. (1995). A functional comparison of CD34 + CD38- cells in cord blood and bone marrow. Blood *86*, 3745-3753.
Hassan, H.T., Stockschlader, M., Schleimer, B., Kruger, W., and Zander, A.R. (1996). Comparison of the content and subpopulations of CD3 and CD34 positive cells in bone marrow harvests and G-CSF-mobilised peripheral blood leukapheresis products from healthy adult donors. Transpl Immunol *4*, 319-323.
Hawkins, E.D., Duarte, D., Akinduro, O., Khorshed, R.A., Passaro, D., Nowicka, M., Straszkowski, L., Scott, M.K., Rothery, S., Ruivo, N.*, et al.* (2016). T-cell acute leukaemia exhibits dynamic interactions with bone marrow microenvironments. Nature *538*, 518-522.
He, L.F., Wang, T.T., Gao, Q.Y., Zhao, G.F., Huang, Y.H., Yu, L.K., and Hou, Y.Y. (2011). Stanniocalcin-1 promotes tumour angiogenesis through up-regulation of VEGF in gastric cancer cells. J Biomed Sci *18*, 39.
Henkenius, K., Greene, B.H., Barckhausen, C., Hartmann, R., Marken, M., Kaiser, T., Rehberger, M., Metzelder, S.K., Parak, W.J., Neubauer, A.*, et al.* (2017). Maintenance of cellular respiration indicates drug resistance in acute myeloid leukemia. Leuk Res *62*, 56-63.
Herault, A., Binnewies, M., Leong, S., Calero-Nieto, F.J., Zhang, S.Y., Kang, Y.A., Wang, X., Pietras, E.M., Chu, S.H., Barry-Holson, K.*, et al.* (2017). Myeloid progenitor cluster formation drives emergency and leukaemic myelopoiesis. Nature *544*, 53-58.
Himburg, H.A., Doan, P.L., Quarmyne, M., Yan, X., Sasine, J., Zhao, L., Hancock, G.V., Kan, J., Pohl, K.A., Tran, E.*, et al.* (2017). Dickkopf-1 promotes hematopoietic regeneration via direct and niche-mediated mechanisms. Nat Med *23*, 91-99.
Hirata, Y., Furuhashi, K., Ishii, H., Li, H.W., Pinho, S., Ding, L., Robson, S.C., Frenette, P.S., and Fujisaki, J. (2018). CD150(high) Bone Marrow Tregs Maintain Hematopoietic Stem Cell Quiescence and Immune Privilege via Adenosine. Cell Stem Cell *22*, 445-453 e445.
Hirschi, K.K. (2012). Hemogenic endothelium during development and beyond. Blood *119*, 4823-4827.
Hoang, V.T., Buss, E.C., Wang, W., Hoffmann, I., Raffel, S., Zepeda-Moreno, A., Baran, N., Wuchter, P., Eckstein, V., Trumpp, A.*, et al.* (2015). The rarity of ALDH(+) cells is the key to separation of normal versus leukemia stem cells by ALDH activity in AML patients. Int J Cancer *137*, 525-536.
Hooper, A.T., Butler, J.M., Nolan, D.J., Kranz, A., Iida, K., Kobayashi, M., Kopp, H.G., Shido, K., Petit, I., Yanger, K.*, et al.* (2009). Engraftment and reconstitution of hematopoiesis is dependent on VEGFR2-mediated regeneration of sinusoidal endothelial cells. Cell Stem Cell *4*, 263-274.
Hornick, N.I., Doron, B., Abdelhamed, S., Huan, J., Harrington, C.A., Shen, R., Cambronne, X.A., Chakkaramakkil Verghese, S., and Kurre, P. (2016). AML suppresses hematopoiesis by releasing exosomes that contain microRNAs targeting c-MYB. Sci Signal *9*, ra88.
Hsu, J.I., Dayaram, T., Tovy, A., De Braekeleer, E., Jeong, M., Wang, F., Zhang, J., Heffernan, T.P., Gera, S., Kovacs, J.J.*, et al.* (2018). PPM1D Mutations Drive Clonal Hematopoiesis in Response to Cytotoxic Chemotherapy. Cell Stem Cell *23*, 700-713 e706.
Huang, L., Zhang, L., Ju, H., Li, Q., Pan, J.S., Al-Lawati, Z., and Sheikh-Hamad, D. (2015). Stanniocalcin-1 inhibits thrombin-induced signaling and protects from bleomycin-induced lung injury. Sci Rep *5*, 18117.
Huck, A., Pozdnyakova, O., Brunner, A., Higgins, J.M., Fathi, A.T., and Hasserjian, R.P. (2015). Prior cytopenia predicts worse clinical outcome in acute myeloid leukemia. Leuk Res *39*, 1034-1040.
Hussong, J.W., Rodgers, G.M., and Shami, P.J. (2000). Evidence of increased angiogenesis in patients with acute myeloid leukemia. Blood *95*, 309-313.

Irigoyen, M., Garcia-Ruiz, J.C., and Berra, E. (2017). The hypoxia signalling pathway in haematological malignancies. Oncotarget *8*, 36832-36844.
Ishikawa, F., Yoshida, S., Saito, Y., Hijikata, A., Kitamura, H., Tanaka, S., Nakamura, R., Tanaka, T., Tomiyama, H., Saito, N.*, et al.* (2007). Chemotherapy-resistant human AML stem cells home to and engraft within the bone-marrow endosteal region. Nat Biotechnol *25*, 1315-1321.
Islam, A., Bielat, K.L., Glomski, C., and Henderson, E.S. (1989). In vitro growth and hemopoietic differentiation of mouse bone marrow-derived adherent stromal cells in long-term culture: formation of spheroidal bodies mimicking hemopoietic anlagen. J Med *20*, 193-207.
Itkin, T., Gur-Cohen, S., Spencer, J.A., Schajnovitz, A., Ramasamy, S.K., Kusumbe, A.P., Ledergor, G., Jung, Y., Milo, I., Poulos, M.G.*, et al.* (2016). Distinct bone marrow blood vessels differentially regulate haematopoiesis. Nature *532*, 323-328.
Ito, K., Turcotte, R., Cui, J., Zimmerman, S.E., Pinho, S., Mizoguchi, T., Arai, F., Runnels, J.M., Alt, C., Teruya-Feldstein, J.*, et al.* (2016). Self-renewal of a purified Tie2+ hematopoietic stem cell population relies on mitochondrial clearance. Science *354*, 1156-1160.
Ito, M., Hiramatsu, H., Kobayashi, K., Suzue, K., Kawahata, M., Hioki, K., Ueyama, Y., Koyanagi, Y., Sugamura, K., Tsuji, K.*, et al.* (2002). NOD/SCID/gamma(c)(null) mouse: an excellent recipient mouse model for engraftment of human cells. Blood *100*, 3175-3182.
Ito, S., Barrett, A.J., Dutra, A., Pak, E., Miner, S., Keyvanfar, K., Hensel, N.F., Rezvani, K., Muranski, P., Liu, P.*, et al.* (2015). Long term maintenance of myeloid leukemic stem cells cultured with unrelated human mesenchymal stromal cells. Stem Cell Res *14*, 95-104.
Ivanovic, Z., Belloc, F., Faucher, J.L., Cipolleschi, M.G., Praloran, V., and Dello Sbarba, P. (2002). Hypoxia maintains and interleukin-3 reduces the pre-colony-forming cell potential of dividing CD34(+) murine bone marrow cells. Exp Hematol *30*, 67-73.
Iversen, P.O., and Wiig, H. (2005). Tumour necrosis factor alpha and adiponectin in bone marrow interstitial fluid from patients with acute myeloid leukemia inhibit normal hematopoiesis. Clin Cancer Res *11*, 6793-6799.
Jacamo, R., Chen, Y., Wang, Z., Ma, W., Zhang, M., Spaeth, E.L., Wang, Y., Battula, V.L., Mak, P.Y., Schallmoser, K.*, et al.* (2014). Reciprocal leukemia-stroma VCAM-1/VLA-4-dependent activation of NF-kappaB mediates chemoresistance. Blood *123*, 2691-2702.
Jacamo, R., Davis, R.E., Ling, X., Sonnylal, S., Wang, Z., Ma, W., Zhang, M., Ruvolo, P., Ruvolo, V., Wang, R.Y.*, et al.* (2017). Tumour Trp53 status and genotype affect the bone marrow microenvironment in acute myeloid leukemia. Oncotarget *8*, 83354-83369.
Jacobson, L.O., Simmons, E.L., Marks, E.K., and Eldredge, J.H. (1951). Recovery from radiation injury. Science *113*, 510-511.
Jaiswal, S., Fontanillas, P., Flannick, J., Manning, A., Grauman, P.V., Mar, B.G., Lindsley, R.C., Mermel, C.H., Burtt, N., Chavez, A.*, et al.* (2014). Age-related clonal hematopoiesis associated with adverse outcomes. N Engl J Med *371*, 2488-2498.
Jalaeikhoo, H., Kashfi, S.M.H., Azimzadeh, P., Narimani, A., Gouhari Moghadam, K., Rajaienejad, M., Ariana, M., and Keyhani, M. (2017). Acute Myeloid Leukemia as the Main Cause of Pancytopenia in Iranian Population. Iran J Pathol *12*, 265-271.
James, K., Seitelbach, M., McCudden, C.R., and Wagner, G.F. (2005). Evidence for stanniocalcin binding activity in mammalian blood and glomerular filtrate. Kidney Int *67*, 477-482.
Jensen, P.O., Mortensen, B.T., Hodgkiss, R.J., Iversen, P.O., Christensen, I.J., Helledie, N., and Larsen, J.K. (2000). Increased cellular hypoxia and reduced proliferation of both normal and leukaemic cells during progression of acute myeloid leukaemia in rats. Cell Prolif *33*, 381-395.

Jepsen, M.R., Kloverpris, S., Mikkelsen, J.H., Pedersen, J.H., Fuchtbauer, E.M., Laursen, L.S., and Oxvig, C. (2015). Stanniocalcin-2 inhibits mammalian growth by proteolytic inhibition of the insulin-like growth factor axis. J Biol Chem *290*, 3430-3439.
Jin, Y., Nie, D., Li, J., Du, X., Lu, Y., Li, Y., Liu, C., Zhou, J., and Pan, J. (2017). Gas6/AXL Signaling Regulates Self-Renewal of Chronic Myelogenous Leukemia Stem Cells by Stabilising beta-Catenin. Clin Cancer Res *23*, 2842-2855.
Jitschin, R., Braun, M., Qorraj, M., Saul, D., Le Blanc, K., Zenz, T., and Mougiakakos, D. (2015). Stromal cell-mediated glycolytic switch in CLL cells involves Notch-c-Myc signaling. Blood *125*, 3432-3436.
Johnston, J., Ramos-Valdes, Y., Stanton, L.A., Ladhani, S., Beier, F., and Dimattia, G.E. (2010). Human stanniocalcin-1 or -2 expressed in mice reduces bone size and severely inhibits cranial intramembranous bone growth. Transgenic Res *19*, 1017-1039.
Jones, D.T., and Harris, A.L. (2006). Identification of novel small-molecule inhibitors of hypoxia-inducible factor-1 transactivation and DNA binding. Mol Cancer Ther *5*, 2193-2202.
Jung, S.N., Yang, W.K., Kim, J., Kim, H.S., Kim, E.J., Yun, H., Park, H., Kim, S.S., Choe, W., Kang, I.*, et al.* (2008). Reactive oxygen species stabilise hypoxia-inducible factor-1 alpha protein and stimulate transcriptional activity via AMP-activated protein kinase in DU145 human prostate cancer cells. Carcinogenesis *29*, 713-721.
Jung, Y.J., Isaacs, J.S., Lee, S., Trepel, J., and Neckers, L. (2003). IL-1beta-mediated up-regulation of HIF-1αlpha via an NFkappaB/COX-2 pathway identifies HIF-1 as a critical link between inflammation and oncogenesis. FASEB J *17*, 2115-2117.
Kanellis, J., Bick, R., Garcia, G., Truong, L., Tsao, C.C., Etemadmoghadam, D., Poindexter, B., Feng, L., Johnson, R.J., and Sheikh-Hamad, D. (2004). Stanniocalcin-1, an inhibitor of macrophage chemotaxis and chemokinesis. Am J Physiol Renal Physiol *286*, F356-362.
Kapp, F.G., Perlin, J.R., Hagedorn, E.J., Gansner, J.M., Schwarz, D.E., O'Connell, L.A., Johnson, N.S., Amemiya, C., Fisher, D.E., Wolfle, U.*, et al.* (2018). Protection from UV light is an evolutionarily conserved feature of the haematopoietic niche. Nature *558*, 445-448.
Kiel, M.J., Radice, G.L., and Morrison, S.J. (2007). Lack of evidence that hematopoietic stem cells depend on N-cadherin-mediated adhesion to osteoblasts for their maintenance. Cell Stem Cell *1*, 204-217.
Kiel, M.J., Yilmaz, O.H., Iwashita, T., Yilmaz, O.H., Terhorst, C., and Morrison, S.J. (2005). SLAM family receptors distinguish hematopoietic stem and progenitor cells and reveal endothelial niches for stem cells. Cell *121*, 1109-1121.
Kim, A., Shim, S., Kim, M.J., Myung, J.K., and Park, S. (2018). Mesenchymal stem cell-mediated Notch2 activation overcomes radiation-induced injury of the hematopoietic system. Sci Rep *8*, 9277.
Kim, Y.W., Koo, B.K., Jeong, H.W., Yoon, M.J., Song, R., Shin, J., Jeong, D.C., Kim, S.H., and Kong, Y.Y. (2008). Defective Notch activation in microenvironment leads to myeloproliferative disease. Blood *112*, 4628-4638.
Kocabas, F., Zheng, J., Thet, S., Copeland, N.G., Jenkins, N.A., DeBerardinis, R.J., Zhang, C., and Sadek, H.A. (2012). Meis1 regulates the metabolic phenotype and oxidant defense of hematopoietic stem cells. Blood *120*, 4963-4972.
Koch, S., and Claesson-Welsh, L. (2012). Signal transduction by vascular endothelial growth factor receptors. Cold Spring Harb Perspect Med *2*, a006502.
Kode, A., Manavalan, J.S., Mosialou, I., Bhagat, G., Rathinam, C.V., Luo, N., Khiabanian, H., Lee, A., Murty, V.V., Friedman, R.*, et al.* (2014). Leukaemogenesis induced by an activating beta-catenin mutation in osteoblasts. Nature *506*, 240-244.
Kojima, K., McQueen, T., Chen, Y., Jacamo, R., Konopleva, M., Shinojima, N., Shpall, E., Huang, X., and Andreeff, M. (2011). p53 activation of mesenchymal stromal cells partially

abrogates microenvironment-mediated resistance to FLT3 inhibition in AML through HIF-1αlpha-mediated down-regulation of CXCL12. Blood *118*, 4431-4439.
Konopleva, M., Thall, P.F., Yi, C.A., Borthakur, G., Coveler, A., Bueso-Ramos, C., Benito, J., Konoplev, S., Gu, Y., Ravandi, F.*, et al.* (2015). Phase I/II study of the hypoxia-activated prodrug PR104 in refractory/relapsed acute myeloid leukemia and acute lymphoblastic leukemia. Haematologica *100*, 927-934.
Korkolopoulou, P., Apostolidou, E., Pavlopoulos, P.M., Kavantzas, N., Vyniou, N., Thymara, I., Terpos, E., Patsouris, E., Yataganas, X., and Davaris, P. (2001). Prognostic evaluation of the microvascular network in myelodysplastic syndromes. Leukemia *15*, 1369-1376.
Korn, C., and Mendez-Ferrer, S. (2017). Myeloid malignancies and the microenvironment. Blood *129*, 811-822.
Kornblau, S.M., Ruvolo, P.P., Wang, R.Y., Battula, V.L., Shpall, E.J., Ruvolo, V.R., McQueen, T., Qui, Y., Zeng, Z., Pierce, S.*, et al.* (2018). Distinct protein signatures of acute myeloid leukemia bone marrow-derived stromal cells are prognostic for patient survival. Haematologica *103*, 810-821.
Krater, M., Jacobi, A., Otto, O., Tietze, S., Muller, K., Poitz, D.M., Palm, S., Zinna, V.M., Biehain, U., Wobus, M.*, et al.* (2017). Bone marrow niche-mimetics modulate HSPC function via integrin signaling. Sci Rep *7*, 2549.
Krevvata, M., Silva, B.C., Manavalan, J.S., Galan-Diez, M., Kode, A., Matthews, B.G., Park, D., Zhang, C.A., Galili, N., Nickolas, T.L.*, et al.* (2014). Inhibition of leukemia cell engraftment and disease progression in mice by osteoblasts. Blood *124*, 2834-2846.
Kuiper, C., Molenaar, I.G., Dachs, G.U., Currie, M.J., Sykes, P.H., and Vissers, M.C. (2010). Low ascorbate levels are associated with increased hypoxia-inducible factor-1 activity and an aggressive tumour phenotype in endometrial cancer. Cancer Res *70*, 5749-5758.
Kumar, B., Garcia, M., Weng, L., Jung, X., Murakami, J.L., Hu, X., McDonald, T., Lin, A., Kumar, A.R., DiGiusto, D.L.*, et al.* (2018). Acute myeloid leukemia transforms the bone marrow niche into a leukemia-permissive microenvironment through exosome secretion. Leukemia *32*, 575-587.
Kunisaki, Y., Bruns, I., Scheiermann, C., Ahmed, J., Pinho, S., Zhang, D., Mizoguchi, T., Wei, Q., Lucas, D., Ito, K.*, et al.* (2013). Arteriolar niches maintain haematopoietic stem cell quiescence. Nature *502*, 637-643.
Kusumbe, A.P., Ramasamy, S.K., and Adams, R.H. (2014). Coupling of angiogenesis and osteogenesis by a specific vessel subtype in bone. Nature *507*, 323-328.
Lagadinou, E.D., Sach, A., Callahan, K., Rossi, R.M., Neering, S.J., Minhajuddin, M., Ashton, J.M., Pei, S., Grose, V., O'Dwyer, K.M.*, et al.* (2013). BCL-2 inhibition targets oxidative phosphorylation and selectively eradicates quiescent human leukemia stem cells. Cell Stem Cell *12*, 329-341.
Lai, K.P., Law, A.Y., Yeung, H.Y., Lee, L.S., Wagner, G.F., and Wong, C.K. (2007). Induction of stanniocalcin-1 expression in apoptotic human nasopharyngeal cancer cells by p53. Biochem Biophys Res Commun *356*, 968-975.
Lane, S.W., Wang, Y.J., Lo Celso, C., Ragu, C., Bullinger, L., Sykes, S.M., Ferraro, F., Shterental, S., Lin, C.P., Gilliland, D.G.*, et al.* (2011). Differential niche and Wnt requirements during acute myeloid leukemia progression. Blood *118*, 2849-2856.
Lansdorp, P.M., Dragowska, W., and Mayani, H. (1993). Ontogeny-related changes in proliferative potential of human hematopoietic cells. J Exp Med *178*, 787-791.
Lapidot, T., Sirard, C., Vormoor, J., Murdoch, B., Hoang, T., Caceres-Cortes, J., Minden, M., Paterson, B., Caligiuri, M.A., and Dick, J.E. (1994). A cell initiating human acute myeloid leukaemia after transplantation into SCID mice. Nature *367*, 645-648.
Laurenti, E., and Gottgens, B. (2018). From haematopoietic stem cells to complex differentiation landscapes. Nature *553*, 418-426.

Law, A.Y., and Wong, C.K. (2013). Stanniocalcin-1 and -2 promote angiogenic sprouting in HUVECs via VEGF/VEGFR2 and angiopoietin signaling pathways. Mol Cell Endocrinol *374*, 73-81.
Lee, T.Y., Chang, W.C., Hsu, J.B., Chang, T.H., and Shien, D.M. (2012). GPMiner: an integrated system for mining combinatorial cis-regulatory elements in mammalian gene group. BMC Genomics *13 Suppl 1*, S3.
Li, H., Ghazanfari, R., Zacharaki, D., Ditzel, N., Isern, J., Ekblom, M., Mendez-Ferrer, S., Kassem, M., and Scheding, S. (2014). Low/negative expression of PDGFR-alpha identifies the candidate primary mesenchymal stromal cells in adult human bone marrow. Stem Cell Reports *3*, 965-974.
Liesveld, J.L., Rosell, K.E., Lu, C., Bechelli, J., Phillips, G., Lancet, J.E., and Abboud, C.N. (2005). Acute myelogenous leukemia--microenvironment interactions: role of endothelial cells and proteasome inhibition. Hematology *10*, 483-494.
Liu, F.D., Tam, K., Pishesha, N., Poon, Z., and Van Vliet, K.J. (2018). Improving hematopoietic recovery through modeling and modulation of the mesenchymal stromal cell secretome. Stem Cell Res Ther *9*, 268.
Liu, G., Yang, G., Chang, B., Mercado-Uribe, I., Huang, M., Zheng, J., Bast, R.C., Lin, S.H., and Liu, J. (2010). Stanniocalcin 1 and ovarian tumourigenesis. J Natl Cancer Inst *102*, 812-827.
Lo Celso, C., Fleming, H.E., Wu, J.W., Zhao, C.X., Miake-Lye, S., Fujisaki, J., Cote, D., Rowe, D.W., Lin, C.P., and Scadden, D.T. (2009). Live-animal tracking of individual haematopoietic stem/progenitor cells in their niche. Nature *457*, 92-96.
Lodish H, B.A., Zipursky SL, et al. (2000). Section 16.2, Electron Transport and Oxidative Phosphorylation. Molecular Cell Biology 4th edition
Long, F. (2011). Building strong bones: molecular regulation of the osteoblast lineage. Nat Rev Mol Cell Biol *13*, 27-38.
Lord, B.I., Testa, N.G., and Hendry, J.H. (1975). The relative spatial distributions of CFUs and CFUc in the normal mouse femur. Blood *46*, 65-72.
Lu, M., Wagner, G.F., and Renfro, J.L. (1994). Stanniocalcin stimulates phosphate reabsorption by flounder renal proximal tubule in primary culture. Am J Physiol *267*, R1356-1362.
Lu, W., Weng, W., Zhu, Q., Zhai, Y., Wan, Y., Liu, H., Yang, S., Yu, Y., Wei, Y., and Shi, J. (2018). Small bone marrow adipocytes predict poor prognosis in acute myeloid leukemia. Haematologica *103*, e21-e24.
Lucas, D., Scheiermann, C., Chow, A., Kunisaki, Y., Bruns, I., Barrick, C., Tessarollo, L., and Frenette, P.S. (2013). Chemotherapy-induced bone marrow nerve injury impairs hematopoietic regeneration. Nat Med *19*, 695-703.
Lv, B., Li, F., Fang, J., Xu, L., Sun, C., Han, J., Hua, T., Zhang, Z., Feng, Z., and Jiang, X. (2017). Hypoxia inducible factor 1alpha promotes survival of mesenchymal stem cells under hypoxia. Am J Transl Res *9*, 1521-1529.
Lymperi, S., Horwood, N., Marley, S., Gordon, M.Y., Cope, A.P., and Dazzi, F. (2008). Strontium can increase some osteoblasts without increasing hematopoietic stem cells. Blood *111*, 1173-1181.
Madiha Iqbal, M.P., Michael Machiorlatti, Sara K. Vesely, Jordan M Morton, Jennifer Holter and Mohamad Cherry (2016). Impact of Duration of Neutropenia and Lymphopenia on AML Patients Undergoing Induction Chemotherapy. ASH Annual Meeting Abstracts *vol. 128 no. 22 5178*.
Madsen, K.L., Tavernini, M.M., Yachimec, C., Mendrick, D.L., Alfonso, P.J., Buergin, M., Olsen, H.S., Antonaccio, M.J., Thomson, A.B., and Fedorak, R.N. (1998). Stanniocalcin: a

novel protein regulating calcium and phosphate transport across mammalian intestine. Am J Physiol *274*, G96-102.
Majmundar, A.J., Wong, W.J., and Simon, M.C. (2010). Hypoxia-inducible factors and the response to hypoxic stress. Mol Cell *40*, 294-309.
Mantel, C.R., O'Leary, H.A., Chitteti, B.R., Huang, X., Cooper, S., Hangoc, G., Brustovetsky, N., Srour, E.F., Lee, M.R., Messina-Graham, S.*, et al.* (2015). Enhancing Hematopoietic Stem Cell Transplantation Efficacy by Mitigating Oxygen Shock. Cell *161*, 1553-1565.
Marlein, C.R., Zaitseva, L., Piddock, R.E., Robinson, S.D., Edwards, D.R., Shafat, M.S., Zhou, Z., Lawes, M., Bowles, K.M., and Rushworth, S.A. (2017). NADPH oxidase-2 derived superoxide drives mitochondrial transfer from bone marrow stromal cells to leukemic blasts. Blood *130*, 1649-1660.
Matsunaga, T., Takemoto, N., Sato, T., Takimoto, R., Tanaka, I., Fujimi, A., Akiyama, T., Kuroda, H., Kawano, Y., Kobune, M.*, et al.* (2003). Interaction between leukemic-cell VLA-4 and stromal fibronectin is a decisive factor for minimal residual disease of acute myelogenous leukemia. Nat Med *9*, 1158-1165.
McCudden, C.R., James, K.A., Hasilo, C., and Wagner, G.F. (2002). Characterisation of mammalian stanniocalcin receptors. Mitochondrial targeting of ligand and receptor for regulation of cellular metabolism. J Biol Chem *277*, 45249-45258.
McIntosh, B.E., Brown, M.E., Duffin, B.M., Maufort, J.P., Vereide, D.T., Slukvin, II, and Thomson, J.A. (2015). Nonirradiated NOD,B6.SCID Il2rgamma-/- Kit(W41/W41) (NBSGW) mice support multilineage engraftment of human hematopoietic cells. Stem Cell Reports *4*, 171-180.
McLeod, C.M., and Mauck, R.L. (2017). On the origin and impact of mesenchymal stem cell heterogeneity: new insights and emerging tools for single cell analysis. Eur Cell Mater *34*, 217-231.
McMahon, S., Charbonneau, M., Grandmont, S., Richard, D.E., and Dubois, C.M. (2006). Transforming growth factor beta1 induces hypoxia-inducible factor-1 stabilisation through selective inhibition of PHD2 expression. J Biol Chem *281*, 24171-24181.
Mead, A.J., Neo, W.H., Barkas, N., Matsuoka, S., Giustacchini, A., Facchini, R., Thongjuea, S., Jamieson, L., Booth, C.A.G., Fordham, N.*, et al.* (2017). Niche-mediated depletion of the normal hematopoietic stem cell reservoir by Flt3-ITD-induced myeloproliferation. J Exp Med *214*, 2005-2021.
Medinger, M., Lengerke, C., and Passweg, J. (2016). Novel therapeutic options in Acute Myeloid Leukemia. Leuk Res Rep *6*, 39-49.
Medvinsky, A., and Dzierzak, E. (1996). Definitive hematopoiesis is autonomously initiated by the AGM region. Cell *86*, 897-906.
Mendez-Ferrer, S., Chow, A., Merad, M., and Frenette, P.S. (2009). Circadian rhythms influence hematopoietic stem cells. Curr Opin Hematol *16*, 235-242.
Mendez-Ferrer, S., Lucas, D., Battista, M., and Frenette, P.S. (2008). Haematopoietic stem cell release is regulated by circadian oscillations. Nature *452*, 442-447.
Mendez-Ferrer, S., Michurina, T.V., Ferraro, F., Mazloom, A.R., Macarthur, B.D., Lira, S.A., Scadden, D.T., Ma'ayan, A., Enikolopov, G.N., and Frenette, P.S. (2010). Mesenchymal and haematopoietic stem cells form a unique bone marrow niche. Nature *466*, 829-834.
Miharada, K., Karlsson, G., Rehn, M., Rorby, E., Siva, K., Cammenga, J., and Karlsson, S. (2011). Cripto regulates hematopoietic stem cells as a hypoxic-niche-related factor through cell surface receptor GRP78. Cell Stem Cell *9*, 330-344.
Miraki-Moud, F., Anjos-Afonso, F., Hodby, K.A., Griessinger, E., Rosignoli, G., Lillington, D., Jia, L., Davies, J.K., Cavenagh, J., Smith, M.*, et al.* (2013). Acute myeloid leukemia does

not deplete normal hematopoietic stem cells but induces cytopenias by impeding their differentiation. Proc Natl Acad Sci U S A *110*, 13576-13581.
Mizuki, M., Fenski, R., Halfter, H., Matsumura, I., Schmidt, R., Muller, C., Gruning, W., Kratz-Albers, K., Serve, S., Steur, C.*, et al.* (2000). Flt3 mutations from patients with acute myeloid leukemia induce transformation of 32D cells mediated by the Ras and STAT5 pathways. Blood *96*, 3907-3914.
Moran-Crusio, K., Reavie, L., Shih, A., Abdel-Wahab, O., Ndiaye-Lobry, D., Lobry, C., Figueroa, M.E., Vasanthakumar, A., Patel, J., Zhao, X.*, et al.* (2011). Tet2 loss leads to increased hematopoietic stem cell self-renewal and myeloid transformation. Cancer Cell *20*, 11-24.
Morrison, S.J., Hemmati, H.D., Wandycz, A.M., and Weissman, I.L. (1995). The purification and characterisation of fetal liver hematopoietic stem cells. Proc Natl Acad Sci U S A *92*, 10302-10306.
Morrison, S.J., and Scadden, D.T. (2014). The bone marrow niche for haematopoietic stem cells. Nature *505*, 327-334.
Morrison, S.J., and Weissman, I.L. (1994). The long-term repopulating subset of hematopoietic stem cells is deterministic and isolatable by phenotype. Immunity *1*, 661-673.
Moschoi, R., Imbert, V., Nebout, M., Chiche, J., Mary, D., Prebet, T., Saland, E., Castellano, R., Pouyet, L., Collette, Y.*, et al.* (2016). Protective mitochondrial transfer from bone marrow stromal cells to acute myeloid leukemic cells during chemotherapy. Blood *128*, 253-264.
Muller, A.M., Medvinsky, A., Strouboulis, J., Grosveld, F., and Dzierzak, E. (1994). Development of hematopoietic stem cell activity in the mouse embryo. Immunity *1*, 291-301.
Muller-Sieburg, C.E., Cho, R.H., Karlsson, L., Huang, J.F., and Sieburg, H.B. (2004). Myeloid-biased hematopoietic stem cells have extensive self-renewal capacity but generate diminished lymphoid progeny with impaired IL-7 responsiveness. Blood *103*, 4111-4118.
Muller-Sieburg, C.E., Cho, R.H., Thoman, M., Adkins, B., and Sieburg, H.B. (2002). Deterministic regulation of hematopoietic stem cell self-renewal and differentiation. Blood *100*, 1302-1309.
Naveiras, O., Nardi, V., Wenzel, P.L., Hauschka, P.V., Fahey, F., and Daley, G.Q. (2009). Bone-marrow adipocytes as negative regulators of the haematopoietic microenvironment. Nature *460*, 259-263.
Ng, S.W., Mitchell, A., Kennedy, J.A., Chen, W.C., McLeod, J., Ibrahimova, N., Arruda, A., Popescu, A., Gupta, V., Schimmer, A.D.*, et al.* (2016). A 17-gene stemness score for rapid determination of risk in acute leukaemia. Nature *540*, 433-437.
Nicolini, F.E., Cashman, J.D., Hogge, D.E., Humphries, R.K., and Eaves, C.J. (2004). NOD/SCID mice engineered to express human IL-3, GM-CSF and Steel factor constitutively mobilise engrafted human progenitors and compromise human stem cell regeneration. Leukemia *18*, 341-347.
Nilsson, S.K., Johnston, H.M., and Coverdale, J.A. (2001). Spatial localisation of transplanted hemopoietic stem cells: inferences for the localisation of stem cell niches. Blood *97*, 2293-2299.
Ninib Baryawno, D.P., Monika Kowalczyk, Youmna Kfoury, Nicolas Severe, Karin Gustafsson, Mercier Francois, Marcin Tabaka, Matan Hofree, Danielle Dionne, Ani Papazian, Dongjun Lee, Orit Rozenblatt-Rosen, Aviv Regev, David Scadden (2019). A cellular taxonomy of the bone marrow stroma in homeostasis and leukemia demonstrates cancer-crosstalk with stroma to impair normal tissue function. BioRxiv *https://doi.org/10.1101/556845*.
Ninomiya, M., Abe, A., Katsumi, A., Xu, J., Ito, M., Arai, F., Suda, T., Ito, M., Kiyoi, H., Kinoshita, T.*, et al.* (2007). Homing, proliferation and survival sites of human leukemia cells in vivo in immunodeficient mice. Leukemia *21*, 136-142.

Nobrega-Pereira, S., Caiado, F., Carvalho, T., Matias, I., Graca, G., Goncalves, L.G., Silva-Santos, B., Norell, H., and Dias, S. (2018). VEGFR2-Mediated Reprogramming of Mitochondrial Metabolism Regulates the Sensitivity of Acute Myeloid Leukemia to Chemotherapy. Cancer Res *78*, 731-741.
Nombela-Arrieta, C., Pivarnik, G., Winkel, B., Canty, K.J., Harley, B., Mahoney, J.E., Park, S.Y., Lu, J., Protopopov, A., and Silberstein, L.E. (2013). Quantitative imageing of haematopoietic stem and progenitor cell localisation and hypoxic status in the bone marrow microenvironment. Nat Cell Biol *15*, 533-543.
Notta, F., Doulatov, S., Laurenti, E., Poeppl, A., Jurisica, I., and Dick, J.E. (2011). Isolation of single human hematopoietic stem cells capable of long-term multilineage engraftment. Science *333*, 218-221.
Notta, F., Zandi, S., Takayama, N., Dobson, S., Gan, O.I., Wilson, G., Kaufmann, K.B., McLeod, J., Laurenti, E., Dunant, C.F.*, et al.* (2016). Distinct routes of lineage development reshape the human blood hierarchy across ontogeny. Science *351*, aab2116.
Oguro, H., Ding, L., and Morrison, S.J. (2013). SLAM family markers resolve functionally distinct subpopulations of hematopoietic stem cells and multipotent progenitors. Cell Stem Cell *13*, 102-116.
Ohkouchi, S., Block, G.J., Katsha, A.M., Kanehira, M., Ebina, M., Kikuchi, T., Saijo, Y., Nukiwa, T., and Prockop, D.J. (2012). Mesenchymal stromal cells protect cancer cells from ROS-induced apoptosis and enhance the Warburg effect by secreting STC1. Mol Ther *20*, 417-423.
Omatsu, Y., Sugiyama, T., Kohara, H., Kondoh, G., Fujii, N., Kohno, K., and Nagasawa, T. (2010). The essential functions of adipo-osteogenic progenitors as the hematopoietic stem and progenitor cell niche. Immunity *33*, 387-399.
Ono, M., Ohkouchi, S., Kanehira, M., Tode, N., Kobayashi, M., Ebina, M., Nukiwa, T., Irokawa, T., Ogawa, H., Akaike, T.*, et al.* (2015). Mesenchymal stem cells correct inappropriate epithelial-mesenchyme relation in pulmonary fibrosis using stanniocalcin-1. Mol Ther *23*, 549-560.
Orkin, S.H., and Zon, L.I. (2008). Hematopoiesis: an evolving paradigm for stem cell biology. Cell *132*, 631-644.
Osawa, M., Hanada, K., Hamada, H., and Nakauchi, H. (1996). Long-term lymphohematopoietic reconstitution by a single CD34-low/negative hematopoietic stem cell. Science *273*, 242-245.
Paciga, M., McCudden, C.R., Londos, C., DiMattia, G.E., and Wagner, G.F. (2003). Targeting of big stanniocalcin and its receptor to lipid storage droplets of ovarian steroidogenic cells. J Biol Chem *278*, 49549-49554.
Palis, J., Robertson, S., Kennedy, M., Wall, C., and Keller, G. (1999). Development of erythroid and myeloid progenitors in the yolk sac and embryo proper of the mouse. Development *126*, 5073-5084.
Palomaki, S., Pietila, M., Laitinen, S., Pesala, J., Sormunen, R., Lehenkari, P., and Koivunen, P. (2013). HIF-1αlpha is upregulated in human mesenchymal stem cells. Stem Cells *31*, 1902-1909.
Pan, J.S., Huang, L., Belousova, T., Lu, L., Yang, Y., Reddel, R., Chang, A., Ju, H., DiMattia, G., Tong, Q.*, et al.* (2015). Stanniocalcin-1 inhibits renal ischemia/reperfusion injury via an AMP-activated protein kinase-dependent pathway. J Am Soc Nephrol *26*, 364-378.
Papaemmanuil, E., Dohner, H., and Campbell, P.J. (2016). Genomic Classification in Acute Myeloid Leukemia. N Engl J Med *375*, 900-901.
Park, D., Spencer, J.A., Koh, B.I., Kobayashi, T., Fujisaki, J., Clemens, T.L., Lin, C.P., Kronenberg, H.M., and Scadden, D.T. (2012). Endogenous bone marrow MSCs are dynamic,

fate-restricted participants in bone maintenance and regeneration. Cell Stem Cell *10*, 259-272.
Park, W.Y., Hong, B.J., Lee, J., Choi, C., and Kim, M.Y. (2016). H3K27 Demethylase JMJD3 Employs the NF-kappaB and BMP Signaling Pathways to Modulate the Tumour Microenvironment and Promote Melanoma Progression and Metastasis. Cancer Res *76*, 161-170.
Passaro, D., Abarrategi, A., Foster, K., Ariza-McNaughton, L., and Bonnet, D. (2017a). Bioengineering of Humanised Bone Marrow Microenvironments in Mouse and Their Visualisation by Live Imageing. J Vis Exp.
Passaro, D., Di Tullio, A., Abarrategi, A., Rouault-Pierre, K., Foster, K., Ariza-McNaughton, L., Montaner, B., Chakravarty, P., Bhaw, L., Diana, G.*, et al.* (2017b). Increased Vascular Permeability in the Bone Marrow Microenvironment Contributes to Disease Progression and Drug Response in Acute Myeloid Leukemia. Cancer Cell *32*, 324-341 e326.
Paydas, S., Ergin, M., Baslamisli, F., Yavuz, S., Zorludemir, S., Sahin, B., and Bolat, F.A. (2002). Bone marrow necrosis: clinicopathologic analysis of 20 cases and review of the literature. Am J Hematol *70*, 300-305.
Pei, W., Feyerabend, T.B., Rossler, J., Wang, X., Postrach, D., Busch, K., Rode, I., Klapproth, K., Dietlein, N., Quedenau, C.*, et al.* (2017). Polylox barcoding reveals haematopoietic stem cell fates realised in vivo. Nature *548*, 456-460.
Pena, C., Cespedes, M.V., Lindh, M.B., Kiflemariam, S., Mezheyeuski, A., Edqvist, P.H., Hagglof, C., Birgisson, H., Bojmar, L., Jirstrom, K.*, et al.* (2013). STC1 expression by cancer-associated fibroblasts drives metastasis of colorectal cancer. Cancer Res *73*, 1287-1297.
Pietras, E.M., Reynaud, D., Kang, Y.A., Carlin, D., Calero-Nieto, F.J., Leavitt, A.D., Stuart, J.M., Gottgens, B., and Passegue, E. (2015). Functionally Distinct Subsets of Lineage-Biased Multipotent Progenitors Control Blood Production in Normal and Regenerative Conditions. Cell Stem Cell *17*, 35-46.
Pollyea, D.A., Stevens, B.M., Jones, C.L., Winters, A., Pei, S., Minhajuddin, M., D'Alessandro, A., Culp-Hill, R., Riemondy, K.A., Gillen, A.E.*, et al.* (2018). Venetoclax with azacitidine disrupts energy metabolism and targets leukemia stem cells in patients with acute myeloid leukemia. Nat Med *24*, 1859-1866.
Poulos, M.G., Crowley, M.J.P., Gutkin, M.C., Ramalingam, P., Schachterle, W., Thomas, J.L., Elemento, O., and Butler, J.M. (2015). Vascular Platform to Define Hematopoietic Stem Cell Factors and Enhance Regenerative Hematopoiesis. Stem Cell Reports *5*, 881-894.
Prendergast, A.M., Kuck, A., van Essen, M., Haas, S., Blaszkiewicz, S., and Essers, M.A. (2017). IFNalpha-mediated remodeling of endothelial cells in the bone marrow niche. Haematologica *102*, 445-453.
Quintas-Cardama, A., Santos, F.P., and Garcia-Manero, G. (2011). Histone deacetylase inhibitors for the treatment of myelodysplastic syndrome and acute myeloid leukemia. Leukemia *25*, 226-235.
Raaijmakers, M.H., Mukherjee, S., Guo, S., Zhang, S., Kobayashi, T., Schoonmaker, J.A., Ebert, B.L., Al-Shahrour, F., Hasserjian, R.P., Scadden, E.O.*, et al.* (2010). Bone progenitor dysfunction induces myelodysplasia and secondary leukaemia. Nature *464*, 852-857.
Rauch, P.J., Ellegast, J.M., Widmer, C.C., Fritsch, K., Goede, J.S., Valk, P.J., Lowenberg, B., Takizawa, H., and Manz, M.G. (2016). MPL expression on AML blasts predicts peripheral blood neutropenia and thrombocytopenia. Blood *128*, 2253-2257.
Reichard, K.K., Zhang, Q.Y., Sanchez, L., Hozier, J., Viswanatha, D., and Foucar, K. (2006). Acute myeloid leukemia of donor origin after allogeneic bone marrow transplantation for precursor T-cell acute lymphoblastic leukemia: case report and review of the literature. Am J Hematol *81*, 178-185.

Reikvam, H., Brenner, A.K., Hagen, K.M., Liseth, K., Skrede, S., Hatfield, K.J., and Bruserud, O. (2015). The cytokine-mediated crosstalk between primary human acute myeloid cells and mesenchymal stem cells alters the local cytokine network and the global gene expression profile of the mesenchymal cells. Stem Cell Res *15*, 530-541.
Reinisch, A., Etchart, N., Thomas, D., Hofmann, N.A., Fruehwirth, M., Sinha, S., Chan, C.K., Senarath-Yapa, K., Seo, E.Y., Wearda, T.*, et al.* (2015). Epigenetic and in vivo comparison of diverse MSC sources reveals an endochondral signature for human hematopoietic niche formation. Blood *125*, 249-260.
Reinisch, A., Thomas, D., Corces, M.R., Zhang, X., Gratsinger, D., Hong, W.J., Schallmoser, K., Strunk, D., and Majeti, R. (2016). A humanised bone marrow ossicle xenotransplantation model enables improved engraftment of healthy and leukemic human hematopoietic cells. Nat Med *22*, 812-821.
RN., P. (2011). Regulation of Tissue Oxygenation. . Morgan & Claypool Life Sciences; 2011 Chapter 4, Oxygen Transport.
Roch, G.J., and Sherwood, N.M. (2011). Stanniocalcin has deep evolutionary roots in eukaryotes. Genome Biol Evol *3*, 284-294.
Rodriguez-Fraticelli, A.E., Wolock, S.L., Weinreb, C.S., Panero, R., Patel, S.H., Jankovic, M., Sun, J., Calogero, R.A., Klein, A.M., and Camargo, F.D. (2018). Clonal analysis of lineage fate in native haematopoiesis. Nature *553*, 212-216.
Rouault-Pierre, K., Lopez-Onieva, L., Foster, K., Anjos-Afonso, F., Lamrissi-Garcia, I., Serrano-Sanchez, M., Mitter, R., Ivanovic, Z., de Verneuil, H., Gribben, J.*, et al.* (2013). HIF-2alpha protects human hematopoietic stem/progenitors and acute myeloid leukemic cells from apoptosis induced by endoplasmic reticulum stress. Cell Stem Cell *13*, 549-563.
Rouault-Pierre, K., Mian, S.A., Goulard, M., Abarrategi, A., Di Tulio, A., Smith, A.E., Mohamedali, A., Best, S., Nloga, A.M., Kulasekararaj, A.G.*, et al.* (2017). Preclinical modeling of myelodysplastic syndromes. Leukemia *31*, 2702-2708.
Rupec, R.A., Jundt, F., Rebholz, B., Eckelt, B., Weindl, G., Hersinger, T., Flaig, M.J., Moosmann, S., Plewig, G., Dorken, B.*, et al.* (2005). Stroma-mediated dysregulation of myelopoiesis in mice lacking I kappa B alpha. Immunity *22*, 479-491.
Russell, S., Wojtkowiak, J., Neilson, A., and Gillies, R.J. (2017). Metabolic Profiling of healthy and cancerous tissues in 2D and 3D. Sci Rep *7*, 15285.
Sacchetti, B., Funari, A., Michienzi, S., Di Cesare, S., Piersanti, S., Saggio, I., Tagliafico, E., Ferrari, S., Robey, P.G., Riminucci, M.*, et al.* (2007). Self-renewing osteoprogenitors in bone marrow sinusoids can organize a hematopoietic microenvironment. Cell *131*, 324-336.
Saito, Y., Uchida, N., Tanaka, S., Suzuki, N., Tomizawa-Murasawa, M., Sone, A., Najima, Y., Takagi, S., Aoki, Y., Wake, A.*, et al.* (2010). Induction of cell cycle entry eliminates human leukemia stem cells in a mouse model of AML. Nat Biotechnol *28*, 275-280.
Sakamuru, S., Attene-Ramos, M.S., and Xia, M. (2016). Mitochondrial Membrane Potential Assay. Methods Mol Biol *1473*, 17-22.
Samudio, I., Fiegl, M., and Andreeff, M. (2009). Mitochondrial uncoupling and the Warburg effect: molecular basis for the reprogramming of cancer cell metabolism. Cancer Res *69*, 2163-2166.
Samudio, I., Fiegl, M., McQueen, T., Clise-Dwyer, K., and Andreeff, M. (2008). The warburg effect in leukemia-stroma co-cultures is mediated by mitochondrial uncoupling associated with uncoupling protein 2 activation. Cancer Res *68*, 5198-5205.
Samudio, I., Harmancey, R., Fiegl, M., Kantarjian, H., Konopleva, M., Korchin, B., Kaluarachchi, K., Bornmann, W., Duvvuri, S., Taegtmeyer, H.*, et al.* (2010). Pharmacologic inhibition of fatty acid oxidation sensitizes human leukemia cells to apoptosis induction. J Clin Invest *120*, 142-156.

Sansone, P., and Bromberg, J. (2012). Targeting the interleukin-6/Jak/stat pathway in human malignancies. J Clin Oncol *30*, 1005-1014.
Sarry, J.E., Murphy, K., Perry, R., Sanchez, P.V., Secreto, A., Keefer, C., Swider, C.R., Strzelecki, A.C., Cavelier, C., Recher, C.*, et al.* (2011). Human acute myelogenous leukemia stem cells are rare and heterogeneous when assayed in NOD/SCID/IL2Rgammac-deficient mice. J Clin Invest *121*, 384-395.
Saultz, J.N., and Garzon, R. (2016). Acute Myeloid Leukemia: A Concise Review. J Clin Med *5*.
Sawai, C.M., Babovic, S., Upadhaya, S., Knapp, D., Lavin, Y., Lau, C.M., Goloborodko, A., Feng, J., Fujisaki, J., Ding, L.*, et al.* (2016). Hematopoietic Stem Cells Are the Major Source of Multilineage Hematopoiesis in Adult Animals. Immunity *45*, 597-609.
Schepers, K., Pietras, E.M., Reynaud, D., Flach, J., Binnewies, M., Garg, T., Wagers, A.J., Hsiao, E.C., and Passegue, E. (2013). Myeloproliferative neoplasia remodels the endosteal bone marrow niche into a self-reinforcing leukemic niche. Cell Stem Cell *13*, 285-299.
Schoedel, K.B., Morcos, M.N.F., Zerjatke, T., Roeder, I., Grinenko, T., Voehringer, D., Gothert, J.R., Waskow, C., Roers, A., and Gerbaulet, A. (2016). The bulk of the hematopoietic stem cell population is dispensable for murine steady-state and stress hematopoiesis. Blood *128*, 2285-2296.
Schofield, C.J., and Ratcliffe, P.J. (2004). Oxygen sensing by HIF hydroxylases. Nat Rev Mol Cell Biol *5*, 343-354.
Schofield, R. (1978). The relationship between the spleen colony-forming cell and the haemopoietic stem cell. Blood Cells *4*, 7-25.
Schroeder, T., Geyh, S., Germing, U., and Haas, R. (2016). Mesenchymal stromal cells in myeloid malignancies. Blood Res *51*, 225-232.
Schutze, S., Wiegmann, K., Machleidt, T., and Kronke, M. (1995). TNF-induced activation of NF-kappa B. Immunobiology *193*, 193-203.
Scortegagna, M., Ding, K., Zhang, Q., Oktay, Y., Bennett, M.J., Bennett, M., Shelton, J.M., Richardson, J.A., Moe, O., and Garcia, J.A. (2005). HIF-2alpha regulates murine hematopoietic development in an erythropoietin-dependent manner. Blood *105*, 3133-3140.
Scortegagna, M., Morris, M.A., Oktay, Y., Bennett, M., and Garcia, J.A. (2003). The HIF family member EPAS1/HIF-2alpha is required for normal hematopoiesis in mice. Blood *102*, 1634-1640.
Serlachius, M., Zhang, K.Z., and Andersson, L.C. (2004). Stanniocalcin in terminally differentiated mammalian cells. Peptides *25*, 1657-1662.
Shafat, M.S., Oellerich, T., Mohr, S., Robinson, S.D., Edwards, D.R., Marlein, C.R., Piddock, R.E., Fenech, M., Zaitseva, L., Abdul-Aziz, A.*, et al.* (2017). Leukemic blasts program bone marrow adipocytes to generate a protumoural microenvironment. Blood *129*, 1320-1332.
Sharma, R., and Sharma, S. (2018). Physiology, Blood Volume. In StatPearls (Treasure Island (FL)).
Sharma S, R.D. (2018). Partial Pressure Of Oxygen (PO2) StatPearls [Internet] Treasure Island (FL): StatPearls Publishing; 2018 Jan- Available from: https://wwwncbinlmnihgov/books/NBK493219/.
Sheikh-Hamad, D., Bick, R., Wu, G.Y., Christensen, B.M., Razeghi, P., Poindexter, B., Taegtmeyer, H., Wamsley, A., Padda, R., Entman, M.*, et al.* (2003). Stanniocalcin-1 is a naturally occurring L-channel inhibitor in cardiomyocytes: relevance to human heart failure. Am J Physiol Heart Circ Physiol *285*, H442-448.
Shi, M., Zhu, J., Wang, R., Chen, X., Mi, L., Walz, T., and Springer, T.A. (2011). Latent TGF-beta structure and activation. Nature *474*, 343-349.

Shlush, L.I., Mitchell, A., Heisler, L., Abelson, S., Ng, S.W.K., Trotman-Grant, A., Medeiros, J.J.F., Rao-Bhatia, A., Jaciw-Zurakowsky, I., Marke, R.*, et al.* (2017). Tracing the origins of relapse in acute myeloid leukaemia to stem cells. Nature *547*, 104-108.
Shlush, L.I., Zandi, S., Mitchell, A., Chen, W.C., Brandwein, J.M., Gupta, V., Kennedy, J.A., Schimmer, A.D., Schuh, A.C., Yee, K.W.*, et al.* (2014). Identification of pre-leukaemic haematopoietic stem cells in acute leukaemia. Nature *506*, 328-333.
Shultz, L.D., Schweitzer, P.A., Christianson, S.W., Gott, B., Schweitzer, I.B., Tennent, B., McKenna, S., Mobraaten, L., Rajan, T.V., Greiner, D.L.*, et al.* (1995). Multiple defects in innate and adaptive immunologic function in NOD/LtSz-scid mice. J Immunol *154*, 180-191.
Silvennoinen, O., and Hubbard, S.R. (2015). Molecular insights into regulation of JAK2 in myeloproliferative neoplasms. Blood *125*, 3388-3392.
Siminovitch, L., McCulloch, E.A., and Till, J.E. (1963). The Distribution of Colony-Forming Cells among Spleen Colonies. J Cell Comp Physiol *62*, 327-336.
Singh, P., Hoggatt, J., Hu, P., Speth, J.M., Fukuda, S., Breyer, R.M., and Pelus, L.M. (2012). Blockade of prostaglandin E2 signaling through EP1 and EP3 receptors attenuates Flt3L-dependent dendritic cell development from hematopoietic progenitor cells. Blood *119*, 1671-1682.
Singh, R.P., Grinenko, T., Ramasz, B., Franke, K., Lesche, M., Dahl, A., Gassmann, M., Chavakis, T., Henry, I., and Wielockx, B. (2018). Hematopoietic Stem Cells but Not Multipotent Progenitors Drive Erythropoiesis during Chronic Erythroid Stress in EPO Transgenic Mice. Stem Cell Reports *10*, 1908-1919.
Sipkins, D.A., Wei, X., Wu, J.W., Runnels, J.M., Cote, D., Means, T.K., Luster, A.D., Scadden, D.T., and Lin, C.P. (2005). In vivo imageing of specialised bone marrow endothelial microdomains for tumour engraftment. Nature *435*, 969-973.
Sivaraj, K.K., and Adams, R.H. (2016). Blood vessel formation and function in bone. Development *143*, 2706-2715.
Slade, I., Bacchelli, C., Davies, H., Murray, A., Abbaszadeh, F., Hanks, S., Barfoot, R., Burke, A., Chisholm, J., Hewitt, M.*, et al.* (2011). DICER1 syndrome: clarifying the diagnosis, clinical features and management implications of a pleiotropic tumour predisposition syndrome. J Med Genet *48*, 273-278.
Song, K., Li, M., Xu, X.J., Xuan, L., Huang, G.N., Song, X.L., and Liu, Q.F. (2014). HIF-1αlpha and GLUT1 gene expression is associated with chemoresistance of acute myeloid leukemia. Asian Pac J Cancer Prev *15*, 1823-1829.
Spencer, J.A., Ferraro, F., Roussakis, E., Klein, A., Wu, J., Runnels, J.M., Zaher, W., Mortensen, L.J., Alt, C., Turcotte, R.*, et al.* (2014). Direct measurement of local oxygen concentration in the bone marrow of live animals. Nature *508*, 269-273.
Sugiyama, T., Kohara, H., Noda, M., and Nagasawa, T. (2006). Maintenance of the hematopoietic stem cell pool by CXCL12-CXCR4 chemokine signaling in bone marrow stromal cell niches. Immunity *25*, 977-988.
Sun, J., Ramos, A., Chapman, B., Johnnidis, J.B., Le, L., Ho, Y.J., Klein, A., Hofmann, O., and Camargo, F.D. (2014). Clonal dynamics of native haematopoiesis. Nature *514*, 322-327.
Swiers, G., Baumann, C., O'Rourke, J., Giannoulatou, E., Taylor, S., Joshi, A., Moignard, V., Pina, C., Bee, T., Kokkaliaris, K.D.*, et al.* (2013). Early dynamic fate changes in haemogenic endothelium characterized at the single-cell level. Nat Commun *4*, 2924.
Tabe, Y., and Konopleva, M. (2015). Role of Microenvironment in Resistance to Therapy in AML. Curr Hematol Malig Rep *10*, 96-103.
Taichman, R.S., and Emerson, S.G. (1994). Human osteoblasts support hematopoiesis through the production of granulocyte colony-stimulating factor. J Exp Med *179*, 1677-1682.

Takenaka, K., Prasolava, T.K., Wang, J.C., Mortin-Toth, S.M., Khalouei, S., Gan, O.I., Dick, J.E., and Danska, J.S. (2007). Polymorphism in Sirpa modulates engraftment of human hematopoietic stem cells. Nat Immunol *8*, 1313-1323.
Takubo, K., Goda, N., Yamada, W., Iriuchishima, H., Ikeda, E., Kubota, Y., Shima, H., Johnson, R.S., Hirao, A., Suematsu, M.*, et al.* (2010). Regulation of the HIF-1αlpha level is essential for hematopoietic stem cells. Cell Stem Cell *7*, 391-402.
Tannahill, G.M., Curtis, A.M., Adamik, J., Palsson-McDermott, E.M., McGettrick, A.F., Goel, G., Frezza, C., Bernard, N.J., Kelly, B., Foley, N.H.*, et al.* (2013). Succinate is an inflammatory signal that induces IL-1beta through HIF-1αlpha. Nature *496*, 238-242.
Tartaglia, M., Mehler, E.L., Goldberg, R., Zampino, G., Brunner, H.G., Kremer, H., van der Burgt, I., Crosby, A.H., Ion, A., Jeffery, S.*, et al.* (2001). Mutations in PTPN11, encoding the protein tyrosine phosphatase SHP-2, cause Noonan syndrome. Nat Genet *29*, 465-468.
Taussig, D.C., Miraki-Moud, F., Anjos-Afonso, F., Pearce, D.J., Allen, K., Ridler, C., Lillington, D., Oakervee, H., Cavenagh, J., Agrawal, S.G.*, et al.* (2008). Anti-CD38 antibody-mediated clearance of human repopulating cells masks the heterogeneity of leukemia-initiating cells. Blood *112*, 568-575.
Taussig, D.C., Vargaftig, J., Miraki-Moud, F., Griessinger, E., Sharrock, K., Luke, T., Lillington, D., Oakervee, H., Cavenagh, J., Agrawal, S.G.*, et al.* (2010). Leukemia-initiating cells from some acute myeloid leukemia patients with mutated nucleophosmin reside in the CD34(-) fraction. Blood *115*, 1976-1984.
Till, J.E., and Mc, C.E. (1961). A direct measurement of the radiation sensitivity of normal mouse bone marrow cells. Radiat Res *14*, 213-222.
Tober, J., Koniski, A., McGrath, K.E., Vemishetti, R., Emerson, R., de Mesy-Bentley, K.K., Waugh, R., and Palis, J. (2007). The megakaryocyte lineage originates from hemangioblast precursors and is an integral component both of primitive and of definitive hematopoiesis. Blood *109*, 1433-1441.
Tohmiya, Y., Koide, Y., Fujimaki, S., Harigae, H., Funato, T., Kaku, M., Ishii, T., Munakata, Y., Kameoka, J., and Sasaki, T. (2004). Stanniocalcin-1 as a novel marker to detect minimal residual disease of human leukemia. Tohoku J Exp Med *204*, 125-133.
Tormin, A., Li, O., Brune, J.C., Walsh, S., Schutz, B., Ehinger, M., Ditzel, N., Kassem, M., and Scheding, S. (2011). CD146 expression on primary nonhematopoietic bone marrow stem cells is correlated with in situ localisation. Blood *117*, 5067-5077.
Trindade, D.M., Silva, J.C., Navarro, M.S., Torriani, I.C., and Kobarg, J. (2009). Low-resolution structural studies of human Stanniocalcin-1. BMC Struct Biol *9*, 57.
Tseng, D.Y., Chou, M.Y., Tseng, Y.C., Hsiao, C.D., Huang, C.J., Kaneko, T., and Hwang, P.P. (2009). Effects of stanniocalcin 1 on calcium uptake in zebrafish (Danio rerio) embryo. Am J Physiol Regul Integr Comp Physiol *296*, R549-557.
Tyner, J.W., Tognon, C.E., Bottomly, D., Wilmot, B., Kurtz, S.E., Savage, S.L., Long, N., Schultz, A.R., Traer, E., Abel, M.*, et al.* (2018). Functional genomic landscape of acute myeloid leukaemia. Nature *562*, 526-531.
Ueda, T., Yoshida, M., Yoshino, H., Kobayashi, K., Kawahata, M., Ebihara, Y., Ito, M., Asano, S., Nakahata, T., and Tsuji, K. (2001). Hematopoietic capability of CD34+ cord blood cells: a comparison with CD34+ adult bone marrow cells. Int J Hematol *73*, 457-462.
Ueno, H., Sakita-Ishikawa, M., Morikawa, Y., Nakano, T., Kitamura, T., and Saito, M. (2003). A stromal cell-derived membrane protein that supports hematopoietic stem cells. Nat Immunol *4*, 457-463.
Uhlen, M., Fagerberg, L., Hallstrom, B.M., Lindskog, C., Oksvold, P., Mardinoglu, A., Sivertsson, A., Kampf, C., Sjostedt, E., Asplund, A.*, et al.* (2015). Proteomics. Tissue-based map of the human proteome. Science *347*, 1260419.

Unnisa, Z., Clark, J.P., Roychoudhury, J., Thomas, E., Tessarollo, L., Copeland, N.G., Jenkins, N.A., Grimes, H.L., and Kumar, A.R. (2012). Meis1 preserves hematopoietic stem cells in mice by limiting oxidative stress. Blood *120*, 4973-4981.
Varghese, R., Gagliardi, A.D., Bialek, P.E., Yee, S.P., Wagner, G.F., and Dimattia, G.E. (2002). Overexpression of human stanniocalcin affects growth and reproduction in transgenic mice. Endocrinology *143*, 868-876.
Velasco-Hernandez, T., Hyrenius-Wittsten, A., Rehn, M., Bryder, D., and Cammenga, J. (2014). HIF-1αlpha can act as a tumour suppressor gene in murine acute myeloid leukemia. Blood *124*, 3597-3607.
Viadana, E., Bross, I.D., and Pickren, J.W. (1978). An autopsy study of the metastatic patterns of human leukemias. Oncology *35*, 87-96.
Visnjic, D., Kalajzic, Z., Rowe, D.W., Katavic, V., Lorenzo, J., and Aguila, H.L. (2004). Hematopoiesis is severely altered in mice with an induced osteoblast deficiency. Blood *103*, 3258-3264.
Vukovic, M., Guitart, A.V., Sepulveda, C., Villacreces, A., O'Duibhir, E., Panagopoulou, T.I., Ivens, A., Menendez-Gonzalez, J., Iglesias, J.M., Allen, L.*, et al.* (2015). HIF-1αlpha and Hif-2alpha synergize to suppress AML development but are dispensable for disease maintenance. J Exp Med *212*, 2223-2234.
Vukovic, M., Sepulveda, C., Subramani, C., Guitart, A.V., Mohr, J., Allen, L., Panagopoulou, T.I., Paris, J., Lawson, H., Villacreces, A.*, et al.* (2016). Adult hematopoietic stem cells lacking HIF-1αlpha self-renew normally. Blood *127*, 2841-2846.
Wagner, G.F., and Dimattia, G.E. (2006). The stanniocalcin family of proteins. J Exp Zool A Comp Exp Biol *305*, 769-780.
Wagner, G.F., Guiraudon, C.C., Milliken, C., and Copp, D.H. (1995). Immunological and biological evidence for a stanniocalcin-like hormone in human kidney. Proc Natl Acad Sci U S A *92*, 1871-1875.
Wagner, G.F., Vozzolo, B.L., Jaworski, E., Haddad, M., Kline, R.L., Olsen, H.S., Rosen, C.A., Davidson, M.B., and Renfro, J.L. (1997). Human stanniocalcin inhibits renal phosphate excretion in the rat. J Bone Miner Res *12*, 165-171.
Walenda, T., Bork, S., Horn, P., Wein, F., Saffrich, R., Diehlmann, A., Eckstein, V., Ho, A.D., and Wagner, W. (2010). Co-culture with mesenchymal stromal cells increases proliferation and maintenance of haematopoietic progenitor cells. J Cell Mol Med *14*, 337-350.
Walkley, C.R., Olsen, G.H., Dworkin, S., Fabb, S.A., Swann, J., McArthur, G.A., Westmoreland, S.V., Chambon, P., Scadden, D.T., and Purton, L.E. (2007). A microenvironment-induced myeloproliferative syndrome caused by retinoic acid receptor gamma deficiency. Cell *129*, 1097-1110.
Walter, R.B., Kantarjian, H.M., Huang, X., Pierce, S.A., Sun, Z., Gundacker, H.M., Ravandi, F., Faderl, S.H., Tallman, M.S., Appelbaum, F.R.*, et al.* (2010). Effect of complete remission and responses less than complete remission on survival in acute myeloid leukemia: a combined Eastern Cooperative Oncology Group, Southwest Oncology Group, and M. D. Anderson Cancer Center Study. J Clin Oncol *28*, 1766-1771.
Wang, L., Zhang, H., Rodriguez, S., Cao, L., Parish, J., Mumaw, C., Zollman, A., Kamoka, M.M., Mu, J., Chen, D.Z.*, et al.* (2014). Notch-dependent repression of miR-155 in the bone marrow niche regulates hematopoiesis in an NF-kappaB-dependent manner. Cell Stem Cell *15*, 51-65.
Wang, W., Stiehl, T., Raffel, S., Hoang, V.T., Hoffmann, I., Poisa-Beiro, L., Saeed, B.R., Blume, R., Manta, L., Eckstein, V.*, et al.* (2017). Reduced hematopoietic stem cell frequency predicts outcome in acute myeloid leukemia. Haematologica *102*, 1567-1577.

Wang, X., Dong, F., Zhang, S., Yang, W., Yu, W., Wang, Z., Zhang, S., Wang, J., Ma, S., Wu, P.*, et al.* (2018). TGF-beta1 Negatively Regulates the Number and Function of Hematopoietic Stem Cells. Stem Cell Reports *11*, 274-287.
Wang, Y., Gao, A., Zhao, H., Lu, P., Cheng, H., Dong, F., Gong, Y., Ma, S., Zheng, Y., Zhang, H.*, et al.* (2016). Leukemia cell infiltration causes defective erythropoiesis partially through MIP-1alpha/CCL3. Leukemia *30*, 1897-1908.
Wang, Y., Huang, L., Abdelrahim, M., Cai, Q., Truong, A., Bick, R., Poindexter, B., and Sheikh-Hamad, D. (2009). Stanniocalcin-1 suppresses superoxide generation in macrophages through induction of mitochondrial UCP2. J Leukoc Biol *86*, 981-988.
Wang, Y., Liu, Y., Malek, S.N., Zheng, P., and Liu, Y. (2011). Targeting HIF1alpha eliminates cancer stem cells in hematological malignancies. Cell Stem Cell *8*, 399-411.
Waskow, C., Madan, V., Bartels, S., Costa, C., Blasig, R., and Rodewald, H.R. (2009). Hematopoietic stem cell transplantation without irradiation. Nat Methods *6*, 267-269.
Weise, F., Fernekorn, U., Hampl, J., Klett, M., and Schober, A. (2013). Analysis and comparison of oxygen consumption of HepG2 cells in a monolayer and three-dimensional high density cell culture by use of a matrigrid(R). Biotechnol Bioeng *110*, 2504-2512.
Whitman, S.P., Kohlschmidt, J., Maharry, K., Volinia, S., Mrozek, K., Nicolet, D., Schwind, S., Becker, H., Metzeler, K.H., Mendler, J.H.*, et al.* (2014). GAS6 expression identifies high-risk adult AML patients: potential implications for therapy. Leukemia *28*, 1252-1258.
Wilson, A., Laurenti, E., Oser, G., van der Wath, R.C., Blanco-Bose, W., Jaworski, M., Offner, S., Dunant, C.F., Eshkind, L., Bockamp, E.*, et al.* (2008). Hematopoietic stem cells reversibly switch from dormancy to self-renewal during homeostasis and repair. Cell *135*, 1118-1129.
Wiseman, D.H. (2011). Donor cell leukemia: a review. Biol Blood Marrow Transplant *17*, 771-789.
Wu, A.M., Till, J.E., Siminovitch, L., and McCulloch, E.A. (1968). Cytological evidence for a relationship between normal hemotopoietic colony-forming cells and cells of the lymphoid system. J Exp Med *127*, 455-464.
Wu, E., Palmer, N., Tian, Z., Moseman, A.P., Galdzicki, M., Wang, X., Berger, B., Zhang, H., and Kohane, I.S. (2008). Comprehensive dissection of PDGF-PDGFR signaling pathways in PDGFR genetically defined cells. PLoS One *3*, e3794.
Wunderlich, M., Chou, F.S., Link, K.A., Mizukawa, B., Perry, R.L., Carroll, M., and Mulloy, J.C. (2010). AML xenograft efficiency is significantly improved in NOD/SCID-IL2RG mice constitutively expressing human SCF, GM-CSF and IL-3. Leukemia *24*, 1785-1788.
Xiao, P., Sandhow, L., Heshmati, Y., Kondo, M., Bouderlique, T., Dolinska, M., Johansson, A.S., Sigvardsson, M., Ekblom, M., Walfridsson, J.*, et al.* (2018). Distinct roles of mesenchymal stem and progenitor cells during the development of acute myeloid leukemia in mice. Blood Adv *2*, 1480-1494.
Xie, Y., Yin, T., Wiegraebe, W., He, X.C., Miller, D., Stark, D., Perko, K., Alexander, R., Schwartz, J., Grindley, J.C.*, et al.* (2009). Detection of functional haematopoietic stem cell niche using real-time imageing. Nature *457*, 97-101.
Xu, P., Wang, M., Jiang, Y., Ouyang, J., and Chen, B.J.T.C.R. (2017). The association between expression of hypoxia inducible factor-1α and multi-drug resistance of acute myeloid leukemia. 2017 *6*, 198-205.
Yamaguchi, T., Mukasa, T., Uchida, E., Kanayasu-Toyoda, T., and Hayakawa, T. (1999). The role of STAT3 in granulocyte colony-stimulating factor-induced enhancement of neutrophilic differentiation of Me2SO-treated HL-60 cells. GM-CSF inhibits the nuclear translocation of tyrosine-phosphorylated STAT3. J Biol Chem *274*, 15575-15581.

Yamamoto, J.F., and Goodman, M.T. (2008). Patterns of leukemia incidence in the United States by subtype and demographic characteristics, 1997-2002. Cancer Causes Control *19*, 379-390.
Yamamoto, R., Morita, Y., Ooehara, J., Hamanaka, S., Onodera, M., Rudolph, K.L., Ema, H., and Nakauchi, H. (2013). Clonal analysis unveils self-renewing lineage-restricted progenitors generated directly from hematopoietic stem cells. Cell *154*, 1112-1126.
Yamamoto, R., Wilkinson, A.C., Ooehara, J., Lan, X., Lai, C.Y., Nakauchi, Y., Pritchard, J.K., and Nakauchi, H. (2018). Large-Scale Clonal Analysis Resolves Ageing of the Mouse Hematopoietic Stem Cell Compartment. Cell Stem Cell *22*, 600-607 e604.
Yamazaki, S., Ema, H., Karlsson, G., Yamaguchi, T., Miyoshi, H., Shioda, S., Taketo, M.M., Karlsson, S., Iwama, A., and Nakauchi, H. (2011). Nonmyelinating Schwann cells maintain hematopoietic stem cell hibernation in the bone marrow niche. Cell *147*, 1146-1158.
Yang, J., AlTahan, A., Jones, D.T., Buffa, F.M., Bridges, E., Interiano, R.B., Qu, C., Vogt, N., Li, J.L., Baban, D.*, et al.* (2015). Estrogen receptor-alpha directly regulates the hypoxia-inducible factor 1 pathway associated with antiestrogen response in breast cancer. Proc Natl Acad Sci U S A *112*, 15172-15177.
Yang, M., Busche, G., Ganser, A., and Li, Z. (2013). Morphology and quantitative composition of hematopoietic cells in murine bone marrow and spleen of healthy subjects. Ann Hematol *92*, 587-594.
Yang, M., Su, H., Soga, T., Kranc, K.R., and Pollard, P.J. (2014). Prolyl hydroxylase domain enzymes: important regulators of cancer metabolism. Hypoxia (Auckl) *2*, 127-142.
Ye, H., Adane, B., Khan, N., Sullivan, T., Minhajuddin, M., Gasparetto, M., Stevens, B., Pei, S., Balys, M., Ashton, J.M.*, et al.* (2016). Leukemic Stem Cells Evade Chemotherapy by Metabolic Adaptation to an Adipose Tissue Niche. Cell Stem Cell *19*, 23-37.
Yeung, B.H., Law, A.Y., and Wong, C.K. (2012). Evolution and roles of stanniocalcin. Mol Cell Endocrinol *349*, 272-280.
Yeung, H.Y., Lai, K.P., Chan, H.Y., Mak, N.K., Wagner, G.F., and Wong, C.K. (2005). Hypoxia-inducible factor-1-mediated activation of stanniocalcin-1 in human cancer cells. Endocrinology *146*, 4951-4960.
Yeung, J., Esposito, M.T., Gandillet, A., Zeisig, B.B., Griessinger, E., Bonnet, D., and So, C.W. (2010). beta-Catenin mediates the establishment and drug resistance of MLL leukemic stem cells. Cancer Cell *18*, 606-618.
Yu, V.W.C., Yusuf, R.Z., Oki, T., Wu, J., Saez, B., Wang, X., Cook, C., Baryawno, N., Ziller, M.J., Lee, E.*, et al.* (2017). Epigenetic Memory Underlies Cell-Autonomous Heterogeneous Behavior of Hematopoietic Stem Cells. Cell *168*, 944-945.
Zeiger, W., Ito, D., Swetlik, C., Oh-hora, M., Villereal, M.L., and Thinakaran, G. (2011). Stanniocalcin 2 is a negative modulator of store-operated calcium entry. Mol Cell Biol *31*, 3710-3722.
Zeng, Z., Shi, Y.X., Tsao, T., Qiu, Y., Kornblau, S.M., Baggerly, K.A., Liu, W., Jessen, K., Liu, Y., Kantarjian, H.*, et al.* (2012). Targeting of mTORC1/2 by the mTOR kinase inhibitor PP242 induces apoptosis in AML cells under conditions mimicking the bone marrow microenvironment. Blood *120*, 2679-2689.
Zhang, B., Ho, Y.W., Huang, Q., Maeda, T., Lin, A., Lee, S.U., Hair, A., Holyoake, T.L., Huettner, C., and Bhatia, R. (2012). Altered microenvironmental regulation of leukemic and normal stem cells in chronic myelogenous leukemia. Cancer Cell *21*, 577-592.
Zhang, J., Niu, C., Ye, L., Huang, H., He, X., Tong, W.G., Ross, J., Haug, J., Johnson, T., Feng, J.Q.*, et al.* (2003). Identification of the haematopoietic stem cell niche and control of the niche size. Nature *425*, 836-841.

Zhang, Q., Zhao, K., Shen, Q., Han, Y., Gu, Y., Li, X., Zhao, D., Liu, Y., Wang, C., Zhang, X.*, et al.* (2015). Tet2 is required to resolve inflammation by recruiting Hdac2 to specifically repress IL-6. Nature *525*, 389-393.
Zhao, M., Perry, J.M., Marshall, H., Venkatraman, A., Qian, P., He, X.C., Ahamed, J., and Li, L. (2014). Megakaryocytes maintain homeostatic quiescence and promote post-injury regeneration of hematopoietic stem cells. Nat Med *20*, 1321-1326.
Zhou, B.O., Yue, R., Murphy, M.M., Peyer, J.G., and Morrison, S.J. (2014). Leptin-receptor-expressing mesenchymal stromal cells represent the main source of bone formed by adult bone marrow. Cell Stem Cell *15*, 154-168.
Zhou, H.S., Carter, B.Z., and Andreeff, M. (2016). Bone marrow niche-mediated survival of leukemia stem cells in acute myeloid leukemia: Yin and Yang. Cancer Biol Med *13*, 248-259.
Zhou, S., Lechpammer, S., Greenberger, J.S., and Glowacki, J. (2005). Hypoxia inhibition of adipocytogenesis in human bone marrow stromal cells requires transforming growth factor-beta/Smad3 signaling. J Biol Chem *280*, 22688-22696.
Zink, F., Stacey, S.N., Norddahl, G.L., Frigge, M.L., Magnusson, O.T., Jonsdottir, I., Thorgeirsson, T.E., Sigurdsson, A., Gudjonsson, S.A., Gudmundsson, J.*, et al.* (2017). Clonal hematopoiesis, with and without candidate driver mutations, is common in the elderly. Blood *130*, 742-752.